

# **Ubiquitous biosynthesis of nano selenium in plants**

Dissertation  
zur  
Erlangung des Doktorgrades (Dr. rer. nat.)  
der  
Mathematisch-Naturwissenschaftlichen Fakultät  
der  
Rheinischen Friedrich-Wilhelms-Universität Bonn

Vorgelegt von  
**Jonas Verstegen**  
aus  
Viersen

Bonn, 2024

Angefertigt mit Genehmigung der Mathematisch-Naturwissenschaftlichen Fakultät der  
Rheinischen Friedrich-Wilhelms-Universität Bonn

Gutachter/Betreuer: Prof. Dr. Klaus Günther  
Gutachter: Prof. Dr. Peter Dörmann  
Gutachterin: Prof. Dr. Gertrud Morlock

Tag der Promotion: 10.04.2025  
Erscheinungsjahr: 2025

*“I think I am quite ready to go on another journey.”*

John Ronald Reuel Tolkien



## Abstract

Selenium, an essential trace element of the chalcogenide group, is involved in a variety of physiological processes, including thyroid metabolism, the antioxidant system, immune functions and male fertility and therefore plays a crucial role in human health. The biological effects of selenium are achieved through incorporation of selenocysteine into the catalytic center of various enzymes.

The impact of selenium on the incidence and prognosis of many chronic diseases such as diabetes mellitus type 2 and various cancers is a subject of ongoing scientific discussion. Some of the studies find inconclusive or contradictory results. We believe that some of this uncertainty arises from insufficient focus on the chemical species of selenium. It is an underrepresented and often overlooked fact, that the chemical form of a nutrient not only influences its resorption and kinetics but can also has a strong impact on the physiological effects it causes.

Selenium is present in many different food groups, including meat, seafood, dairy products, nuts, grains, fruits and vegetables. Past analysis of selenium species in plants and in food primarily focused on distinguishing between organic compounds, such as selenocysteine and selenomethionine and inorganic compounds like selenite and selenate. Selenium nanoparticles (SeNP) were not part of the scientific discourse and there is no mention of naturally occurring biosynthesis of SeNP in plants in the relevant literature.

Among higher plants selenium is not considered an essential nutrient. Yet many beneficial effects, such as increased resistance to stressors like drought and cold, are observed. The reductive potential of the antioxidant biomolecules that are present in plant cells suggest however, that formation of selenium nanoparticles could happen naturally in living plant cells. Those molecules include amino acids, enzymes, flavonoids, phenolic compounds, proteins, saponins, sugars and tannins. Enzymatic detoxification and degradation of selenocysteine into alanine (Ala) and  $\text{Se}^0$  could also contribute to SeNP formation. Our aim was to investigate the potential synthesis of SeNP in plants and we hypothesized that it does not only happen

as an isolated event but is a widespread phenomenon within the plant kingdom.

To test this hypothesis, a hydroponic system was set up to grow plants under controlled conditions. In this system the plants were nourished with a nutritional solution with added selenite and no other form of selenium to rule out contamination. Seeds were germinated and grown in the hydroponic system. A tailored procedure for preparing and digesting root and shoot tissues was designed for analysis using a new sp-ICP-MS method, which was developed as a part of this project. Post-harvest, the plant treatment included physical and enzymatic breakdown of the tissues and a specifically developed dialysis method that was used to reduce the dissolved selenium in the plant samples and thus to reduce noise and false positive results.

The sp-ICP-MS method was developed for the Perkin Elmer NexION 350D and we were the first ones to be able to analyze SeNP with that system. The method development included evaluating the most suitable selenium isotope to focus on and fine-tuning of system-specific parameters including ideal conditions for the dynamic reaction cell, that was necessary to clear the signal from interferences due to the argon gas that is used for the creation of the plasma.

Successfully applying the analytical method on the complex matrix of plant tissue we discovered, for the first time, evidence for the natural occurrence of SeNP in plants. A substantial number of nanoparticles were found in the root and shoot tissues of the observed plants. The size distribution showed some variation among the different plant species, as did the particle number, however the size distribution was very narrow for most plants and the main share of particles spans around 40 to 60 nm.

Consequently, we put a special focus on including a diverse variety of plants from different families and orders of Angiospermae in our study for the purpose of exploring the commonness of SeNP in plants. Remarkably, SeNP were found in every included plant species, providing strong evidence for the ubiquitous occurrence of nanoparticles in plants. The further choice of analytes consisted of a selection of food plants whose shoots or roots

are part of the human diet including salads, herbs and root vegetables. SeNP were found in all included species of food plants as well. This marks another main finding of this study, which is the recognition that SeNP are regular constituents of plant-based food and therefore consumed by almost all humans on a daily basis.

## Content

<b>Abbreviations .....</b>	vi
<b>List of publications .....</b>	vii
<b>Introduction .....</b>	1
History of selenium.....	1
Selenium biochemistry .....	2
Selenium requirements and availability .....	4
Selenium deficiency and selenosis.....	7
Selenium in plants – physiology and biochemistry .....	9
Nanoparticles .....	11
<b>Method development .....</b>	13
Investigation on the lower concentration limit.....	19
Repeatability.....	21
Comparison between the $^{78}\text{Se}$ and the $^{80}\text{Se}$ isotope .....	24
Inspection of the possibility of particle aggregation .....	25
Improvement of the daily optimized parameters.....	28
Measuring time optimization.....	30
Plant treatment.....	32
<b>Biosynthesis of nano selenium in plants.....</b>	41
Contribution .....	41
Summary .....	41
Introduction .....	41
Materials and Methods .....	42
Results and Discussion .....	43

<b>Ubiquitous Occurrence of Nano Selenium in Food Plants.....</b>	44
Contribution.....	44
Summary.....	44
Introduction.....	44
Materials and Methods .....	45
Results and Discussion .....	46
<b>Discussion and Conclusion .....</b>	48
<b>References.....</b>	50
<b>Appendix.....</b>	64
Appendix A: Biosynthesis of nano selenium in plants .....	64
Appendix B: Ubiquitous Occurrence of Nano Selenium in Food Plants .....	74
Appendix C: Method development .....	90
<b>Acknowledgments .....</b>	128

## Abbreviations

AI	adequate intake
Ala	alanine
Cys	cysteine
DMDSe	dimethyldiselenide
DMSe	dimethylselenide
DI	deionized
DRC	dynamic reaction cell
Efsa	European Food Safety Authority
GPx	glutathione peroxidase
GSH	glutathione
HASTs	high affinity sulphate transporters
HS	Hoagland solution
KBD	Kashin-Beck disease
KD	Keshan disease
LOAEL	lowest-observed-adverse-effect-level
MWCO	molecular weight cut-off
NifS	nitrogen fixation sulfur
RCT	randomized controlled trial
ROS	reactive oxygen species
SECIS	selenocysteine insertion sequence
SeCys	selenocysteine
SeMet	selenomethionine
SeNP	selenium nanoparticle
Ser	serine
Sp-ICP-MS	single particle inductively coupled mass spectrometry
TrxR	thioredoxin reductase
UL	upper tolerable limit
VSSA	volume specific surface area

## List of publications

### Articles (peer-review)

1. Verstegen, J.; Günther, K. Biosynthesis of nano selenium in plants, *Artificial cells, nanomedicine, and biotechnology*. **2023**, 51, pp. 13–21.  
DOI: 10.1080/21691401.2022.2155660
2. Verstegen, J.; Günther, K. Ubiquitous Occurrence of Nano Selenium in Food Plants, *Foods*. **2023**, 12(17) p. 3203. DOI: 10.3390/foods12173203

### Abstracts (conference participation)

1. Verstegen, J.; Günther, K. Biosynthese von Selennanopartikeln in Pflanzen, *Lebensmittelchemie*. **2023**, p. 77. DOI: 10.1002/lemi.202359016

## Introduction

### History of Selenium

Selenium is an element of the 16<sup>th</sup> group and the 4<sup>th</sup> period of the periodic table. Selenium's atomic number is 34, its standard atomic weight is 78.971 and its symbol is Se. Selenium was discovered by the Swedish chemist Jöns Jacob Berzelius in 1817. Berzelius was searching for toxins impacting the health of workers in acid plants<sup>1</sup>. The lead chamber process, a procedure used for the synthesis of sulfuric acid resulted in a waste sludge that contained selenium alongside with tellurium. Originally misidentified as tellurium, selenium was identified as an element of its own. By analogy to the similar tellurium which is named after the Latin word "tellus" which means earth, but is also used in a divine sense as "mother earth" or in Latin also "tellus mater", Berzelius named the newly discovered element after the Greek "Σελήνη" or "selene", which translates to moon (goddess)<sup>1</sup>.

Selenium was first classified as toxin and feared for its impact on livestock and only later, selenium was recognized to be an essential trace element with many functions in the human organism. Scientific papers connected to the keyword "selenoprotein" were first published in the 1970s. Simultaneously, first mentions of the keyword "selenocysteine" were published<sup>2</sup>. Selenocysteine (SeCys) is a very unique amino acid and the compound that is responsible for selenium's role in physiology. The UGA codon is typically a stop codon. However, with specific adjacent genetic structure this codon fulfills a double role and can dictate the insertion of SeCys. This discovery led to the first expansion of the genetic code since it was originally described<sup>3</sup>. In the following years up to now 25 genes and their respective selenoproteins were identified in the human genome<sup>4,5</sup>. Selenium's essentiality was confirmed in the 1980s in China. In regions with particularly low levels of selenium in soil a congestive cardiomyopathy today known as "Keshan disease" was endemic. The often-fatal disease can be prevented by adequate selenium intake from diet or selenium supplementation.

## Selenium biochemistry

20 amino acids were originally described with the discovery of the genetic code in the 1960s<sup>3</sup>. Each of the 64 codons consisting of 3 nucleotides encodes for a specific amino acid or one of the 3 stop codons which terminate a protein synthesis. Only years later, it was discovered that the UGA codon, which usually functions as a stop codon, can also encode for SeCys. This phenomenon is present in eubacteria, archaea, and eukaryotes. The incorporation of SeCys into a protein in eukaryotes is performed cotranslationally by the selenocysteine insertion sequence (SECIS). It's worthwhile noticing that this sequence is found commonly in humans and other animals, in algae and lower plants, but not in higher plants or fungi<sup>6</sup>. Along with this finding goes the widely accepted assumption that selenium is an essential nutrient for humans and many other animals, but not for higher plants.

In SeCys there is a selenium atom where an oxygen is in serine (Ser) and a sulfur in cysteine (Cys). The selenol group in selenocysteine has a pKa of 5.2 to 5.3, whereas the thiol group in cysteine has a pKa of 8.3 to 8.5<sup>5,7</sup>. The increased strength in acidity of SeCys is associated with the larger atomic radius and bond length of selenium and thus its increased polarizability<sup>7</sup>. Compared to their Cys homologues selenoproteins have an activity that can be 100- to 1000-fold higher in mammals<sup>8</sup>. However, there are orthologous enzymes, like the thioredoxin reductase (TrxR) in *Drosophila melanogaster* that naturally contain Cys instead of SeCys in the active center and show equal activity to their corresponding mammalian selenoproteins<sup>7</sup>.

Except for Selenoprotein P, which consists of multiple SeCys, the mRNA for all selenoproteins contains only 1 UGA codon encoding for SeCys. Located in the untranslated 3' region of the mRNA often multiple hundreds of bases downstream from the UGA codon, there is the SECIS element, a stem-loop structure that directs the insertion of SeCys<sup>9</sup>. The second crucial factor for the biosynthesis of selenoproteins are the two isoforms of tRNA <sup>[Ser]Sec</sup>. The two isoforms are essential factors for another subclass of selenoproteins each. One is part in the biosynthesis of housekeeping proteins, the other one is involved in the translation of stress-related proteins<sup>10</sup>. tRNA <sup>[Ser]Sec</sup> is the longest tRNA of its kind in

eukaryotes. It has 96 nucleotides compared to the average 75 nucleotides in other tRNAs, hinting its more complex task. Unlike other amino acids SeCys is not just bound to its tRNA and transported to its destination, but instead it is synthesized on the spot. The educts of SeCys synthesis are Ser and hydrogen selenide<sup>11</sup>. In the first step, seryl-tRNA synthetase attaches Ser to tRNA<sup>[Ser]Sec</sup>. Secondly, the serine's side chain -OH group is phosphorylated by O-phosphoseryl-tRNA<sup>Sec</sup> kinase and selenophosphate 2 synthetase yields dihydrogen selenophosphate from hydrogen selenide. Thirdly, the selenium is transferred onto the activated serine by O-phospho-L-seryl-tRNASEc:L-selenocysteinyl-tRNA synthase<sup>11,12</sup>.

So far 25 genes have been identified, that translate to 25 selenoproteins<sup>5</sup>. Among the most prominent classes of selenoproteins are glutathione peroxidases (GPx). The human GPx family consists of 8 members, GPx 1 to 8. Only GPx 1 to 4 and 6 are selenoproteins, while the others have a Cys in the catalytic center instead of a SeCys. All GPx are catalysts for the reduction of peroxides, using glutathione (GSH) as cofactor<sup>5</sup>.

GPx1 and GPx4 are both expressed ubiquitously in the human body and play a crucial role in maintaining redox homeostasis. GPx1 levels are highly correlated with oxidative stress and the selenium status and also play a special role in cancer prevention and progression. Acting as a major player in regulating intracellular levels of reactive oxygen species (ROS), GPx1 can protect DNA from alteration and cells in general from damage and death. However, GPx1 is a controversial factor when comparing different kinds of cancer. Its levels are found to be increased in lung cancer cells and renal cell carcinoma yet decreased in hepatic tumors and pancreatic cancer. For breast cancer cells, a lack of Gpx1 expression and declining GPx1 throughout the cancer progression was observed<sup>5,13–15</sup>.

GPx4 is the only member of the GPx family that reduces cholesterol and phospholipid peroxides. It is therefore a direct and main protector of cell membranes. GPx4 can also reduce cell damage and death caused by radiation<sup>16</sup>.

Thioredoxin reductase (TrxR) is a selenium enzyme, for which there are three mammalian isoforms. The cytosolic TrxR1, the mitochondrial TrxR2 and the TrxR3, which is primarily

expressed in the testes and also shortened TGR as it is a thioredoxin glutathione reductase. TrxR is a dithiol-disulfide reductase and works by reductively reactivating thioredoxin in the presence of NADPH and H<sup>+</sup>. The two ubiquitous isoforms are involved in multiple essential processes including reduction of H<sub>2</sub>O<sub>2</sub> and regulation of apoptosis, DNA synthesis, immunomodulation, protein repair mechanisms and protein disulfide reduction<sup>5,17</sup>. TrxR3 is most present in the testes and responsible for many reductive processes during the sperm maturation and quality control. Unlike for the other two isoforms, TrxR3 knockout mice are viable. They are not sterile, yet the impaired oxidoreductive homeostasis leads to decreased fertility. Contrary to the common assumption, TrxR3 is not testes-specific. It was shown in mice that TrxR3 is involved in antioxidant activity in the colon, and its overexpression has a positive impact on the death of colon cancer cells and control of ulcerative colitis<sup>5,18,19</sup>.

The family of iodothyronine deiodinases consists of three members, D1, D2 and D3, that are integral membrane proteins whose catalytic center is located intracellular. They are essential actors in thyroid gland homeostasis and the activation and inactivation of thyroid hormones. Thyroxine (T4) is activated by D1 and D2 to triiodothyronine (T3) through monodeiodination on the outer ring. D1 and D3 are responsible for the inactivation of T3 through monodeiodination on the inner ring and thus creating diiodothyronine (T2). T4 can also directly be inactivating by D1 and D3 in which case the removal of an iodine from the inner ring results in reverse triiodothyronine (rT3). D2's affinity to T4 is 1000-fold higher than D1's affinity which has a higher affinity to rT3. This fact, combined with the unique distribution of all three enzymes throughout the human body shows how selenoenzymes control the thyroid hormones and how a suboptimal selenium status can hinder the activation and inactivation of those hormones<sup>5,20,21</sup>.

## Selenium requirements and availability

Selenium is an essential trace element in the human diet. With careful consideration of reference values of various food organizations including German speaking D-A-CH organization and the World Health Organization and the Food and Agriculture organization

of the United Nations, the European Food Safety Authority (efsa) presented 70 µg/day as an adequate intake (AI) für adult men and women. The average selenium intake of newborns and infants is based on the average of breast milk intake which is estimated to be 0.8 l/day and an average selenium concentration in breast milk of 15 µg/l. It is therefore estimated to be 12 µg/day. Full efsa recommendations for the selenium AI is presented in table 1<sup>22</sup>.

*Table 1: Adequate intake for selenium for various age groups<sup>22</sup>.*

<b>Age</b>	<b>Adequate Intake (µg/day)</b>
7–11 months	15
1–3 years	15
4–6 years	20
7–10 years	35
11–14 years	55
15–17 years	70
≥ 18 years	70
Pregnancy	70
Lactation	85

Giving precise selenium intake recommendations is a challenging task, since selenium is a nutrient with a particular narrow therapeutic range and there is still an ongoing discussion about the ideal marker for selenium status. The expression and activity of many selenoproteins like GPx can be saturated at comparably low levels. Those are therefore able to give valuable information about a manifest deficiency but cannot be used to give satisfying statement on the exact status.

Some studies show a saturation of selenoprotein P at a daily intake between 100 and 150

µg/day<sup>23</sup>, others describe an optimal expression at a daily intake between 100 and 300 µg/day<sup>24</sup>. The most recent efsa publication on the matter describes a lowest-observed-adverse-effect-level (LOAEL) of 330 µg/day and therefore state and upper tolerable limit (UL) of 225 µg/day, based on an uncertainty factor of 1,3<sup>25</sup>. Selenium toxicity can be life threatening at blood levels of 300 µg/l and above<sup>26</sup>.

The estimated daily intake differs regionally, with an average daily intake of 30 µg or lower in countries such as Croatia, Egypt, Saudi Arabia and Slovenia and 100 µg and above in Canada, Japan, USA and Venezuela<sup>27</sup>. Germany is located in the lower midfield with an average daily intake of 35 µg of selenium.

Nevertheless, the selenium status of over 8000 German adults that were observed in a systematic review including 37 studies was found to be at a mean of 82 µg/l in plasma or serum<sup>28</sup>. The authors describe these selenium levels as satisfactory and further explain that the selenium intake in Germany cannot be sufficiently assessed and only estimates can be calculated based on food analysis.

The strong variation in both recommendations and actual intakes presumably correlates with the negligence towards the binding form of selenium in food. Usually, only the total amount of selenium in foods is given. Grains and animal-based products are the most common sources of selenium<sup>29</sup> Beef, bread, pork, chicken and eggs combined make up around 50 % of the total selenium in US diets<sup>30</sup>.

The most prominent form of selenium in food cannot clearly be stated but is estimated to be selenomethionine<sup>29</sup>. Its intestinal absorption takes place through amino acid transporters and results in resorption rates as high as 96 %. The absorption of selenite was described in different studies to be between 62 and 76 %, while absorption rates of 94 % are described for selenate. Participants in a study that were given servings of 100 g of selenium rich shrimp, were observed to resorb 83 % of the containing selenium in unspecified binding form. Unspecified selenium from food is shown to improve plasma selenium concentrations better than inorganic selenium, which was shown in a study, comparing selenite, selenium enriched

yeast, and selenium enriched wheat. Higher excretion rates are found for selenate, hinting that it passes the body faster and is therefore, despite its high absorption, not physiologically available for the body, while SeMet can be non-specifically incorporated into proteins and thus stored<sup>31</sup>. Since SeNP have not been described as naturally occurring forms of selenium in food before the results of the herein presented research was published, nothing is known about the share of nano selenium in total selenium in food.

## **Selenium deficiency and selenosis**

The variety of essential physiological functions selenium is involved in underlines the cruciality for public health to understand and recognize the signs, symptoms and causes of either excessive or insufficient selenium supply.

The high variability of selenium content is most prominently described for brazil nuts but can be observed in a multitude of foods and range sometimes as widely as 0,19 - 2,17 mg/kg in beef or 0,11 - 7,74 mg/kg of wheat flakes<sup>27</sup>. The concentrations range even wider for brazil nuts, where selenium contents between 1,61 and 153 mg/kg can be found<sup>32</sup>. These differences could theoretically cause both deficiency and selenosis without a change in diet and show the difficulties for an appropriate selenium intake.

A selenium deficiency can be defined by a plasma selenium concentration below the necessary value for optimal activity of iodothyronine deiodinase (< 64,8 ng/mL) or glutathione peroxidase 3 (< 86,9 ng/mL)<sup>33</sup>.

Many symptoms of selenium deficiency are unspecific. They include discoloration and dysfunction of skin and nails, and tiredness<sup>26</sup>.

The most prominent and most specific danger of selenium deficiency is the emergence of Keshan disease (KD). This illness can manifest itself in acute, subacute, chronic, or latent form. While the latter form can be easily overlooked and often shows no symptoms at all, the other three forms are serious and potentially fatal diseases. Acute KD can include acute heart

failure and acute pulmonary symptoms, cardiogenic fainting or cardiogenic shock and severe arrhythmia. The clinical manifestation of subacute KD is similar to the acute form, but with a less rapid onset. Slowly progressing chronic KD varies in its clinical ranges in the typical range of heart failure and cardiac insufficiency. Dilated heart chambers, cardiomyopathy and myocardial fibrosis can occur in different severity. Chronic KD can be the result of acute or subacute KD. KD is an endemic disease and the result of selenium deficient soil and therefrom selenium deficient food. It occurs in rural and poor areas, mostly in China, Korea and Japan<sup>34,35</sup>. In the recent past, the prevalence of KD was lowered. It can now be considered controlled and in some areas even eliminated<sup>36</sup>. A reduction of KD prevalence and selenium deficiency can be achieved by biofortification. Selenium enriched crops, for example *Allium* and *Brassica* species who are known as selenium accumulators can offer great amounts of selenium. The biofortification can be performed by foliar or soil application and leads to additional beneficial phytochemicals, including methylated forms of selenium, carotenoids, phenolic compounds and anthocyanins offering among others antioxidant and chemopreventive properties<sup>37-39</sup>.

Kashin-Beck disease (KBD) is another endemic disease that is connected to the same epidemiological factors and low Se eco-environment as KD. The osteochondral disease occurs in China, Russia, Siberia, North Korea, Tibet and Vietnam<sup>40,41</sup>. KBD leads to necrosis and deformation, growth retardation, and shortened limbs and fingers<sup>42</sup>.

Genetic causes for the illness were ruled out and environmental factors were found to be the reason for KBD, based on the observation that no more cases occurred in families who emigrated from the endemic areas and new ones occurred in families that immigrated to those areas. Selenium deficiency was discovered to be the main cause of KBD alongside T-2 mycotoxin. KBD prevalence is well under control through preventive matters, such as reduction of the exposure to the toxin and selenium biofortification of crops and can safely be assumed to be eradicated completely in the foreseeable future<sup>41,43,44</sup>.

Diseases that are caused by selenium deficiency are often observed alongside insufficient vitamin E status as well<sup>45,46</sup>.

Selenium deficiency can be caused by a poor selenium intake, insufficient selenium absorption or excessive oxidative stress, usually associated with chronic diseases that can lead to a depletion of antioxidative selenium species<sup>47</sup>. While selenium deficiency can occur in individual persons, mostly associated with either metabolic diseases or restrictive diets, it is a phenomenon that typically affects an entire community or population and is caused by low selenium levels in local soil and therefore local food<sup>46</sup>. Biofortification is therefore the most promising action to prevent selenium deficiency.

Excess of selenium is less common and usually appears only in randomized controlled trials (RCTs), that include high doses of selenium, in cases of drug or food supplement overdoses or fabrication errors and extreme diets, for example those including an unusually high amount of brazil nuts<sup>48</sup>. Selenosis can lead to death in severe cases. Apart from gastrointestinal symptoms including nausea, vomiting and diarrhea, patients with life threatening cases of selenium toxicity usually suffer from pulmonary and cardiac symptoms as well.

## **Selenium in plants – physiology and biochemistry**

Being arguably one of the most intriguing micronutrients, selenium can induce multiple beneficial effects in higher plants, without being an essential trace element. While many mammalian genes encode for selenoproteins, their corresponding plant homologues contain Cys instead of SeCys. Selenium is in many ways chemically similar to sulfur, forms equivalent inorganic compounds and amino acids. Correspondingly, selenium shares many physiological properties, pathways, and transporters with sulfur. Selenate and selenite are the most common forms of selenium in soils. More precisely, selenite is more common in anaerobic and acidic environments while selenate is more common in oxic and basic soils, which are also the typical conditions in agriculturally utilized areas. Selenite is absorbed into the root by phosphate transporters while sulphate transporters are responsible for the uptake of selenate<sup>49</sup>. It should be noted that foliar application of selenium in the form of selenate or selenite can strongly increase the selenium concentration in various plants as well<sup>50–52</sup>. The

amount of selenium uptake is mostly dependent on the concentration of selenium in the soil, however there are species-specific differences. Plant species can be divided into hyperaccumulators that reach selenium concentrations of >1000 mg/kg dry weight, secondary accumulators, and non-accumulators with 100-1000 or <100 mg/kg dry weight respectively. Selenium uptake is favored over sulfur uptake in hyperaccumulators and vice versa in non-accumulators<sup>53</sup>. For most angiosperms however, the Se/S ratio is similar and increased concentrations of selenium usually occur alongside of increase concentrations of sulfur<sup>54</sup>.

High concentrations of selenium in plant tissue can increase the expression of enzymes and transporters that play crucial roles in the sulfur metabolism and can thus increase sulfur absorption and utilization. Therefore sulfur dependent physiological processes including those connected to stress resistance and plants growth are enhanced, showing a possible way how selenium can benefit plants as a non-essential nutrient<sup>54</sup>.

Following its accumulation, selenite is mostly converted to organic compounds such as SeMet or SeCys following sulfur pathways<sup>54,55</sup>. Those are either unspecifically incorporated into proteins and thus might cause toxic effects, reduced to  $\text{Se}^0$ , or are metabolized to other compounds including Methyl-SeCys or  $\gamma$ -glutamyl-Se-methyl-SeCys. The methylation of SeCys is a crucial step to detoxify SeCys and therefore avoid its accidental incorporation into proteins, which is an important factor for selenium hyperaccumulation<sup>56</sup>.

Unlike selenite, selenate is transported through the symplast and xylem into the shoot of the plant. Selenate reaches the leaves via sulfur transporters and is mostly stored in the vacuole. Selenate can be reductively converted to selenite and then follow the same metabolic pathways.

Other selenium metabolites in plants include further analogues to sulfur compounds such as selenogluathione. Selenium can also be detoxified via the methylation of SeCys and SeMet to Methyl-SeCys and Methyl-SeMet and then further metabolism to Dimethylselenide (DMSe) and Dimethyldiselenide (DMDSe). Plants that are selenium hyperaccumulators mainly produce DMDSe and plants that are non-accumulator mainly release DMSe<sup>54,55</sup>.

SeCys can also be broken down into Ala and Se<sup>0</sup> in the same way that Cys is converted into Ala and S<sup>0</sup>. The NifS-like (nitrogen fixation sulfur) proteins that are responsible for this reaction are present in mitochondria, chloroplasts and the cytosol and are a key factor in the formation of Fe-S clusters<sup>57,58</sup>. The fact that SeCys can also be targeted by NifS-like proteins suggests that Se might also be falsely incorporated into Fe-S clusters. It definitely means that elemental selenium can be present in plants and overexpression of NifS-like proteins is associated with increased selenium tolerance and selenium hyperaccumulation<sup>59,60</sup>. It is not unreasonable to think about the possible formation of elemental insoluble selenium nanoparticles via this pathway.

## Nanoparticles

Nanotechnology is a multidisciplinary field that is based on the fundamentally different behavior of materials on a nanoscale compared to the macroscopic scale. This behavior derives from factors like surface area, shape and size<sup>61</sup>. The materials that are treated in the context of nanotechnology are nanomaterials or nanoparticles. Principles from physics, chemistry and biology are integral components of nanotechnology and nanomaterials can find applications across many domains including electronics, medicine, materials science and engineering. Nanoparticles are and were used in consumer products including medicinal products, foods, cosmetics and biocides before they were fully understood and scientifically defined. Therefore, different definitions arose and are used in various regulations concerning each individual group of products. These regulations help to ensure the safety of consumers products, but may pose problems due to uncertain definitions<sup>62</sup>. A universal definition of nanoparticles or nanomaterials that is applicable to all concerning industries and all the relevant regulations does not yet exist. A more scientific approach to define nanomaterial was proposed by Kreyling et al. who suggest a definition based on the volume specific surface area (VSSA)<sup>61</sup>. Based on the fact that one of the main aspects of nanoparticles is their notably high specific surface they suggest that materials with a VSSA  $\geq 60 \text{ m}^2/\text{cm}^3$  should be classified as nanomaterials.

The efsa published a statement that aims to offer guidance on the risk assessment of nanomaterials in food and feed chain and that refers to the Regulation (EU) No 2015/2283 on novel foods which states that: “engineered nanomaterial’ means any intentionally produced material that has one or more dimensions of the order of 100 nm or less or that is composed of discrete functional parts, either internally or at the surface, many of which have one or more dimensions of the order of 100 nm or less, including structures, agglomerates or aggregates, which may have a size above the order of 100 nm but retain properties that are characteristic of the nanoscale. Properties that are characteristic of the nanoscale include:

- (i) those related to the large specific surface area of the materials considered; and/or
- (ii) specific physico-chemical properties that are different from those of the non-nanoform of the same material”<sup>63,64</sup>.

The definition stated in the Regulation (EC) No 1223/2009 on cosmetic products offers some similarities and some differences: “nanomaterial’ means an insoluble or biopersistent and intentionally manufactured material with one or more external dimensions, or an internal structure, on the scale from 1 to 100 nm”<sup>65</sup>. It can firstly be stated that the size ranges of 1 to 100 nm are generally agreed on<sup>62</sup>. The EU regulation on food however does include larger particles in their definition as long as they show nano-specific features, hinting towards the desirability to find a definition that focuses on the function of nanomaterials rather than solely their size. This definition based on function bears regulatory and analytical challenges. The differences between different regulations and definitions and the combination of size and function-based factors shows, how these challenges are being partly avoided.

It is generally agreed upon that for a material to fall under the definition of nanomaterial it has to be intentionally produced leading to the question of whether naturally occurring particles with a size between 1 and 100 nm in one or more external dimensions can even be labeled nanoparticles. From a regulatory perspective it does not seem that way, however for the sake of readability particles in the nanoscale will be called nanoparticles throughout this dissertation.

There is also no reason to believe that naturally occurring nanoparticles should not show the specific features and behavior of manufactured nanomaterial. We know that different binding forms of a nutrient can behave differently in terms of resorption and function. SeNP have been shown to lead to completely different effects in adolescent rats compared to selenite<sup>66</sup>.

Furthermore, we should not neglect the possibility to intentionally manufacture nanoparticles using plants. This has been described for plant extracts<sup>67–70</sup>. Additionally, the presented results in this dissertation show evidence for the biosynthesis of SeNP in plants, which in theory could be utilized and upscaled to a dimension that might be considered intentional manufacturing.

While naturally occurring nanoparticles seem to not be covered by the existing regulations, it is highly desirable to evaluate their functions and specific effects, because it is not unlikely that their features and biochemical effects are as specific and as strong as those which are manufactured intentionally.

The imprecise definitions of nanoparticles in some respects, particularly those focused on regulatory aspects, may partly be attributed to the fact that the research articles featured in this work are among the first to mention the naturally occurring biosynthesis of nanoparticles in plants.

## Method development

The analysis was performed on a NexION350D by Perkin Elmer.

In the harsh conditions that create the plasma, Argon-dimer cations can be created. Given the relative abundance of the <sup>40</sup>Ar isotope of 99.6 % these dimers are most likely to create noise over the <sup>80</sup>Se signal, but the formation of <sup>38</sup>Ar-<sup>40</sup>Ar-dimer cations can also cause disturbance. The NexION350D was equipped with a universal cell to eliminate disturbances. By introducing hydrogen gas into the cell, using it as a dynamic reaction cell (DRC mode) the signal can be cleaned, as hydrogen molecules react with argon-dimer cations. In order to compare the detection capabilities of the <sup>78</sup>Se isotope with a relative abundance of 23.78 %

and the  $^{80}\text{Se}$  isotope with a relative abundance of 49.61 %, the first steps of method development were carried out simultaneously for both isotopes. For each analyte the appropriate flowrate of the reaction gas had to be examined individually. For the  $^{80}\text{Se}$  isotope a flowrate of 4.4 ml hydrogen per minute and for the  $^{78}\text{Se}$  isotope a flowrate of 2.8 ml hydrogen per minute was established.

The following parameters were used as starting conditions to compare the  $^{78}\text{Se}$  and the  $^{80}\text{Se}$  isotopes as sp-ICP-MS analytes:

- RF power	1450 W
- Plasma Ar flow rate	15 L/min
- Reaction cell flow rate for $^{78}\text{Se}$ ( $\text{H}_2$ )	2.8 mL/min
- Reaction cell flow rate for $^{80}\text{Se}$ ( $\text{H}_2$ )	4.4 mL/min
- Dwell time:	50 $\mu\text{s}$
- Measuring time:	60 s
- Deflector Attractor Voltage:	-135 V
- Deflector Entrance Lens:	-50 V

Some parameters were optimized daily in order to achieve the best possible results, by adapting to fluctuating environmental conditions. Due to these changes no values for these parameters are presented here. The changing parameters are:

- The torch alignment, which is a mechanical procedure, aiming to physically align the torch and therefore the ion stream with the cone interface to maximize the signal strength.
- The nebulizer flow rate, which represents the amount of argon gas per time that is used to disperse the sample to be introduced into the plasma.
- The QID voltages, that are responsible for redirecting the ion flow in a  $90^\circ$  angle into the second and third quadrupole.

Focusing on either isotope a 50 nm and a 100 nm SeNP standard were measured with

concentrations between 0.1, 0.2, 0.4 and 0.8 µg/l. Figures 1 to 16 show the results of this analysis.

<sup>80</sup>Se was shown to be a more suitable analyte for lower concentrated samples of the 50 nm standard. Not only more, but also a broader variety of nanoparticles sizes was detected than with respective <sup>78</sup>Se measurements. A similar observation was made for the 100 nm standard, however it appeared that these concentrations of 0.1 and 0.2 µg/l were generally too low for a proper size histogram of the 100 nm standard.

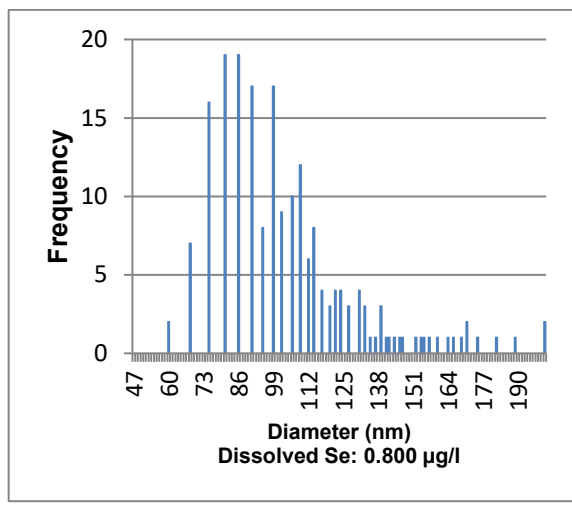


Figure 1: Size histogram of 50 nm SeNP standard (0.1 µg/l) based on the detection of  $^{78}\text{Se}$ .

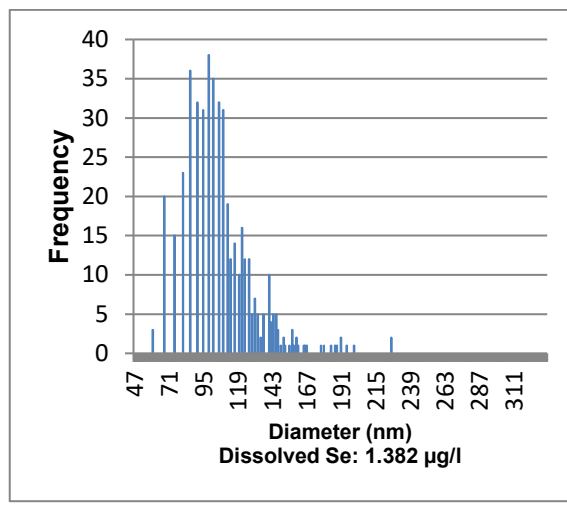


Figure 2: Size histogram of 50 nm SeNP standard (0.2 µg/l) based on the detection of  $^{78}\text{Se}$ .

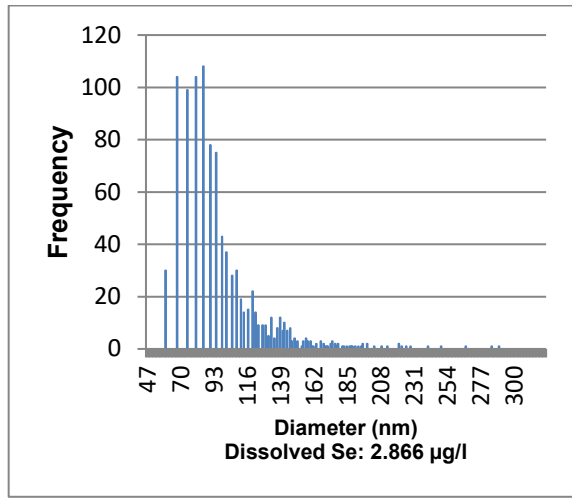


Figure 3: Size histogram of 50 nm SeNP standard (0.4 µg/l) based on the detection of  $^{78}\text{Se}$ .

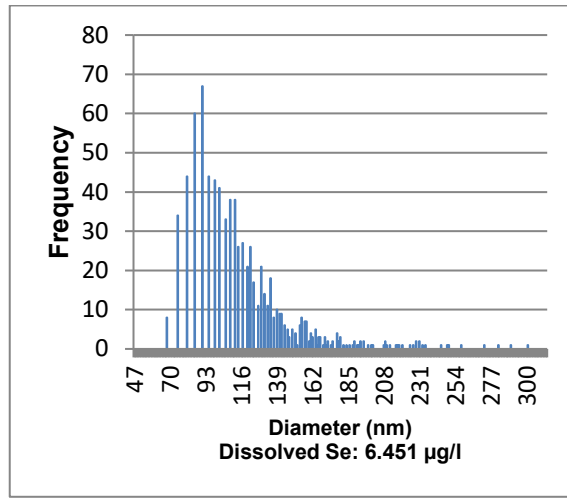


Figure 4: Size histogram of 50 nm SeNP standard (0.8 µg/l) based on the detection of  $^{78}\text{Se}$ .

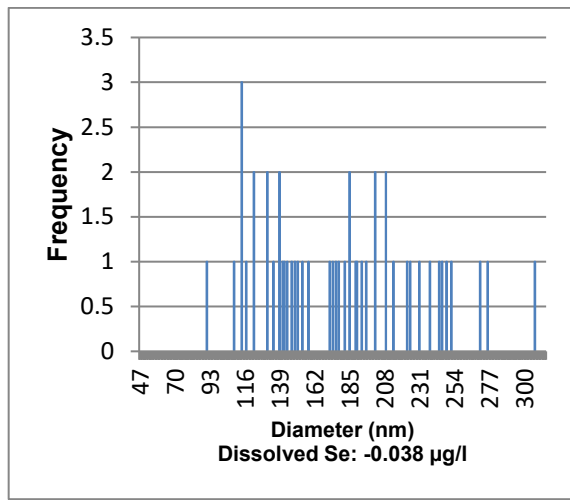


Figure 5: Size histogram of 100 nm SeNP standard (0.1 µg/l) based on the detection of  $^{78}\text{Se}$ .

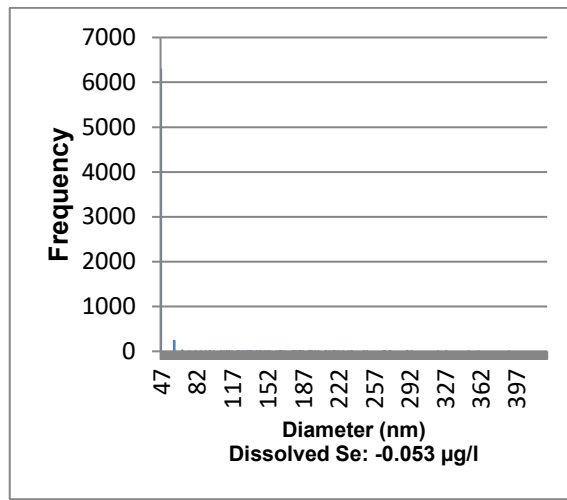


Figure 6: Size histogram of 100 nm SeNP standard (0.2 µg/l) based on the detection of  $^{78}\text{Se}$ .

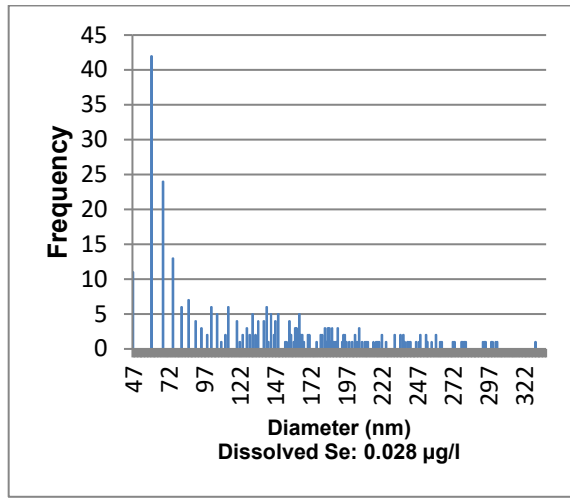


Figure 7: Size histogram of 100 nm SeNP standard (0.4 µg/l) based on the detection of  $^{78}\text{Se}$ .

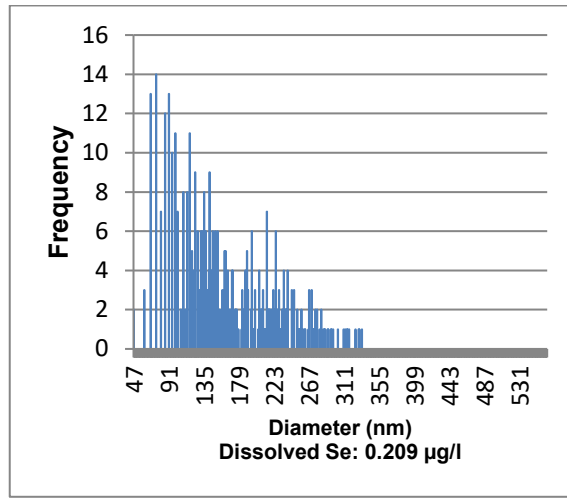


Figure 8: Size histogram of 100 nm SeNP standard (0.8 µg/l) based on the detection of  $^{78}\text{Se}$ .

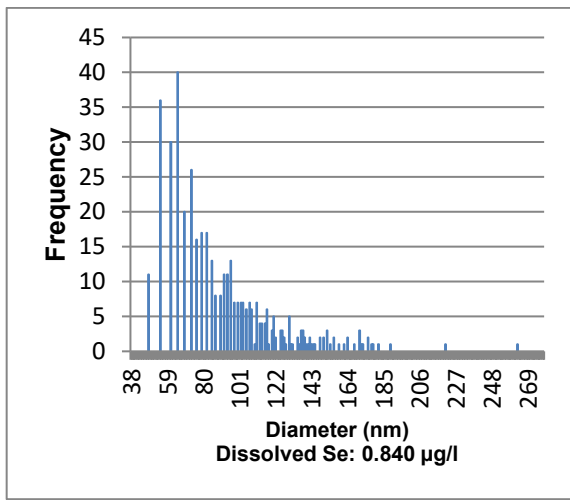


Figure 9: Size histogram of 50 nm SeNP standard (0.1 µg/l) based on the detection of  $^{80}\text{Se}$ .

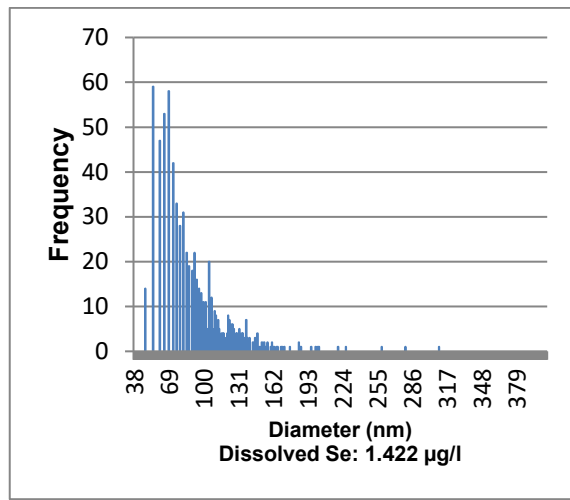


Figure 10: Size histogram of 50 nm SeNP standard (0.2 µg/l) based on the detection of  $^{80}\text{Se}$ .

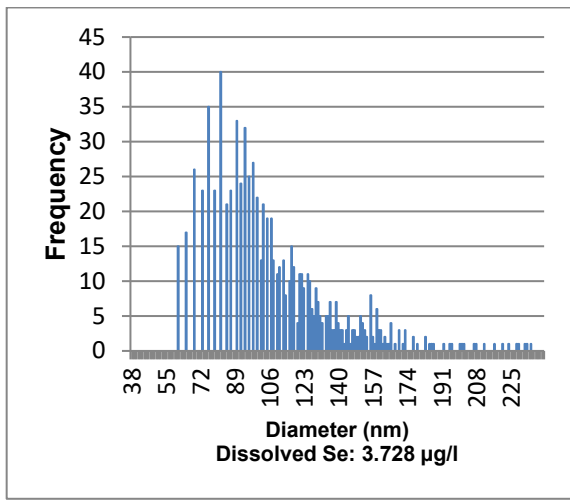


Figure 11: Size histogram of 50 nm SeNP standard (0.4 µg/l) based on the detection of  $^{80}\text{Se}$ .

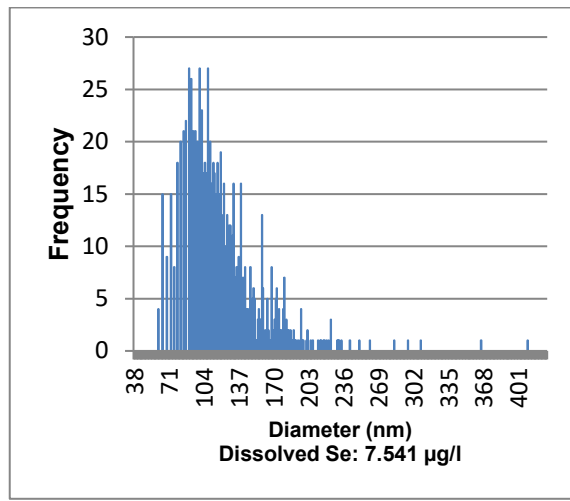


Figure 12: Size histogram of 50 nm SeNP standard (0.8 µg/l) based on the detection of  $^{80}\text{Se}$ .

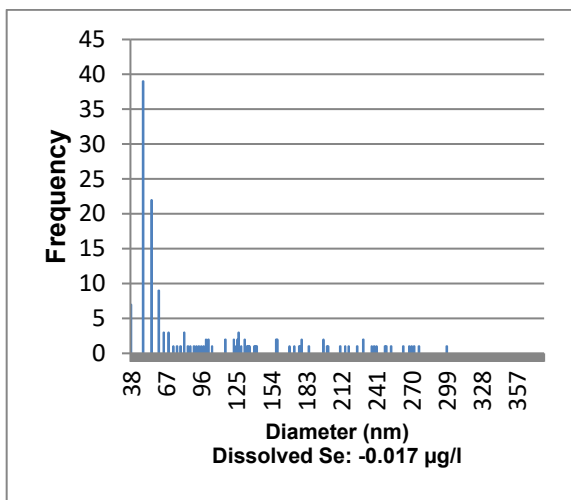


Figure 13: Size histogram of 100 nm SeNP standard (0.1 µg/l) based on the detection of  $^{80}\text{Se}$ .

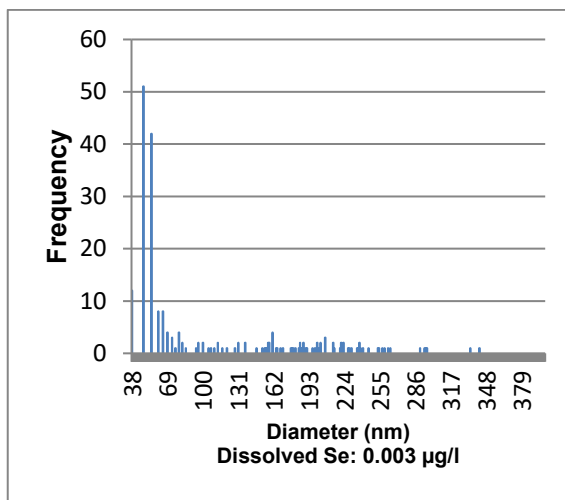


Figure 14: Size histogram of 100 nm SeNP standard (0.2 µg/l) based on the detection of  $^{80}\text{Se}$ .

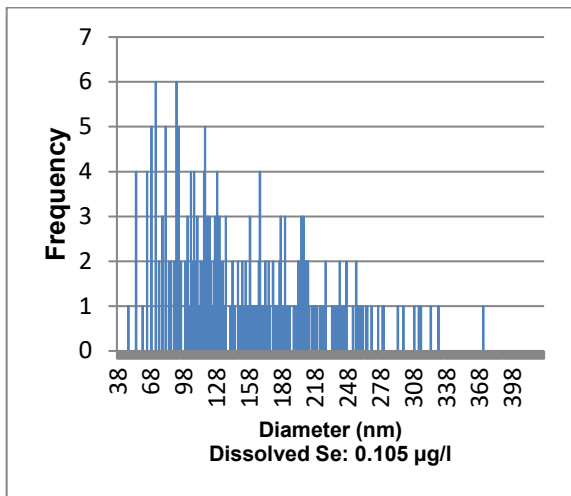


Figure 15: Size histogram of 100 nm SeNP standard (0.4 µg/l) based on the detection of  $^{80}\text{Se}$ .

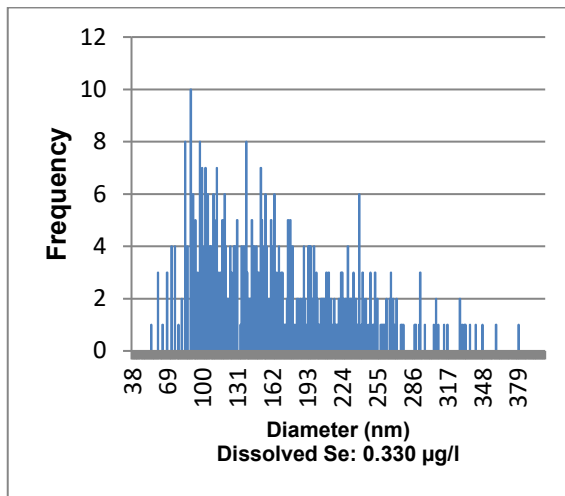


Figure 16: Size histogram of 100 nm SeNP standard (0.8 µg/l) based on the detection of  $^{80}\text{Se}$ .

## Investigation on the lower concentration limit

To further assess analytical performance on low concentrations, the SeNP standards were analyzed within the concentration range of 0.01 to 0.08 µg/l. Since both standards appeared to be near the detection limit, our objective was to observe and describe the transition in shape and size distribution of histograms.

This observation proved successful for all four arms of the examination as illustrated in figures

63 to 110 in appendix C. For both isotopes and both SeNP standards each subsequent higher concentration resulted in a more evenly distributed histogram, transitioning from an L-shaped to a bell-curve-shaped distribution. Alongside this transition, a moderate size shift was noted. As concentrations increased, both the mean and median size consistently grew, prompting questions about the precision of nanoparticle size measurement or the accuracy of labeled sizes in the standard solutions.

A direct comparison of both standards in a concentration of 0.08 µg/l revealed that the most frequently detected particle size in the 50 nm standard was 73 nm while in the 100 nm standard it was 62 nm. The results for <sup>80</sup>Se are closer to the labeled sizes, as the most frequent particle size detecting in the 50 nm standard is 57 nm and 63 nm for the 100 nm standard.

Two notable findings emerged from this series of measurements: first, a slight tendency toward the detection mode focusing on the <sup>80</sup>Se isotope and second, it must be noted, that the histograms created from 0.08 µg/l of SeNP 100 nm standard solution resembled the SeNP 50 nm standard solutions with a concentration of 0.04 µg/l in terms of general shape. This suggests that the concentration of 0.08 µg/l might be too low for the detection of a bell curve shaped histogram thereby masking the true average size of the nanoparticles in this sample. The overall shift in size distribution detected in samples with either very low or slightly higher concentration helps to gain insight into the evaluation of sp-ICP-MS results and assessing whether the analytes' concentration might be too low.

The histograms obtained with the 50 nm SeNP standard and the <sup>80</sup>Se detection mode exhibited the highest quality among the four arms of the analysis in terms of shape and distribution (figures 17 to 20). Both the standard and the method proved to be particularly suitable for future analyses.

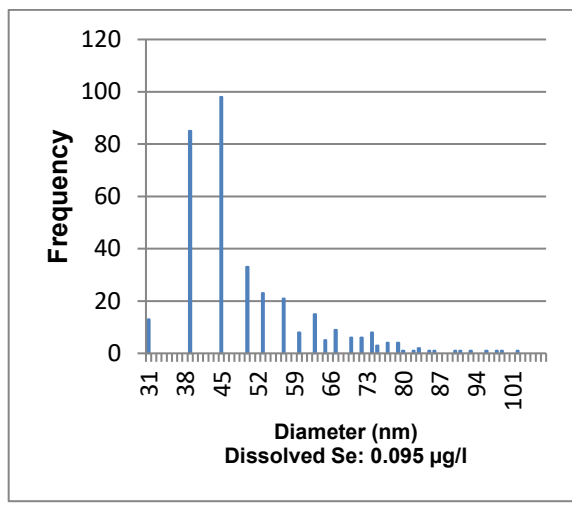


Figure 17: Size histogram of 50 nm SeNP standard (0.01 µg/l) based on the detection of  $^{80}\text{Se}$ .

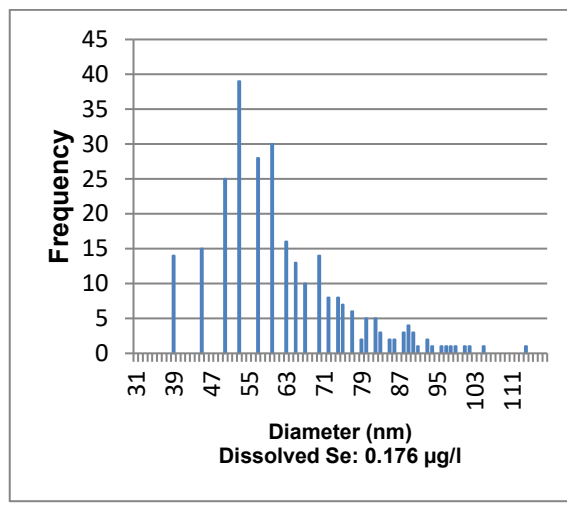


Figure 18: Size histogram of 50 nm SeNP standard (0.02 µg/l) based on the detection of  $^{80}\text{Se}$ .

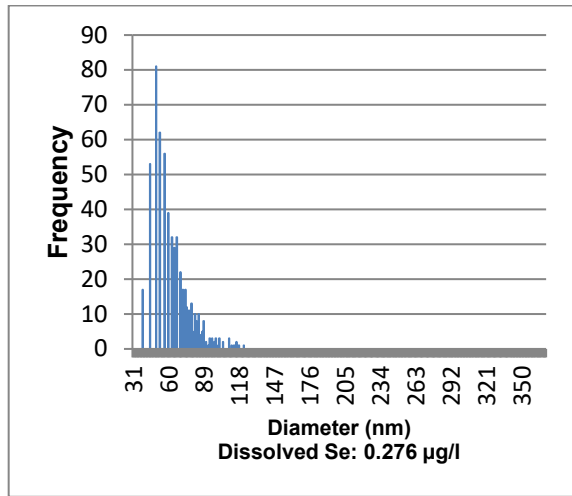


Figure 19: Size histogram of 50 nm SeNP standard (0.04 µg/l) based on the detection of  $^{80}\text{Se}$ .

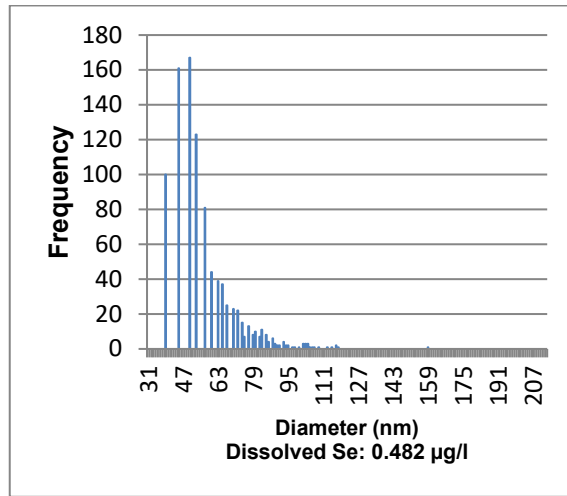


Figure 20: Size histogram of 50 nm SeNP standard (0.08 µg/l) based on the detection of  $^{80}\text{Se}$ .

## Repeatability

To comprehensively assess the performance of NexION 350D with low concentration SeNP solutions and variations across multiple analytical runs with the same sample, both nanoparticles standards were subjected to repeated measurements on both the  $^{78}\text{Se}$  and the  $^{80}\text{Se}$  isotope with concentrations of 0.01 and 0.1 µg/l.

The repeatability of results (shown in figures 111 to 134 in appendix C) demonstrated

excellent consistency and high similarity in repeated runs of the same sample. However, certain borderline cases posed challenges where the system struggled to distinctly differentiate between dissolved selenium and nano selenium. In contrast to the minor deviations in most samples, these borderline cases could lead to the detection of a notable number of nanoparticles or almost none at all.

This issue was observed similarly for both isotopes and is characteristic of either very low concentrations of total selenium content or very high concentrations of dissolved selenium. In such cases, the actual presence of nanoparticles may have been obscured or resulted in false-positive outcomes.

Figures 21 to 26 exhibit excellent repeatability, indicating that when the selenium concentration is not near the detection limit, the previously discussed problem does not occur and is concentration dependent. The amount, size, and distribution of detected SeNP varied only slightly.

A notable difference between the two isotopes was not apparent in this context. However, considering that a given concentration in  $\mu\text{g/l}$  translates to different concentration in particles per ml it becomes more evident, that the SeNP 100 nm standard must be analyzed at a higher concentration to contain a suitable amount of SeNP.

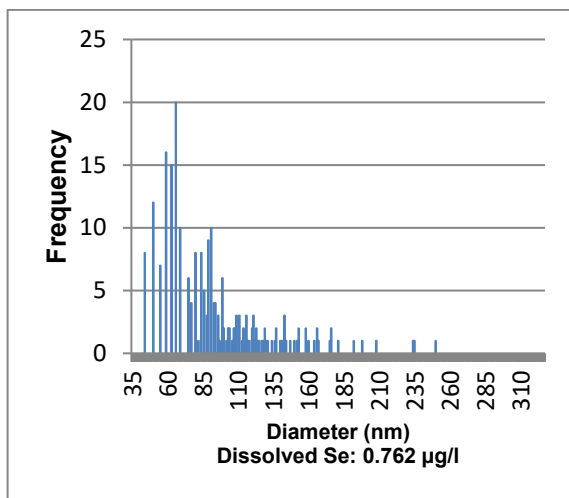


Figure 21: Size histogram of 50 nm SeNP standard (0.1 µg/l) based on the detection of  $^{80}\text{Se}$ . Run 1

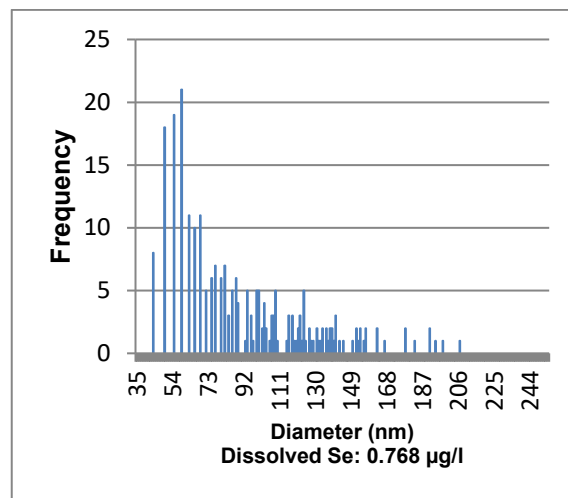


Figure 22: Size histogram of 50 nm SeNP standard (0.1 µg/l) based on the detection of  $^{80}\text{Se}$ . Run 2

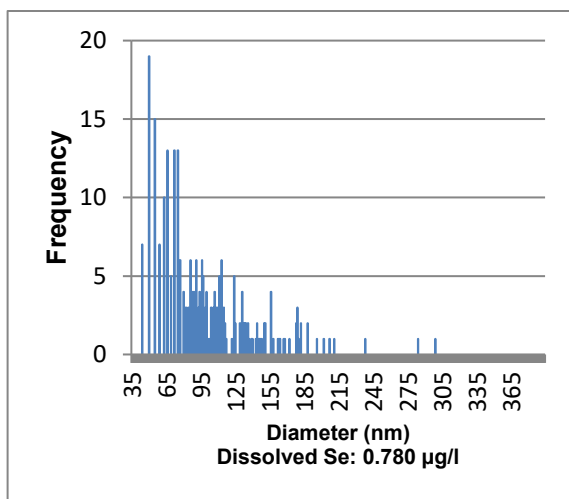


Figure 23: Size histogram of 50 nm SeNP standard (0.1 µg/l) based on the detection of  $^{80}\text{Se}$ . Run 3

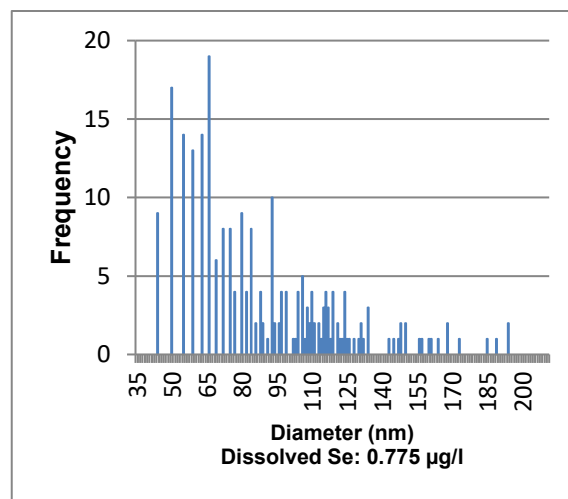


Figure 24: Size histogram of 50 nm SeNP standard (0.1 µg/l) based on the detection of  $^{80}\text{Se}$ . Run 4

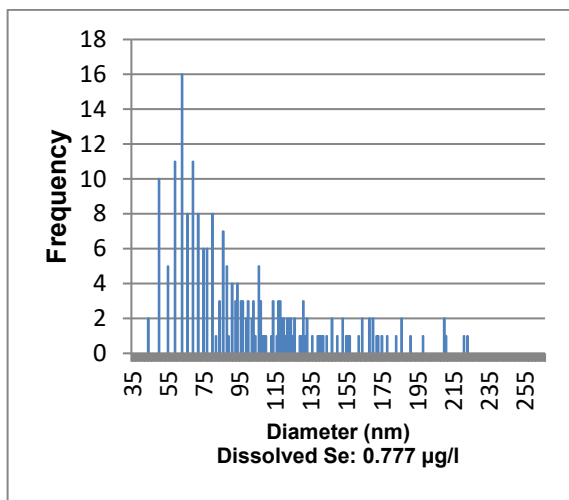


Figure 25: Size histogram of 50 nm SeNP standard ( $0.1 \mu\text{g/l}$ ) based on the detection of  $^{80}\text{Se}$ . Run 5

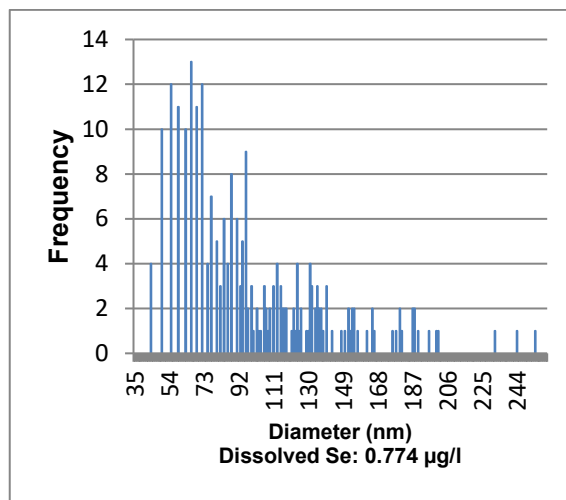


Figure 26: Size histogram of 50 nm SeNP standard ( $0.1 \mu\text{g/l}$ ) based on the detection of  $^{80}\text{Se}$ . Run 6

## Comparison between the $^{78}\text{Se}$ and the $^{80}\text{Se}$ isotope

The method development undertaken to this point leaned towards favoring the  $^{80}\text{Se}$  isotope instead of the  $^{78}\text{Se}$  isotope. In addition to the earlier findings, a comparison was made of calibrations of the system under nearly identical conditions, differing only in the mass filter's isotope setting. The results for this comparison are shown in figure 27. The coefficient of determination was satisfactory for both isotopes:  $R^2 = 0.99990$  for  $^{80}\text{Se}$ ,  $R^2 = 0.99998$  for  $^{78}\text{Se}$ . The decisive difference was found in the slope. With 0.1866 counts per  $\mu\text{g/l}$  the slope of the graph was notably higher for  $^{80}\text{Se}$  than 0.1263 count per  $\mu\text{g/l}$  for  $^{78}\text{Se}$ . A higher slope suggests better accuracy and sensitivity in the analytical method. As a result, we decided to proceed with all future analyses focusing on the  $^{80}\text{Se}$  isotope.

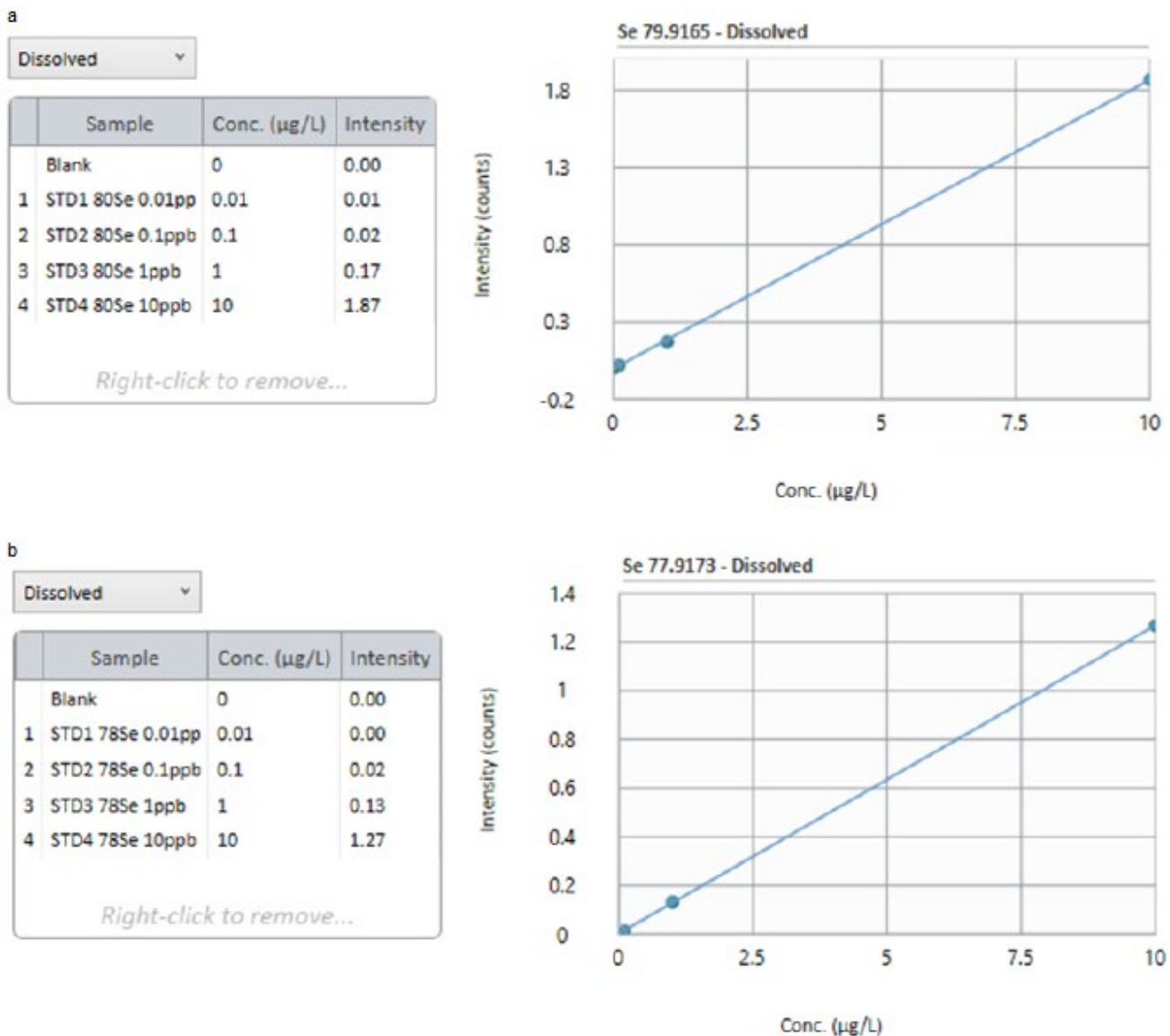


Figure 27: Comparison of ICP-MS calibration of  $^{80}\text{Se}$  (a) with  $^{78}\text{Se}$  (b).

## Inspection of the possibility of particle aggregation

To evaluate the possibility of SeNP cohesion and aggregation and consequently, the risk of misinterpreting multiple particles as a single entity and thus overestimating particle sizes, identical samples of both 50 and 100 nm nano standard solutions were compared, either after sonication for 1 minute or direct measurement.

The initial interpretation of these measurements might seem ambiguous. For the 0.02 µg/l samples of the SeNP 50nm standard, almost identical patterns of particle size distribution were observed with the only discernible difference being a slight decrease in the overall particle frequency for the sonicated samples. Conversely, for the 0.2 µg/l samples the opposite trend was observed, with an increased number of particles in the sonicated samples. However, such variations fall within the typical ranges of sp-ICP-MS. With more advanced technologies and complex mathematical procedures a variation in this magnitude is to be expected and must not be overestimated. The samples with a 0.08 µg/l concentration of the 50 nm standard are shown exemplary in figures 28 to 33. The histograms for the full series of measurements are shown in figures 135 to 170 in appendix C.

This observation extends to the measurements of the 100 nm samples. While some inconsistencies were noted, particularly regarding the histogram shapes discussed earlier, the irregularities do not appear to be influenced by the sonication, as they manifest similarly in both sonicated and non-sonicated samples.

Based on these findings, it can be asserted that SeNP aggregation does not occur in a notable manner. Consequently, the available standards were deemed suitable and continued to be employed for further method development.

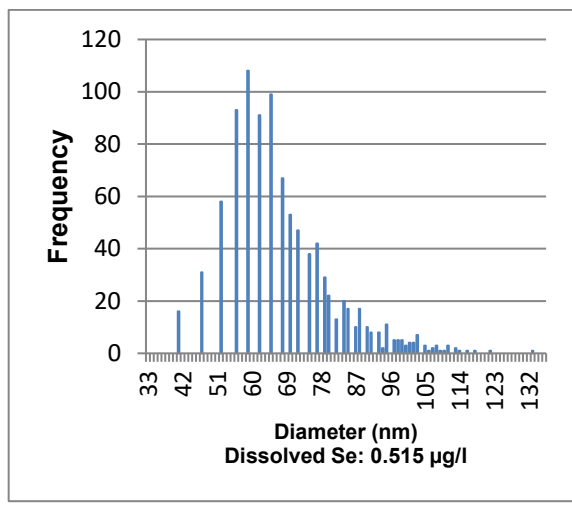


Figure 28: Size histogram of 50 nm SeNP standard (0.08 µg/l), not sonicated. Run 1

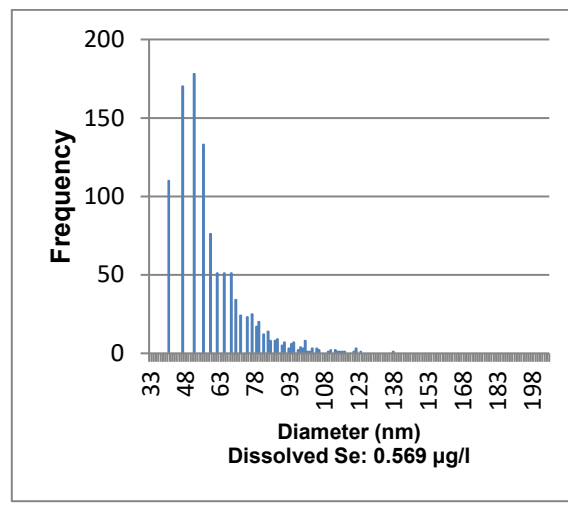


Figure 29: Size histogram of 50 nm SeNP standard (0.08 µg/l), not sonicated. Run 2

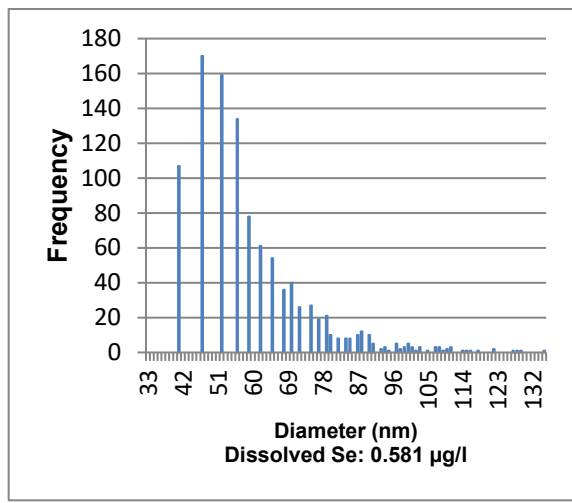


Figure 30: Size histogram of 50 nm SeNP standard (0.08 µg/l), not sonicated. Run 3

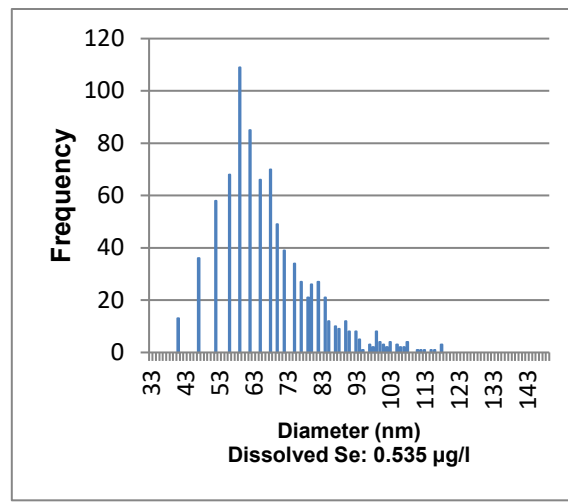


Figure 31: Size histogram of 50 nm SeNP standard (0.08 µg/l), sonicated. Run 1

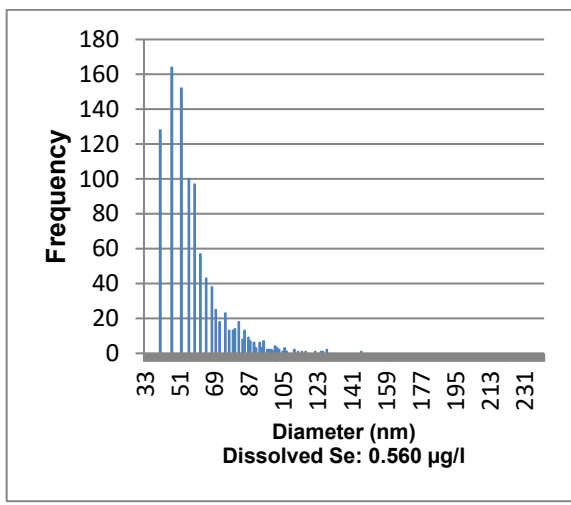


Figure 32: Size histogram of 50 nm SeNP standard (0.08 µg/l), sonicated. Run 2

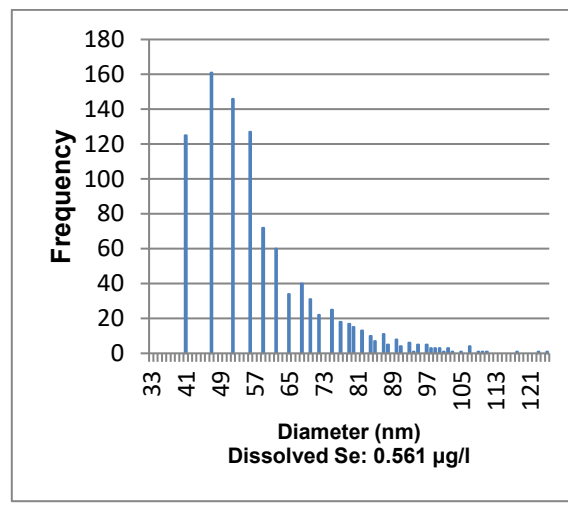


Figure 33: Size histogram of 50 nm SeNP standard (0.08 µg/l), sonicated. Run 3

## Improvement of the daily optimized parameters

Some of the measuring conditions need to be optimized daily for sp-ICP-MS measurements. These conditions include the torch alignment, the nebulizer gas flow and the QID voltages. For most common approaches this is performed using Perkin Elmer's "Setup Solution", a standard solution that contains a variety of analytes covering a broad variety of masses and properties to ensure a consistent quality across the spectrum. While certain adjustments may enhance signal strength for specific analytes, they also carry the risk of creating divalent ions or oxides.

In the context of the nano application in Syngistix software, the optimization can take a different approach, as there is only one aim, to achieve the highest possible signal strength for the isotope of interest.

Therefore, our aim was to establish a set of conditions most suitable for the detection of selenium nanoparticles. Given that sp-ICP-MS is a very new technique especially in its applications to SeNP analysis, it is not well established yet. To our knowledge, this research project represents the first ever analysis of SeNP using an ICP-MS by Perkin Elmer.

To create conditions optimal for the analysis of selenium and SeNP, a solution of sodium selenite (1 µg/l) was prepared, and the daily parameters optimization was performed using  $^{80}\text{Se}$  as the sole analyte.

For each given concentration both the 50 nm and the 100 nm standards resulted in improved histograms. Even the 100 nm standard at a concentration of 0.02 µg/l, which was previously considered too strongly diluted, produced a well distributed histogram. While the torch alignment is hardly different in default and nano conditions, both the QID voltages and the nebulizer gas flow were increased during the development of nano conditions.

Subsequently, the newly implemented measuring conditions were evaluated across a broader range of concentrations. As figures 34 to 37 show, the newly implemented conditions generally performed well in terms of particle distribution and repeatability. Moreover, in size histogram of samples with low concentrations, strong results were obtained.

In comparison to the 50 nm standard, the 100 nm samples yielded less reliable outcomes. Its broader distribution on the one hand and the mean particle size being far smaller than the assigned size on the other hand led to the decision to continue the method development with a focus on the 50 nm standard, which appeared to exhibit higher quality. A full overview of this series of measurements is shown in figures 171 to 194 in appendix C.

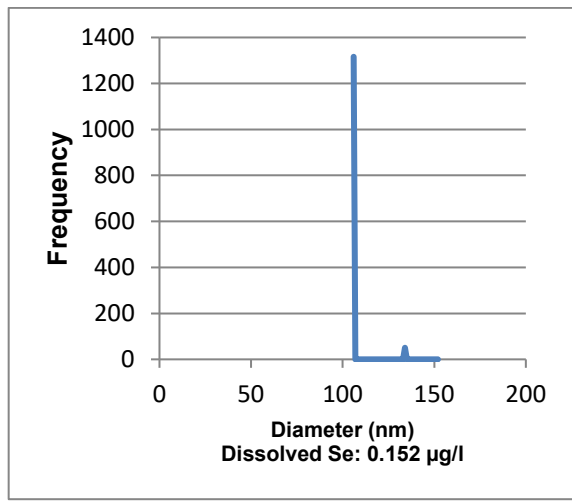


Figure 34: Size histogram of 50 nm SeNP standard (0.02 µg/l) default conditions. Run 1

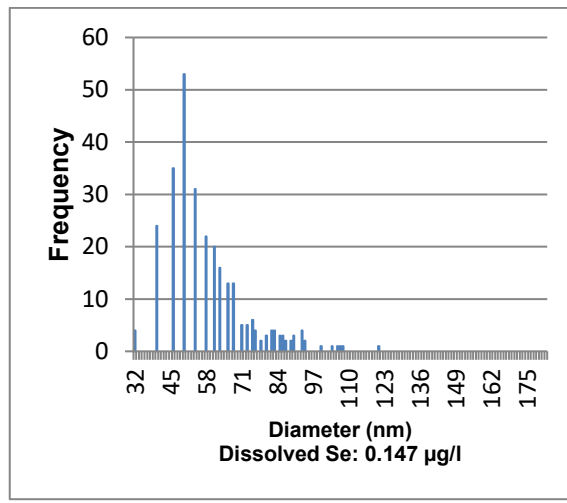


Figure 35: Size histogram of 50 nm SeNP standard (0.02 µg/l) nano conditions. Run 1

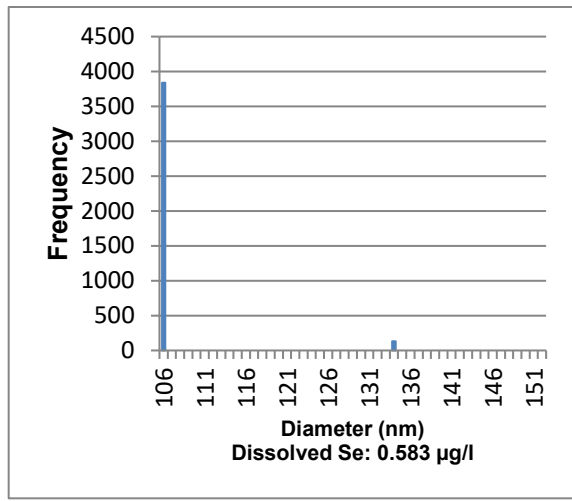


Figure 36: Size histogram of 50 nm SeNP standard (0.08 µg/l) default conditions. Run 1

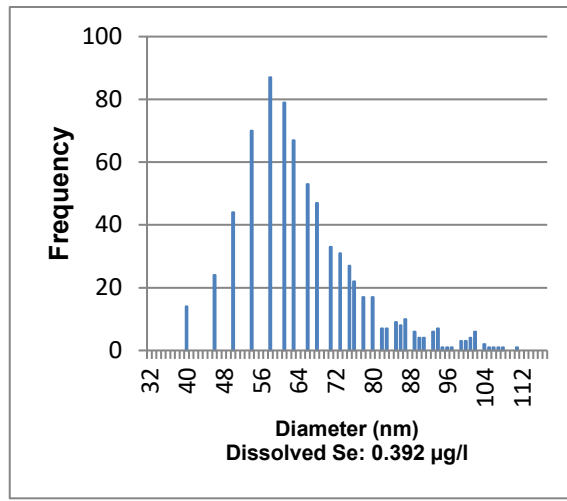


Figure 37: Size histogram of 50 nm SeNP standard (0.08 µg/l) nano conditions. Run 1

## Measuring time optimization

With a dwell time of 50 µs and a measuring time of 60 s every measurement comprises of 1.2 million data points, representing either a nanoparticle or background noise, due to dissolved selenium. Doubling or halving the measuring time accordingly doubles or halves the amount of data points. Increasing the amount of data points served two beneficial

purposes. Firstly, a larger sample was measured, resulting in a more representative outcome, as twice as many nanoparticles should be detected. Secondly, assuming an unchanged actual variation within a population, the measured standard deviation decreases with a higher sample size. Since the detection of a nanoparticle is achieved mathematically by identifying it as an outlier from the deviation of noise created by dissolved selenium, an increased measuring time, which lowers the standard deviation of noise, should facilitate the identification and detection of even smaller particles.

A marker for noise is the threshold defining the number of counts that must be detected in the time window of one dwell time for the system to declare its source as a nanoparticle. To evaluate the relationship between measuring time and threshold, identical samples of various concentration were measured with a measuring time of 30, 60 and 120 s. Samples with a manually defined threshold were measured as comparison. Figures 195 to 254 in appendix C display the results of the measuring time optimization.

The most obvious observation was that a threshold that is too low can lead to a strong overestimation of the containing SeNP. Especially for low concentrations an increased measuring time markedly improved the results. Both the steps from 30 to 60 and from 60 to 120 s resulted in a greater number of detected particles leading to more evenly distributed histograms. It is crucial to take both the measured dissolved selenium and the calculated threshold into account. The impact the measuring time can have on the quality of the analysis is highlighted in figures 38 to 40.

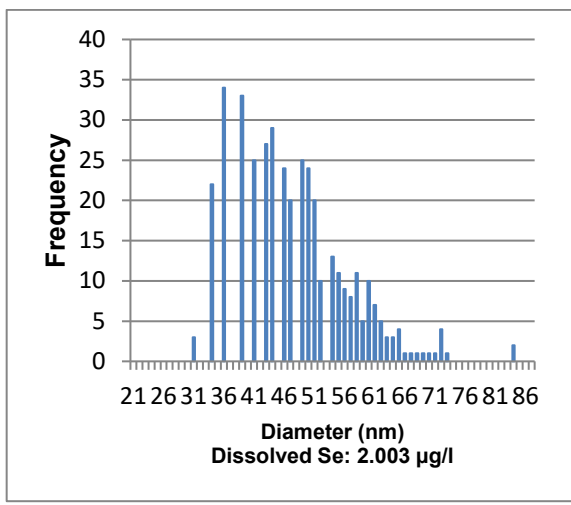


Figure 38: Size histogram of 50 nm SeNP standard (0.5 µg/l)  
30 s Measuring Time. Run 1. Automatic Threshold: 2.41

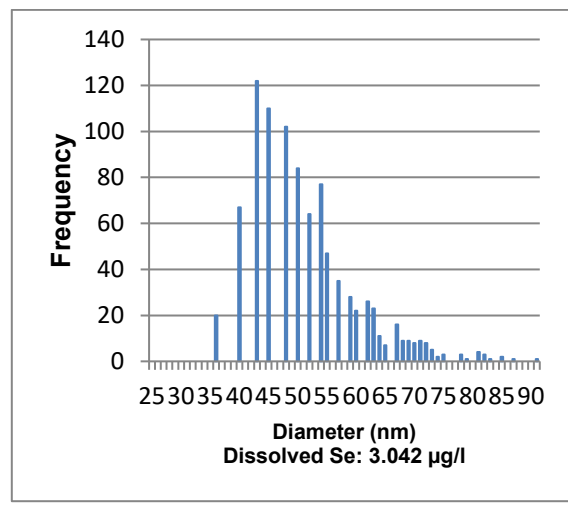


Figure 39: Size histogram of 50 nm SeNP standard (0.5 µg/l)  
60 s Measuring Time. Run 1. Automatic Threshold: 2.33

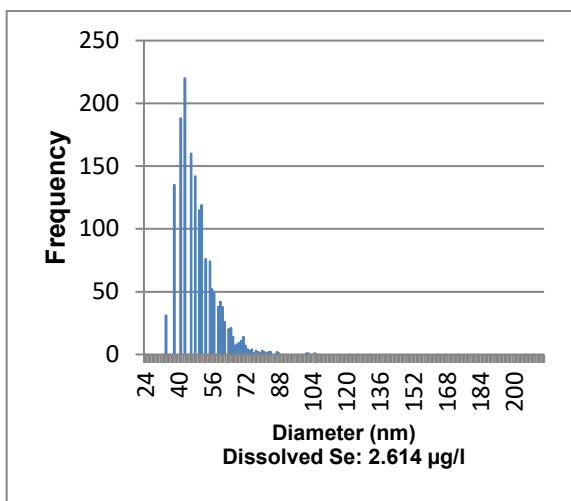


Figure 40: Size histogram of 50 nm SeNP standard (0.5 µg/l)  
120 s Measuring Time. Run 1. Automatic Threshold: 2.31

## Plant treatment

To explore the potential biosynthesis of SeNP in plants it is imperative to analyze plants that have never been exposed to SeNP. Consequently, we opted to cultivate plants under controlled conditions using hydroponics. Working with a hydroponic system facilitates precise control over the environment and influences the growing plants are objected to<sup>71</sup>. A nutritional solution can be selected based on the individual aims of the research project. Quarter

strength Hoagland solution (HS) was used as a basis. The dilution of HS to quarter strength can prevent adverse osmotic effects and was proven to yield satisfactory growth in hydroponic applications<sup>72,73</sup>. HS does not contain any selenium. The solution was therefore spiked with sodium selenite to achieve a concentration of 5 mg/l, equivalent to a selenium concentration of 28.91 µmol/l.

Lighting was provided by two neon tubes with a color temperature of 6500 K and a power of 55 W placed within a reflector approximately 30 cm above the plants. The day was divided into a lighted period of 16 hours and an 8-hour period with no artificial illumination. At 6 a.m. and 10 p.m. the lights were turned on or off respectively.

In the beginning of every growth cycle the hydroponic system was prepared with a fresh batch of growth solution. The Terra Aquatica GrowStream that we used was run on a volume of 40 l of growth solution. During the growth period the loss of water due to evaporation and consumption by the plants was offset every other day maintaining a constant water level. Importantly, no additional minerals or selenium were introduced with this compensation, but only deionized (DI) water was added.

The initial step in every growth cycle involved the surface sterilization of the seeds. This was done to prevent growth of mold, algae, or any other unwanted growth within the hydroponic system. The seeds were sterilized in a 10 % formalin solution for 10 minutes and thoroughly rinsed with DI water afterwards. The seeds were then soaked in DI water for 10 minutes and subsequently transferred onto a piece of filter paper that was kept moist. Under exclusion of light the seeds were allowed to sprout. Once the seedlings reached an adequate size, they were transferred to the hydroponic system.

The growth period in the hydroponic system varied for the different plant species. A time between 4 and 8 weeks was needed for the plants to grow sufficiently and to form well developed shoot and roots. The growth of selected plants will be described later in detail. Upon harvesting, root and shoot were separated to be analyzed individually and the root crown was removed and discarded to prevent intermixing. Both parts of the plants were rinsed

thoroughly with DI water. To ensure that any detected SeNP in the root sample resulted from nanoparticle synthesis by the plants, an extensive cleansing process was implemented. A pH 6 citrate buffer solution (0.1 M) was prepared using disodium hydrogen citrate and citric acid. The roots were cut roughly and transferred to the buffer solution where they were stirred for 48 hours. After that period, the root samples were rinsed again with DI water. This procedure aimed to avoid false positive results that could potentially be caused by root exudates or microbial SeNP synthesis.

Roots and shoots were cut finely with a razorblade and 100 mg samples were taken. 8.0 ml of citrate buffer were added to the samples, and subsequently they were homogenized for 2 minutes with a Qiagen TissueRuptor II. The suspensions were spiked with 2 ml of a solution of Macerozyme R-10 (50 mg/ml) and 50 µl of Proteinase K (20 mg/ml) and shaken for 24 hours at a temperature of 37 °C. Macerozyme was used to digest cell walls and release the cells' content and Proteinase K was added to digest the contained proteins in order to facilitate the following dialysis.

0.500 ml supernatant of the digestion were mixed with 0.500 ml of ethanol absolute and diluted to 5.0 ml with citrate buffer. That mixture was introduced into a dialysis tubing with a Molecular Weigh Cut-Off (MWCO) of 3.5 kDa. The MWCO was chosen to ensure that protein debris was able to penetrate the membrane while retaining NP. The dialysis tubing was closed and stirred for 24 hours in 500 ml of citrate buffer. After dialysis the samples were diluted appropriately and analyzed with the newly developed sp-ICP-MS method.

The plants exhibited healthy growth with no signs of discoloration or abnormalities. This study observed 16 different plant species, 15 of those were grown under the described conditions, with the only exception being Brazil nuts (*Bertholletia excelsa*). Since time and effort would have been far beyond the scope of this work to grow those, the nuts were bought at local grocery stores, because the role of brazil nuts as a source of plant-based selenium is too notable to be dismissed in this study.

The other species that were observed are brown mustard (*Brassica juncea*), barley (*Hordeum*

*vulgare*), flax (*Linum usitatissimum*), lentil (*Lens culinaris*), bell pepper (*capsicum annuum*), butter lettuce (*Lactuca sativa*), carrot (*Daucus carota subsp. sativus*), cucumber (*Cucumis sativus*), basil (*Ocimum basilicum*), dill (*Anethum graveolens*), chard (*Beta vulgaris*), spinach (*Spinacia oleracea*), brussels sprouts (*Brassica oleracea var. gemmifera*), broccoli (*Brassica oleracea var. italica*), and lamb's lettuce (*Valerianella locusta*). In the following the growth process of three plants will be exemplarily presented more thoroughly.

The carrot seeds were let to germinate for a week and transferred to the hydroponic system on day 8 as shown in figure 41. The cotyledons had not fully emerged from the seed and to do so they took longer than those of the other plant species. The growth state on days 17 and 23 is shown in figures 42 and 43. In these few days the carrot plants grew beyond their cotyledons and developed a more mature shoot. Feathery secondary leaves began to form in a characteristic pinnately compound arrangement. The shoots branched out in the following days as depicted in figures 44 and 45. The branching out of the carrot plants took place at the root crown which is typically at or just above the soil surface. Though there is no soil in a hydroponic system, this region still marks the transitional region between root and shoot systems. Leaflets in the crown regions that stabilize the shoots and foliage started to show. Figure 45 shows a carrot plant on day 46 of its growth, which was the final day of the growth period. On this day the plants were removed from the hydroponic system and prepared for the analysis in the earlier described manner. Figure 46 also shows the roots of the newly harvested plant.



Figure 41: Carrot seedling on day 8.



Figure 42: Carrot seedling on day 17.



Figure 43: Carrot plant on day 23.



Figure 44: Carrot plant on day 36.



Figure 45: Carrot plant on day 46.



Figure 46: Harvested carrot plant on day 46.

The cucumber seeds were let to germinate for a few days and transferred to the hydroponic system on day 5 when seedlings had been formed. The cotyledons were fully unfurled on day 14 as shown in figure 47. Initial leaves began to spread right after and leave expression became more pronounced as shown in figures 48 and 49. Elongation of the stem and general increase in height took place. Up to day 48 as shown in figures 50 to 52 the foliage became denser. Lateral shoots began to show between the days 38 and 48 leading to a more complex structure in each plant's branching pattern. During the last days of the growth cycle the first flower buds became noticeable, which can be seen in figures 51 and 52. The plants were harvested on day 48. In figures 53 and 54 a cucumber plant is shown in full size including the

root system.



Figure 47: Cucumber plant on day 14.



Figure 48: Cucumber plant on day 23.



Figure 49: Cucumber plant on day 31.



Figure 50: Cucumber plant on day 38.

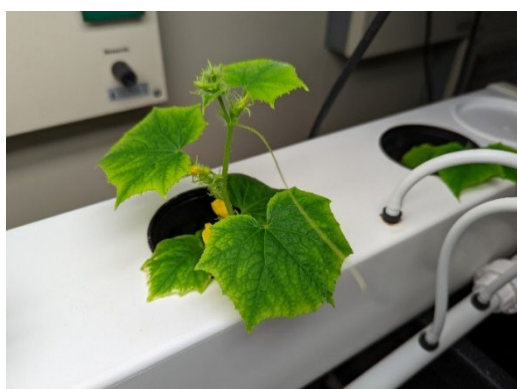


Figure 51: Cucumber plant on day: 48.



Figure 52: Cucumber plant on day 48.



Figure 53: Harvested Cucumber plant on day 48.



Figure 54: Harvested Cucumber plant on day 48.

Germination took place quickly for brown mustard seeds as shown in figure 55. Figure 56 shows 5-day old seedlings with cotyledons and an early stages root. On this day, the seedlings were transferred into the hydroponic system as shown in figure 57. Few days later, the cotyledons had transformed into a pair of characteristic heart-shaped leaves as depicted in figure 58. The cotyledons continued to increase in width while the stem elongated. Figure 59 also shows pinnately lobed leaves that started to develop between the days 8 and 15. As the stem elongation continued by day 23 the alternate phyllotaxis became more noticeable as shown in figure 60. The expansion of foliage continued in the following days and happened alongside a division of the stem into secondary branches. Figure 61 shows that this division into branches marked a period of brown mustard growth in which elongation of the stem and spread in width took place equally. The plants were harvested on day 30. Figure 62 shows a close-up of the root system.

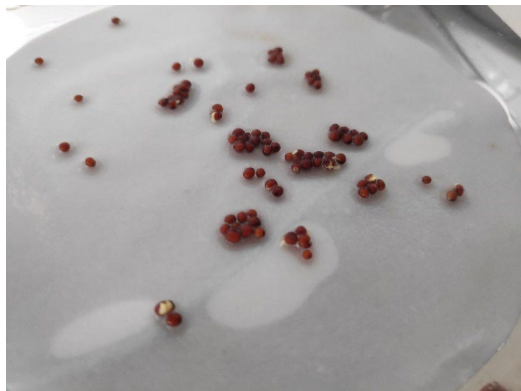


Figure 55: Brown mustard seeds on day 3.



Figure 56: Sprouted brown mustard seeds on day 5.



Figure 57: Sprouted brown mustard seed on day 5.



Figure 58: Brown mustard plant on day 8.



Figure 59: Brown mustard plant on day 15.



Figure 60: Brown mustard plant on day 23.



Figure 61: Brown mustard plant on day 30.



Figure 62: Brown mustard roots after harvesting on day 30.

## Biosynthesis of nano selenium in plants

Jonas Versteegen<sup>1,2</sup>, Klaus Günther<sup>1,3</sup>

<sup>1</sup> University of Bonn, Institute of Nutritional and Food Sciences, Germany.

<sup>2</sup> Federal Institute for Drugs and Medical Devices, Bonn, Germany.

<sup>3</sup> Research Centre Juelich, Institute of Bio- and Geosciences, IBG-2, Plant Sciences. Germany.

*Artificial cells, nanomedicine, and biotechnology.* **2023**, 51, pp. 13–21

This publication is listed in appendix A.

### Contribution

I contributed to the design of the experiments. I performed the method development, experiments, and the data analysis. I prepared the figures and the data presentation and contributed to writing the manuscript. Klaus Günther contributed to the design of the experiments and to writing the manuscript. All of my work was supervised by Klaus Günther.

### Summary

#### Introduction

Selenium is not an essential nutrient for plants, but it can enhance factors like growth and resistance against multiple stressors. The most common forms of selenium in soil are selenite and selenate. Selenium shares metabolic pathways and transporters with sulfur, including those that are responsible for the uptake into the roots. Plants can be divided into selenium hyper-, secondary, and non-accumulators, reaching selenium concentrations of >1000 mg/kg, 100-1000 mg/kg or <100 mg/kg dry weight respectively<sup>1,49,53,54,60,74–76</sup>. The

inorganic selenium species are metabolized to SeCys. This amino acid can increase the activity of enzymes when incorporated instead of Cys, however the unspecific misincorporation of SeCys into proteins is mostly associated with loss of function, explaining the toxicity of selenium<sup>77</sup>. SeCys can be targeted by proteins that are responsible for the creation of iron-sulfur clusters, leading to the formation of Se<sup>0</sup><sup>59</sup>. In the context of the general reductive potential in plants, this led to the hypothesis that plants should be able to naturally form selenium nanoparticles. SeNP synthesis has been described for yeast and bacteria in the past, but also using plant extracts. Sometimes reducing agents were added, but often naturally occurring molecules such as tannins or flavonoids offered sufficient reductive potential<sup>67,68,78–81</sup>.

## Materials and Methods

8 different plants were led to germinate and subsequently grown in a hydroponic system. The growth solution was spiked with sodium selenite to ensure a controlled environment, in which the plants were subjected to selenium, but never to SeNP. The plants were grown for 28 to 42 days and afterwards harvested and cleaned thoroughly. The plants were then divided into roots and shoots. Samples were taken from the plants and homogenized with a TissueRuptor. This was followed by an enzymatic digestion with Macerozyme R-10 and Proteinase K and a dialysis to wash out dissolved selenium.

Following the presented procedure for plant treatment, brown mustard (*Brassica juncea*), barley (*Hordeum vulgare*), flax (*Linum usitatissimum*), lentil (*Lens culinaris*), bell pepper (*capsicum annuum*), butter lettuce (*Lactuca sativa*), carrot (*Daucus carota subsp. sativus*), and cucumber (*Cucumis sativus*) were included. Two growth cycles were performed for every species, each consisted of completely separated germination, hydroponic environment and nutritional solution, sample preparation and analysis. The selected plants belong to a variety of families and orders of Angiospermae, and they were chosen that way specifically to gain insight into the commonness of naturally occurring biosynthesis of SeNP.

A method was developed using the Syngistix software with nano application measuring the <sup>80</sup>Se isotope with a relative abundance of 49.61 %. Argon-dimer interference was removed

using hydrogen in a dynamic reaction cell (DRC). The dwell time was set to 50 µs and measuring time to 120 s, while see settling time was eliminated completely. The sample flow rate was determined daily.

## Results and Discussion

All plants were healthy. Shape and colour were unremarkable and primary and secondary roots developed normally. SeNP were found in all observed plants. There was variation in number, size, and distribution among the plant species, but similarities were found as well. Higher concentrations of dissolved selenium correlated with increased SeNP numbers. Their sizes were commonly falling between 30 and 65 nm with the primary size generally below 50 nm. Few particles with sizes of up to 400 nm were discovered. Barley displayed similar SeNP distribution patterns in both root and shoot tissue. Linum roots showed a broader distribution and a higher number of SeNP than linum shoots. Lentils exhibited inconsistent results across samples. Capsicum consistently displayed more SeNP in shoot samples than in root tissues. Lettuce samples showed an overall broad distribution of SeNP, with variations among different plants. Cucumbers exhibited a relatively narrow size distribution, with a sharp cut around 75 to 90 nm. Carrots showed differences in root and shoot tissues, with more particles and a broader distribution in the roots. In mustard samples, the most abundant particle size was between 30 and 45 nm and therefore smaller than the overall average between 46 and 50 nm.

This article was the first one ever to describe and find evidence for the natural biosynthesis of SeNP in living plants. The average number of selenium atoms per nanoparticles were calculated to be 2.1 million. Many aspects of this work have been newly developed and therefore bear some uncertainties, further research is desired, however the detection of SeNP in all included plants species leads to the conviction, that a new pathway of plant biochemistry that leads to the biosynthesis of SeNP was discovered in this work.

The publication furthermore expresses the importance of SeNP for human health and nutrition, due to the superiority of SeNP towards other binding forms of selenium and the importance of optimized selenium levels for multiple chronic and deadly diseases<sup>4,5,82–86</sup>.

# Ubiquitous Occurrence of Nano Selenium in Food Plants

Jonas Verstegen<sup>1,2</sup>, Klaus Günther<sup>1,3</sup>

<sup>1</sup> University of Bonn, Institute of Nutritional and Food Sciences, Germany.

<sup>2</sup> Federal Institute for Drugs and Medical Devices, Bonn, Germany.

<sup>3</sup> Research Centre Juelich, Institute of Bio- and Geosciences, IBG-2, Plant Sciences. Germany.

*Foods* **2023**, *12*(17) 3203.

This publication is listed in appendix B.

## Contribution

I contributed to the design of the experiments. I performed the method development, experiments, and the data analysis. I prepared the figures and the data presentation and contributed to writing the manuscript. Klaus Günther contributed to the design of the experiments and to writing the manuscript. All of my work was supervised by Klaus Günther.

## Summary

### Introduction

The European Food Safety Authority recommends a daily intake for selenium of 70 µg/day for adults<sup>22</sup>. In comparison with other micronutrients, the intestinal absorption of selenium is generally good. The absorption of selenium in an unknown chemical state from food was found to be 83%, yet there is not much information on the selenium species in food and practically no research on naturally occurring nano selenium in food at all. Selenium rich foods are often animal-based, and the fodder for livestock is not rarely enriched with selenium<sup>31,87–89</sup>. Grains and other plant-based foods can be reliable sources of selenium as well, but they are dependent on the selenium content in soil. Selenium-enriched fertilizer can

increase the selenium content of the farmed plants. This can also be achieved through foliar application<sup>90–92</sup>. Since our previous discovery of naturally occurring biosynthesis of SeNP in plants, we aimed to explore the commonness of this biochemical novelty with a special focus on food plants including herbs, salads, cruciferous vegetables, and brazil nuts<sup>93</sup>.

SeNP are a highly desirable form of selenium for the human diet because they combine high bioavailability, low toxicity, and high biological activity. They perform particularly well at protecting against heavy-metal toxicity and showed great potential for the treatment of various kinds of cancer<sup>94–101</sup>.

## Materials and Methods

The analytical procedure used in this research article is essentially identical with the procedure that was also applied in the previous article. 7 different plants were led to germinate and subsequently grown in a hydroponic system. The growth solution was spiked with sodium selenite to ensure a controlled environment, in which the plants were subjected to selenium, but never to SeNP. The plants were grown for 28 to 42 days and afterwards harvested and cleaned thoroughly. The plants were then divided into roots and shoots. Samples were taken from the plants and homogenized with a TissueRuptor. This was followed by an enzymatic digestion with Macerozyme R-10 and Proteinase K and a dialysis to wash out dissolved selenium.

Following the presented procedure for plant treatment Basil (*Ocimum basilicum*), dill (*Anethum graveolens*), chard (*Beta vulgaris*), spinach (*Spinacia oleracea*), brussels sprouts (*Brassica oleracea* var. *gemmifera*), broccoli (*Brassica oleracea* var. *italica*) and lamb's lettuce (*Valerianella locusta*), were included. Additionally, brazil nuts (*Bertholletia excelsa*) were purchased at local supermarkets and homogenized, digested, and treated with dialysis like the other samples.

A method was developed using the Syngistix software with nano application measuring the <sup>80</sup>Se isotope with a relative abundance of 49.61 %. Argon-dimer interference was removed using hydrogen in a dynamic reaction cell (DRC). The dwell time was set to 50 µs and

measuring time to 120 s, while see settling time was eliminated completely. The sample flow rate was determined daily.

## Results and Discussion

The roots and shoots of all included plants were found to contain SeNP, as did the brazil nuts. In basil plants, a relatively low number of SeNP was found. The size distribution of SeNP especially in the shoots was found to be particularly narrow and strongly focused between 30 and 50 nm. The dill samples exhibited very pronounced similarities between roots and shoots and all included samples were found to contain few particles with a size between 300 and 500 nm. The chard plants had an overall remarkably high selenium accumulation and a great number of SeNP. The total selenium content and the number of nanoparticles was higher in the roots than in the shoots. The spinach plants had a slightly narrower size distribution than the chard plants, with SeNP being mostly between 40 and 70 nm in diameter. Brussels sprouts contained a great number of SeNP, especially the root samples. While in the shoots, the detected nanoparticles were mostly between 40 and 60 nm in diameter, a large number of SeNP were found in the roots. Many particles with diameters over 100 nm were found. Broccoli exhibited many similarities with brussels sprouts, which belongs to the same plant family of Brassicaceae that is often associated with selenium hyperaccumulation. In lamb's lettuce, an overall low concentration of selenium was found. Correspondingly, only few SeNP were found. Brazil nuts were found to contain a high number SeNP, that are mainly found in the range between 40 and 60 nm. The differences between the individual nuts were great.

The results gave clear indication that SeNP are ubiquitously present in plants, given that a total of 16 different species were now examined with the analytical procedure and every single species did biosynthesize SeNP. With the focus being shifted to plants whose shoots or roots are commonly eaten as herbs, salads or vegetables, the findings of this article also build strong evidence that selenium in nano form is not only an occasional constituent of food, but an ingredient that is consumed daily by most humans.

The article furthermore discusses the differences between SeNP and other binding forms of

selenium and highlights the benefits of SeNP towards other forms of selenium in terms of bioavailability and ability to yield positive results in combating diseases associated with poor selenium status<sup>66,102,103</sup>.

The potential benefits of SeNP are huge in the context of selenium deficiency as a worldwide problem. Selenium biofortification can not only increase the amount of selenium in human diets to a healthy level, but also improve the quality of selenium, as SeNP show unique beneficial metabolic effects that other forms do not. These nanoparticles are particularly promising because their size is associated with good resorption and bioavailability<sup>104–110</sup>.

Selenium biofortification can furthermore increase accumulation of valuable compounds including vitamin c and flavonoids, it can also increase crop yield in plants<sup>90,91,111–115</sup>.

In the context of global ecology, nutrition and health the potential uses of this new discovery are highlighted. The ubiquitous occurrence of nano selenium in food plants can henceforth be considered proven. Further research is desired, especially studies focusing on the internal and external structure of these naturally occurring SeNP, thus gaining insight into the coating of these particles and the modification of selenium inside.

## Discussion and Conclusion

Within the context of the presented dissertation a sp-ICP-MS method was developed and applied on a multitude of samples, which derived from a variety of plants. A plant treatment procedure was established that enabled the physical breakdown and enzymatic digestion of shoots, roots and nuts to allow sp-ICP-MS analysis without destroying the nanoparticles.

The objective to find evidence for the natural biosynthesis of SeNP was achieved successfully. SeNP were found in all included plants. This was the first time ever that nanoparticle synthesis was observed in living plants. Therefore, many follow up questions arise and the observations that were made have implications on many different scientific fields.

First of all, the consistent detection of SeNP throughout a variety of plant orders and families suggests a ubiquitous phenomenon that can safely be assumed to have purpose and function in plant physiology. Since this is the first time that naturally occurring SeNP are described in plants, nothing is known with certainty about the biochemical pathway that leads to their synthesis or the roles they potentially possess in plant physiology or biochemistry. Selenium is not considered an essential nutrient for plants, which makes a targeted synthesis for SeNP even more surprising. However, beneficial effects of SeNP on plants growth and crop yield have been proven successfully and we see great potential in the further investigation of the biochemical reasoning for this. Selenium can increase the concentrations of beneficial compounds such as flavonoids or vitamin c. The potential of biofortification of crops with selenium should include its acting as a biostimulant and the potential to combat selenium deficiency that is estimated to affect up to a billion people.

During the later stage of the research project, great emphasis was placed on food plants. The constant detection of SeNP took place as much as it did in other plants and it therefore has to be stated with great vigor, that these nanoparticles are universally present in food. Furthermore, the detected sizes of nanoparticles are highly bioavailable. The literature referenced in this dissertation and the included research articles describes the different physiological effects that different selenium compounds in food can cause in mammals.

SeNP were never before discussed as natural ingredients in foods, but the results presented in this dissertation require a close look and thorough investigation on the potential of different kinds of foods as selenium sources. This includes an evaluation of dose-dependent nanoparticle synthesis in plants and quantitative studies investigating the percentage of selenium that is transformed into nano form.

As the binding form of a nutrient strongly impacts its bioavailability and function it is of the utmost importance to identify the composition and coating of nanoparticles. The coating of a particle can impact its properties in the same way. Further research on the coating can therefore give important insight in its function and the way it is synthesized but can also help to understand how plant-based SeNP act in the human body. The characterization of those particles also needs to include a determination of the selenium modification or modifications that are found in the core of the nanoparticles. Red (Se rings) or grey (Se chains) modification have very different reaction behaviors.

Lastly, the findings of this dissertation may aid the path to a sustainable and efficient way to yield high quality SeNP for the development and production of superior selenium food supplements and drugs. The narrow size distribution that was found in the different plants and the high number of particles within that range in some of the specimen hint towards a great potential for medical applications and usage in the field of nutraceuticals.

These additional questions very clearly show the challenges that still need to be overcome in the future for an accurate characterization of selenium nanoparticles.

Finally, there is no reason to believe that natural formation of nanoparticles in plants should be limited to selenium. A greater system of nano physiology and nano biochemistry, including a variety of metalloid and metals, especially those that function as micronutrients is not unlikely, considering the findings discussed here. The implications and opportunities of this cannot be put into words yet. The possibilities for further research concerning that matter however seem to hold great potential and scientific curiosity might lead to a whole new area of plant physiology.

## References

- (1) Reich, H. J.; Hondal, R. J. Why Nature Chose Selenium, *ACS chemical biology*. **2016**, *11*, pp. 821–841.
- (2) Arnér, E. S. J. History of Selenium Research. In *Selenium*; Hatfield, D. L.; Berry, M. J.; Gladyshev, V. N., Eds.; Springer New York: New York, NY, 2012, pp. 1–19.
- (3) Hatfield, D. L.; Gladyshev, V. N. How selenium has altered our understanding of the genetic code, *Molecular and cellular biology*. **2002**, *22*, pp. 3565–3576.
- (4) Kryukov, G. V.; Castellano, S.; Novoselov, S. V.; Lobanov, A. V.; Zehtab, O.; Guigó, R.; Gladyshev, V. N. Characterization of mammalian selenoproteomes, *Science (New York, N.Y.)*. **2003**, *300*, pp. 1439–1443.
- (5) Reeves, M. A.; Hoffmann, P. R. The human selenoproteome: recent insights into functions and regulation, *Cellular and molecular life sciences : CMLS*. **2009**, *66*, pp. 2457–2478.
- (6) Turanov, A. A.; Xu, X.-M.; Carlson, B. A.; Yoo, M.-H.; Gladyshev, V. N.; Hatfield, D. L. Biosynthesis of selenocysteine, the 21st amino acid in the genetic code, and a novel pathway for cysteine biosynthesis, *Advances in nutrition (Bethesda, Md.)*. **2011**, *2*, pp. 122–128.
- (7) Gromer, S.; Johansson, L.; Bauer, H.; Arscott, L. D.; Rauch, S.; Ballou, D. P.; Williams, C. H.; Schirmer, R. H.; Arnér, E. S. J. Active sites of thioredoxin reductases: why selenoproteins?, *Proceedings of the National Academy of Sciences of the United States of America*. **2003**, *100*, pp. 12618–12623.
- (8) Kim, H.-Y.; Gladyshev, V. N. Different catalytic mechanisms in mammalian selenocysteine- and cysteine-containing methionine-R-sulfoxide reductases, *PLoS biology*. **2005**, *3*, e375.
- (9) Hoffmann PR, B. M. J. Selenoprotein Synthesis: A Unique Translational Mechanism Used by a Diverse Family of Proteins, *Thyroid*. **2005**, pp. 765–775.
- (10) Carlson, B. A.; Lee, B. J.; Tsuji, P. A.; Copeland, P. R.; Schweizer, U.; Gladyshev, V. N.; Hatfield, D. L. Selenocysteine tRNASerSec, the Central Component of

Selenoprotein Biosynthesis: Isolation, Identification, Modification, and Sequencing, *Methods in molecular biology (Clifton, N.J.)*. **2018**, 1661, pp. 43–60.

- (11) Vindry, C.; Ohlmann, T.; Chavatte, L. Translation regulation of mammalian selenoproteins, *Biochimica et biophysica acta. General subjects*. **2018**, 1862, pp. 2480–2492.
- (12) Schmidt, R. L.; Simonović, M. Synthesis and decoding of selenocysteine and human health, *Croatian medical journal*. **2012**, 53, pp. 535–550.
- (13) R. Steven Esworthy; Margaret A. Baker; Fong-Fong Chu Expression of Selenium-dependent Glutathione Peroxidase in Human Breast Tumor Cell Lines, *Cancer Res.* **1995**, 55, pp. 957–962.
- (14) Zhao, Y.; Wang, H.; Zhou, J.; Shao, Q. Glutathione Peroxidase GPX1 and Its Dichotomous Roles in Cancer, *Cancers*. **2022**, 14, p. 2560.
- (15) Cheng, Y.; Xu, T.; Li, S.; Ruan, H. GPX1, a biomarker for the diagnosis and prognosis of kidney cancer, promotes the progression of kidney cancer, *Aging*. **2019**, 11, pp. 12165–12176.
- (16) Yant, L. J.; Ran, Q.; Rao, L.; van Remmen, H.; Shibatani, T.; Belter, J. G.; Motta, L.; Richardson, A.; Prolla, T. A. The selenoprotein GPX4 is essential for mouse development and protects from radiation and oxidative damage insults, *Free radical biology & medicine*. **2003**, 34, pp. 496–502.
- (17) Arnér, E. S.; Holmgren, A. Physiological functions of thioredoxin and thioredoxin reductase, *European journal of biochemistry*. **2000**, 267, pp. 6102–6109.
- (18) Dou, Q.; Turanov, A. A.; Mariotti, M.; Hwang, J. Y.; Wang, H.; Lee, S.-G.; Paulo, J. A.; Yim, S. H.; Gygi, S. P.; Chung, J.-J.; Gladyshev, V. N. Selenoprotein TXNRD3 supports male fertility via the redox regulation of spermatogenesis, *The Journal of biological chemistry*. **2022**, 298, p. 102183.
- (19) Liu, Q.; Du, P.; Zhu, Y.; Zhang, X.; Cai, J.; Zhang, Z. Thioredoxin reductase 3 suppression promotes colitis and carcinogenesis via activating pyroptosis and necrosis, *Cellular and molecular life sciences : CMLS*. **2022**, 79, p. 106.

- (20) Köhrle, J.; Frädrich, C. Deiodinases control local cellular and systemic thyroid hormone availability, *Free radical biology & medicine*. **2022**, 193, pp. 59–79.
- (21) Russo, S. C.; Salas-Lucia, F.; Bianco, A. C. Deiodinases and the Metabolic Code for Thyroid Hormone Action, *Endocrinology*. **2021**, 162, bqab059.
- (22) Scientific Opinion on Dietary Reference Values for selenium, *EFSA Journal*. **2014**, 12, p. 3846.
- (23) Brodin, O.; Hackler, J.; Misra, S.; Wendt, S.; Sun, Q.; Laaf, E.; Stoppe, C.; Björnstedt, M.; Schomburg, L. Selenoprotein P as Biomarker of Selenium Status in Clinical Trials with Therapeutic Dosages of Selenite, *Nutrients*. **2020**, 12, p. 1067.
- (24) Schomburg, L. Selenoprotein P - Selenium transport protein, enzyme and biomarker of selenium status, *Free radical biology & medicine*. **2022**, 191, pp. 150–163.
- (25) Turck, D.; Bohn, T.; Castenmiller, J.; Henauw, S. de; Hirsch-Ernst, K.-I.; Knutsen, H. K.; Maciuk, A.; Mangelsdorf, I.; McArdle, H. J.; Peláez, C.; Pentieva, K.; Siani, A.; Thies, F.; Tsabouri, S.; Vinceti, M.; Aggett, P.; Crous Bou, M.; Cubadda, F.; Ciccolallo, L.; Sesmaisons Lecarré, A. de; Fabiani, L.; Titz, A.; Naska, A. Scientific opinion on the tolerable upper intake level for selenium, *EFSA Journal*. **2023**, 21, e07704.
- (26) Hadrup, N.; Ravn-Haren, G. Acute human toxicity and mortality after selenium ingestion: A review, *Journal of trace elements in medicine and biology : organ of the Society for Minerals and Trace Elements (GMS)*. **2020**, 58, p. 126435.
- (27) Rayman, M. P. Food-chain selenium and human health: emphasis on intake, *The British journal of nutrition*. **2008**, 100, pp. 254–268.
- (28) Liaskos, M.; Fark, N.; Ferrario, P.; Engelbert, A. K.; Merz, B.; Hartmann, B.; Watzl, B. First review on the selenium status in Germany covering the last 50 years and on the selenium content of selected food items, *European journal of nutrition*. **2023**, 62, pp. 71–82.
- (29) Combs, G. F. Biomarkers of selenium status, *Nutrients*. **2015**, 7, pp. 2209–2236.

- (30) Combs, G. F. Selenium in global food systems, *The British journal of nutrition.* **2001**, *85*, pp. 517–547.
- (31) Hadrup, N.; Ravn-Haren, G. Absorption, distribution, metabolism and excretion (ADME) of oral selenium from organic and inorganic sources: A review, *Journal of trace elements in medicine and biology : organ of the Society for Minerals and Trace Elements (GMS).* **2021**, *67*, p. 126801.
- (32) Alcântara, D. B.; Dionísio, A. P.; Artur, A. G.; Silveira, B. K. S.; Lopes, A. F.; Guedes, J. A. C.; Luz, L. R.; Nascimento, R. F.; Lopes, G. S.; Hermsdorff, H. H. M.; Zocolo, G. J. Selenium in Brazil nuts: An overview of agronomical aspects, recent trends in analytical chemistry, and health outcomes, *Food chemistry.* **2022**, *372*, p. 131207.
- (33) Phiri, F. P.; Ander, E. L.; Bailey, E. H.; Chilima, B.; Chilimba, A. D. C.; Gondwe, J.; Joy, E. J. M.; Kalimbira, A. A.; Kumssa, D. B.; Lark, R. M.; Phuka, J. C.; Salter, A.; Suchdev, P. S.; Watts, M. J.; Young, S. D.; Broadley, M. R. The risk of selenium deficiency in Malawi is large and varies over multiple spatial scales, *Scientific reports.* **2019**, *9*, p. 6566.
- (34) Yan, C.; Luo, R.; Li, F.; Liu, M.; Li, J.; Hua, W.; Li, X. The epidemiological status, environmental and genetic factors in the etiology of Keshan disease, *Cardiovascular endocrinology & metabolism.* **2021**, *10*, pp. 14–21.
- (35) Jia, Y.; Han, S.; Hou, J.; Wang, R.; Li, G.; Su, S.; Qi, L.; Wang, Y.; Du, L.; Sun, H.; Hao, S.; Feng, C.; Wang, Y.; Liu, X.; Zou, Y.; Zhang, Y.; Li, D.; Wang, T. Spatial Epidemiological Analysis of Keshan Disease in China, *Annals of global health.* **2022**, *88*, p. 79.
- (36) Hou, J.; Zhu, L.; Chen, C.; Feng, H.; Li, D.; Sun, S.; Xing, Z.; Wan, X.; Wang, X.; Li, F.; Guo, X.; Xiong, P.; Zhao, S.; Li, S.; Liu, J.; Sun, D. Association of selenium levels with the prevention and control of Keshan disease: A cross-sectional study, *Journal of trace elements in medicine and biology : organ of the Society for Minerals and Trace Elements (GMS).* **2021**, *68*, p. 126832.

- (37) Newman, R.; Waterland, N.; Moon, Y.; Tou, J. C. Selenium Biofortification of Agricultural Crops and Effects on Plant Nutrients and Bioactive Compounds Important for Human Health and Disease Prevention - a Review, *Plant foods for human nutrition (Dordrecht, Netherlands)*. **2019**, *74*, pp. 449–460.
- (38) Schiavon, M.; Nardi, S.; Dalla Vecchia, F.; Ertani, A. Selenium biofortification in the 21st century: status and challenges for healthy human nutrition, *Plant and soil*. **2020**, *453*, pp. 245–270.
- (39) D'Amato, R.; Regni, L.; Falcinelli, B.; Mattioli, S.; Benincasa, P.; Dal Bosco, A.; Pacheco, P.; Proietti, P.; Troni, E.; Santi, C.; Businelli, D. Current Knowledge on Selenium Biofortification to Improve the Nutraceutical Profile of Food: A Comprehensive Review, *Journal of agricultural and food chemistry*. **2020**, *68*, pp. 4075–4097.
- (40) Shi, Y.; Yang, W.; Tang, X.; Yan, Q.; Cai, X.; Wu, F. Keshan Disease: A Potentially Fatal Endemic Cardiomyopathy in Remote Mountains of China, *Frontiers in pediatrics*. **2021**, *9*, p. 576916.
- (41) Wang, K.; Yu, J.; Liu, H.; Liu, Y.; Liu, N.; Cao, Y.; Zhang, X.; Sun, D. Endemic Kashin-Beck disease: A food-sourced osteoarthropathy, *Seminars in arthritis and rheumatism*. **2020**, *50*, pp. 366–372.
- (42) Wang, J.; Zhao, S.; Yang, L.; Gong, H.; Li, H.; Nima, C. Assessing the Health Loss from Kashin-Beck Disease and Its Relationship with Environmental Selenium in Qamdo District of Tibet, China, *International journal of environmental research and public health*. **2020**, *18*(1), p. 11.
- (43) Yu, F.-F.; Qi, X.; Shang, Y.-N.; Ping, Z.-G.; Guo, X. Prevention and control strategies for children Kashin-Beck disease in China: A systematic review and meta-analysis, *Medicine*. **2019**, *98*, e16823.
- (44) Li, D.; Han, J.; Guo, X.; Qu, C.; Yu, F.; Wu, X. The effects of T-2 toxin on the prevalence and development of Kashin-Beck disease in China: a meta-analysis and systematic review, *Toxicology research*. **2016**, *5*, pp. 731–751.

- (45) Klein, E. A. Selenium and vitamin E cancer prevention trial, *Annals of the New York Academy of Sciences*. **2004**, *1031*, pp. 234–241.
- (46) Shreenath, A. P.; Ameer, M. A.; Dooley, J. *StatPearls. Selenium Deficiency*: Treasure Island (FL), 2023.
- (47) Chariot, P.; Bignani, O. Skeletal muscle disorders associated with selenium deficiency in humans, *Muscle & nerve*. **2003**, *27*, pp. 662–668.
- (48) Rayman, M. P. Selenium intake, status, and health: a complex relationship, *Hormones (Athens, Greece)*. **2020**, *19*, pp. 9–14.
- (49) White, P. J. Selenium accumulation by plants, *Annals of botany*. **2016**, *117*, pp. 217–235.
- (50) Boldrin, P. F.; Faquin, V.; Ramos, S. J.; Boldrin, K. V. F.; Ávila, F. W.; Guilherme, L. R. G. Soil and foliar application of selenium in rice biofortification, *Journal of Food Composition and Analysis*. **2013**, *31*, pp. 238–244.
- (51) Drahoňovský, J.; Száková, J.; Mestek, O.; Tremlová, J.; Kaňa, A.; Najmanová, J.; Tlustoš, P. Selenium uptake, transformation and inter-element interactions by selected wildlife plant species after foliar selenate application, *Environmental and Experimental Botany*. **2016**, *125*, pp. 12–19.
- (52) Duborská, E.; Šebesta, M.; Matulová, M.; Zvěřina, O.; Urík, M. Current Strategies for Selenium and Iodine Biofortification in Crop Plants, *Nutrients*. **2022**, *14*, p. 4717.
- (53) Gupta, M.; Gupta, S. An Overview of Selenium Uptake, Metabolism, and Toxicity in Plants, *Frontiers in plant science*. **2016**, *7*, p. 2074.
- (54) White, P. J. Selenium metabolism in plants, *Biochimica et biophysica acta. General subjects*. **2018**, *1862*, pp. 2333–2342.
- (55) Pilon-Smits, E. A. H.; Quinn, C. F. Selenium Metabolism in Plants. In *Cell Biology of Metals and Nutrients*; Hell, R.; Mendel, R.-R., Eds.; Springer Berlin Heidelberg: Berlin, Heidelberg, 2010, pp. 225–241.
- (56) Freeman, J. L.; Tamaoki, M.; Stushnoff, C.; Quinn, C. F.; Cappa, J. J.; Devonshire, J.; Fakra, S. C.; Marcus, M. A.; McGrath, S. P.; van Hoewyk, D.; Pilon-Smits, E. A. H.

Molecular mechanisms of selenium tolerance and hyperaccumulation in *Stanleya pinnata*, *Plant physiology*. **2010**, 153, pp. 1630–1652.

(57) van Hoewyk, D.; Pilon, M.; Pilon-Smits, E. A. The functions of NifS-like proteins in plant sulfur and selenium metabolism, *Plant Science*. **2008**, 174, pp. 117–123.

(58) Ye, H.; Pilon, M.; Pilon-Smits, E. A. H. CpNifS-dependent iron-sulfur cluster biogenesis in chloroplasts, *New Phytologist*. **2006**, 171, pp. 285–292.

(59) van Hoewyk, D.; Garifullina, G. F.; Ackley, A. R.; Abdel-Ghany, S. E.; Marcus, M. A.; Fakra, S.; Ishiyama, K.; Inoue, E.; Pilon, M.; Takahashi, H.; Pilon-Smits, E. A. H. Overexpression of AtCpNifS enhances selenium tolerance and accumulation in *Arabidopsis*, *Plant physiology*. **2005**, 139, pp. 1518–1528.

(60) Lima, L. W.; Pilon-Smits, E. A. H.; Schiavon, M. Mechanisms of selenium hyperaccumulation in plants: A survey of molecular, biochemical and ecological cues, *Biochimica et biophysica acta. General subjects*. **2018**, 1862, pp. 2343–2353.

(61) Kreyling, W. G.; Semmler-Behnke, M.; Chaudhry, Q. A complementary definition of nanomaterial, *Nano today*. **2010**, 5, pp. 165–168.

(62) Miernicki, M.; Hofmann, T.; Eisenberger, I.; Kammer, F. von der; Praetorius, A. Legal and practical challenges in classifying nanomaterials according to regulatory definitions, *Nature nanotechnology*. **2019**, 14, pp. 208–216.

(63) REGULATION (EU) 2015/2283 OF THE EUROPEAN PARLIAMENT AND OF THE COUNCIL of 25 November 2015 on novel foods, amending Regulation (EU) No 1169/2011 of the European Parliament and of the Council and repealing Regulation (EC) No 258/97 of the European Parliament and of the Council and Commission Regulation (EC) No 1852/2001, 2015.

(64) More, S.; Bampidis, V.; Benford, D.; Bragard, C.; Halldorsson, T.; Hernández-Jerez, A.; Hougaard Bennekou, S.; Koutsoumanis, K.; Lambré, C.; Machera, K.; Naegeli, H.; Nielsen, S.; Schlatter, J.; Schrenk, D.; Silano Deceased, V.; Turck, D.; Younes, M.; Castenmiller, J.; Chaudhry, Q.; Cubadda, F.; Franz, R.; Gott, D.; Mast, J.; Mortensen, A.; Oomen, A. G.; Weigel, S.; Barthelemy, E.; Rincon, A.; Tarazona, J.;

- Schoonjans, R. Guidance on risk assessment of nanomaterials to be applied in the food and feed chain: human and animal health, *EFSA Journal*. **2021**, *19*, e06768.
- (65) REGULATION (EC) No 1223/2009 OF THE EUROPEAN PARLIAMENT AND OF THE COUNCIL of 30 November 2009 on cosmetic products, 30.11.2009.
- (66) Ojeda, M. L.; Nogales, F.; Carreras, O.; Pajuelo, E.; Del Gallego-López, M. C.; Romero-Herrera, I.; Begines, B.; Moreno-Fernández, J.; Díaz-Castro, J.; Alcudia, A. Different Effects of Low Selenite and Selenium-Nanoparticle Supplementation on Adipose Tissue Function and Insulin Secretion in Adolescent Male Rats, *Nutrients*. **2022**, *14*, p. 3571.
- (67) Anu, K.; Singaravelu, G.; Murugan, K.; Benelli, G. Green-Synthesis of Selenium Nanoparticles Using Garlic Cloves (*Allium sativum*): Biophysical Characterization and Cytotoxicity on Vero Cells, *J Clust Sci.* **2017**, *28*, pp. 551–563.
- (68) Cittrarasu, V.; Kaliannan, D.; Dharman, K.; Maluventhen, V.; Easwaran, M.; Liu, W. C.; Balasubramanian, B.; Arumugam, M. Green synthesis of selenium nanoparticles mediated from *Ceropegia bulbosa Roxb* extract and its cytotoxicity, antimicrobial, mosquitocidal and photocatalytic activities, *Scientific reports*. **2021**, *11*, p. 1032.
- (69) Ghaderi, R. S.; Adibian, F.; Sabouri, Z.; Davoodi, J.; Kazemi, M.; Amel Jamehdar, S.; Meshkat, Z.; Soleimanpour, S.; Daroudi, M. Green synthesis of selenium nanoparticle by *Abelmoschus esculentus* extract and assessment of its antibacterial activity, *Materials Technology*. **2022**, *37*, pp. 1289–1297.
- (70) Pyrzynska, K.; Sentkowska, A. Biosynthesis of selenium nanoparticles using plant extracts, *J Nanostruct Chem.* **2022**, *12*, pp. 467–480.
- (71) Niu, G.; Masabni, J. Hydroponics. In *Plant Factory Basics, Applications and Advances*; Elsevier, 2022, pp. 153–166.
- (72) Howard, H. F.; Watschke, T. L. Hydroponic Culture of Grass Plants for Physiological Experiments 1, *Crop Science*. **1984**, *24*, pp. 991–992.

- (73) SMITH, G. S.; JOHNSTON, C. M.; CORNFORTH, I. S. COMPARISON OF NUTRIENT SOLUTIONS FOR GROWTH OF PLANTS IN SAND CULTURE, *New Phytologist*. **1983**, 94, pp. 537–548.
- (74) Schiavon, M.; Pilon-Smits, E. A. H. The fascinating facets of plant selenium accumulation - biochemistry, physiology, evolution and ecology, *The New phytologist*. **2017**, 213, pp. 1582–1596.
- (75) Bela, K.; Horváth, E.; Gallé, Á.; Szabados, L.; Tari, I.; Csiszár, J. Plant glutathione peroxidases: emerging role of the antioxidant enzymes in plant development and stress responses, *Journal of plant physiology*. **2015**, 176, pp. 192–201.
- (76) Kolbert, Z.; Molnár, Á.; Feigl, G.; van Hoewyk, D. Plant selenium toxicity: Proteome in the crosshairs, *Journal of plant physiology*. **2019**, 232, pp. 291–300.
- (77) Hoffman, K. S.; Vargas-Rodriguez, O.; Bak, D. W.; Mukai, T.; Woodward, L. K.; Weerapana, E.; Söll, D.; Reynolds, N. M. A cysteinyl-tRNA synthetase variant confers resistance against selenite toxicity and decreases selenocysteine misincorporation, *The Journal of biological chemistry*. **2019**, 294, pp. 12855–12865.
- (78) Shoeibi, S.; Mashreghi, M. Biosynthesis of selenium nanoparticles using *Enterococcus faecalis* and evaluation of their antibacterial activities, *Journal of trace elements in medicine and biology : organ of the Society for Minerals and Trace Elements (GMS)*. **2017**, 39, pp. 135–139.
- (79) Jiménez-Lamana, J.; Abad-Álvaro, I.; Bierla, K.; Laborda, F.; Szpunar, J.; Lobinski, R. Detection and characterization of biogenic selenium nanoparticles in selenium-rich yeast by single particle ICPMS, *J. Anal. At. Spectrom.* **2018**, 33, pp. 452–460.
- (80) Nayak, V.; Singh, K. R. B.; Singh, A. K.; Singh, R. P. Potentialities of selenium nanoparticles in biomedical science, *New J. Chem.* **2021**, 45, pp. 2849–2878.
- (81) Janthima, R.; Siri, S. Cellular biogenesis of metal nanoparticles by water velvet (*Azolla pinnata*): different fates of the uptake Fe<sup>3+</sup> and Ni<sup>2+</sup> to transform into nanoparticles, *Artificial cells, nanomedicine, and biotechnology*. **2021**, 49, pp. 471–482.

- (82) Rayman, M. P. Selenium and human health, *Lancet (London, England)*. **2012**, 379, pp. 1256–1268.
- (83) Carlisle, A. E.; Lee, N.; Matthew-Onabanjo, A. N.; Spears, M. E.; Park, S. J.; Youkana, D.; Doshi, M. B.; Peppers, A.; Li, R.; Joseph, A. B.; Smith, M.; Simin, K.; Zhu, L. J.; Greer, P. L.; Shaw, L. M.; Kim, D. Selenium detoxification is required for cancer-cell survival, *Nature metabolism*. **2020**, 2, pp. 603–611.
- (84) Kang, D.; Lee, J.; Wu, C.; Guo, X.; Lee, B. J.; Chun, J.-S.; Kim, J.-H. The role of selenium metabolism and selenoproteins in cartilage homeostasis and arthropathies, *Experimental & molecular medicine*. **2020**, 52, pp. 1198–1208.
- (85) Lin, Z.; Li, Y.; Guo, M.; Xiao, M.; Wang, C.; Zhao, M.; Xu, T.; Xia, Y.; Zhu, B. Inhibition of H1N1 influenza virus by selenium nanoparticles loaded with zanamivir through p38 and JNK signaling pathways, *RSC Adv.* **2017**, 7, pp. 35290–35296.
- (86) He, L.; Zhao, J.; Wang, L.; Liu, Q.; Fan, Y.; Li, B.; Yu, Y.-L.; Chen, C.; Li, Y.-F. Using nano-selenium to combat Coronavirus Disease 2019 (COVID-19)?, *Nano today*. **2021**, 36, p. 101037.
- (87) Melse-Boonstra, A. Bioavailability of Micronutrients From Nutrient-Dense Whole Foods: Zooming in on Dairy, Vegetables, and Fruits, *Frontiers in nutrition*. **2020**, 7, p. 101.
- (88) Hurrell, R.; Egli, I. Iron bioavailability and dietary reference values, *The American journal of clinical nutrition*. **2010**, 91, pp. 1461–1467.
- (89) Gu, X.; Gao, C.-Q. New horizons for selenium in animal nutrition and functional foods, *Animal nutrition (Zhongguo xu mu shou yi xue hui)*. **2022**, 11, pp. 80–86.
- (90) Alfthan, G.; Eurola, M.; Ekholm, P.; Venäläinen, E.-R.; Root, T.; Korkalainen, K.; Hartikainen, H.; Salminen, P.; Hietaniemi, V.; Aspila, P.; Aro, A. Effects of nationwide addition of selenium to fertilizers on foods, and animal and human health in Finland: From deficiency to optimal selenium status of the population, *Journal of trace elements in medicine and biology : organ of the Society for Minerals and Trace Elements (GMS)*. **2015**, 31, pp. 142–147.

- (91) Silva, M. A.; Sousa, G. F. de; Corquinha, A. P. B.; Lima Lessa, J. H. de; Dinali, G. S.; Oliveira, C.; Lopes, G.; Amaral, D.; Brown, P.; Guilherme, L. R. G. Selenium biofortification of soybean genotypes in a tropical soil via Se-enriched phosphate fertilizers, *Frontiers in plant science*. **2022**, *13*, p. 988140.
- (92) Hossain, A.; Skalicky, M.; Breštic, M.; Maitra, S.; Sarkar, S.; Ahmad, Z.; Vemuri, H.; Garai, S.; Mondal, M.; Bhatt, R.; Kumar, P.; Banerjee, P.; Saha, S.; Islam, T.; Laing, A. M. Selenium Biofortification: Roles, Mechanisms, Responses and Prospects, *Molecules (Basel, Switzerland)*. **2021**, *26*, p. 881.
- (93) Versteegen, J.; Günther, K. Biosynthesis of nano selenium in plants, *Artificial cells, nanomedicine, and biotechnology*. **2023**, *51*, pp. 13–21.
- (94) Menon, S.; Shruthi Devi, K.; Santhiya, R.; Rajeshkumar, S.; Venkat Kumar, S. Selenium nanoparticles: A potent chemotherapeutic agent and an elucidation of its mechanism, *Colloids and surfaces. B, Biointerfaces*. **2018**, *170*, pp. 280–292.
- (95) Shimada, B. K.; Alfulaij, N.; Seale, L. A. The Impact of Selenium Deficiency on Cardiovascular Function, *International journal of molecular sciences*. **2021**, *22*, p. 10713.
- (96) Hughes, D. J.; Duarte-Salles, T.; Hybsier, S.; Trichopoulou, A.; Stepien, M.; Aleksandrova, K.; Overvad, K.; Tjønneland, A.; Olsen, A.; Affret, A.; Fagherazzi, G.; Boutron-Ruault, M.-C.; Katzke, V.; Kaaks, R.; Boeing, H.; Bamia, C.; Lagiou, P.; Peppa, E.; Palli, D.; Krogh, V.; Panico, S.; Tumino, R.; Sacerdote, C.; Bueno-de-Mesquita, H. B.; Peeters, P. H.; Engeset, D.; Weiderpass, E.; Lasheras, C.; Agudo, A.; Sánchez, M.-J.; Navarro, C.; Ardanaz, E.; Dorronsoro, M.; Hemmingsson, O.; Wareham, N. J.; Khaw, K.-T.; Bradbury, K. E.; Cross, A. J.; Gunter, M.; Riboli, E.; Romieu, I.; Schomburg, L.; Jenab, M. Prediagnostic selenium status and hepatobiliary cancer risk in the European Prospective Investigation into Cancer and Nutrition cohort, *The American journal of clinical nutrition*. **2016**, *104*, pp. 406–414.
- (97) Rai, R. K.; Karri, R.; Dubey, K. D.; Roy, G. Regulation of Tyrosinase Enzyme Activity by Glutathione Peroxidase Mimics, *Journal of agricultural and food chemistry*. **2022**, *70*, pp. 9730–9747.

- (98) Kristal, A. R.; Darke, A. K.; Morris, J. S.; Tangen, C. M.; Goodman, P. J.; Thompson, I. M.; Meyskens, F. L.; Goodman, G. E.; Minasian, L. M.; Parnes, H. L.; Lippman, S. M.; Klein, E. A. Baseline selenium status and effects of selenium and vitamin e supplementation on prostate cancer risk, *Journal of the National Cancer Institute*. **2014**, *106*, djt456.
- (99) Sun, X.-H.; Lv, M.-W.; Zhao, Y.-X.; Zhang, H.; Ullah Saleem, M. A.; Zhao, Y.; Li, J.-L. Nano-Selenium Antagonized Cadmium-Induced Liver Fibrosis in Chicken, *Journal of agricultural and food chemistry*. **2023**, *71*, pp. 846–856.
- (100) Abd-Rabou, A. A.; Ahmed, H. H.; Shalby, A. B. Selenium Overcomes Doxorubicin Resistance in Their Nano-platforms Against Breast and Colon Cancers, *Biological trace element research*. **2020**, *193*, pp. 377–389.
- (101) Liao, G.; Tang, J.; Di Wang; Zuo, H.; Zhang, Q.; Liu, Y.; Xiong, H. Selenium nanoparticles (SeNPs) have potent antitumor activity against prostate cancer cells through the upregulation of miR-16, *World journal of surgical oncology*. **2020**, *18*, p. 81.
- (102) Chen, J.; Guo, Y.; Zhang, X.; Liu, J.; Gong, P.; Su, Z.; Fan, L.; Li, G. Emerging Nanoparticles in Food: Sources, Application, and Safety, *Journal of agricultural and food chemistry*. **2023**, *71*, pp. 3564–3582.
- (103) Dolai, J.; Mandal, K.; Jana, N. R. Nanoparticle Size Effects in Biomedical Applications, *ACS Appl. Nano Mater.* **2021**, *4*, pp. 6471–6496.
- (104) Bakaloudi, D. R.; Halloran, A.; Rippin, H. L.; Oikonomidou, A. C.; Dardavessis, T. I.; Williams, J.; Wickramasinghe, K.; Breda, J.; Chourdakis, M. Intake and adequacy of the vegan diet. A systematic review of the evidence, *Clinical nutrition (Edinburgh, Scotland)*. **2021**, *40*, pp. 3503–3521.
- (105) Bhattacharjee, A.; Basu, A.; Bhattacharya, S. Selenium nanoparticles are less toxic than inorganic and organic selenium to mice in vivo, *Nucleus*. **2019**, *62*, pp. 259–268.
- (106) Jia, X.; Li, N.; Chen, J. A subchronic toxicity study of elemental Nano-Se in Sprague-Dawley rats, *Life sciences*. **2005**, *76*, pp. 1989–2003.

- (107) Peng, D.; Zhang, J.; Liu, Q.; Taylor, E. W. Size effect of elemental selenium nanoparticles (Nano-Se) at supranutritional levels on selenium accumulation and glutathione S-transferase activity, *Journal of inorganic biochemistry*. **2007**, *101*, pp. 1457–1463.
- (108) Skalickova, S.; Milosavljevic, V.; Cihalova, K.; Horky, P.; Richtera, L.; Adam, V. Selenium nanoparticles as a nutritional supplement, *Nutrition (Burbank, Los Angeles County, Calif.)*. **2017**, *33*, pp. 83–90.
- (109) Wang, H.; Zhang, J.; Yu, H. Elemental selenium at nano size possesses lower toxicity without compromising the fundamental effect on selenoenzymes: comparison with selenomethionine in mice, *Free radical biology & medicine*. **2007**, *42*, pp. 1524–1533.
- (110) Weder, S.; Zerback, E. H.; Wagener, S. M.; Koeder, C.; Fischer, M.; Alexy, U.; Keller, M. How Does Selenium Intake Differ among Children (1-3 Years) on Vegetarian, Vegan, and Omnivorous Diets? Results of the VeChi Diet Study, *Nutrients*. **2022**, *15*(1), p. 34.
- (111) Hossain, M. A.; Ahammed, G. J.; Kolbert, Z.; El-Ramady, H.; Islam, M. T.; Schiavon, M., Eds. *Selenium and Nano-Selenium in Environmental Stress Management and Crop Quality Improvement*, 1st ed.; Springer, 2022.
- (112) Cheng, C.; Coldea, T. E.; Yang, H.; Zhao, H. Selenium Uptake, Translocation, and Metabolization Pattern during Barley Malting: A Comparison of Selenate, Selenite, and Selenomethionine, *Journal of agricultural and food chemistry*. **2023**, *71*, pp. 5240–5249.
- (113) Silva Junior, E. C.; Wadt, L. H. O.; Silva, K. E.; Lima, R. M. B.; Batista, K. D.; Guedes, M. C.; Carvalho, G. S.; Carvalho, T. S.; Reis, A. R.; Lopes, G.; Guilherme, L. R. G. Natural variation of selenium in Brazil nuts and soils from the Amazon region, *Chemosphere*. **2017**, *188*, pp. 650–658.
- (114) Zou, C.; Du, Y.; Rashid, A.; Ram, H.; Savasli, E.; Pieterse, P. J.; Ortiz-Monasterio, I.; Yazici, A.; Kaur, C.; Mahmood, K.; Singh, S.; Le Roux, M. R.; Kuang, W.; Onder, O.; Kalayci, M.; Cakmak, I. Simultaneous Biofortification of Wheat with Zinc,

Iodine, Selenium, and Iron through Foliar Treatment of a Micronutrient Cocktail in Six Countries, *Journal of agricultural and food chemistry*. **2019**, *67*, pp. 8096–8106.

(115) Dima, S.-O.; Neamțu, C.; Desliu-Avram, M.; Ghiurea, M.; Capra, L.; Radu, E.; Stoica, R.; Faraon, V.-A.; Zamfiropol-Cristea, V.; Constantinescu-Aruxandei, D.; Oancea, F. Plant Biostimulant Effects of Baker's Yeast Vinasse and Selenium on Tomatoes through Foliar Fertilization, *Agronomy*. **2020**, *10*, p. 133.

## **Appendix**

### **Appendix A**

#### **Biosynthesis of nano selenium in plants**

## Biosynthesis of nano selenium in plants

Jonas Verstegen<sup>a,b</sup>  and Klaus Günther<sup>a,c</sup> 

<sup>a</sup>Institute of Nutritional and Food Sciences, University of Bonn, Bonn, Germany; <sup>b</sup>Federal Institute for Drugs and Medical Devices, Department 45: Pharmacopoeia, Bonn, Germany; <sup>c</sup>Institute of Bio- and Geosciences, IBG-2, Plant Sciences, Research Centre Juelich, Juelich, Germany

### ABSTRACT

Selenium is a non-essential element with beneficial and toxic effects on plants, whose exact role in plant physiology leaves many unanswered questions. Various species of hydroponically grown plants produce defined selenium nano particles (SeNP) with a narrow size distribution and about 2 million selenium atoms by biosynthesis when being exposed to selenite, proving that green synthesis of SeNP is not only possible in plants extracts, but also in living organisms. The detection was performed with single particle inductively coupled plasma mass spectrometry. These results require a new view of the selenium biochemistry in plants and its impact on nutrition, food sciences and medicine. To the best of our knowledge, this is the first report on the synthesis of elemental nanoparticles in general and selenium nanoparticles in particular by living plants.

### ARTICLE HISTORY

Received 26 August 2022  
 Revised 14 November 2022  
 Accepted 22 November 2022

### KEYWORDS

Selenium; nanoparticles;  
 sp-ICP-MS;  
 biosynthesis; plant

## Introduction

Selenium is an element of the chalcogenide group and one of the most versatile trace elements. In contrast to other species, selenium is not considered essential for plants [1,2]. While among other mammals humans rely on selenocysteine (SeCys) in the catalytic centre of enzymes like glutathione peroxidase (GPx) or thioredoxin reductase (TrxR), the plant homologues contain cysteine (Cys) [3]. Though not considered essential, selenium can still have beneficial impact on plants and increase the activity of said enzymes while also improving the resistance against cold, drought and metallic stress [4]. Still, selenium accumulation bears the danger to impair cell integrity and metabolism. Toxic effects of selenium in plants are mostly caused by unintentional incorporation of SeCys and selenomethionine (SeMet) into proteins [5], but also include oxidative and nitrosative stress [2].

Selenium occurs in multiple oxidative states ranging from -II to +VI just like sulphur and coherently it forms analogous compounds, including selenide ( $\text{Se}^{2-}$ ), selenite ( $\text{SeO}_3^{2-}$ ) and selenate ( $\text{SeO}_4^{2-}$ ). Plants are able to take up a variety of selenium compounds, but the most abundant forms of selenium in soil are selenate in alkaline and oxic environments and selenite in anaerobic and acidic environments. Selenate uptake is catalysed by high-affinity sulphate transporters (HASTs) while phosphate transporters such as OsPt2 and aquaporin channels such as OsNIP2;1 catalyse selenite uptake [6]. Generally, the similarities between selenium and sulphur hint towards many functions of selenium in biochemistry.

Selenium shows superiority to sulphur in the catalytic centre of enzymes in the form of increased catalytic activity. Due to selenium being a good nucleophile and electrophile, peroxidases containing SeCys instead of Cys can more easily regenerate throughout an oxidoreductive cycle, leading to the hypothesis that one of selenium's functions is the prevention of irreversible oxidative inactivation [7]. Selenium's ability to be both rapidly oxidised and reduced, also known as 'selenium paradox' could explain why non selenium dependent species such as those within the plant kingdom may profit from low doses of selenium, as the unintentional incorporation of SeCys into the active centre of enzymes can benefit their activity.

Due to their similar biochemical characteristics selenium and sulphur share metabolic pathways and are substrates to the same enzymes, which can cause damage. A high concentration of selenium in plant tissues is overall associated with a high concentration of sulphur. In terms of selenium uptake plants can be divided in non-accumulators, secondary accumulators and hyperaccumulators. They are classified by their selenium concentration of either  $>1000 \text{ mg/kg}$ ,  $100\text{--}1000 \text{ mg/kg}$  or  $<100 \text{ mg/kg}$  dry weight [2,4]. Selenium hyperaccumulators show a greater ratio of selenium to sulphur concentrations than non-accumulators. Selenate uptake decreases drastically in soil with an excess of sulphate over selenate for non-accumulators, this does not apply for hyperaccumulators [8].

Inorganic selenium compounds can be reductively converted to SeCys [2]. Furthermore, it has been shown that the

**CONTACT** Klaus Günther  [\[k.guenther@fz-juelich.de\]\(mailto:k.guenther@fz-juelich.de\)](mailto:k.guenther@fz-juelich.de)  Institute of Nutritional and Food Sciences, University of Bonn, Bonn, Germany; Institute of Bio- and Geosciences, IBG-2, Plant Sciences, Research Centre Juelich, Juelich, Germany

 Supplemental data for this article is available online at <https://doi.org/10.1080/21691401.2022.2155660>.

© 2023 The Author(s). Published by Informa UK Limited, trading as Taylor & Francis Group  
 This is an Open Access article distributed under the terms of the Creative Commons Attribution License (<http://creativecommons.org/licenses/by/4.0/>), which permits unrestricted use, distribution, and reproduction in any medium, provided the original work is properly cited.

chloroplastic CpNifS protein that is involved in the formation of iron-sulphur clusters can also target SeCys [9]. For different plants the selenium speciation in different tissues varies due to the selenium compounds the plant is exposed to.

Signs for natural formation of SeNP in plants are so far unknown. The synthesis of selenium nanomaterials has been described using microorganisms like *Enterococcus faecalis* [10] or yeast [11,12], but it was also found that various plant extracts [13,14] can be used to synthesise SeNP. Sometimes reducing agents such as ascorbic acid were added to the mixture of plant extract and a selenium compound, but mostly it was found that the reductive potential of biomolecules within the plant extract had sufficient reductive potential for the synthesis of SeNP. Those molecules include amino acids, enzymes, flavonoids, phenolic compounds, proteins, saponins, sugars and tannins. While these studies on plant extracts and homogenates give no insight in the natural formation of nano particles in plants, it was our aim to investigate the potential synthesis of SeNP in intact cells of living plants. The cellular synthesis of iron oxide nano particles has already been described, however these are not elemental nanoparticles, but chemical compounds of the iron cations [15]. However, the synthesis of elemental nanoparticles in intact plants has not yet been described.

In this study it was our aim to prove the hypothesis that natural formation of SeNP takes place in plants when being objected to selenite. To do so, we grew plants under controlled conditions, to ensure they were not exposed to SeNP. These findings may not only have an impact on the green biosynthesis of nanoparticles (NP), but also raise questions on the role that NP might have in plant physiology and biochemistry. In contrast to previous research that focussed on plant extracts, we investigated the occurrence of so far unmentioned SeNP synthesis in living plant cells and analysed their size distribution using single particle inductively coupled mass spectrometry (sp-ICP-MS). By proving that nanoparticle synthesis is a naturally occurring phenomenon, it is safe to conclude that selenium nano particles are ingested by humans and animals. We see great necessity to investigate the impacts of this matter.

In contrast to plants, selenium is an essential element in the human organism. Selenium impacts thyroid metabolism, the antioxidant system and immune functions. Selenium supplementation has shown beneficial effects on male fertility, various kinds of cancer and then incidence of eclampsia, whereas selenium deficiency can cause cardiovascular and inflammatory diseases [16–21]. Furthermore, anti-infective properties have been described for selenium in general and for selenium nano particles (SeNP) specifically. Anti-viral properties of SeNP have been proven and latest publications even linked selenium levels in patients with the disease progression of Covid-19 and express the desirability to investigate the use of SeNP to fight the viral pandemic [22,23].

On the other hand, the possibility of toxic selenium concentrations and the narrow therapeutic range call for attention. Due to selenium's chemical similarity with sulphur, unusual seleno-amino acid, mostly SeCys and SeMet, can non-specifically replace their respective sulphuric equivalents, leading to faulty proteins [24]. It is therefore worth noticing that various

animal trials state lower toxicity and better bioavailability for SeNP in comparison with both inorganic and organic selenium [25–28]. SeNP are especially promising candidates for cancer treatment since improved efficiency and reduced toxicity can even be enhanced by conjugation with targeting agents on the surface [27]. Different kinds of modified and unmodified SeNP have been proven to be efficient in inducing selective cell death in different kinds of cancer, including cervical carcinoma cells, oestrogen receptor  $\alpha$ -positive breast cancer cells and prostate cancer cells [12,27,29]. It has also been shown in mice that, when given the same amount of selenium in form of SeNP of different sizes, the smaller SeNP showed greater increase in the activity of SeCys dependent enzymes like GPx or TrxR. This size effect gives a necessity to synthesise SeNP in a narrow size range, to achieve precise effects in the treated organisms [30]. GIT absorption of SeNP is also size dependent, thus a way to reliably synthesise small SeNP can strongly enhance their pharmacokinetic properties and potential as drugs and food supplements [31].

## Materials and methods

Ultrapure water (18.2 M $\Omega$ ·cm) was produced by Sartorius arium® pro ultrapure water system. For homogenisation of the plants tissues a Qiagen Tissue Ruptor II was used. For plant digestion Macerozyme R-10 enzyme derived from *Rhizopus* sp. was purchased from bioWorld. Proteinase K was purchased from GeneON. Citric acid and disodium hydrogen citrate for the preparation of a citrate buffer were purchased from Sigma-Aldrich. Gold and selenium reference standard solutions for calibration were purchased from Perkin Elmer. SeNP reference standard suspensions were purchased from Nanocs. Spectra/Por® 3 dialysis membrane MWCO 3.5 kD and Spectra/Por® closures were purchased from Fisher Scientific.

The hydroponic system was purchased from growland. So was the GHE TriPart series of nutritional solutions. Hoagland's solution was purchased from Biozol. The sodium selenite was purchased from Sigma-Aldrich. Formalin solution 10% was purchased from Sigma-Aldrich. Ethanol 96% was purchased from Merck. All seeds were purchased from local supermarkets.

The sp-ICP-MS analysis was performed with a Perkin Elmer NexION 350D equipped with a quartz cyclonic spray chamber (Perkin Elmer, Waltham MA, USA) and a glass nebuliser (Ar 1.0 SLPM @ 43 psi, Golden CO, USA). Peristaltic pump tubing (polyvinyl chloride) was obtained from Perkin Elmer, with an inner diameter of 0.38 mm and flared ends. Samples were prepared in 50 ml polypropylene tubes (Sarstedt AG and Co.KG, Nümbrecht, Germany) or 15 ml sterile polypropylene tubes (CELLSTAR® TUBES, Germany).

## Plant treatment

Brown mustard (*Brassica juncea*), barley (*Hordeum vulgare*), flax (*Linum usitatissimum*), lentil (*Lens culinaris*), bell pepper (*capsicum annuum*), butter lettuce (*Lactuca sativa*), carrot (*Daucus carota subsp. sativus*) and cucumber (*Cucumis sativus*) were used in our research.

The seeds were surface sterilised with 10% formalin solution for 10 min and rinsed thoroughly with ultrapure water. For up to 7 days the seeds were germinated on filter paper, moisturised with ultrapure water, and subsequently transferred into a hydroponic system, containing a growth solution with all essential nutrients that was spiked with sodium selenite. The concentration of sodium selenite in the nutritional solution was 5 mg/l, equivalent to a selenium concentration of 28.91 µM/l. For barley and brown mustard the GHE TriPart Series was used as nutritional solution, for the other plants Hoagland Solution at quarter strength was used. Water was added every other day to keep the water level roughly constant. Light was distributed with two 55 W neon tubes and a reflector. The neon tubes emitted a colour temperature of 6500 K. The days were split into a 16-h light and an 8-h darkness period, in which no artificial light was emitted. The light source was placed about 30 cm above the seeds and was powered from 6 am to 10 pm. The plants grew 28 to 42 days. Following the harvesting, shoot and root were separated and rinsed with the root crown being disposed to avoid intermixing.

The root tissues were cleaned with DI water, roughly cut, and stirred in 0.1 M citrate buffer (pH 6) for 48 h to clean the surface from the nutritional solution, and afterwards again rinsed with DI water. After cleaning 100 mg of root tissue were transferred in 8 ml of 0.1 M citrate buffer and homogenised with a tissue ruptor for 2 min. The shoot tissue was just rinsed with DI water without being washed and stirred for 48 h before being homogenised. 2 ml of Macerozyme R-10 solution (50 mg/ml) and 50 µl of Proteinase K (20 mg/ml) were added to the homogenate and shaken for 24 h at 37 °C. 500 µl of the supernatant were spiked with 500 µl of ethanol, and diluted to 5 ml with 0.1 M citrate buffer (pH 6) and transferred into a piece of dialysis tubing made from regenerated cellulose with a MWCO of 3500 Da. The closed tubing was stirred in a mixture of 50 ml ethanol and 450 ml of aforementioned citrate buffer for 24 h. Subsequently the content of the tubing was diluted back to a volume of 5 ml. 500 µl of dialysis product were diluted to 5 ml with ultrapure water and measured directly. The study was performed with two individual growth cycles for every plant. Each time, three plants per species were grown and their roots and shoots were analysed, making for a total of six specimens per plant that were included in the study. If the analysis resulted in a concentration of dissolved selenium greater than 1 ppb, which was found to be prone to false positive results, 500 µl of dialysis product were instead spiked with 50 µl of ethanol and diluted to 10 ml, resulting in an analysis at half concentration compared to the rest. This was done for the following samples: Carrot 2 and 3 root in the first replicate. Butter lettuce 2 root and shoot in the second replicate. Capsicum 2 shoot in the second replicate. Lens 1, 2 and 3 root in the second replicate.

#### **ICP-MS method and parameters**

A method was developed using the Syngistix software with nano application measuring the  $^{80}\text{Se}$  isotope with a relative

abundance of 49.61%. Argon-dimer interference was removed using hydrogen in a dynamic reaction cell (DRC). The dwell time was set to 50 µs and measuring time to 120 s, while see settling time was eliminated completely. The sample flow rate was determined daily. Further instrumental parameters included:

RF power	1300 W
Plasma Ar flow	15 L/min
Reaction cell gas flow ( $\text{H}_2$ )	4.4 ml/min
RPq	0.8 V
Deflector attractor	-135 V
Deflector entrance lens	-50 V
Transport efficiency	3.69%

#### **Results**

All plants were healthy. Shape and colour were unremarkable and primary and secondary roots developed normally.

The sp-ICP-MS analysis was performed on a NexION 350 D system. We utilised the system's ability to reduce the dwell time to 50 µs to decrease noise and detection limit. The detection of  $^{80}\text{Se}$ , the isotope of interest, is highly interfered by  $^{40}\text{Ar}$  dimer cations, we used the direct reaction cell (DRC) technology and introduced hydrogen gas to eliminate the disturbance. This may have been affecting the selenium signal strength. The slope, indicating the ratio between selenium concentration and signal strength is not large enough to allow for precise size differentiation in the lower nm area, therefore steps of 5 nm are used in the following figures, which is intended to represent a more realistic distribution of particles within the samples.

While the majority of particles is in the size range between 30 and 65 nm, few particles were found with diameters up to 400 nm. For the sake of clarity these outliers have not been included in the histograms in Figures 1–4, please consult the [supplementary information](#) for the full list.

In general, no clear tendency can be observed for the difference in root and shoot tissues regarding number or size distribution of SeNP. A broader size distribution and a larger number of SeNP appears to manifest in both root and shoot tissue of the respective plant.

In mustard there is a slight shift for the most abundant particle size. While in the root tissue of all plants the maximum was observed between 46 and 50 nm, the most frequently detected particle sizes in the shoot tissue were between 30 and 45 nm.

Barley root and shoot tissue show very similar SeNP distribution pattern, with just few slightly larger particles in the root tissues.

Linum roots show a broader distribution and a higher number of SeNP than linum shoots. The large number of detected particles and the shapes of the histograms of linum root tissue also suggest a considerable amount of SeNP with a diameter of 30 nm or less, that were not detected due to the size detection limit.

The results for lentils in both root and shoot tissues a very inconsistent. While all plants clearly show occurrence of SeNP

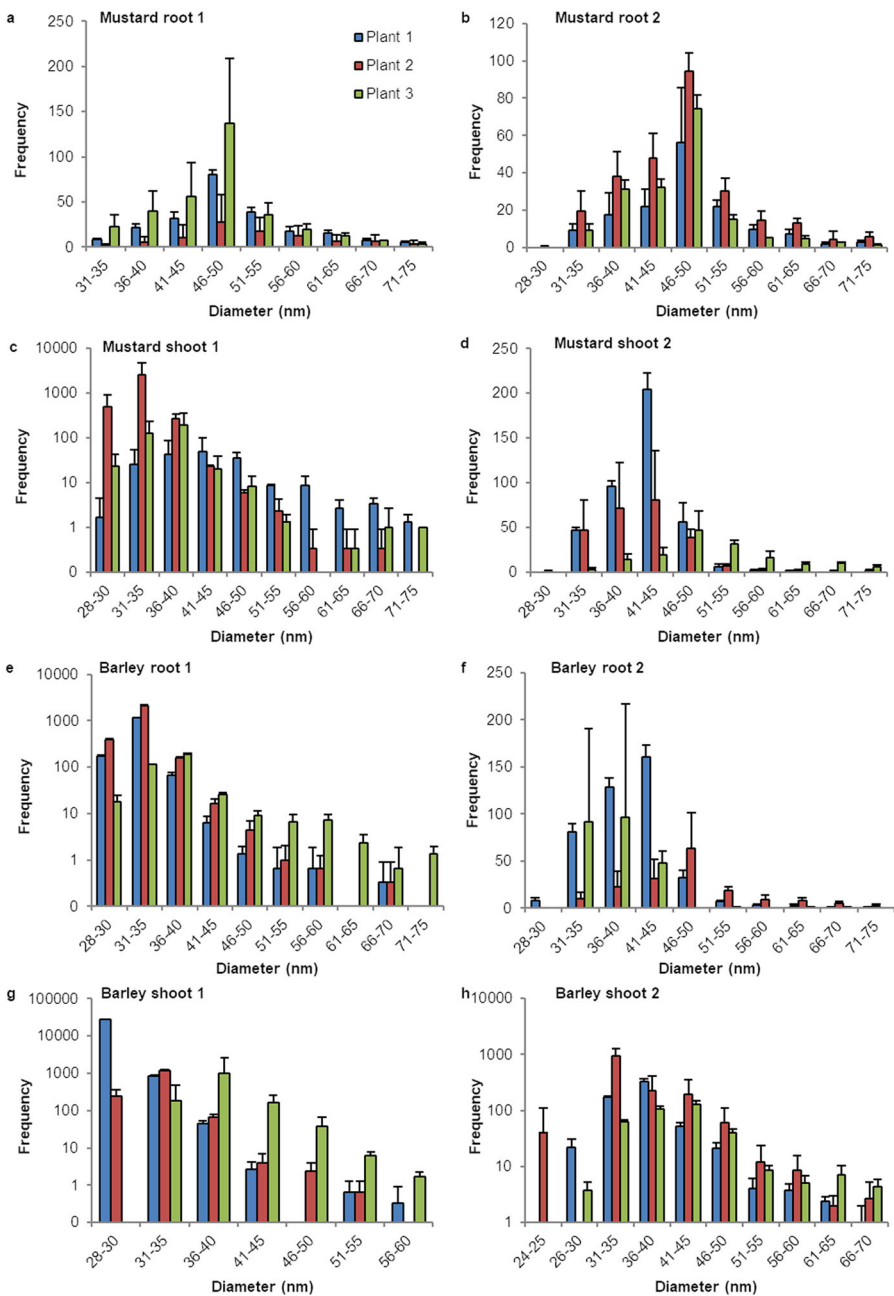


**Figure 1.** Size distribution of SeNP in root and shoot tissues of barley and brown mustard plants. Histograms for the sp-ICP-MS analysis of the first duplicate of (a) mustard root, (c) mustard shoot, (e) barley root and (g) barley shoot and the second duplicate of (b) mustard root, (d) mustard shoot, (f) barley root and (h) barley shoot. The error indicators represent the standard deviation for the three replicates that were measured from every sample. While in some measurements, nano particles with a size of up to 400 nm where detected, these histograms are cropped to show the main distribution of SeNP. A full list of the results and histograms showing individual data points for every run can be found in the [supplementary information](#).

the number of particles, the size range and size distribution vary strongly among all samples.

Unlike the other species *capsicum* shows consistently more SeNP in the shoot samples in comparison the root tissues. While all root samples show strong selenium nano signals mostly ranging from 40 to 90 nm with a maximum between 46 and 60 nm, the corresponding shoot tissues contain larger amounts of nano particles in a broader distribution ranging from 30 to 160 nm.

The lettuce samples showed overall broad distribution of SeNP. While there was a lot of variation among the different plants of this species and maximum particle numbers lying

between 40 and 70 nm, particles were detected with diameters of up to 110–140 nm in all root and shoot samples.

Cucumbers have a rather narrow size distribution of SeNP compared to the large number of particles that can be found in root and shoot tissue. With no clear differences between the two plant parts, a quite sharp cut off can be seen around 75–90 nm. However, the shape of the histograms suggests the existence of particle with a size of less than 30 nm that fell below the size detection limit, especially in the roots.

Carrots show many SeNP in root and shoot samples, yet clear differences can be observed. Generally, there are more particles in the root tissue with a broader distribution from

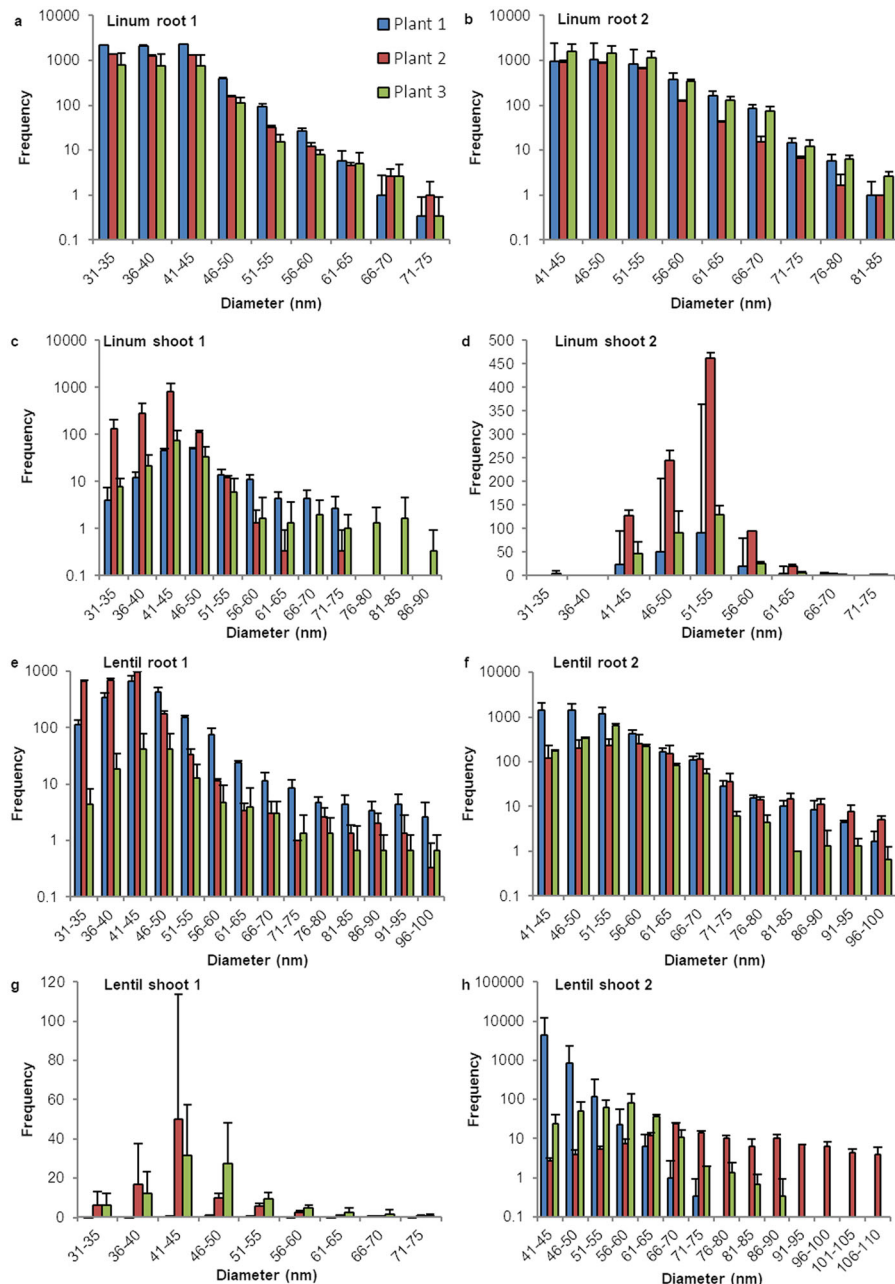


**Figure 2.** Size distribution of SeNP in root and shoot tissues of linum and lens plants. Histograms for the sp-ICP-MS analysis of the first duplicate of (a) linum root, (c) linum shoot, (e) lens root and (g) lens shoot and the second duplicate of (b) linum root, (d) linum shoot, (f) lens root and (h) lens shoot. The error indicators represent the standard deviation for the three replicates that were measured from every sample. While in some measurements, nano particles with a size of up 400 nm where detected, these histograms are cropped to show the main distribution of SeNP. A full list of the results and histograms showing individual data points for every run can be found in the [supplementary information](#).

36 to 120 nm, whereas the observed carrot shoots contain particles mostly in the area between 36 and 65 nm.

## Discussion

With a flow rate of about 0.25 ml/min, a measuring time of 2 min, and a concentration of either 100 µg/ml or 50 µg/ml, each histogram in Figures 1–4 represents the amount of SeNP that are detected in a sample that represents 50 µg or 25 µg of root or shoot tissue. With the developed method we detected SeNP in root and shoot tissue of all observed species. We observed variation within the results in terms of

number, size, and distribution of nano particles but nonetheless noticed some patterns and consistency. For most species the most detected particle size was located between 30 and 65 nm. Samples with a narrow size distribution usually showed a symmetrical size distribution on both sides of the maximum. Samples with a wider size distribution often lacked symmetry in size distribution with a large quantity of SeNP bigger than the mean. The fairly bell-shaped histograms for barley, brown mustard and lens raise the assumption, that the actual size distribution for other plants might be more symmetrical than the one portrayed here, which is restricted by the size detection limit.

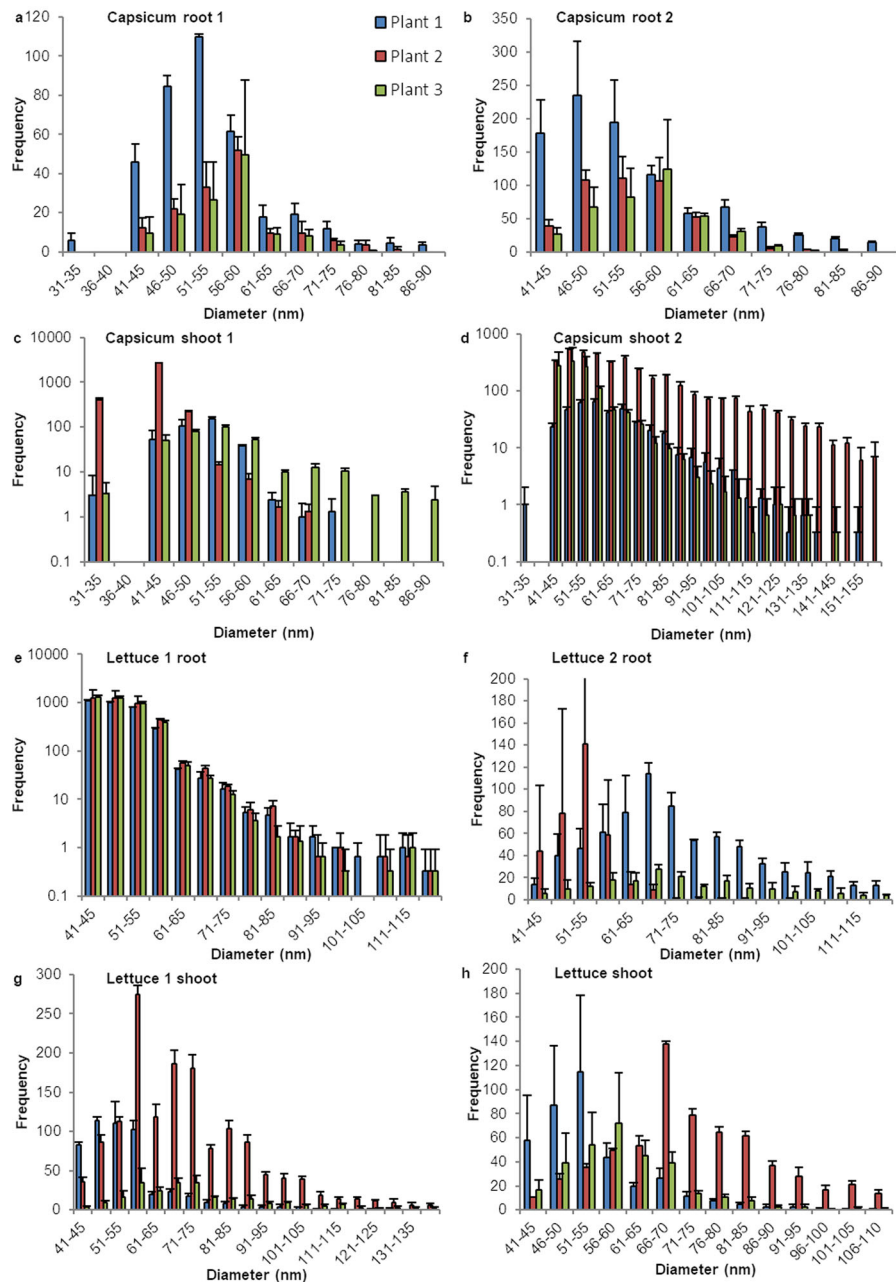


**Figure 3.** Size distribution of SeNP in root and shoot tissues of capsicum and butter lettuce plants. Histograms for the sp-ICP-MS analysis of the first duplicate of (a) capsicum root, (c) capsicum shoot, (e) butter lettuce root and (g) butter lettuce shoot and the second duplicate of (b) capsicum root, (d) capsicum shoot, (f) butter lettuce root and (h) butter lettuce shoot. The error indicators represent the standard deviation for the three replicates that were measured from every sample. While in some measurements, nano particles with a size of up 400 nm where detected, these histograms are cropped to show the main distribution of SeNP. A full list of the results and histograms showing individual data points for every run can be found in the [supplementary information](#).

It should be kept in mind, that not only sp-ICP-MS is quite a new method, but even more the analysis of SeNP with an sp-ICP-MS method has rarely ever been done. Furthermore, given that no naturally derived SeNP in plants have ever been analysed before, the newly developed digestion and dialysis methods create many unknown variables and therefore the quantitative aspect of the given results should not be overestimated. However, several hundred to several thousand particles were found in every sample and the results clearly indicate the occurrence of SeNP in both plant shoots and roots, for all the included plants. The consistent

detection of NP in a specific range suggests the existence of a system within the plant physiology that leads to the synthesis of SeNP. Samples were taken from the nutrient solutions of different growth cycles and tested for SeNP. None were found, from which we concluded, that the nano particle synthesis was not caused by microorganisms within the solution but took place within the plants.

Given, that the main share of NP found in this study is no larger than 50 nm in diameter and the earlier described size effect stating that smaller NP can have a stronger impact on the activity of selenium dependent enzymes, the here

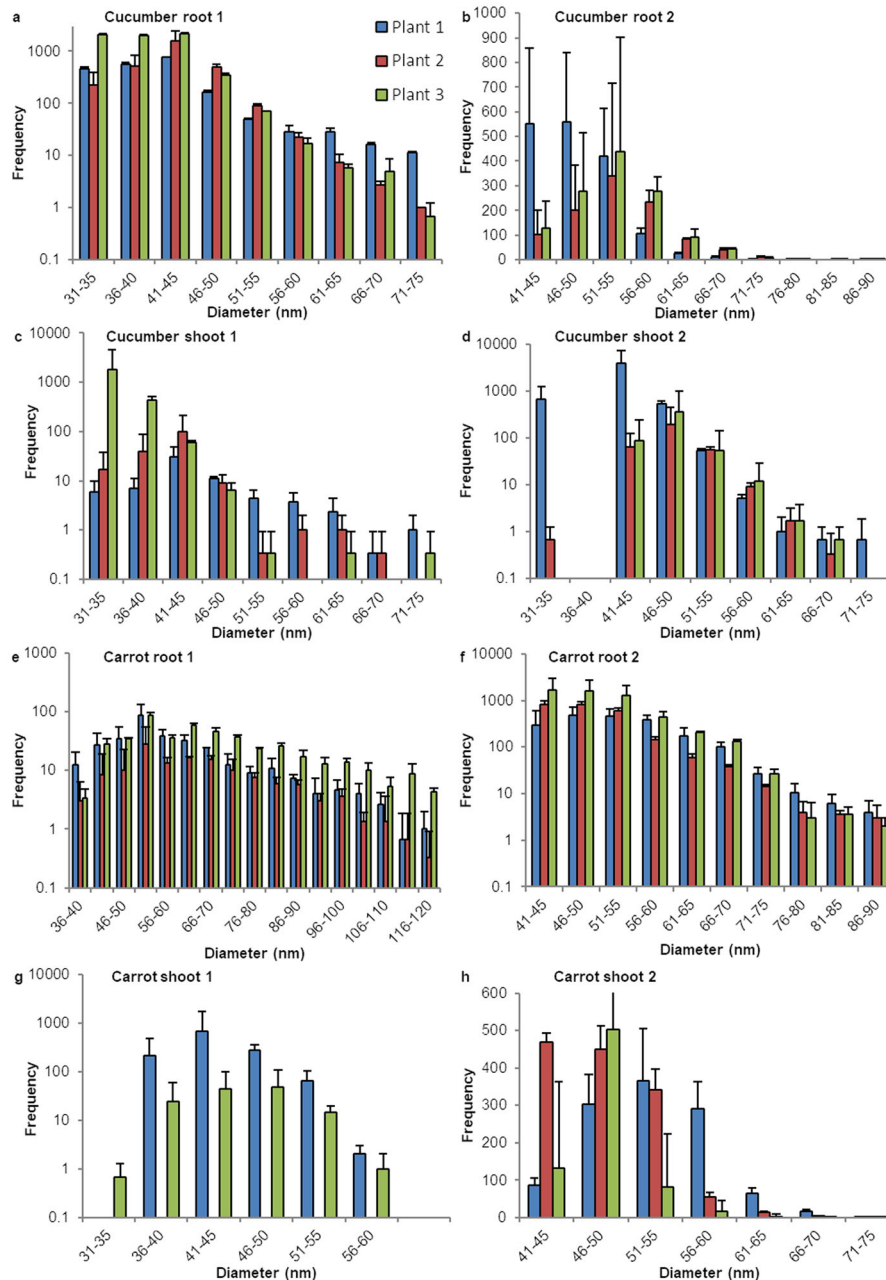


**Figure 4.** Size distribution of SeNP in root and shoot tissues of cucumber and carrot plants. Histograms for the sp-ICP-MS analysis of the first duplicate of (a) cucumber root, (c) cucumber shoot, (e) carrot root and (g) carrot shoot and the second duplicate of (b) cucumber root, (d) cucumber shoot, (f) carrot root and (h) carrot shoot. The error indicators represent the standard deviation for the three replicates that were measured from every sample. While in some measurements, nano particles with a size of up 400 nm where detected, these histograms are cropped to show the main distribution of SeNP. A full list of the results and histograms showing individual data points for every run can be found in the [supplementary information](#).

described NP or plants containing those NP are very promising candidates for the treatment and prevention of diseases that are linked to a low selenium status.

Previous research focussed on the synthesis of SeNP using plant extracts. The materials used include leaves, fruits, peels and flowers. Different temperatures, times and the use of a microwave oven or use of additional reductive agents like ascorbic acid are mentioned [16]. This form of green synthesis is described to produce stable nano particles and is reliable, eco-friendly, and cost effective [13].

The particles synthesised with plant extracts show similar size distributions as the naturally grown ones in our study [13,32]. Phytochemicals with reductive properties including

polyphenols, flavonoids and saponins are also discussed as stabilising agents within the particles. Following the assumptions that the SeNP formed in living plants are constituted in the same way, their actual size might be larger than described in this study, since the sp-ICP-MS size calculation is based solely on the detected selenium isotopes. However, given that the nanoparticles derived from plant extracts are formed in a few hours, sometimes under the influence of heat, it is safe to assume that they do not contain the same components in the same ratio.

While the role of SeNP in plants and their commonness or even ubiquitousness in the plant kingdom call for further research, the developed method was able to proof the

biosynthesis of SeNP in living plants. All species that were analysed belong to very different orders of Angiospermae. In addition to that, plants like brown mustard are known to be selenium accumulators unlike other like barley, which is a non-accumulator. Still, all observed plants form SeNP, which is a strong hint that the formation of SeNP is not an isolated event, but one that occurs in plants with very different selenium tolerances and is part of a so far undiscovered metabolic pathway. These findings indicate that NP might be considerably more common in plants than expected and could be part of a physiological system that is to be studied.

Concerning human health and nutrition it can be stated that SeNP act superior to other selenium sources in terms of toxicity and effectiveness. Due to their small size and narrow size distribution, plant based SeNP are promising candidates for food supplements and drugs as they can also be expected to show great bioavailability.

Aside from the medical potential, we see cause for future research on three main botanical questions that we aim to investigate in the future: Is the biosynthesis of SeNP ubiquitous within the plant kingdom? How common are SeNP in edible parts of plants, such as fruits and vegetables? Is there a physiological system that involves the synthesis and metabolism of NP of further elements?

The formation of selenium nanoparticles in the metabolism of intact plants has not yet been described. By means of a combination method developed and optimised by us using enzymes, dialysis and single-particle mass spectrometry with inductively coupled plasma, selenium nanoparticles were reliably detected in both shoots and roots of eight different plant species. The existence of selenium nanoparticles thus appears to be a newly discovered natural biological principle commonly found in the plant kingdom. The very common selenium nanoparticles found in most plants have a mean size diameter of about 48 nm (30–65 nm).

According to the formulas

$$\text{NSe (30 nm)} = \frac{4}{3} * 3.14 * (30/2)^3 * 4.8 * 6 \\ \times 10^{23} / 79 * 10^{-21}$$

$$\text{NSe (48 nm)} = \frac{4}{3} * 3.14 * (48/2)^3 * 4.8 * 6 \\ \times 10^{23} / 79 * 10^{-21}$$

$$\text{NSe (65 nm)} = \frac{4}{3} * 3.14 * (65/2)^3 * 4.8 * 6 \\ \times 10^{23} / 79 * 10^{-21}$$

the nanoparticles consist of 0.52, 2.1, and 5.2 million selenium atoms with a size of 30 nm, 48 nm, and 65 nm, respectively. It would be interesting to clarify the internal structure and the coating of the surface, and of course the plant physiological function.

## Acknowledgments

We thank the German Federal Institute for Drugs and Medical Devices for providing the laboratory equipment that was used for this study and Dr. Norwig for his work and support.

## Author contributions

J.V. and K.G. designed the experiments. J.V. performed the experiments and analysed the data with supervision by K.G. J.V. and K.G. wrote the manuscript.

## Disclosure statement

No potential conflict of interest was reported by the author(s).

## Funding

The laboratory equipment, analytical instruments and materials used were funded by: Federal Institute for Drugs and Medical Devices [PN 20570003].

## ORCID

Jonas Verstegen  <http://orcid.org/0000-0002-4339-5087>

Klaus Günther  <http://orcid.org/0000-0003-0541-6980>

## Data availability statement

The data for Figures 1–4 are shown in the supplementary information.

## References

- [1] Schiavon M, Pilon-Smits EAH. The fascinating facets of plant selenium accumulation – biochemistry, physiology, evolution and ecology. *New Phytol.* 2017;213(4):1582–1596.
- [2] White PJ. Selenium metabolism in plants. *Biochim Biophys Acta Gen Subj.* 2018;1862(11):2333–2342.
- [3] Bela K, Horváth E, Gallé Á, et al. Plant glutathione peroxidases: emerging role of the antioxidant enzymes in plant development and stress responses. *J Plant Physiol.* 2015;176:192–201.
- [4] Gupta M, Gupta S. An overview of selenium uptake, metabolism, and toxicity in plants. *Front Plant Sci.* 2016;7:2074.
- [5] Kolbert Z, Molnár Á, Feigl G, et al. Plant selenium toxicity: proteome in the crosshairs. *J Plant Physiol.* 2019;232:291–300.
- [6] White PJ. Selenium accumulation by plants. *Ann Bot.* 2016;117(2):217–235.
- [7] Reich HJ, Hondal RJ. Why nature chose selenium. *ACS Chem Biol.* 2016;11(4):821–841.
- [8] Lima LW, Pilon-Smits EAH, Schiavon M. Mechanisms of selenium hyperaccumulation in plants: a survey of molecular, biochemical and ecological cues. *Biochim Biophys Acta Gen Subj.* 2018;1862(11):2343–2353.
- [9] Van Hoewyk D, Garifullina GF, Ackley AR, et al. Overexpression of AtCpNifS enhances selenium tolerance and accumulation in arabidopsis. *Plant Physiol.* 2005;139(3):1518–1528.
- [10] Shoeibi S, Mashreghi M. Biosynthesis of selenium nanoparticles using *Enterococcus faecalis* and evaluation of their antibacterial activities. *J Trace Elem Med Biol.* 2017;39:135–139.
- [11] Jiménez-Lamana J, Abad-Álvaro I, Bierla K, et al. Detection and characterization of biogenic selenium nanoparticles in selenium-rich yeast by single particle ICPMS. *J Anal At Spectrom.* 2018;33(3):452–460.
- [12] Nayak V, Singh KRB, Singh AK, et al. Potentialities of selenium nanoparticles in biomedical science. *New J Chem.* 2021;45(6):2849–2878.
- [13] Anu K, Singaravelu G, Murugan K, et al. Green-Synthesis of selenium nanoparticles using garlic cloves (*Allium sativum*): biophysical characterization and cytotoxicity on vero cells. *J Clust Sci.* 2017;28(1):551–563.
- [14] Cittrarasu V, Kaliannan D, Dharman K, et al. Green synthesis of selenium nanoparticles mediated from *ceropogia bulbosa* roxb

- extract and its cytotoxicity, antimicrobial, mosquitocidal and photocatalytic activities. *Sci Rep.* 2021;11(1):1032.
- [15] Janthima R, Siri S. Cellular biogenesis of metal nanoparticles by water velvet (*Azolla pinnata*): different fates of the uptake Fe<sup>3+</sup> and Ni<sup>2+</sup> to transform into nanoparticles. *Artif Cells Nanomed Biotechnol.* 2021;49(1):471–482.
- [16] Kryukov GV, Castellano S, Novoselov SV, et al. Characterization of mammalian selenoproteomes. *Science.* 2003;300(5624):1439–1443.
- [17] Reeves MA, Hoffmann PR. The human selenoproteome: recent insights into functions and regulation. *Cell Mol Life Sci.* 2009; 66(15):2457–2478.
- [18] Rayman PM. Selenium and human health. *Lancet.* 2012;379(9822): 1256–1268.
- [19] Carlisle AE, Lee N, Matthew-Onabanjo AN, et al. Selenium detoxification is required for cancer-cell survival. *Nat Metab.* 2020;2(7): 603–611.
- [20] Kang D, Lee J, Wu C, et al. The role of selenium metabolism and selenoproteins in cartilage homeostasis and arthropathies. *Exp Mol Med.* 2020;52(8):1198–1208.
- [21] Pyrzynska K, Sentkowska A. Biosynthesis of selenium nanoparticles using plant extracts. *J Nanostruct Chem.* 2022;12(4): 467–480.
- [22] Lin Z, Li Y, Guo M, et al. Inhibition of H1N1 influenza virus by seleniumnanoparticles loaded with zanamivir through p38and JNK signaling pathways. *RSC Adv.* 2017;7(56):35290–35296.
- [23] He L, Zhao J, Wang L, et al. Using nano-selenium to combat coronavirus disease 2019 (COVID-19)? *Nano Today.* 2021;36:101037.
- [24] Hoffman KS, Vargas-Rodriguez O, Bak DW, et al. A cysteinyl-tRNA synthetase variant confers resistance against selenite toxicity and decreases selenocysteine misincorporation. *J Biol Chem.* 2019; 294(34):12855–12865.
- [25] Jia X, Li N, Chen J. A subchronic toxicity study of elemental nano-Se in Sprague-Dawley rats. *Life Sci.* 2005;76(17):1989–2003.
- [26] Wang H, Zhang J, Yu H. Elemental selenium at nano size possesses lower toxicity without compromising the fundamental effect on selenoenzymes: comparison with selenomethionine in mice. *Free Radic Biol Med.* 2007;42(10):1524–1533.
- [27] Menon S, Devi KS, Santhiya R, et al. Selenium nanoparticles: a potent chemotherapeutic agent and an elucidation of its mechanism. *Colloids Surf B Biointerfaces.* 2018;170:280–292.
- [28] Bhattacharjee A, Basu A, Bhattacharya S. Selenium nanoparticles are less toxic than inorganic and organic selenium to mice in vivo. *Nucleus.* 2019;62(3):259–268.
- [29] Liao G, Tang J, Wang D, et al. Selenium nanoparticles (SeNPs) have potent antitumor activity against prostate cancer cells through the upregulation of miR-16. *World J Surg Oncol.* 2020; 18(1):81.
- [30] Peng D, Zhang J, Liu Q, et al. Size effect of elemental selenium nanoparticles (nano-Se) at supranutritional levels on selenium accumulation and glutathione S-transferase activity. *J Inorg Biochem.* 2007;101(10):1457–1463.
- [31] Skalickova S, Milosavljevic V, Cihalova K, et al. Selenium nanoparticles as a nutritional supplement. *Nutrition.* 2017;33:83–90.
- [32] Ghaderi RS, Adibian F, Sabouri Z, et al. Green synthesis of selenium nanoparticle by abelmoschus esculentus extract and assessment of its antibacterial activity. *Mater Technol.* 2022;37: 1289–1297.

## **Appendix B**

### **Ubiquitous Occurrence of Nano Selenium in Food Plants**

## Article

# Ubiquitous Occurrence of Nano Selenium in Food Plants

Jonas Verstegen <sup>1,2</sup>  and Klaus Günther <sup>1,3,\*</sup> 

<sup>1</sup> Institute of Nutritional and Food Sciences, University of Bonn, 53115 Bonn, Germany

<sup>2</sup> Federal Institute for Drugs and Medical Devices, 53175 Bonn, Germany

<sup>3</sup> Research Centre Juelich, Institute of Bio- and Geosciences, IBG-2, Plant Sciences, 52428 Jülich, Germany

\* Correspondence: k.guenther@fz-juelich.de

**Abstract:** Selenium is an essential trace element in human nutrition. Recent findings suggest that the biosynthesis of selenium nano particles (SeNPs) in plants might be a ubiquitous phenomenon. We investigated the potential of SeNP biosynthesis in food plants and our core objective was to explore the commonness and possible ubiquitousness of nano selenium in food plants and consequently in the human diet. By growing a variety of plants in controlled conditions and the presence of selenite we found strong evidence that SeNPs are widely present in vegetables. The shoots and roots of seven different plants, and additionally Brazil nuts, were analyzed with single-particle inductively coupled plasma mass spectrometry with a focus on edible plants including herbs and salads. SeNPs were found in every plant of our study, hence we conclude, that SeNPs are common ingredients in plant-based food and are therefore eaten daily by most humans. Considering the concerning worldwide prevalence of selenium deficiency and the great physiological properties of SeNPs, we see a high potential in utilizing this discovery.

**Keywords:** selenium; nanoparticles; sp-ICP-MS; biosynthesis; plant; nutrition; crop science

## 1. Introduction

Selenium is an essential trace element with great importance for human health. The oxidative states it occurs in are similar to sulfur-II to +VI and accordingly, selenium can be found in corresponding compounds, including selenide ( $\text{Se}^{2-}$ ), selenite ( $\text{SeO}_3^{2-}$ ), and selenate ( $\text{SeO}_4^{2-}$ ). The two latter ones, alongside organic compounds, namely selenomethionine (SeMet) and selenocysteine (SeCys), are well-described forms of selenium in human nutrition. The European Food Safety Authority (EFSA) recommends a daily intake of 70 µg/day for adult men and women and a progressive weight dependent amount between 15 µg/day (for ages 1 to 3 years and a reference body weight of 11.9 kg) and 55 µg/day (for ages 11 to 14 years and a reference body weight of 45.7 kg) for children. An adjusted intake during pregnancy is not recommended. Yet, the average daily intake is estimated by the EFSA to be between 31.0 and 65.6 µg/day in adults ( $\geq 18$  years) and 20.6 to 45.9 µg/day in children aged 3 to <10 years [1].

Intestinal absorption of selenium is generally good, particularly in comparison to other micronutrients, for example zinc (25% from milk and dairy food [2]) and iron (14 to 18% from mixed diets and 5 to 12% from vegetarian diets [3]). Absorption from selenite was found to be between 62 and 76% and above 90% for selenomethionine and selenate. The absorption of selenium in an unknown chemical state from food was found to be 83%, as tested on an intake of 100 g shrimp/day [4].

Selenium rich foods are mainly animal-based, they include fish, shellfish, and meat. Often in agriculture, fodder is enriched with selenium [5]. Plant-based food can be a less reliable source of selenium, as the selenium intake of plants is dependent on salinity, pH-levels, and soil composition, including the strong variation of the selenium content in soil [1,6]. The reliability of plants as selenium sources can be increased by using selenium-enriched fertilizer [7]. While small amounts of selenium can show beneficial effects on resistance



**Citation:** Verstegen, J.; Günther, K. Ubiquitous Occurrence of Nano Selenium in Food Plants. *Foods* **2023**, *12*, 3203. <https://doi.org/10.3390/foods12173203>

Academic Editor: Soledad Cerutti

Received: 2 August 2023

Revised: 15 August 2023

Accepted: 22 August 2023

Published: 25 August 2023



**Copyright:** © 2023 by the authors. Licensee MDPI, Basel, Switzerland. This article is an open access article distributed under the terms and conditions of the Creative Commons Attribution (CC BY) license (<https://creativecommons.org/licenses/by/4.0/>).

against stress factors like heat and drought, it is not considered an essential element for plants [8,9], and with few exceptions, only small amounts of selenium are tolerable for plants. Plant species can be divided into three groups, selenium non-accumulators, selenium accumulators, and selenium hyperaccumulators and concentrations of <100 mg/kg, 100–1000 mg/kg, or >1000 mg/kg dry weight can be found in those plants, given that there is sufficient selenium available in the soil [8,10].

A total of 25 human selenoproteins have been identified so far and play important roles in human physiology. Their functions include key roles in the immune system and cancer prevention, thyroid metabolism, brain function, fertility, and antioxidant processes [11–13]. Selenium deficiency is associated with cardiovascular disease, cancer, liver disease, osteoarthritis, and Keshan disease [14–18]. Selenium impacts apoptosis and autophagy in cardiomyocytes, therefore a deficiency cannot only cause Keshan disease, but other forms of cardiomyopathy as well [17]. The antiviral properties of selenium are especially promising in nano particles. Zanamivir-loaded SeNPs showed superior cell viability than zanamivir or SeNP alone and selenium is also associated with good outcomes in COVID-19 infections [19,20].

Due to its heavier and larger nature, selenium in the form of SeCys can be superior to sulfur and Cys in enzymes, as it is both a good electrophile and nucleophile. Sulfur is less polarizable than selenium and can therefore not regenerate to its active form within the catalytic cycle as easily and quickly [9].

Even for a micronutrient, the therapeutic range of selenium is noteworthy narrow, therefore food sources and food supplements containing selenium require to be of high quality with a minimized danger of toxicity. Thus, recommendations for selenium supplementation should be made with careful consideration for the soil of the respective area and the selenium supply due to food. Toxic effects of selenium mostly occur in protein biosynthesis where SeCys and SeMet might mistakenly be put in the place of Cys or Met [21]. This replacement can happen non-specifically and subsequently cause faulty proteins. Due to the important role of Cys in the structure and function of many proteins, it being replaced by SeCys bears a greater danger than Met being replaced by SeMet. SeNPs excel in that matter, since despite their great bioavailability and activity, their toxicity is lower than that of other selenium compounds [13,22–26].

Among the most promising applications for SeNPs are treatments for various kinds of cancer. An optimal selenium supply can decrease the incidence of cancer. Mostly its antioxidant nature and ability to control reactive oxygen species (ROS) and radicals factor into its chemopreventive nature. Decreased levels of selenium and seleno-enzymes, like glutathione peroxidase (GPx) for example, are associated with malignant melanoma, colorectal cancer, lung cancer, hepatocellular carcinoma, and gallbladder and biliary tract cancers [14,18,26,27]. However, increased levels of selenium can increase the risk of cancer as well. This double-edged relationship between selenium intake and cancer is particularly well described for prostate cancer [12,28,29].

SeNPs are superior to other forms of selenium as food supplements, due to their high bioavailability, low toxicity, and high biological activity [13]. Additionally, SeNPs were shown to be present in an elemental state and the  $\text{Se}^0$  is acting particularly well at protecting against heavy-metal toxicity [13,30]. This is achieved partly by direct reductive activity, but also by the induction of several pathways and enzymes like Nrf2, GSH, and hemoglobin oxygenase.

A modification of SeNPs can be performed and a conjugation with another agent that can, for example, be used to specifically target the tumor cells can enhance the antitumor activity while lowering its toxicity [24]. Successful applications of SeNPs include trials with estrogen receptor  $\alpha$ -positive breast cancer cells, colon cancer cells, prostate cancer cells, and cervical carcinoma cells [24,26,31–33]. The size effect of SeNPs and nano particles in general is still discussed. While some researchers find inconclusive results, some studies find that the activities of GPx, thioredoxin reductase, and other selenium dependent enzymes increase more when a given amount of SeNP is applied with smaller particles [34,35]. It is

therefore of great interest to the nutritional and medicinal science community to find ways to produce selenium in nano form with a small size and a narrow size distribution.

Recently, we found evidence that plants are able to naturally produce SeNP when exposed to selenite [26]. This was found for species from many different orders of plants and might turn out to be a ubiquitous phenomenon. Generally, selenium is not an essential nutrient for plants and so far, no genes that encode for SeCys or SeMet were found in a plant genome [8,9]. For most plants, selenium is mainly a potential toxin, potentially causing oxidative and nitrosative stress. Additionally, as in animals, seleno amino acids might be confused with their sulfuric equivalents and cause faulty proteins in plants as well [8,26,36]. Selenium can on the other hand still cause positive effects for plant organisms in small doses, like resistance to stress from factors like metallic stress and drought [10]. Furthermore, selenium can enhance plant growth and crop yield [37–39].

Selenium has a high bioavailability for organic and inorganic compounds. The uptake of selenate and selenite mostly happens through sulfate and phosphate transporters, respectively [6,40]. Many of the earlier described selenium hyperaccumulators belong to the family of Brassicaceae. Various food plants, namely cruciferous vegetables, belong to that family. In this research, it was our aim to investigate the potential synthesis of SeNPs in food plants and potentially find evidence that nano selenium is already part of many humans' diets. As a continuation of our previous work, we grew plants under controlled conditions in the presence of selenite and analyzed their SeNP content with single-particle mass spectrometry with inductively coupled plasma (sp-ICP-MS). It was our aim to quantify the amount of nano selenium and find insight into their size and size distribution and thus on the presence of nano selenium in food.

## 2. Materials and Methods

### 2.1. Chemicals and Instruments

A Sartorius arium® pro system was used to produce ultrapure water (18.2 MΩ·cm). A Qiagen Tissue Ruptor II was used to homogenize the plant samples. Macerozyme R-10 derived from *Rhizopus* sp. and Proteinase K were used for plant digestion. They were purchased from GeneON and bioWorld, respectively. For the buffer preparation, disodium hydrogen citrate and citric acid were purchase from Sigma-Aldrich. Dialysis membrane Spectra/Por® 3 with a MWCO of 3.5 kDa and the corresponding closures were purchased from Fisher Scientific.

For the plant growth, a hydroponic system by growland was used. Hoagland solution was prepared from a salt base that was purchased from Biozol. Sodium selenite to spike the growth solution and formalin solution to surface sterilize the seeds were purchased from Merck. Ethanol 96% that was used during the dialysis was purchased from Sigma-Aldrich.

A NexION 350D sp-ICP-MS by Perkin Elmer (Waltham, MA, USA) was used for the analysis. It was equipped with a quartz cyclonic spray chamber and a glass nebulizer (Ar 1.0 SLPM @ 43 psi). The peristaltic pump tubing with flared ends and an inner diameter of 0.38 mm was made of polyvinyl chloride.

Polypropylene tubes with a volume of 50 mL were purchased from Sarstedt AG & Co.KG (Nümbrecht, Germany) and tubes with a volume of 15 mL were purchased from Cellstar.

### 2.2. Plant Treatment

Basil (*Ocimum basilicum*), dill (*Anethum graveolens*), chard (*Beta vulgaris*), spinach (*Spinacia oleracea*), brussels sprouts (*Brassica oleracea var. gemmifera*), broccoli (*Brassica oleracea var. italica*), lamb's lettuce (*Valerianella locusta*), and Brazil nuts (*Bertholletia excelsa*) were used in our research.

The plant treatment was performed in the same way as in our previous work on SeNPs in plants [26]. Formalin solution with a 10% concentration was used to perform a surface sterilization on the seeds for 10 min. Ultrapure water was used to rinse of any remaining formalin. The seeds were transferred onto filter paper that was kept moist and dark in order

to allow germination for up to 7 days. After germination, the seedlings were conveyed to a hydroponic system, where they were grown for 28 to 42 days. Hoagland solution was used as growth solution, after it was diluted to quarter strength and was spiked with 5 mg/L sodium selenite, resulting in a concentration von 28.91 µmol/L of selenium.

Water absorption by the plants and evaporation was compensated every 2 to 3 days. Two neon tubes with a power of 55 W and a color temperature of 6500 K and a reflector were placed at a distance of 30 cm above the seeds. The plants were grown in 8 h of darkness and 16 h of artificial light. The light period started at 6 a.m. and ended at 10 p.m. After the growth period, the plants were harvested from the hydroponic system and the shoots were separated from the roots. Intermixing was avoided by disposing of the root crowns. Both tissues were rinsed with DI water.

The root surface was further cleaned. After a second rinse with DI water, rough cuts of the root tissue were prepared and subsequently transferred to a pH 6 M citrate buffer (0.1 M). The roots were stirred for 48 h to rinse off any residues of growth solution. The buffer solution was then rinsed off with DI water and a sample of 100 mg was taken from the tissue. Without the 48 h period, the shoots were treated in the same manner and samples of 100 mg were taken. A tissue ruptor was used to homogenize the samples in 8 mL of the earlier-described citrate buffer for 2 min.

A total of 2 mL of a 50 mg/mL solution of Macerozyme R-10 was added to the mixture as well as 50 µL of a 20 mg/mL solution of Proteinase K. The mixture was shaken at 37 °C. After 24 h, 0.500 mL of ethanol was mixed with 0.500 mL of supernatant and 4.000 mL of earlier-described citrate buffer. A dialysis was performed in 450 mL of buffer and 50 mL of ethanol. The dialysis tubing had a 3.5 kDa MWCO and after being filled with the 5 mL sample, it was stirred for 24 h.

The sample was removed from the tubing afterwards and if necessary, citrate buffer was added to a volume of 5 mL. The mixture was diluted by a factor of 10 with ultrapure water before being analyzed.

For every species, three individual plants were used and treated as described. If a concentration higher than 1 µg/L of dissolved selenium was found in a sample, the last dilution step was not performed with a factor of 10, but instead 50 µL of ethanol was added to 500 µL of sample, which was then diluted with ultrapure water to 10 mL, resulting in a dilution factor of 20 instead of 10. Sample 1 and Sample 2 of chard root required this treatment.

The Brazil nuts were cut into small pieces and samples of 100 mg were treated in the same manner as the root and shoot tissues. Two different brands of Brazil nuts were purchased from two different supermarkets and since they contained very different amounts of selenium, the second batch of Brazil nuts was analyzed without the last dilution step (1000 µg/mL) while the first batch was diluted to 50 mL in the last sample preparation step resulting in a concentration of 10 µg/mL.

### 2.3. ICP-MS Method and Parameters

A method was developed using the Syngistix software version 2.4 with nano application, measuring the 80Se isotope with a relative abundance of 49.61%. Argon-dimer interference was removed using hydrogen in a dynamic reaction cell (DRC). The dwell time was set to 50 µs and measuring time to 120 s, while the settling time was eliminated completely. The sample flow rate was determined daily. Further instrumental parameters included:

RF power	1300 W
Plasma Ar flow	15 L/min
Reaction cell gas flow (H <sub>2</sub> )	4.4 mL/min
RPq	0.8 V
Deflector Attractor	-135 V
Deflector Entrance Lens	-50 V
Transport Efficiency	7.26%

### 3. Results

The sp-ICP-MS analyses for basil and dill plants are displayed in Figure 1 and Table 1. All basil plants show moderate concentrations of dissolved selenium with 0.15 to 0.3 µg/L in the root and a low concentration between 0.05 and 0.1 µg/L in the shoot samples. The root tissues show fairly symmetrical histograms of nano particles with a narrow size distribution between 35 and 80 nm and a maximum between 50 and 55 nm. In accordance with the dissolved selenium, the number of nano particles is low to mediocre compared to other plants. The shoot samples appear to only have a very narrow size distribution with a surprisingly high number of particles in the range between 30 and 50 nm.

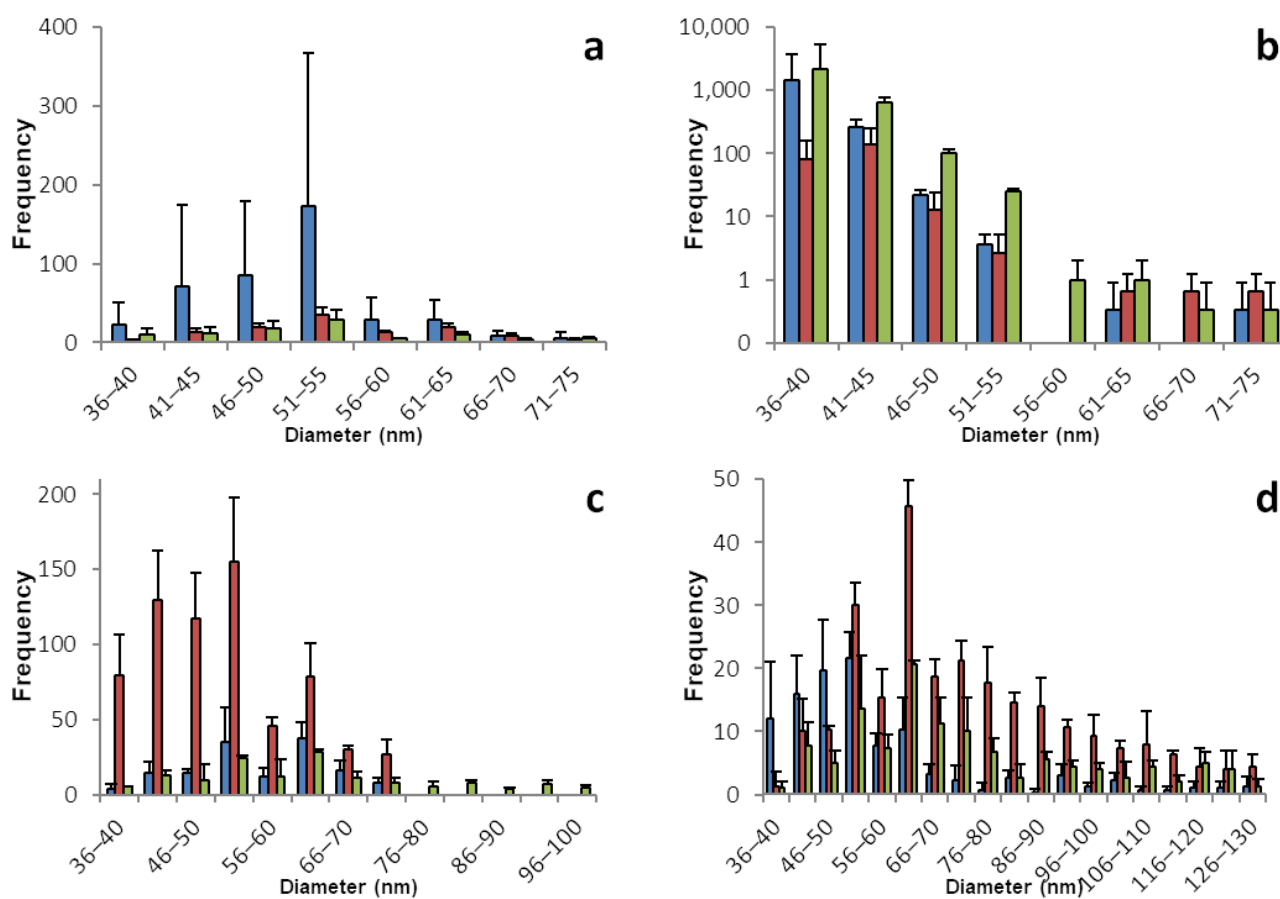


**Figure 1.** Size distribution of SeNPs in root and shoot tissues of basil and dill plants. These histograms show the sp-ICP-MS analysis of (a) basil root, (b) basil shoot, (c) dill root, and (d) dill shoot. Three specimens of each plant were grown, and each bar color represents a single plant. The standard deviation depicted describes the variation for 3 replicates of the same sample. Nano particles with a size of up to 531 nm were detected, however the histograms in this figure are meant to show the main distribution of SeNPs and were therefore cropped. Supplementary information S1 shows the full results. Supplementary information S2 shows histograms including all detected data points for the individual replicates.

Dill shows an astonishing amount of similarity between the root and shoot tissues. SeNPs are found in every plant. The dissolved selenium ranges from 0.3 to 0.5 µg/L in the roots and from 0.3 to 0.8 µg/L in the shoot samples. The maximum for both parts of the plant is between 40 and 60 nm. The histograms show a steep decline for the particles smaller than the maximum and a very flat and slow decline for the particles bigger than the maximum with few particles with a diameter between 300 and 500 nm found in all samples.

**Table 1.** Concentrations of dissolved selenium corresponding to the histograms shown in Figure 1.

	Root			Shoot		
Basil	1	2	3	1	2	3
Mean concentration of dissolved Se [ $\mu\text{g/L}$ ]	0.288	0.258	0.166	0.073	0.056	0.106
Standard deviation	0.003	0.006	0.005	0.005	0.003	0.001
Mass of Se per kg plant mass (fresh weight) [mg]	2.88	2.58	1.66	0.73	0.56	1.06
Dill						
Mean concentration of dissolved Se [ $\mu\text{g/L}$ ]	0.495	0.433	0.339	0.374	0.817	0.579
Standard deviation	0.029	0.011	0.007	0.003	0.019	0.007
Mass of Se per kg plant mass (fresh weight) [mg]	4.95	4.33	3.39	3.74	8.17	5.79

The sp-ICP-MS analyses for chard and spinach plants are displayed in Figure 2 and Table 2. Selenium nano particles were found in all chard plants. The samples prepared from plants 1 and 2 had high concentrations above 1 ppm of dissolved selenium, which are connected to an increased potential for false positive results. Those samples were remeasured at half concentration. All root samples show a great number of SeNPs in a broad range with the main share being between 40 and 80 nm in diameter. Fewer particles were found in the shoot tissue, especially for plants 1 and 2, which goes along with a lower concentration of dissolved selenium. Interestingly, the ratio of dissolved to nano selenium in root and shoot tissues for plants 1 and 2 is about 5:1 while for plant 3 the ratio is roughly 3:2. This comes along with a higher number of SeNPs in the shoot of plant 3, hinting that the ratio between dissolved and particulate selenium is not dependent on the organ, but rather the number of SeNPs in a plant part is dependent on the overall selenium concentration.

**Table 2.** Concentrations of dissolved selenium corresponding to the histograms shown in Figure 2.

	Root			Shoot		
Chard	1	2	3	1	2	3
Mean concentration of dissolved Se [ $\mu\text{g/L}$ ]	0.404	0.453	0.742	0.194	0.176	0.462
Standard deviation	0.012	0.009	0.023	0.009	0.004	0.006
Mass of Se per kg plant mass (fresh weight) [mg]	4.04	4.53	7.42	1.94	1.76	4.62
Spinach						
Mean concentration of dissolved Se [ $\mu\text{g/L}$ ]	0.565	0.560	0.362	0.357	0.552	0.378
Standard deviation	0.032	0.021	0.010	0.007	0.011	0.009
Mass of Se per kg plant mass (fresh weight) [mg]	5.65	5.60	3.62	3.57	5.52	3.78

All spinach plants formed similar amounts of selenium nano particles. With a slightly narrower distribution than chard, SeNPs can be found mostly in the range between 40 and 70 nm. While in plant 1 there is a ratio of roughly 3:2 of dissolved selenium in root compared to shoot samples, the ratio in plants 2 and 3 is close to 1:1. However, here, we can see a larger number of nano particles in the root tissues compared to the respective shoot samples. Keeping in mind that the used method is prone for variation and the exact quantification should not be overestimated it is noticeable here, that unlike in chard

plants, there is a tissue-dependent gradient and root samples have a larger amount of their selenium stored as SeNPs than their shoot counterparts.

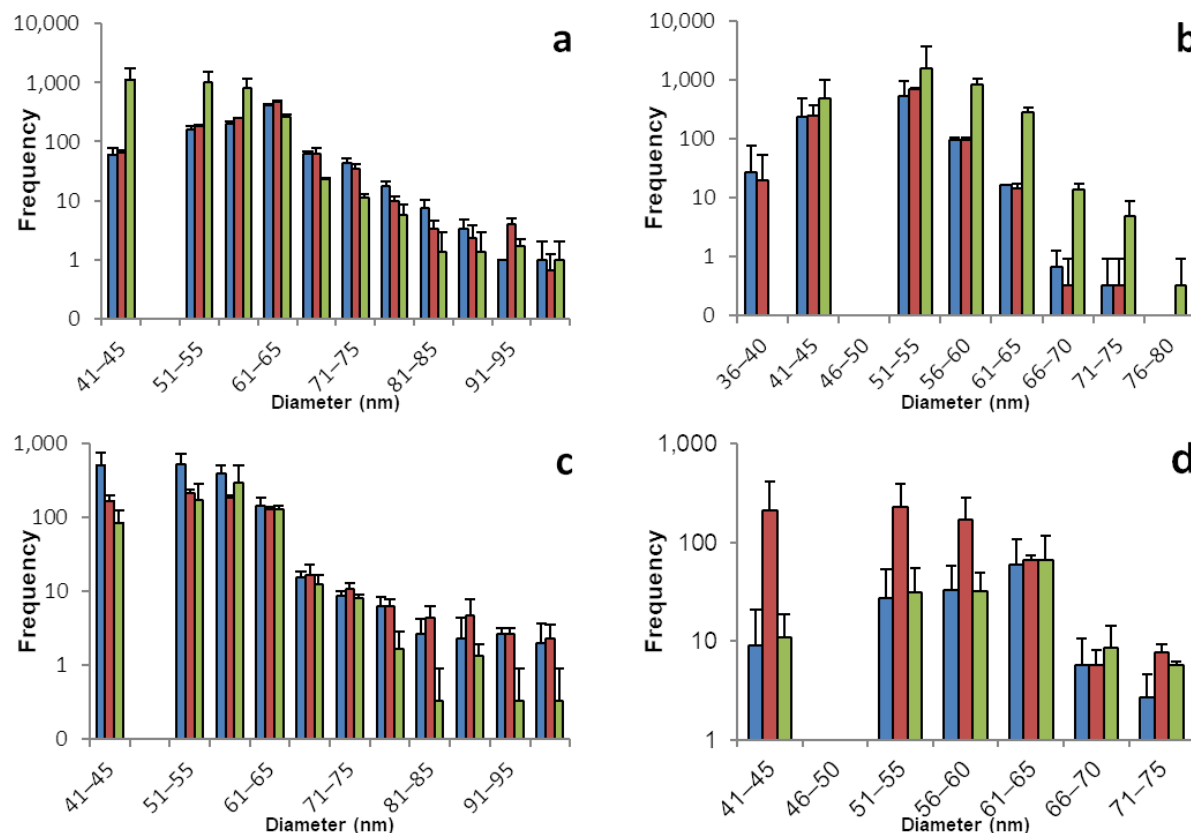


**Figure 2.** Size distribution of SeNPs in root and shoot tissues of chard and spinach plants. These histograms show the sp-ICP-MS analysis of (a) chard root, (b) chard shoot, (c) spinach root, and (d) spinach shoot. Three specimens of each plant were grown, and each bar color represents a single plant. The standard deviation depicted describes the variation for 3 replicates of the same sample. Nano particles with a size of up to 242 nm were detected, however the histograms in this figure are meant to show the main distribution of SeNPs and were therefore cropped. Supplementary information S1 shows the full results. Supplementary information S2 shows histograms including all detected data points for the individual replicates.

The sp-ICP-MS analyses for brussels sprouts and broccoli are displayed in Figure 3 and Table 3. Selenium. Brussels sprouts, especially the root samples show a great number of SeNPs. With a maximum between 50 and 65 nm, all root samples contained nano particles, which were up to 400 nm and over in diameter. In contrast to other plants with few particles larger than 100 nm in diameter, in brussels sprouts roots there was a dense and broad distribution of larger particles. The shoots, on the other hand, had a rather narrow distribution of nano particles, and overall fewer nano particles, mostly in the range between 40 and 60 nm in diameter. Analogous to the particles, the concentration of dissolved selenium was between 0.5 and 0.9 µg/L in the root samples and only between 0.1 and 0.3 µg/L in the shoot samples.

Broccoli, just like brussels sprouts, belongs to the plant family Brassicaceae, which contains all the cruciferous vegetables and that is known to contain many selenium accumulators. Unsurprisingly, the broccoli samples show selenium patterns that are similar to brussels sprouts. A great number of particles with a maximum between 60 and 75 nm in a broad distribution ranging up 500 nm is found in the root samples, which have a concentration of dissolved selenium between 0.4 and 0.6 µg/L.

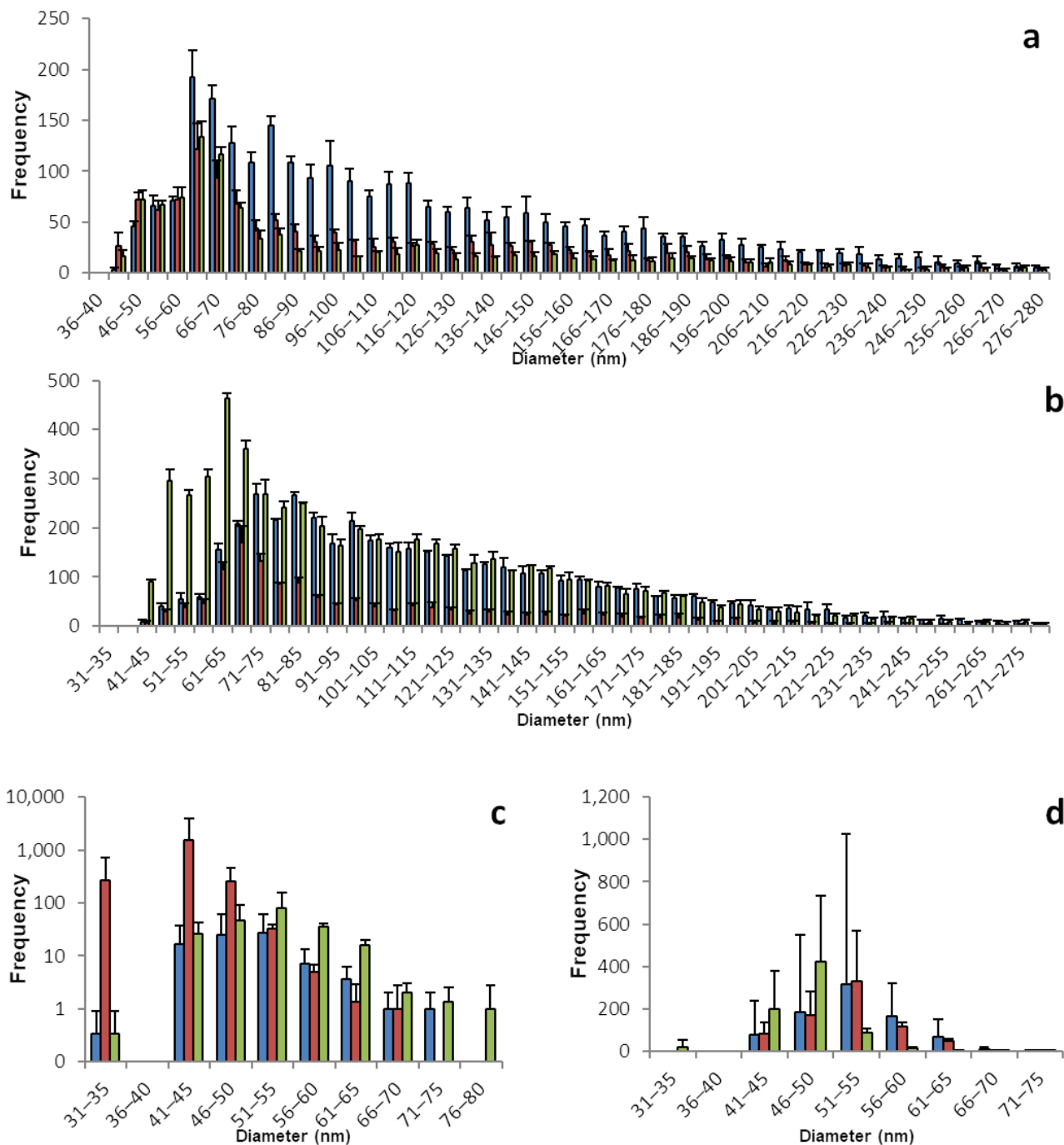


**Figure 3.** Size distribution of SeNPs in root and shoot tissues of brussels sprout and broccoli plants. These histograms show the sp-ICP-MS analysis of (a) brussels sprout root, (c) brussels sprout shoot, (b) broccoli root, and (d) broccoli shoot. Three specimens of each plant were grown, and each bar color represents a single plant. The standard deviation depicted describes the variation for 3 replicates of the same sample. Nano particles with a size of up to 536 nm were detected, however the histograms in this figure are meant to show the main distribution of SeNPs and were therefore cropped. Supplementary information S1 shows the full results. Supplementary information S2 shows histograms including all detected data points for the individual replicates.

**Table 3.** Concentrations of dissolved selenium corresponding to the histograms shown in Figure 3.

	Root			Shoot		
Brussels Sprout	1	2	3	1	2	3
Mean concentration of dissolved Se [ $\mu\text{g}/\text{L}$ ]	0.941	0.522	0.698	0.205	0.133	0.284
Standard deviation	0.007	0.009	0.002	0.002	0.001	0.001
Mass of Se per kg plant mass (fresh weight) [mg]	9.41	5.22	6.98	2.05	1.33	2.84
Broccoli						
Mean concentration of dissolved Se [ $\mu\text{g}/\text{L}$ ]	0.461	0.420	0.601	0.400	0.373	0.192
Standard deviation	0.017	0.001	0.001	0.007	0.034	0.002
Mass of Se per kg plant mass (fresh weight) [mg]	4.61	4.20	6.01	4.00	3.73	1.92

Equally, the shoot samples of broccoli plants are similar to brussels sprouts with a narrow distribution of nano particles and a maximum between 50 and 60 nm. However, there is less of a gradient in the overall number of nano particles or dissolved selenium in broccoli, compared to brussels sprouts. The shoot samples contain 0.2 to 0.4  $\mu\text{g}/\text{L}$  dissolved selenium and a higher number of particles.

The sp-ICP-MS analyses for lamb's lettuce and brazil nuts are displayed in Figure 4 and Table 4. Most of the lamb's lettuce samples do not give conclusive results. While all of the histograms show SeNPs, most of them do not show a trustworthy distribution. Only a few bars being present in the histograms, often with very high numbers and very low concentrations of dissolved selenium, is a strong hint for false positive results. The case is less clear for lamb's lettuce roots. Those samples show a more trustworthy distribution of SeNPs ranging from 36 to 70 nm. It can be assumed that the overall low concentration of selenium in lamb's lettuce is strongly correlated to the lack of SeNPs and especially the shoot samples show close to no reliable hint for the presence of SeNPs, leading to the assumption that unlike the other plants, the consumption of lamb's lettuce does not include the ingestion of selenium nano particles, as most of lamb's lettuce's SeNPs are stored in the roots.

Brazil nuts, being the most prominent representative source of plant-based selenium, have been widely discussed lately for the huge variation of selenium content, which is most probably linked to the strongly varying selenium content of the soil, which Brazil nut trees grow on. We did not grow any plants of this species ourselves, but instead bought two different brands of Brazil nuts from two different local grocery stores. The nuts were treated in the same manner as the plants and the analysis was performed accordingly [41].

And just as the current state of scientific knowledge suggests, the selenium content varies hugely. This is true for the two brands being different from each other, but even the nuts from the same package differ strongly from each other. This also applies to the different runs of sp-ICP-MS analysis that were performed with the exact same sample. When comparing the two batches, referring to the two different bags of nuts, please pay attention to the different dilutions. Replicate 1 was diluted by a factor of 100, compared to replicate number 2.

A reason for the strong differences between the three runs of a sample might be due to aggregation. While we were not yet able to investigate the coating of naturally occurring SeNPs in plants, it is safe to assume that there is a coating around the selenium core. With the exceptionally high amounts of selenium that can be accumulated in Brazil nuts, there might be a unique coating for SeNPs that allows for more efficient detoxification and selenium storage. An aggregation due to the coating might be a reason for a lack of homogenous distribution of SeNPs within the samples.

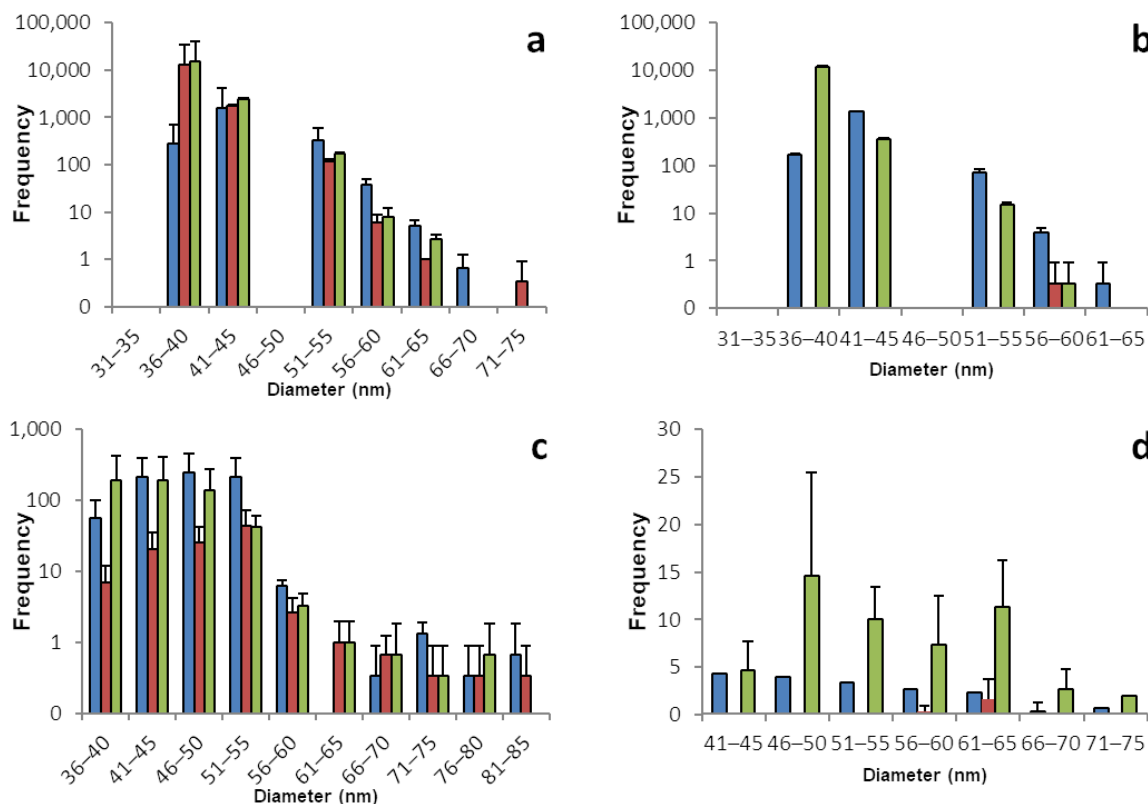


**Figure 4.** Size distribution of SeNPs in root and shoot tissues of lamb's lettuce and in Brazil nuts: These histograms show the sp-ICP-MS analysis of (a) lamb's lettuce root, (b) lamb's lettuce shoot, (c) the first batch of Brazil nuts, and (d) the second batch of Brazil nuts. Three specimens of each plant were grown, and each bar color represents a single plant. The standard deviation depicted describes the variation for 3 replicates of the same sample. Nano particles with a size of up to 273 nm were detected, however the histograms in this figure are meant to show the main distribution of SeNPs and were therefore cropped. Supplementary information S1 shows the full results. Supplementary information S2 shows histograms including all detected data points for the individual replicates.

**Table 4.** Concentrations of dissolved selenium corresponding to the histograms shown in Figure 4.

	Root			Shoot		
Lamb's Lettuce	1	2	3	1	2	3
Mean concentration of dissolved Se [ $\mu\text{g/L}$ ]	0.204	0.084	0.113	0.062	0.040	0.002
Standard deviation	0.023	0.006	0.004	0.003	0.003	0.001
Mass of Se per kg plant mass (fresh weight) [mg]	2.04	0.84	1.13	0.62	0.40	0.02
Brazil Nut	Batch 1			Batch 2		
Mean concentration of dissolved Se [ $\mu\text{g/L}$ ]	0.419	0.173	0.309	0.647	0.476	0.854
Standard deviation	0.229	0.008	0.003	0.011	0.009	0.018
Mass of Se per kg plant mass (fresh weight) [mg]	41.9	17.3	30.9	0.647	0.476	0.854
Mass of Se per Brazil nut (assuming an average weight of 5 g/nut) [ $\mu\text{g}$ ]	209.5	86.5	154.5	3.234	2.36	4267

It should be kept in mind that the analytical method was optimized to reduce dissolved selenium and by doing so, minimizing the potential of false positive results. For Brazil nuts, with naturally high concentrations of selenium, a stronger dilution was needed to avoid false positives. At the expense of a more representative size histogram, we achieved valid and trustworthy results, thus being able to prove that Brazil nuts also contain selenium nano particles. Additionally, it must be kept in mind that nuts are a more complex matrix to work with than shoot and root tissues. The different composition of compounds, especially the lower amount of water in the matrix and the high amounts of proteins and fats, may complicate the extraction of nano particles. Since little is known about naturally occurring SeNPs, it is hard to make an assumption about their resistance to factors like heat or acidity and therefore care has to be taken during the extraction process.

It is, on the other hand, safe to say that Brazil nuts with a high overall concentration of selenium produce a larger number of SeNPs, mainly in the range between 40 and 60 nm. The size distribution of SeNPs in Brazil nuts is rather sharp, with more particles larger than the most frequent size. The histograms overall show a similarity in shape to the ones obtained from shoot and root samples. Despite the dialysis of dissolved selenium, some of the Brazil nuts contain huge amounts of selenium. With a single Brazil nut, the daily recommended dose of selenium could be exceeded by far. On the contrary, some of the Brazil nuts do contain comparably low amounts of selenium and a handful of them might be needed to meet the daily dose of selenium.

#### 4. Discussion

SeNPs were found in every observed plant. The nano particles are present in root and shoot tissues and in the case of Brazil nuts, in the nuts themselves as well. The data acquisition time was 120 s and the flow rate was 0.25 mL/min, therefore the SeNPs in 50 µg of plant mass are shown in every histogram, with the exceptions being the chard root samples 1 and 2 representing 25 µg, the first batch of Brazil nuts representing 5 µg, and the second batch of Brazil nuts representing 500 µg as described in the plant treatment section. To ensure that the particles we detected were not root exudates or have a microbiological origin, samples were taken from the growth solution and analyzed in the same way as the plant tissues. No SeNPs were detected by the sp-ICP-MS in those samples. There are differences in the size and size distribution of the particles in the different plant species as well as in the number and proportion of SeNPs. Some observations, however, can be generalized to some extent. Typically, a higher concentration of dissolved selenium is associated with a higher number of SeNPs. The maximum number of SeNPs was found between 40 and 70 nm in all species and the main size ranges are usually not larger than 50 nm. This narrow size distribution is, on the one hand, highly advantageous for possible applications as food supplement or medicinal products and can, on the other hand, be interpreted as a sign for an active metabolic pathway that leads to the nano particle synthesis. In our previous research, we already grew eight different species of plants under the same conditions to evaluate the botanical commonness of SeNP biosynthesis in plants [26]. With these additional plants, we see strong evidence that the naturally occurring synthesis of SeNPs is in fact a ubiquitous phenomenon and we firmly predict that SeNPs can be found in any plant and hence every food plant. It is therefore safe to assume that SeNPs are ubiquitously present in every human's diet on a daily basis.

The impact of a suboptimal selenium status on human health is not yet fully understood and requires further research. While clear selenium deficiency is well known and described, as well as selenosis from chronic selenium intoxication, there are still many unknown factors for the ideal selenium supply. A high but not oversaturated selenium is linked to reduced mortality by multiple causes including systemic inflammatory response syndrome, sepsis, and cancer mortality including reduced all-cause mortality in prospective studies [12]. Aside from mammals and plants, SeNPs can also have beneficial effects on fish. SeNPs can improve the growth and final weight as well as the antioxidant and immune

function in fish. Enriching plant-based fish feed with selenium can therefore supply fish with beneficial SeNPs as well.

A size effect for nano particles was found to be significant for absorption in the gut. For all observed species, the highest count of detected particles was well under 100 nm, mostly between 40 and 70 nm, which is an ideal size for bioavailability in humans. Therefore, we see great nutritive potential for these particles. This particle size is also associated with great cell-barrier penetration. The large surface of SeNPs can, on the other hand, be a disadvantage as well, due to their high surface energy and the potential of precipitation, however compounds such as polyphenols, polysaccharides, and proteins are known to be stabilizing agents. The abundance of such compounds in plants suggests a higher stability of plant-based SeNPs compared to SeNPs that are derived by chemical synthesis.

These findings raise two main questions: What does this mean for agriculture and nutrition? What research is needed in the future? As for nutrition, we know that SeNPs are a great source of selenium, due to their high bioavailability and effect and their low toxicity. These properties make them a highly desirable compound in food. Throughout the last decade, a trend was observed showing that an increasing number of people choose to eat fully plant-based diets with all animal-derived foods excluded. Many experts believe that climate change will force everyone to focus their diet more on plants and massively reduce animal-derived foods. Since selenium is a potentially critical nutrient in the vegan diet, measures need to be taken to ensure a sufficient supply of selenium for the population.

SeNPs are highly desirable candidates for future food supplements. They show great bioavailability and low toxicity, but beyond that, they have unique beneficial effects on health that cannot be observed for other forms of selenium. While a selenite supplement affected pancreatic function and increased adipogenesis and general anabolism in adolescent rats, SeNP supplementation significantly reduced white adipose tissue and BMI [13,42].

The great variations in selenium content of the observed Brazil nuts show even more how complicated selenium nutrition can be. The selenium content of the soil in which Brazil nuts and other plants are grown can be safely assumed to be one of the most critical factors for uptake in plants. Even among trace elements, the range of recommended intake for selenium is particularly narrow. For such a nutrient, it is very important to be aware of the compounds in which it can be found in food [43,44]. In many regions, for example, Nordic countries, the selenium concentration in soil is very low. To achieve sufficient selenium supply, different measures are taken. Unlike the common approach of enriching animal fodder with selenium, Finland took the measure of adding selenium to fertilizers nationwide and thus increased the average daily intake of selenium from 25 µg/day/10 MJ in the 1970s to 80 µg/day/10 MJ today [7]. This is a great example of the benefits of plant-based selenium, and we firmly believe that SeNPs play a huge role in this matter. In many more applications and for a variety of plants, selenium biofortification has proven to be a great way to improve crop selenium content and the nutritive value of plants. The biofortification of crops has been shown to yield promising results through foliar application as well. Therefore, we see potential for future research investigating the binding forms of selenium in crops that have been treated in that manner, as it is more resource-efficient and can help answer the question of whether all plant cells are able to synthesize SeNPs [37,39,45,46].

Selenium is acting as a biostimulant. It can increase the accumulation of bioactive compounds such as vitamin c or flavonoids, which further aid the antioxidant properties of selenium [38,47]. Beneficial effects of selenium on agricultural plants and SeNPs on human health can therefore be achieved simultaneously.

## 5. Conclusions

For the future, we see cause for further research to evaluate the dose-dependent nano particle synthesis in plants and quantitative studies to judge the proportion of selenium that is present in nano form. Selenium deficiency is estimated to affect up to 1 billion people worldwide [48]. Our research shows that it is a highly desirable approach to address this

problem by biofortification of crops with selenium. The ubiquitous biosynthesis of SeNPs in food plants results in a high-quality selenium source with great safety and sustainability.

Furthermore, we see cause for research on the coating of these nano particles, as the surface may impact its biological function massively. For this purpose, single-particle-ICP-MS and organic triple-quadrupole mass spectrometry must be combined in the future to determine the organic ligands on the surface of selenium nanoparticles. A complete characterization also requires the determination of the selenium modification present in the core of the nanoparticles. For example, the question arises whether the selenium is present in the red (Se rings) or grey (Se chains) modification, which would cause very different reaction behaviors. To fully assess the potential of plant-based SeNPs as food supplements and components in both natural foods and those enhanced by biofortification, an enhanced method has to be developed that differentiates between organic, inorganic, and nano selenium and can quantify the percentage of selenium that is in nano form. These additional questions very clearly show the challenges that still need to be overcome in the future for an accurate characterization of selenium nanoparticles.

**Supplementary Materials:** The following supporting information can be downloaded at: <https://www.mdpi.com/article/10.3390/foods12173203/s1>, Supplementary Information S1: Raw data of the *sp*-ICP-MS results included in this study; Supplementary Information S2: all individual data points for the histograms included in Figures 1–4.

**Author Contributions:** J.V. and K.G. designed the experiments. J.V. performed the experiments and analyzed the data with supervision by K.G. J.V. and K.G. wrote the manuscript. All authors have read and agreed to the published version of the manuscript.

**Funding:** The laboratory equipment, analytical instruments and materials used were funded by the Federal Institute for Drugs and Medical Devices PN 20570003.

**Data Availability Statement:** The data for Figures 1–4 are shown in the supplementary information.

**Acknowledgments:** We thank the German Federal Institute for Drugs and Medical Devices for providing the laboratory equipment that was used for this study.

**Conflicts of Interest:** The authors declare no conflict of interest. The funders had no role in the design of the study; in the collection, analyses, or interpretation of data; in the writing of the manuscript; or in the decision to publish the results.

## References

- EFSA Panel on Dietetic Products, Nutrition and Allergies (NDA). Scientific Opinion on Dietary Reference Values for selenium. *EFSA J.* **2014**, *12*, 3846. [[CrossRef](#)]
- Melse-Boonstra, A. Bioavailability of Micronutrients From Nutrient-Dense Whole Foods: Zooming in on Dairy, Vegetables, and Fruits. *Front. Nutr.* **2020**, *7*, 101. [[CrossRef](#)]
- Hurrell, R.; Egli, I. Iron bioavailability and dietary reference values. *Am. J. Clin. Nutr.* **2010**, *91*, 1461S–1467S. [[CrossRef](#)]
- Hadrup, N.; Ravn-Haren, G. Absorption, distribution, metabolism and excretion (ADME) of oral selenium from organic and inorganic sources: A review. *J. Trace Elem. Med. Biol.* **2021**, *67*, 126801. [[CrossRef](#)]
- Gu, X.; Gao, C.-Q. New horizons for selenium in animal nutrition and functional foods. *Anim. Nutr.* **2022**, *11*, 80–86. [[CrossRef](#)]
- White, P.J. Selenium accumulation by plants. *Ann. Bot.* **2016**, *117*, 217–235. [[CrossRef](#)]
- Alfthan, G.; Eurola, M.; Ekhholm, P.; Venäläinen, E.-R.; Root, T.; Korkalainen, K.; Hartikainen, H.; Salminen, P.; Hietaniemi, V.; Aspila, P.; et al. Effects of nationwide addition of selenium to fertilizers on foods, and animal and human health in Finland: From deficiency to optimal selenium status of the population. *J. Trace Elem. Med. Biol.* **2015**, *31*, 142–147. [[CrossRef](#)]
- White, P.J. Selenium metabolism in plants. *Biochim. Biophys. Acta Gen. Subj.* **2018**, *1862*, 2333–2342. [[CrossRef](#)]
- Schiavon, M.; Pilon-Smits, E.A.H. The fascinating facets of plant selenium accumulation—Biochemistry, physiology, evolution and ecology. *New Phytol.* **2017**, *213*, 1582–1596. [[CrossRef](#)]
- Gupta, M.; Gupta, S. An Overview of Selenium Uptake, Metabolism, and Toxicity in Plants. *Front. Plant. Sci.* **2016**, *7*, 2074. [[CrossRef](#)]
- Reeves, M.A.; Hoffmann, P.R. The human selenoproteome: Recent insights into functions and regulation. *Cell. Mol. Life Sci.* **2009**, *66*, 2457–2478. [[CrossRef](#)] [[PubMed](#)]
- Rayman, M.P. Selenium and human health. *Lancet* **2012**, *379*, 1256–1268. [[CrossRef](#)] [[PubMed](#)]
- Chen, J.; Guo, Y.; Zhang, X.; Liu, J.; Gong, P.; Su, Z.; Fan, L.; Li, G. Emerging Nanoparticles in Food: Sources, Application, and Safety. *J. Agric. Food Chem.* **2023**, *71*, 3564–3582. [[CrossRef](#)]

14. Carlisle, A.E.; Lee, N.; Matthew-Onabanjo, A.N.; Spears, M.E.; Park, S.J.; Youkana, D.; Doshi, M.B.; Peppers, A.; Li, R.; Joseph, A.B.; et al. Selenium detoxification is required for cancer-cell survival. *Nat. Metab.* **2020**, *2*, 603–611. [[CrossRef](#)] [[PubMed](#)]
15. Kang, D.; Lee, J.; Wu, C.; Guo, X.; Lee, B.J.; Chun, J.-S.; Kim, J.-H. The role of selenium metabolism and selenoproteins in cartilage homeostasis and arthropathies. *Exp. Mol. Med.* **2020**, *52*, 1198–1208. [[CrossRef](#)]
16. Pyrzynska, K.; Sentkowska, A. Biosynthesis of selenium nanoparticles using plant extracts. *J. Nanostruct. Chem.* **2022**, *12*, 467–480. [[CrossRef](#)]
17. Shimada, B.K.; Alfulaij, N.; Seale, L.A. The Impact of Selenium Deficiency on Cardiovascular Function. *Int. J. Mol. Sci.* **2021**, *22*, 10713. [[CrossRef](#)]
18. Hughes, D.J.; Duarte-Salles, T.; Hybsier, S.; Trichopoulou, A.; Stepien, M.; Aleksandrova, K.; Overvad, K.; Tjønneland, A.; Olsen, A.; Affret, A.; et al. Prediagnostic selenium status and hepatobiliary cancer risk in the European Prospective Investigation into Cancer and Nutrition cohort. *Am. J. Clin. Nutr.* **2016**, *104*, 406–414. [[CrossRef](#)]
19. Lin, Z.; Li, Y.; Guo, M.; Xiao, M.; Wang, C.; Zhao, M.; Xu, T.; Xia, Y.; Zhu, B. Inhibition of H1N1 influenza virus by selenium nanoparticles loaded with zanamivir through p38 and JNK signaling pathways. *RSC Adv.* **2017**, *7*, 35290–35296. [[CrossRef](#)]
20. He, L.; Zhao, J.; Wang, L.; Liu, Q.; Fan, Y.; Li, B.; Yu, Y.-L.; Chen, C.; Li, Y.-F. Using nano-selenium to combat Coronavirus Disease 2019 (COVID-19)? *Nano Today* **2021**, *36*, 101037. [[CrossRef](#)]
21. Hoffman, K.S.; Vargas-Rodriguez, O.; Bak, D.W.; Mukai, T.; Woodward, L.K.; Weerapana, E.; Söll, D.; Reynolds, N.M. A cysteinyl-tRNA synthetase variant confers resistance against selenite toxicity and decreases selenocysteine misincorporation. *J. Biol. Chem.* **2019**, *294*, 12855–12865. [[CrossRef](#)] [[PubMed](#)]
22. Jia, X.; Li, N.; Chen, J. A subchronic toxicity study of elemental Nano-Se in Sprague-Dawley rats. *Life Sci.* **2005**, *76*, 1989–2003. [[CrossRef](#)] [[PubMed](#)]
23. Wang, H.; Zhang, J.; Yu, H. Elemental selenium at nano size possesses lower toxicity without compromising the fundamental effect on selenoenzymes: Comparison with selenomethionine in mice. *Free Radic. Biol. Med.* **2007**, *42*, 1524–1533. [[CrossRef](#)] [[PubMed](#)]
24. Menon, S.; Ks, S.D.; Santhiya, R.; Rajeshkumar, S.; Kumar, V. Selenium nanoparticles: A potent chemotherapeutic agent and an elucidation of its mechanism. *Colloids Surf. B Biointerfaces* **2018**, *170*, 280–292. [[CrossRef](#)]
25. Bhattacharjee, A.; Basu, A.; Bhattacharya, S. Selenium nanoparticles are less toxic than inorganic and organic selenium to mice in vivo. *Nucleus* **2019**, *62*, 259–268. [[CrossRef](#)]
26. Verstegen, J.; Günther, K. Biosynthesis of nano selenium in plants. *Artif. Cells Nanomed. Biotechnol.* **2023**, *51*, 13–21. [[CrossRef](#)]
27. Rai, R.K.; Karri, R.; Dubey, K.D.; Roy, G. Regulation of Tyrosinase Enzyme Activity by Glutathione Peroxidase Mimics. *J. Agric. Food Chem.* **2022**, *70*, 9730–9747. [[CrossRef](#)]
28. Kristal, A.R.; Darke, A.K.; Morris, J.S.; Tangen, C.M.; Goodman, P.J.; Thompson, I.M.; Meyskens, F.L.; Goodman, G.E.; Minasian, L.M.; Parnes, H.L.; et al. Baseline selenium status and effects of selenium and vitamin e supplementation on prostate cancer risk. *J. Natl. Cancer Inst.* **2014**, *106*, djt456. [[CrossRef](#)]
29. Rayman, M.P. Selenium intake, status, and health: A complex relationship. *Hormones* **2020**, *19*, 9–14. [[CrossRef](#)]
30. Sun, X.-H.; Lv, M.-W.; Zhao, Y.-X.; Zhang, H.; Ullah Saleem, M.A.; Zhao, Y.; Li, J.-L. Nano-Selenium Antagonized Cadmium-Induced Liver Fibrosis in Chicken. *J. Agric. Food Chem.* **2023**, *71*, 846–856. [[CrossRef](#)]
31. Nayak, V.; Singh, K.R.B.; Singh, A.K.; Singh, R.P. Potentialities of selenium nanoparticles in biomedical science. *New J. Chem.* **2021**, *45*, 2849–2878. [[CrossRef](#)]
32. Liao, G.; Tang, J.; Wang, D.; Zuo, H.; Zhang, Q.; Liu, Y.; Xiong, H. Selenium nanoparticles (SeNPs) have potent antitumor activity against prostate cancer cells through the upregulation of miR-16. *World J. Surg. Oncol.* **2020**, *18*, 81. [[CrossRef](#)] [[PubMed](#)]
33. Abd-Rabou, A.A.; Ahmed, H.H.; Shalby, A.B. Selenium Overcomes Doxorubicin Resistance in Their Nano-platforms Against Breast and Colon Cancers. *Biol. Trace Elem. Res.* **2020**, *193*, 377–389. [[CrossRef](#)] [[PubMed](#)]
34. Peng, D.; Zhang, J.; Liu, Q.; Taylor, E.W. Size effect of elemental selenium nanoparticles (Nano-Se) at supranutritional levels on selenium accumulation and glutathione S-transferase activity. *J. Inorg. Biochem.* **2007**, *101*, 1457–1463. [[CrossRef](#)] [[PubMed](#)]
35. Dolai, J.; Mandal, K.; Jana, N.R. Nanoparticle Size Effects in Biomedical Applications. *ACS Appl. Nano Mater.* **2021**, *4*, 6471–6496. [[CrossRef](#)]
36. Kolbert, Z.; Molnár, Á.; Feigl, G.; van Hoewyk, D. Plant selenium toxicity: Proteome in the crosshairs. *J. Plant Physiol.* **2019**, *232*, 291–300. [[CrossRef](#)]
37. Silva, M.A.; de Sousa, G.F.; Corquinha, A.P.B.; de Lima Lessa, J.H.; Dinali, G.S.; Oliveira, C.; Lopes, G.; Amaral, D.; Brown, P.; Guilherme, L.R.G. Selenium biofortification of soybean genotypes in a tropical soil via Se-enriched phosphate fertilizers. *Front. Plant Sci.* **2022**, *13*, 988140. [[CrossRef](#)]
38. Hossain, M.A.; Ahammed, G.J.; Kolbert, Z.; El-Ramady, H.; Islam, T.; Schiavon, M. *Selenium and Nano-Selenium in Environmental Stress Management and Crop Quality Improvement*; Springer International Publishing: Cham, Switzerland, 2022; ISBN 978-3-031-07062-4.
39. Hossain, A.; Skalicky, M.; Brestic, M.; Maitra, S.; Sarkar, S.; Ahmad, Z.; Vemuri, H.; Garai, S.; Mondal, M.; Bhatt, R.; et al. Selenium Biofortification: Roles, Mechanisms, Responses and Prospects. *Molecules* **2021**, *26*, 881. [[CrossRef](#)]
40. Cheng, C.; Coldea, T.E.; Yang, H.; Zhao, H. Selenium Uptake, Translocation, and Metabolization Pattern during Barley Malting: A Comparison of Selenate, Selenite, and Selenomethionine. *J. Agric. Food Chem.* **2023**, *71*, 5240–5249. [[CrossRef](#)]

41. Silva Junior, E.C.; Wadt, L.H.O.; Silva, K.E.; Lima, R.M.B.; Batista, K.D.; Guedes, M.C.; Carvalho, G.S.; Carvalho, T.S.; Reis, A.R.; Lopes, G.; et al. Natural variation of selenium in Brazil nuts and soils from the Amazon region. *Chemosphere* **2017**, *188*, 650–658. [[CrossRef](#)]
42. Ojeda, M.L.; Nogales, F.; Carreras, O.; Pajuelo, E.; Del Gallego-López, M.C.; Romero-Herrera, I.; Begines, B.; Moreno-Fernández, J.; Díaz-Castro, J.; Alcudia, A. Different Effects of Low Selenite and Selenium-Nanoparticle Supplementation on Adipose Tissue Function and Insulin Secretion in Adolescent Male Rats. *Nutrients* **2022**, *14*, 3571. [[CrossRef](#)] [[PubMed](#)]
43. Bakaloudi, D.R.; Halloran, A.; Rippin, H.L.; Oikonomidou, A.C.; Dardavesis, T.I.; Williams, J.; Wickramasinghe, K.; Breda, J.; Chourdakis, M. Intake and adequacy of the vegan diet. A systematic review of the evidence. *Clin. Nutr.* **2021**, *40*, 3503–3521. [[CrossRef](#)]
44. Weder, S.; Zerback, E.H.; Wagener, S.M.; Koeder, C.; Fischer, M.; Alexy, U.; Keller, M. How Does Selenium Intake Differ among Children (1–3 Years) on Vegetarian, Vegan, and Omnivorous Diets? Results of the VeChi Diet Study. *Nutrients* **2022**, *15*, 34. [[CrossRef](#)] [[PubMed](#)]
45. Zou, C.; Du, Y.; Rashid, A.; Ram, H.; Savasli, E.; Pieterse, P.J.; Ortiz-Monasterio, I.; Yazici, A.; Kaur, C.; Mahmood, K.; et al. Simultaneous Biofortification of Wheat with Zinc, Iodine, Selenium, and Iron through Foliar Treatment of a Micronutrient Cocktail in Six Countries. *J. Agric. Food Chem.* **2019**, *67*, 8096–8106. [[CrossRef](#)] [[PubMed](#)]
46. Duborská, E.; Šebesta, M.; Matulová, M.; Zvěřina, O.; Urík, M. Current Strategies for Selenium and Iodine Biofortification in Crop Plants. *Nutrients* **2022**, *14*, 4717. [[CrossRef](#)] [[PubMed](#)]
47. Dima, S.-O.; Neamțu, C.; Desliu-Avram, M.; Ghiurea, M.; Capra, L.; Radu, E.; Stoica, R.; Faraon, V.-A.; Zamfiropol-Cristea, V.; Constantinescu-Aruxandei, D.; et al. Plant Biostimulant Effects of Baker's Yeast Vinasé and Selenium on Tomatoes through Foliar Fertilization. *Agronomy* **2020**, *10*, 133. [[CrossRef](#)]
48. Shreenath, A.P.; Ameer, M.A.; Dooley, J. StatPearls: Selenium Deficiency. In *Treasure Island*; Broadview Press: Peterborough, ON, Canada, 2023.

**Disclaimer/Publisher's Note:** The statements, opinions and data contained in all publications are solely those of the individual author(s) and contributor(s) and not of MDPI and/or the editor(s). MDPI and/or the editor(s) disclaim responsibility for any injury to people or property resulting from any ideas, methods, instructions or products referred to in the content.

## **Appendix C**

### **Method development**

### Investigation on lower detection limit

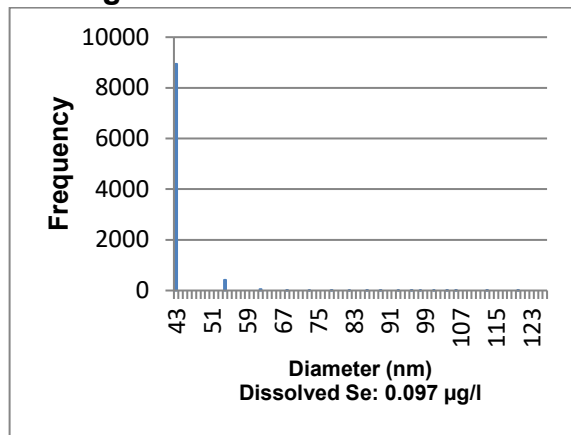


Figure 63: Size histogram of 50 nm SeNP standard (0.01 µg/l) based on the detection of  $^{78}\text{Se}$ . Run 1

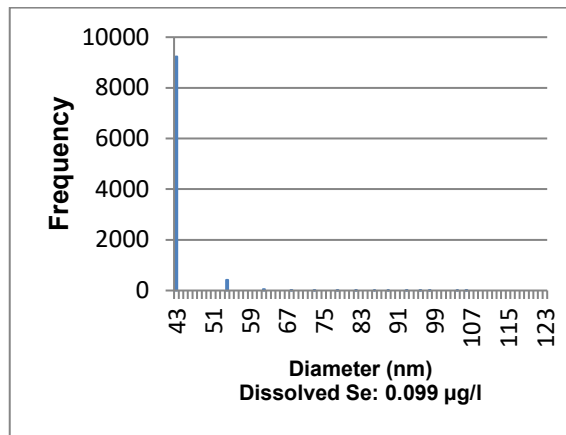


Figure 64: Size histogram of 50 nm SeNP standard (0.01 µg/l) based on the detection of  $^{78}\text{Se}$ . Run 2

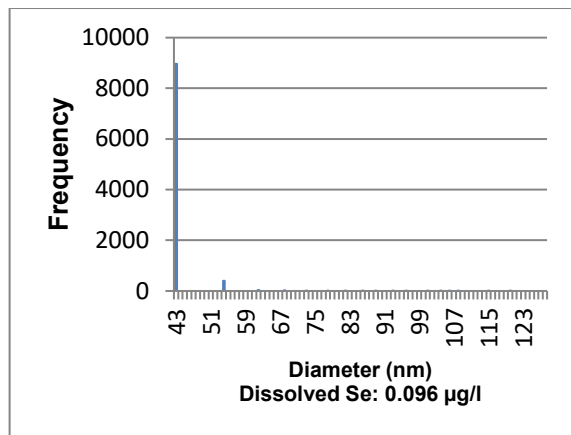


Figure 65: Size histogram of 50 nm SeNP standard (0.01 µg/l) based on the detection of  $^{78}\text{Se}$ . Run 3

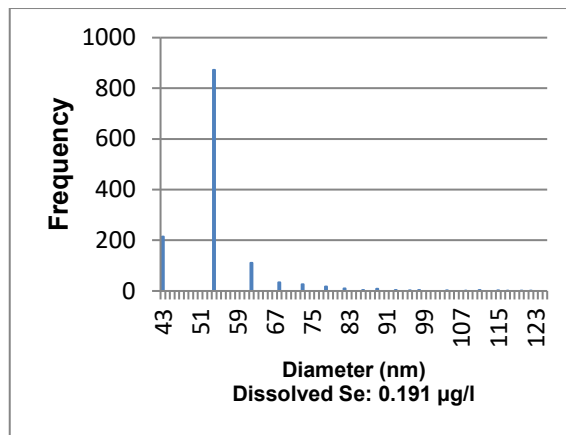


Figure 66: Size histogram of 50 nm SeNP standard (0.02 µg/l) based on the detection of  $^{78}\text{Se}$ . Run 1

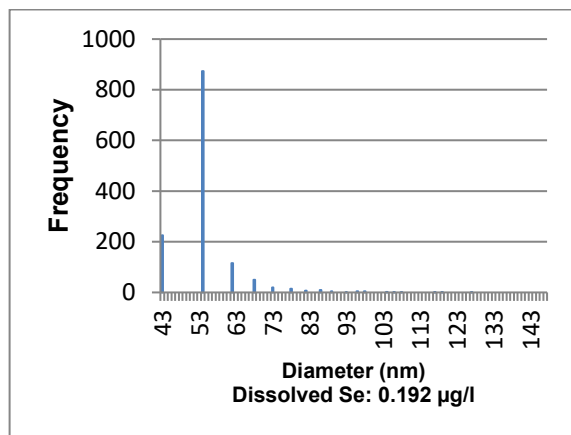


Figure 67: Size histogram of 50 nm SeNP standard (0.02 µg/l) based on the detection of  $^{78}\text{Se}$ . Run 2

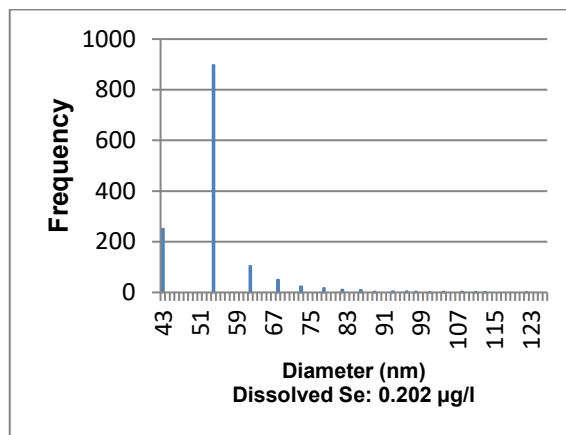


Figure 68: Size histogram of 50 nm SeNP standard (0.02 µg/l) based on the detection of  $^{78}\text{Se}$ . Run 3

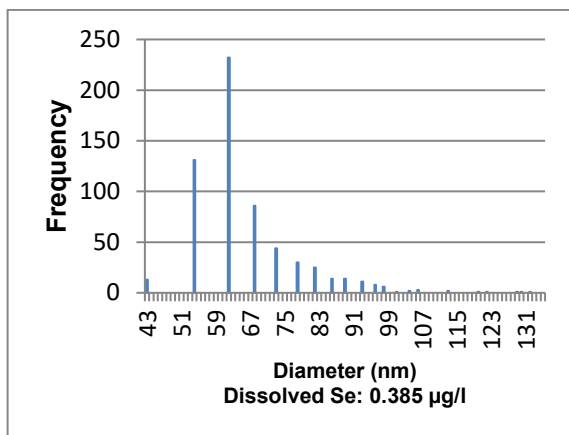


Figure 69: Size histogram of 50 nm SeNP standard (0.04 µg/l) based on the detection of  $^{78}\text{Se}$ . Run 1

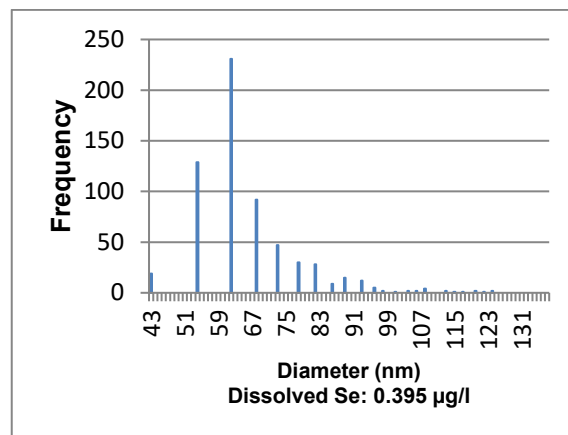


Figure 70: Size histogram of 50 nm SeNP standard (0.04 µg/l) based on the detection of  $^{78}\text{Se}$ . Run 2

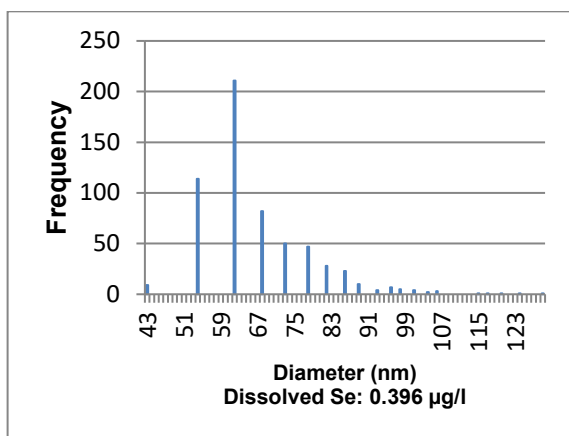


Figure 71: Size histogram of 50 nm SeNP standard (0.04 µg/l) based on the detection of  $^{78}\text{Se}$ . Run 3

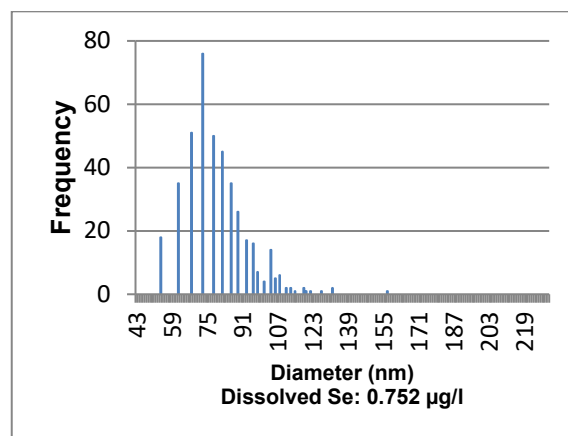


Figure 72: Size histogram of 50 nm SeNP standard (0.08 µg/l) based on the detection of  $^{78}\text{Se}$ . Run 1

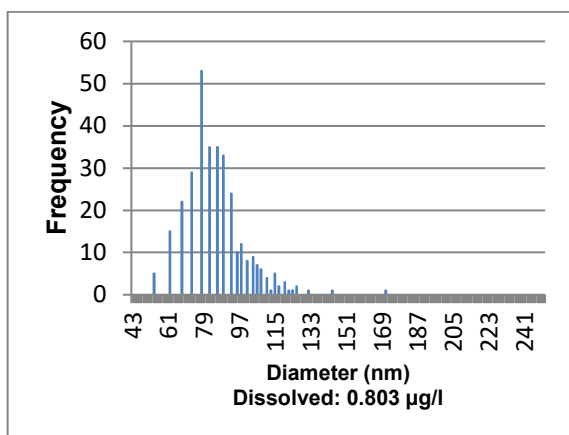


Figure 73: Size histogram of 50 nm SeNP standard (0.08 µg/l) based on the detection of  $^{78}\text{Se}$ . Run 2

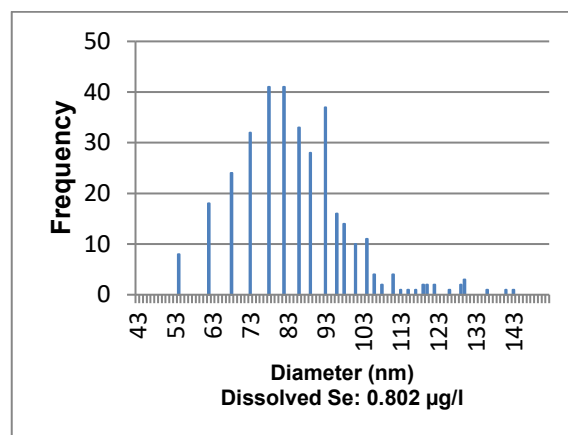


Figure 74: Size histogram of 50 nm SeNP standard (0.02 µg/l) based on the detection of  $^{78}\text{Se}$ . Run 3

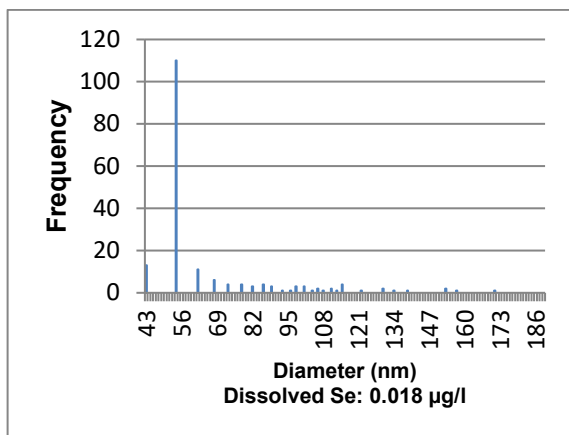


Figure 75: Size histogram of 100 nm SeNP standard (0.01 µg/l) based on the detection of  $^{78}\text{Se}$ . Run 1

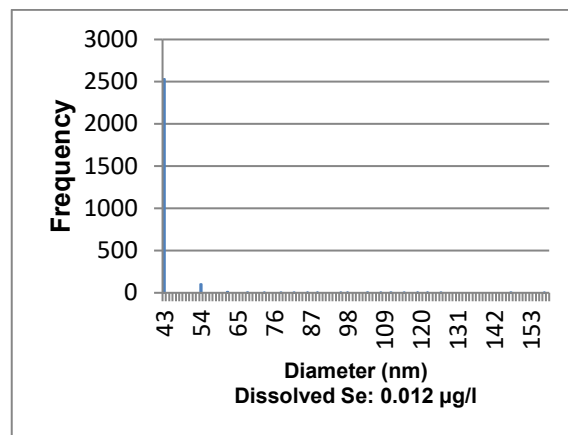


Figure 76: Size histogram of 100 nm SeNP standard (0.01 µg/l) based on the detection of  $^{78}\text{Se}$ . Run 2

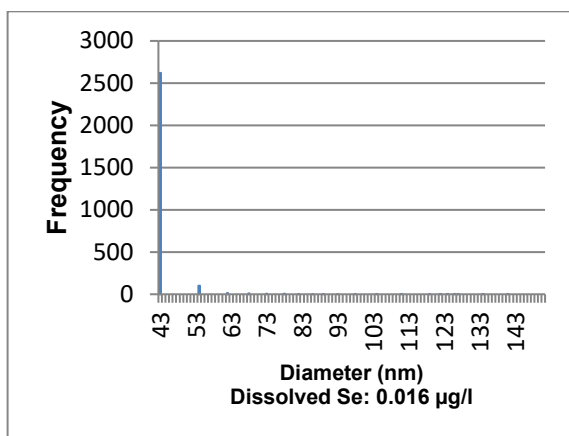


Figure 77: Size histogram of 100 nm SeNP standard (0.01 µg/l) based on the detection of  $^{78}\text{Se}$ . Run 3

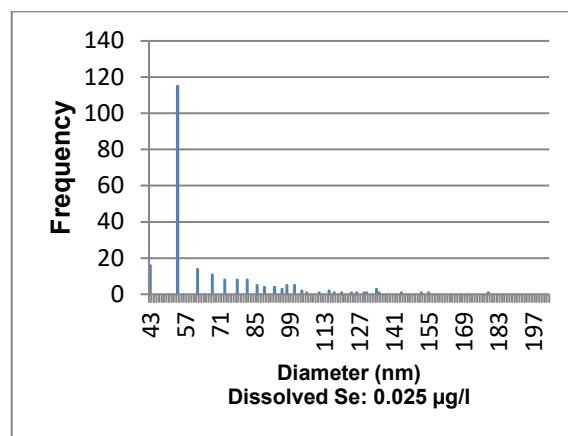


Figure 78: Size histogram of 100 nm SeNP standard (0.02 µg/l) based on the detection of  $^{78}\text{Se}$ . Run 1

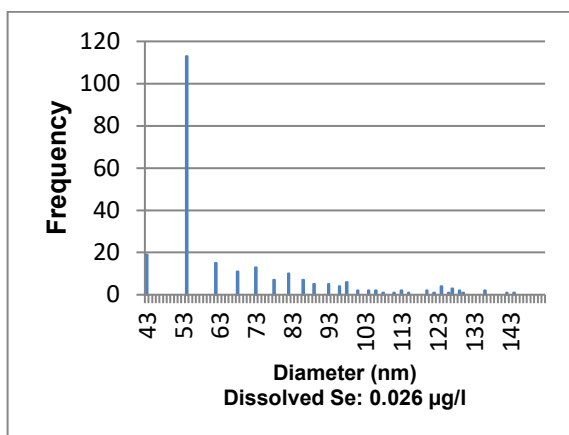


Figure 79: Size histogram of 100 nm SeNP standard (0.02 µg/l) based on the detection of  $^{78}\text{Se}$ . Run 2

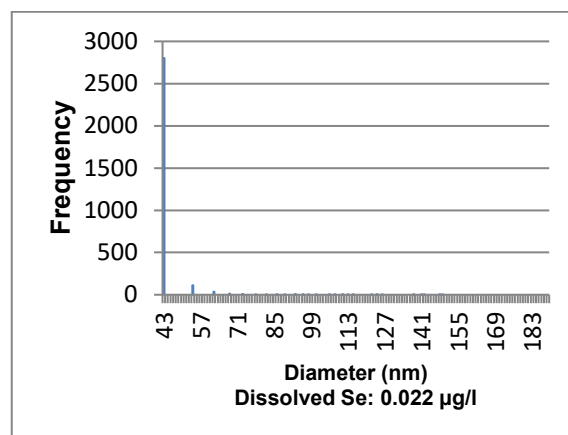


Figure 80: Size histogram of 100 nm SeNP standard (0.02 µg/l) based on the detection of  $^{78}\text{Se}$ . Run 3

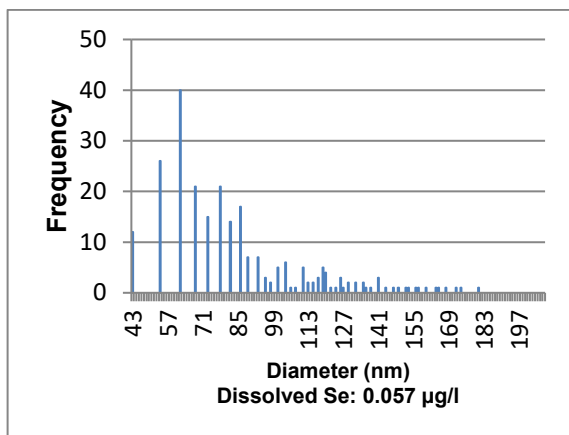


Figure 81: Size histogram of 100 nm SeNP standard (0.04 µg/l) based on the detection of  $^{78}\text{Se}$ . Run 1

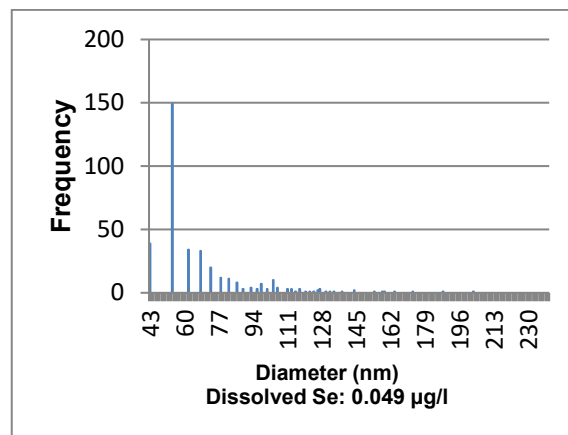


Figure 82: Size histogram of 100 nm SeNP standard (0.04 µg/l) based on the detection of  $^{78}\text{Se}$ . Run 2

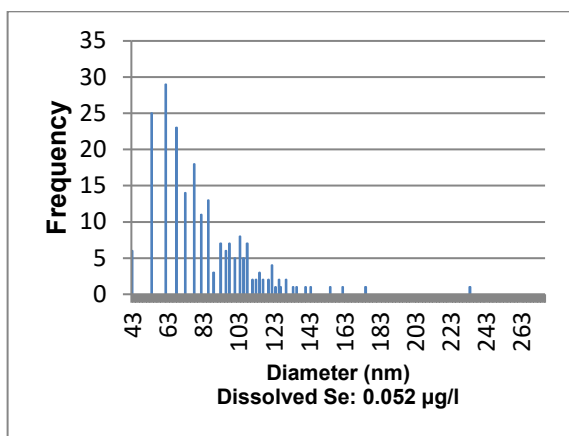


Figure 83: Size histogram of 100 nm SeNP standard (0.04 µg/l) based on the detection of  $^{78}\text{Se}$ . Run 3

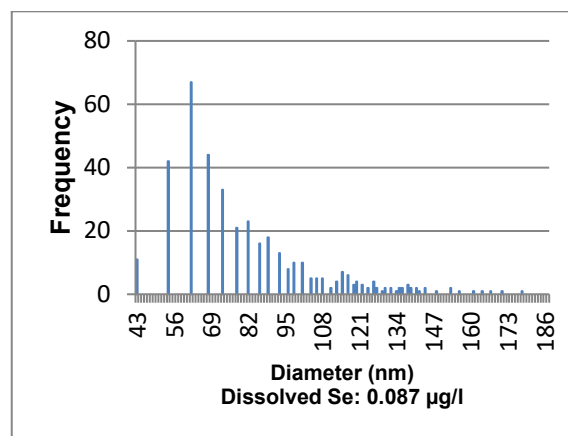


Figure 84: Size histogram of 100 nm SeNP standard (0.08 µg/l) based on the detection of  $^{78}\text{Se}$ . Run 1

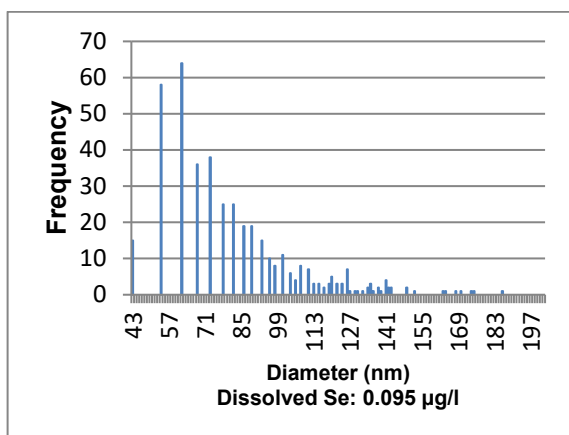


Figure 85: Size histogram of 100 nm SeNP standard (0.08 µg/l) based on the detection of  $^{78}\text{Se}$ . Run 2

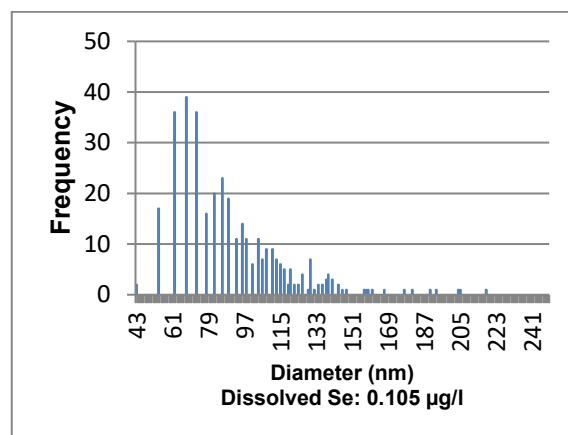


Figure 86: Size histogram of 100 nm SeNP standard (0.08 µg/l) based on the detection of  $^{78}\text{Se}$ . Run 3

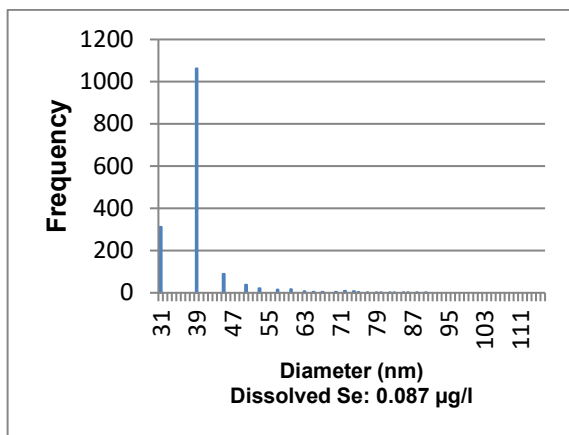


Figure 87: Size histogram of 50 nm SeNP standard (0.01 µg/l) based on the detection of  $^{80}\text{Se}$ . Run 1

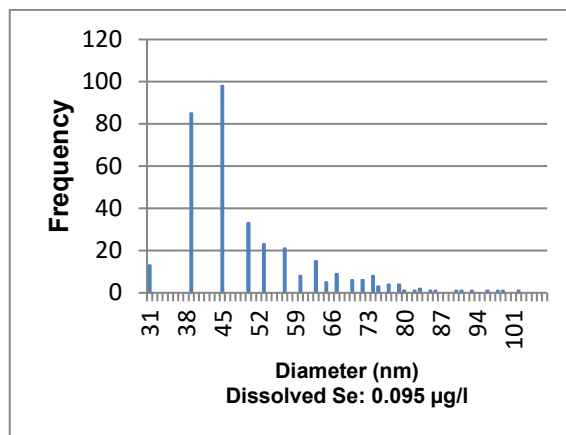


Figure 88: Size histogram of 50 nm SeNP standard (0.01 µg/l) based on the detection of  $^{80}\text{Se}$ . Run 2

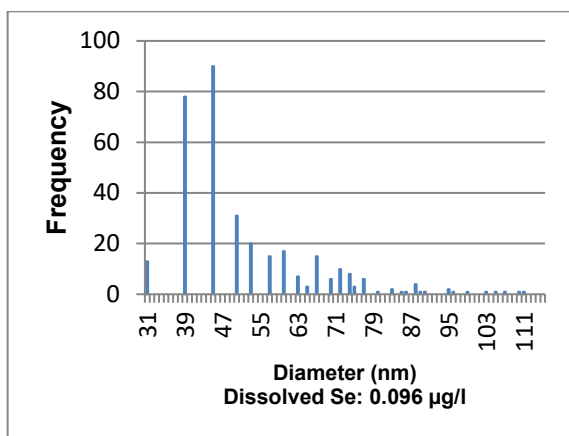


Figure 89: Size histogram of 50 nm SeNP standard (0.01 µg/l) based on the detection of  $^{80}\text{Se}$ . Run 3

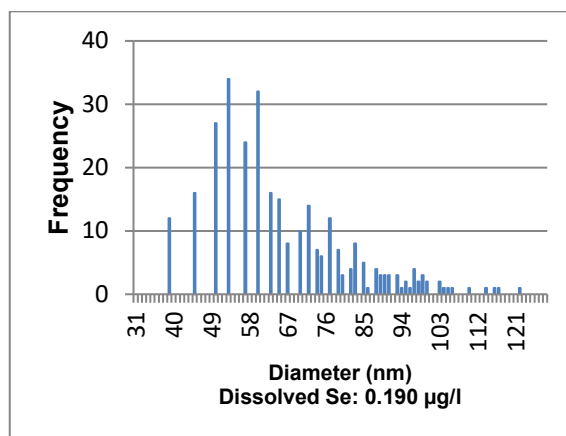


Figure 90: Size histogram of 50 nm SeNP standard (0.02 µg/l) based on the detection of  $^{80}\text{Se}$ . Run 1

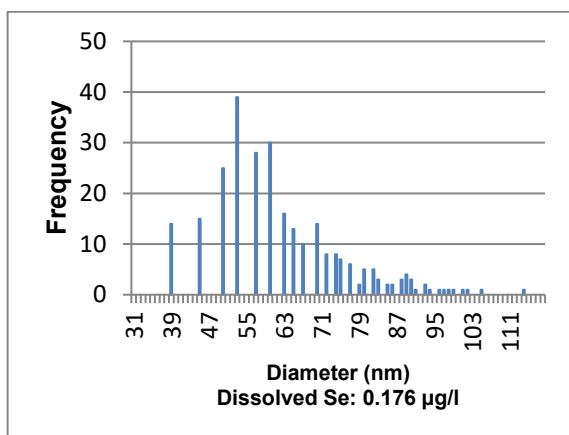


Figure 91: Size histogram of 50 nm SeNP standard (0.02 µg/l) based on the detection of  $^{80}\text{Se}$ . Run 2

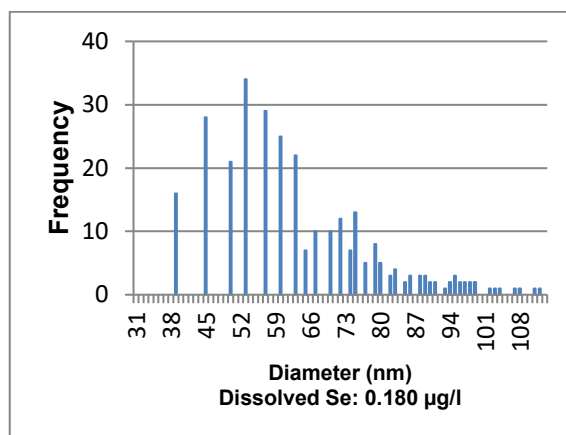


Figure 92: Size histogram of 50 nm SeNP standard (0.02 µg/l) based on the detection of  $^{80}\text{Se}$ . Run 3

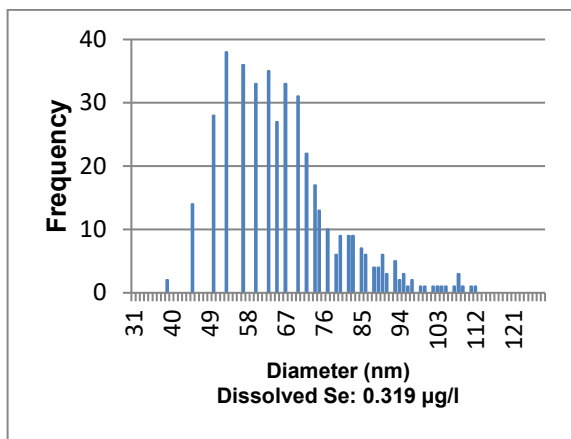


Figure 93: Size histogram of 50 nm SeNP standard (0.04 µg/l) based on the detection of  $^{80}\text{Se}$ . Run 1

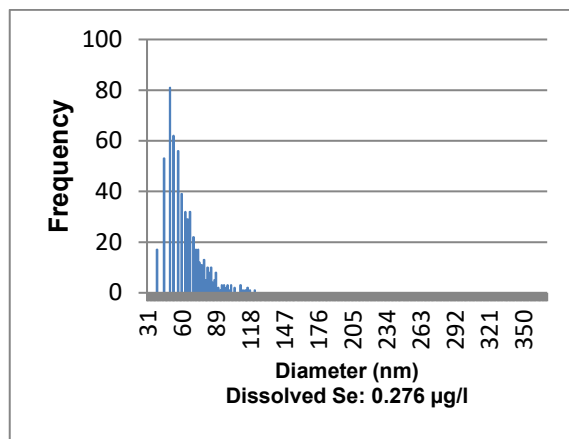


Figure 94: Size histogram of 50 nm SeNP standard (0.04 µg/l) based on the detection of  $^{80}\text{Se}$ . Run 2

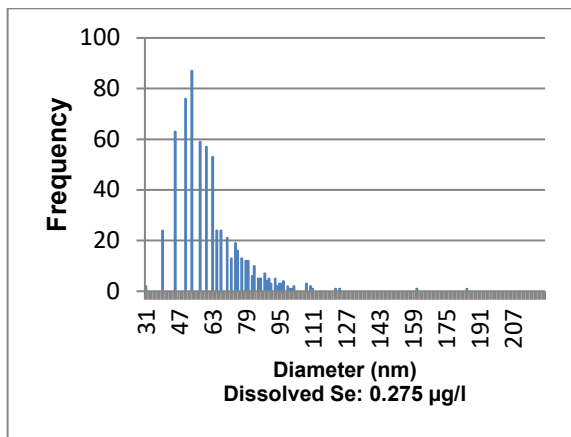


Figure 95: Size histogram of 50 nm SeNP standard (0.04 µg/l) based on the detection of  $^{80}\text{Se}$ . Run 3

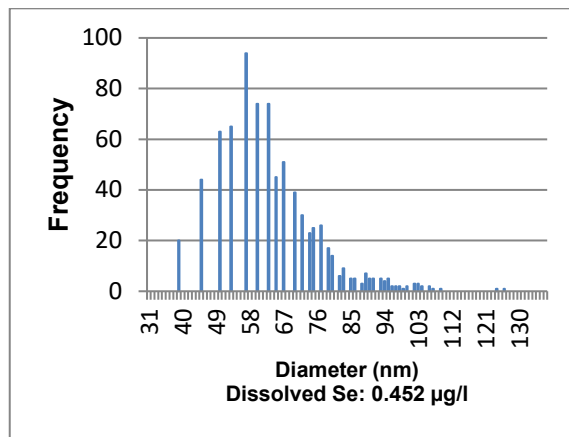


Figure 96: Size histogram of 50 nm SeNP standard (0.08 µg/l) based on the detection of  $^{80}\text{Se}$ . Run 1

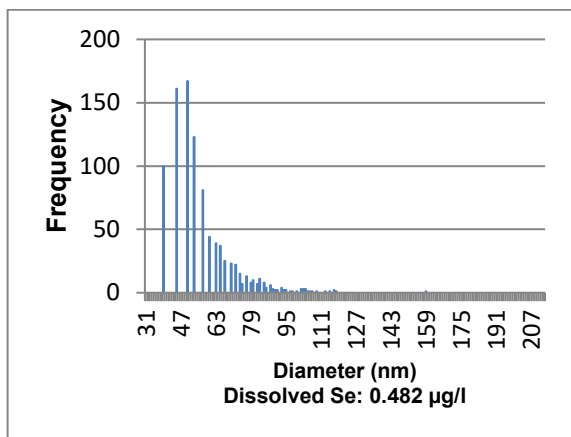


Figure 97: Size histogram of 50 nm SeNP standard (0.08 µg/l) based on the detection of  $^{80}\text{Se}$ . Run 2

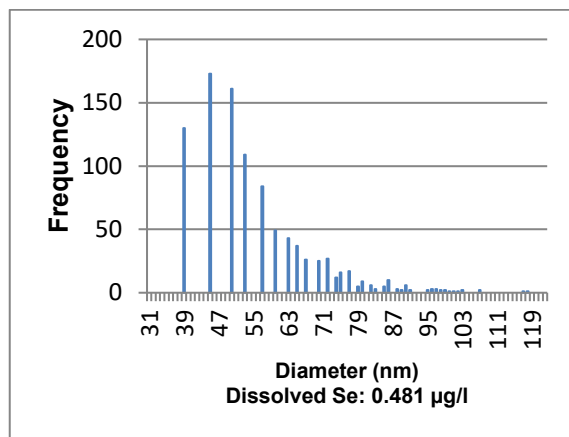


Figure 98: Size histogram of 50 nm SeNP standard (0.08 µg/l) based on the detection of  $^{80}\text{Se}$ . Run 3

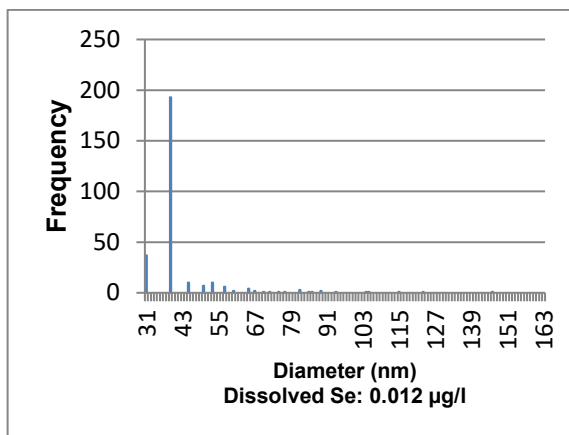


Figure 99: Size histogram of 100 nm SeNP standard (0.01 µg/l) based on the detection of  $^{80}\text{Se}$ . Run 1

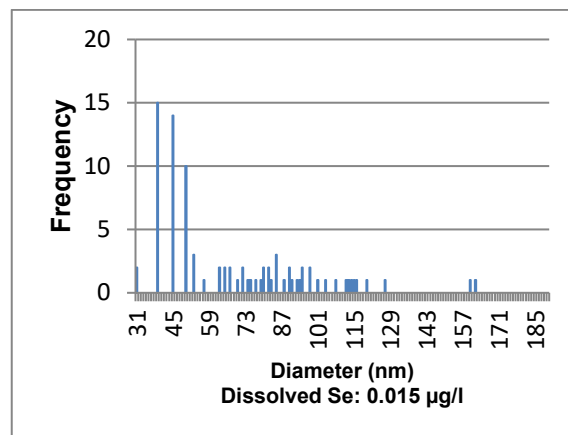


Figure 100: Size histogram of 100 nm SeNP standard (0.01 µg/l) based on the detection of  $^{80}\text{Se}$ . Run 2

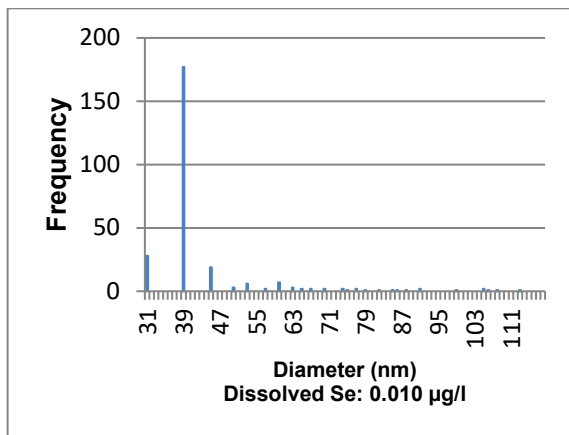


Figure 101: Size histogram of 100 nm SeNP standard (0.01 µg/l) based on the detection of  $^{80}\text{Se}$ . Run 3

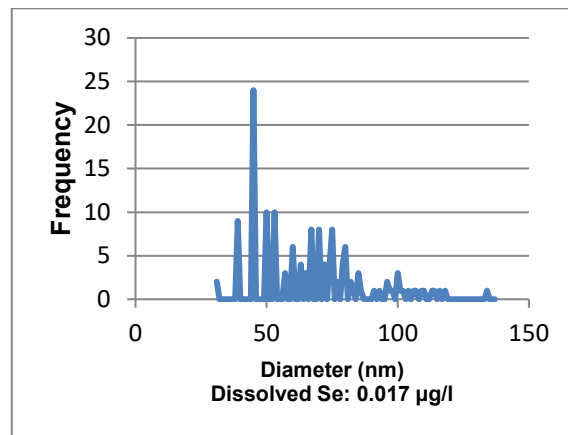


Figure 102: Size histogram of 100 nm SeNP standard (0.02 µg/l) based on the detection of  $^{80}\text{Se}$ . Run 1

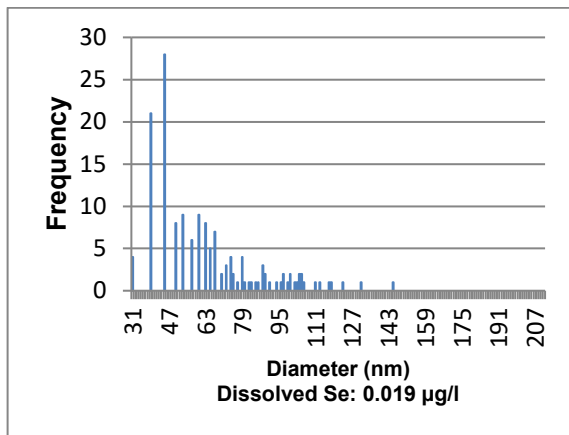


Figure 103: Size histogram of 100 nm SeNP standard (0.02 µg/l) based on the detection of  $^{80}\text{Se}$ . Run 2

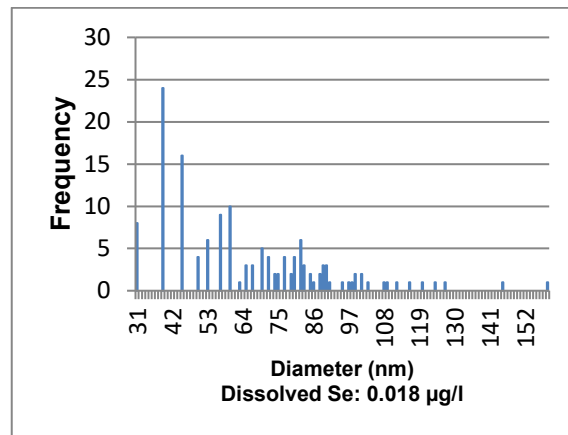


Figure 104: Size histogram of 100 nm SeNP standard (0.02 µg/l) based on the detection of  $^{80}\text{Se}$ . Run 3

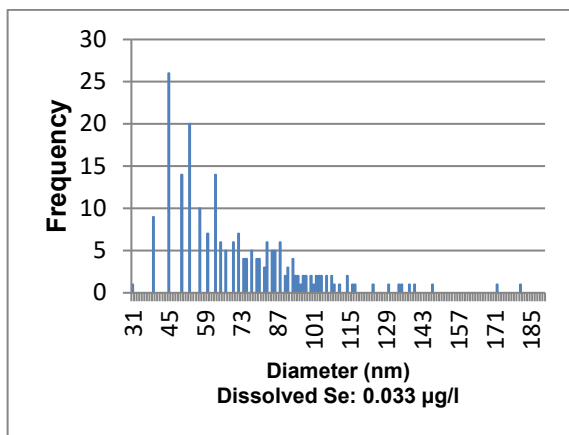


Figure 105: Size histogram of 100 nm SeNP standard (0.04 µg/l) based on the detection of  $^{80}\text{Se}$ . Run 1

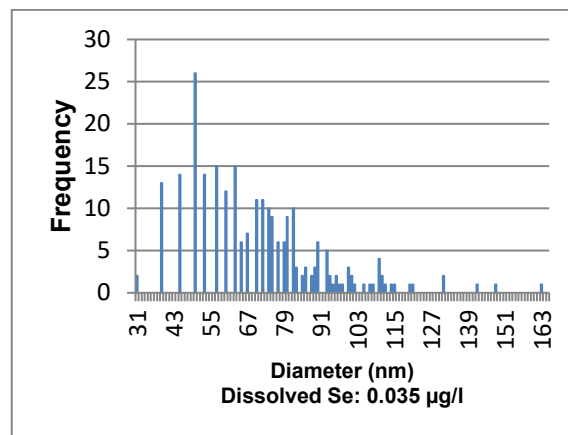


Figure 106: Size histogram of 100 nm SeNP standard (0.04 µg/l) based on the detection of  $^{80}\text{Se}$ . Run 2

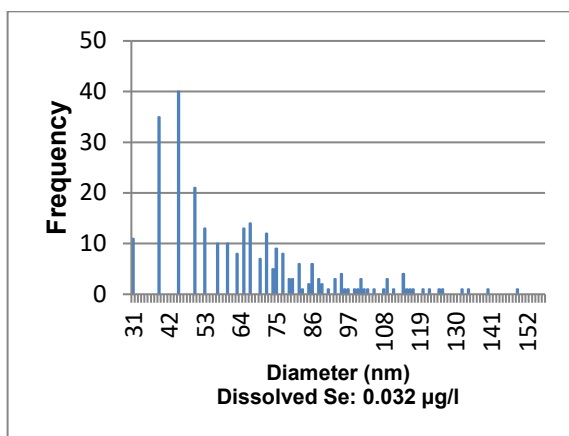


Figure 107: Size histogram of 100 nm SeNP standard (0.04 µg/l) based on the detection of  $^{80}\text{Se}$ . Run 3

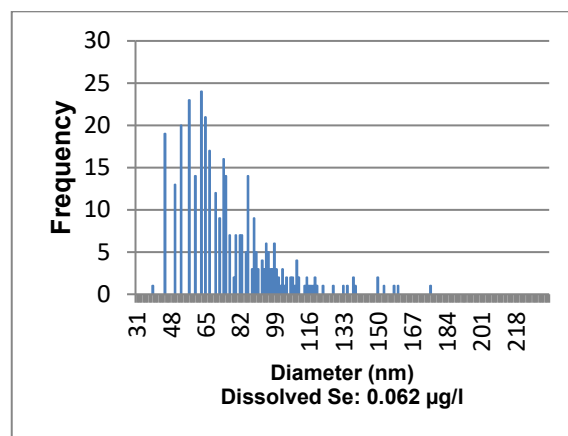


Figure 108: Size histogram of 100 nm SeNP standard (0.08 µg/l) based on the detection of  $^{80}\text{Se}$ . Run 1

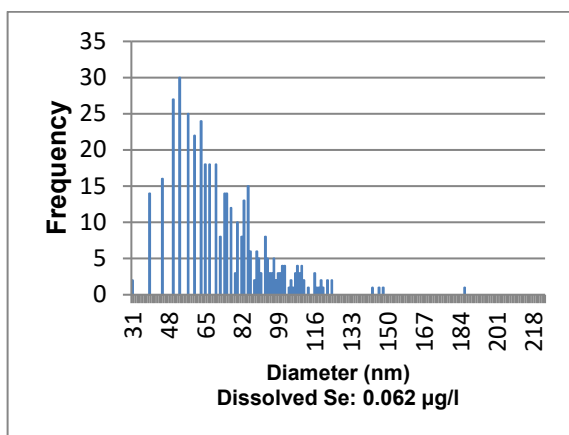


Figure 109: Size histogram of 100 nm SeNP standard (0.08 µg/l) based on the detection of  $^{80}\text{Se}$ . Run 2

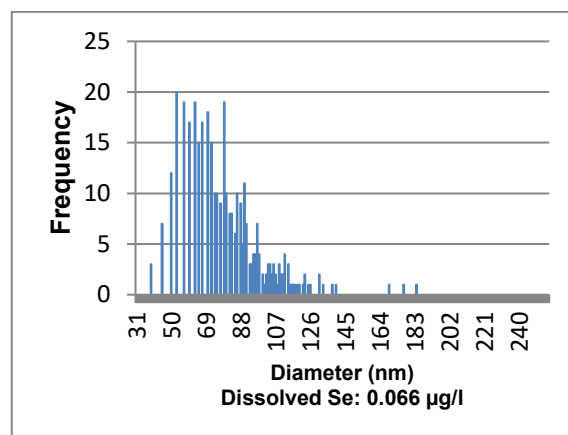


Figure 110: Size histogram of 100 nm SeNP standard (0.02 µg/l) based on the detection of  $^{80}\text{Se}$ . Run 3

## Repeatability

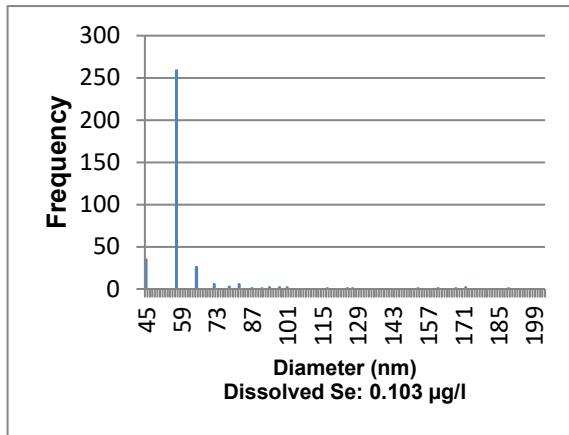


Figure 111: Size histogram of 50 nm SeNP standard (0.01 µg/l) based on the detection of  $^{78}\text{Se}$ . Run 1

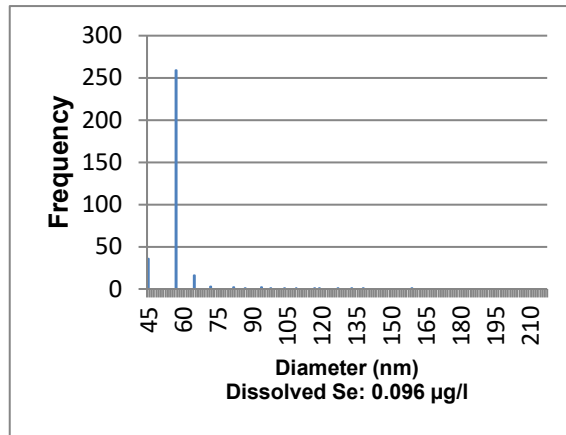


Figure 112: Size histogram of 50 nm SeNP standard (0.01 µg/l) based on the detection of  $^{78}\text{Se}$ . Run 2

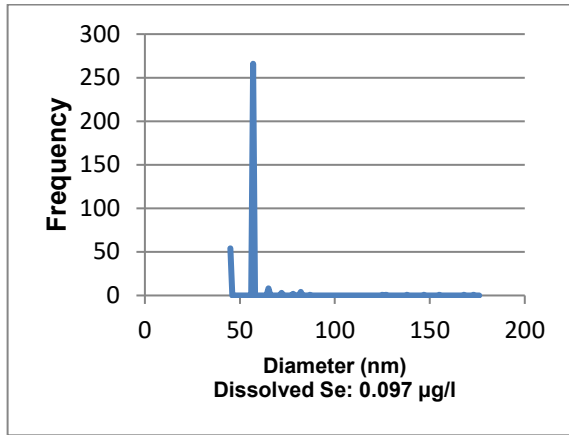


Figure 113: Size histogram of 50 nm SeNP standard (0.01 µg/l) based on the detection of  $^{78}\text{Se}$ . Run 3

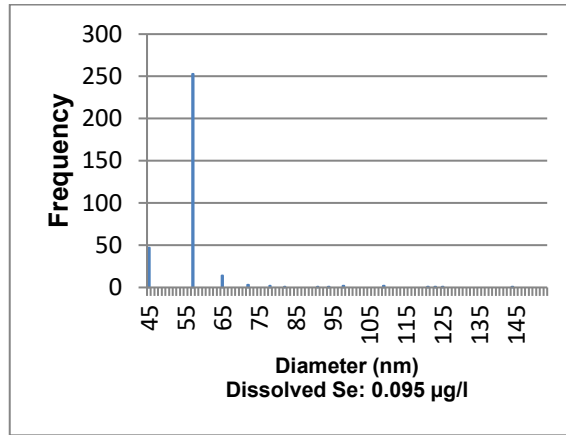


Figure 114: Size histogram of 50 nm SeNP standard (0.01 µg/l) based on the detection of  $^{78}\text{Se}$ . Run 4

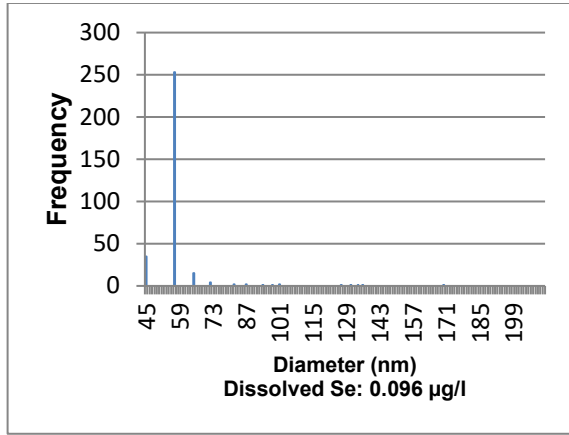


Figure 115: Size histogram of 50 nm SeNP standard (0.01 µg/l) based on the detection of  $^{78}\text{Se}$ . Run 5

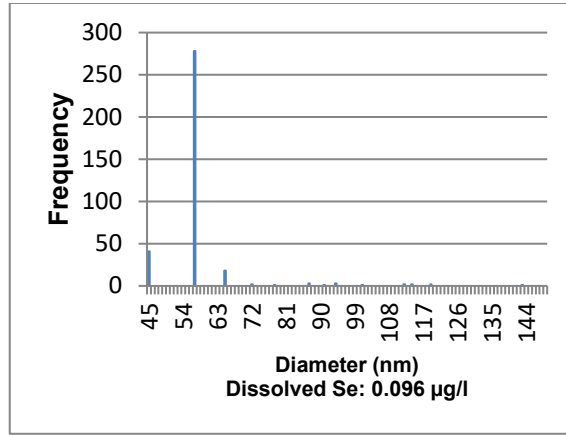


Figure 116: Size histogram of 50 nm SeNP standard (0.01 µg/l) based on the detection of  $^{78}\text{Se}$ . Run 6

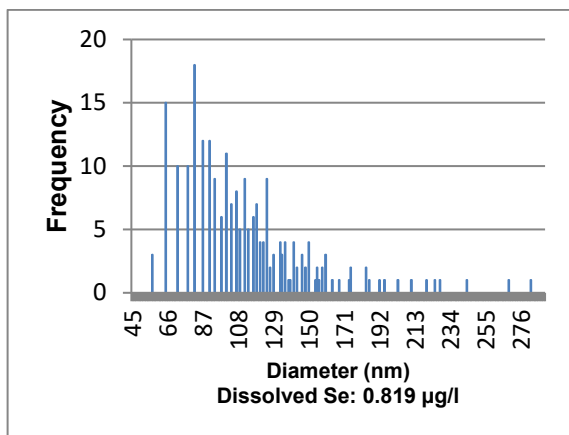


Figure 117: Size histogram of 50 nm SeNP standard (0.1 µg/l) based on the detection of  $^{78}\text{Se}$ . Run 1

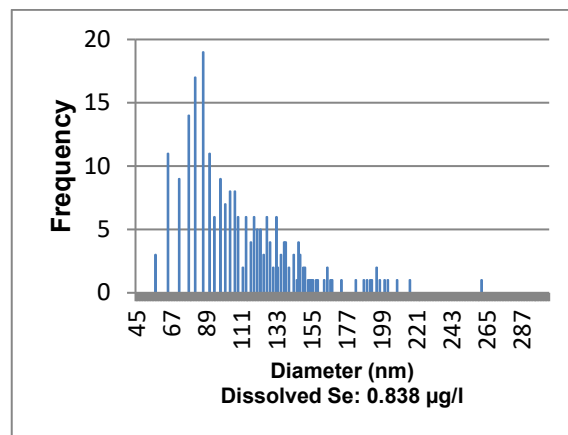


Figure 118: Size histogram of 50 nm SeNP standard (0.1 µg/l) based on the detection of  $^{78}\text{Se}$ . Run 2

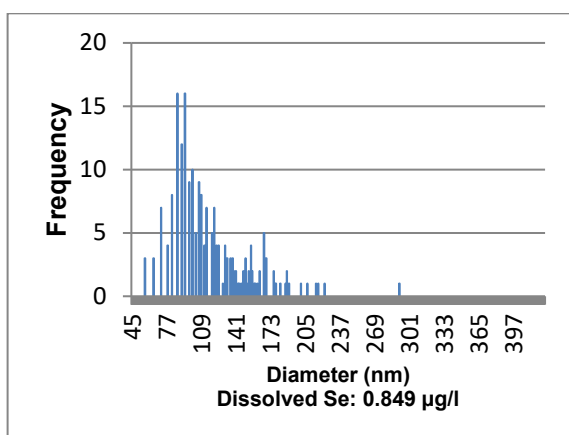


Figure 119: Size histogram of 50 nm SeNP standard (0.1 µg/l) based on the detection of  $^{78}\text{Se}$ . Run 3

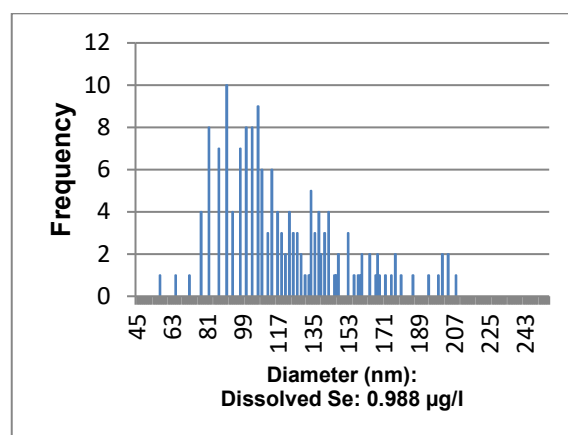


Figure 120: Size histogram of 50 nm SeNP standard (0.1 µg/l) based on the detection of  $^{78}\text{Se}$ . Run 4

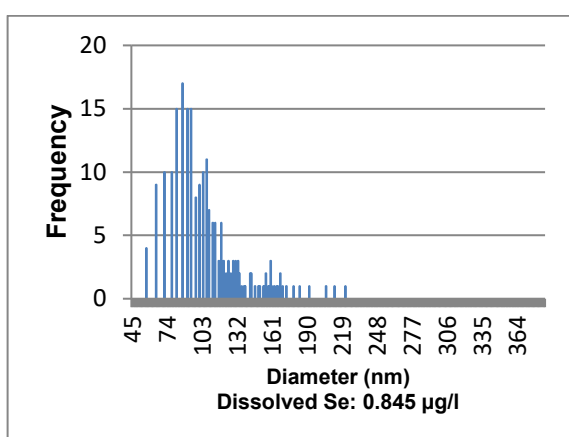


Figure 121: Size histogram of 50 nm SeNP standard (0.1 µg/l) based on the detection of  $^{78}\text{Se}$ . Run 5

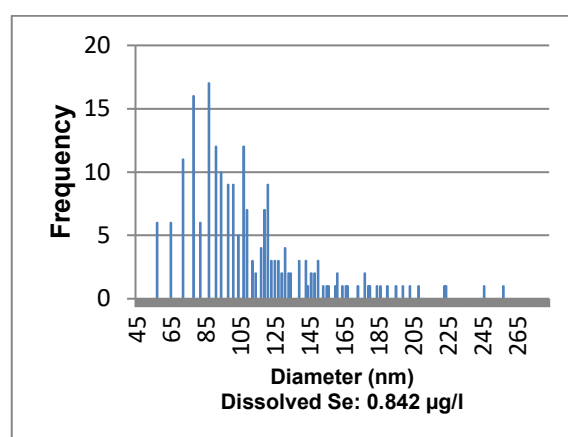


Figure 122: Size histogram of 50 nm SeNP standard (0.1 µg/l) based on the detection of  $^{78}\text{Se}$ . Run 6

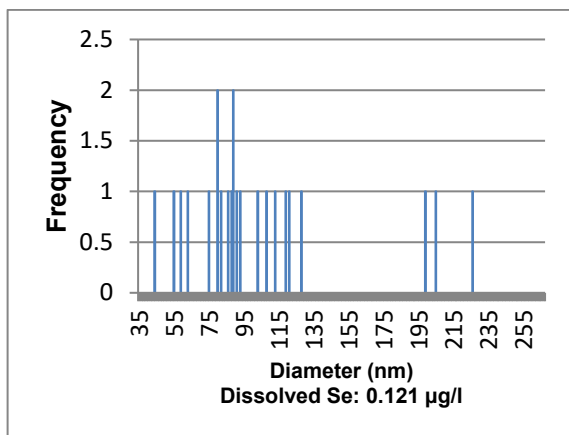


Figure 123: Size histogram of 50 nm SeNP standard (0.01 µg/l) based on the detection of  $^{80}\text{Se}$ . Run 1

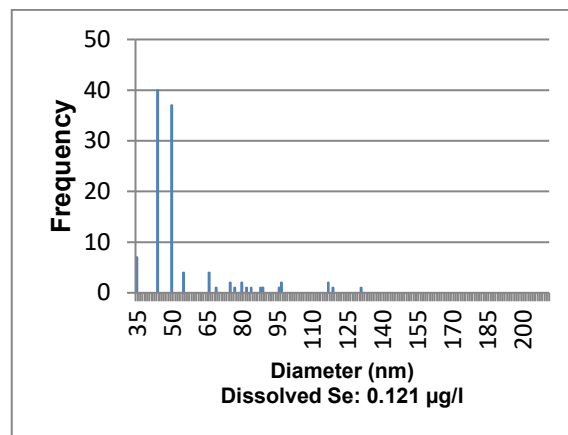


Figure 124: Size histogram of 50 nm SeNP standard (0.01 µg/l) based on the detection of  $^{80}\text{Se}$ . Run 2

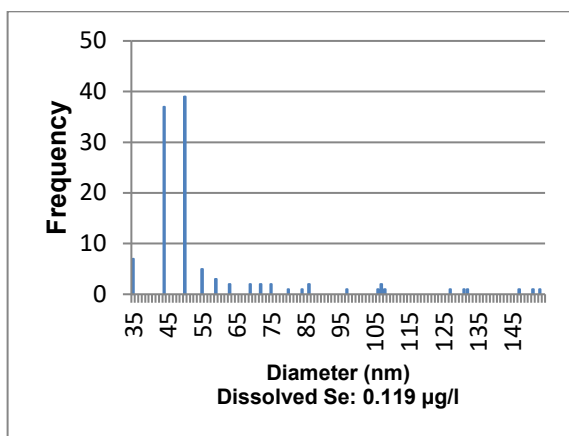


Figure 125: Size histogram of 50 nm SeNP standard (0.01 µg/l) based on the detection of  $^{80}\text{Se}$ . Run 3

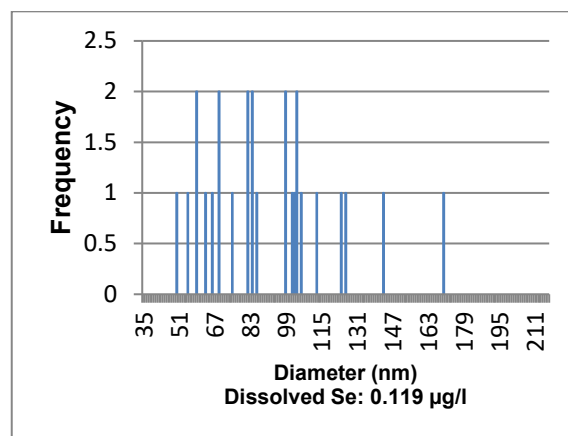


Figure 126: Size histogram of 50 nm SeNP standard (0.01 µg/l) based on the detection of  $^{80}\text{Se}$ . Run 4

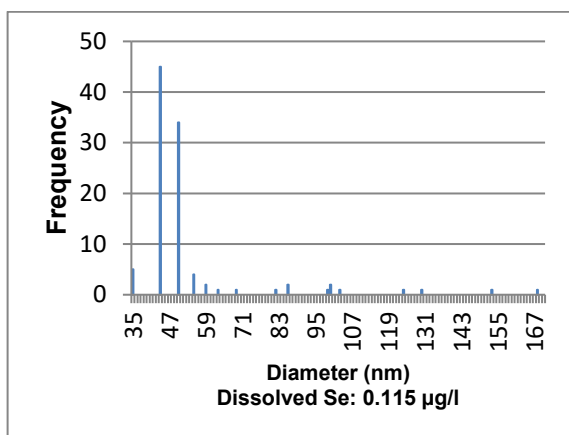


Figure 127: Size histogram of 50 nm SeNP standard (0.01 µg/l) based on the detection of  $^{80}\text{Se}$ . Run 5

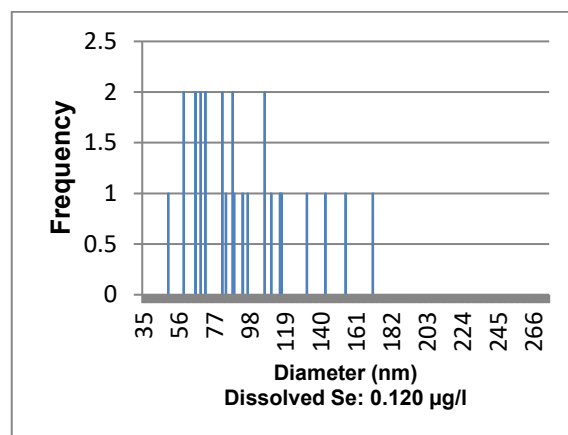


Figure 128: Size histogram of 50 nm SeNP standard (0.01 µg/l) based on the detection of  $^{80}\text{Se}$ . Run 6

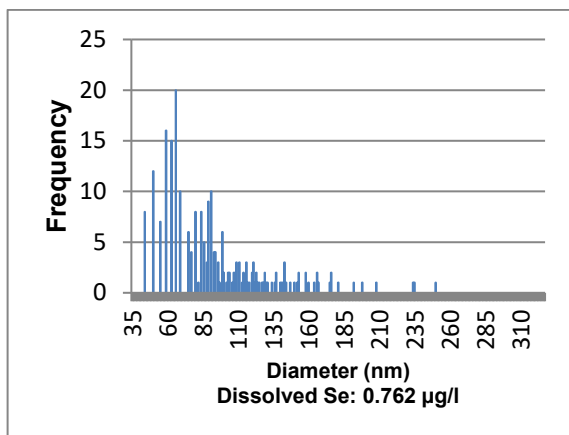


Figure 129: Size histogram of 50 nm SeNP standard (0.1 µg/l) based on the detection of  $^{80}\text{Se}$ . Run 1

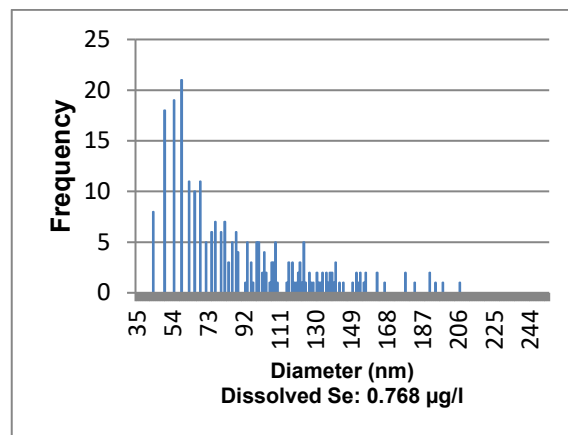


Figure 130: Size histogram of 50 nm SeNP standard (0.1 µg/l) based on the detection of  $^{80}\text{Se}$ . Run 2

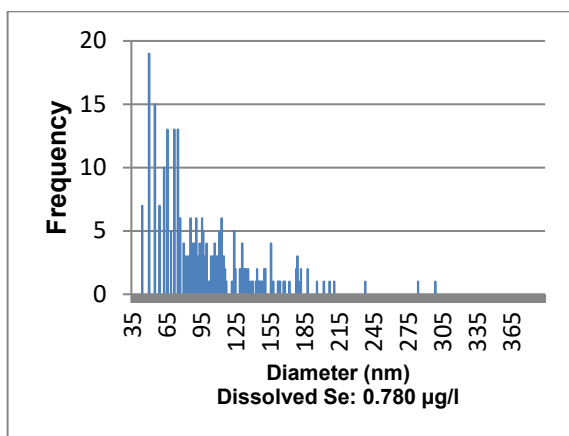


Figure 131: Size histogram of 50 nm SeNP standard (0.1 µg/l) based on the detection of  $^{80}\text{Se}$ . Run 3

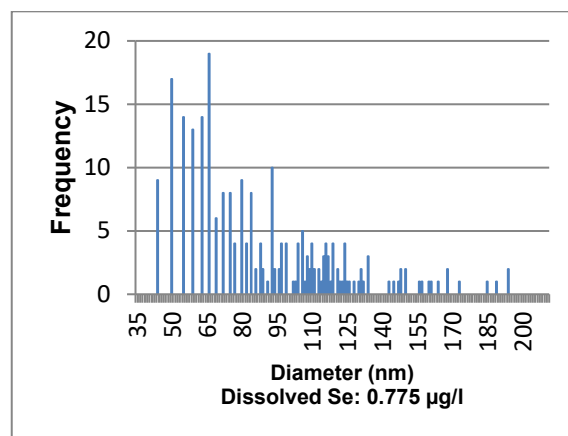


Figure 132: Size histogram of 50 nm SeNP standard (0.1 µg/l) based on the detection of  $^{80}\text{Se}$ . Run 4

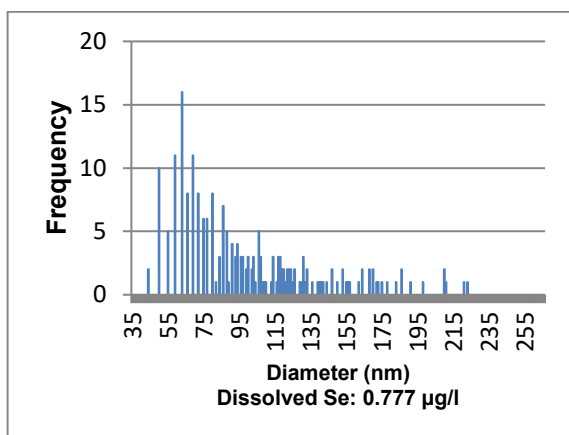


Figure 133: Size histogram of 50 nm SeNP standard (0.1 µg/l) based on the detection of  $^{80}\text{Se}$ . Run 5

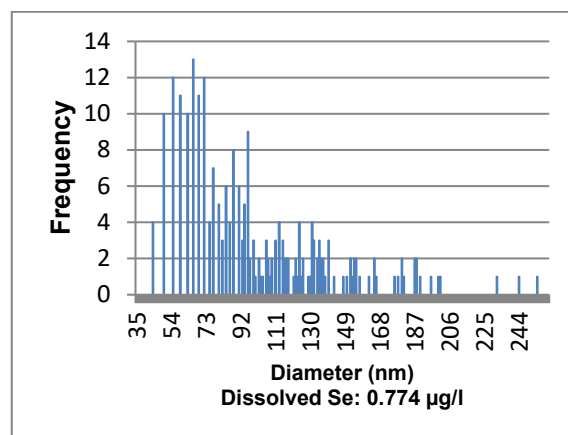


Figure 134: Size histogram of 50 nm SeNP standard (0.1 µg/l) based on the detection of  $^{80}\text{Se}$ . Run 6

## Inspection of the possibility of particle aggregation

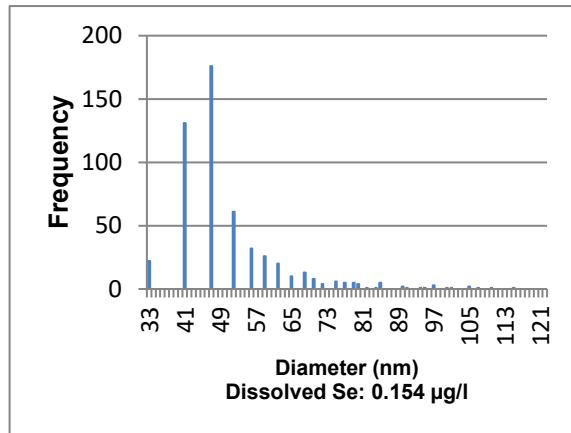


Figure 135: Size histogram of 50 nm SeNP standard (0.02 µg/l), not sonicated. Run 1

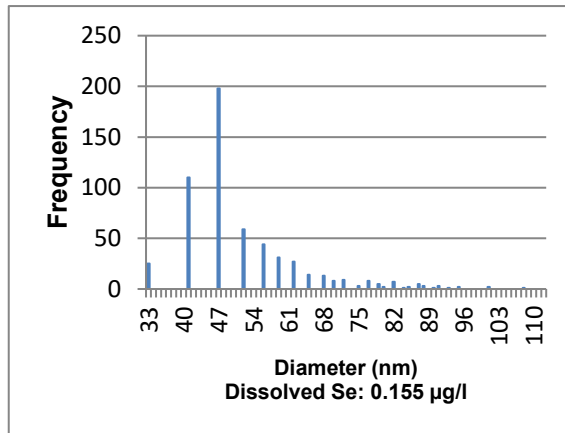


Figure 136: Size histogram of 50 nm SeNP standard (0.02 µg/l), not sonicated. Run 2

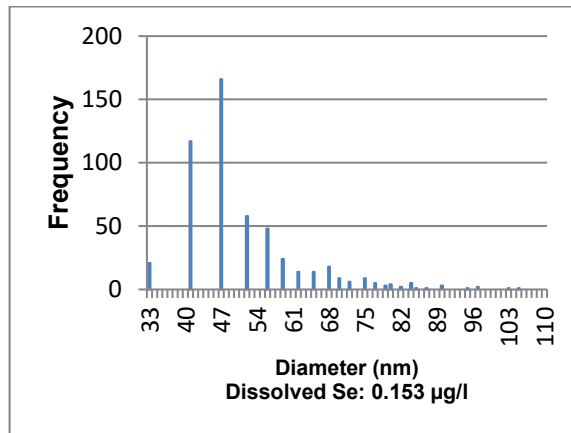


Figure 137: Size histogram of 50 nm SeNP standard (0.02 µg/l), not sonicated. Run 3

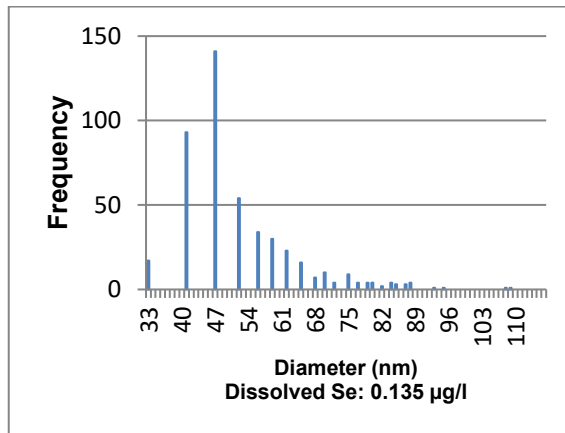


Figure 138: Size histogram of 50 nm SeNP standard (0.02 µg/l), sonicated. Run 1

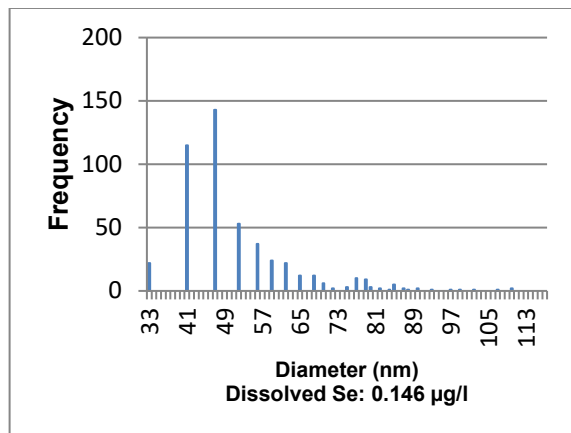


Figure 139: Size histogram of 50 nm SeNP standard (0.02 µg/l), sonicated. Run 2

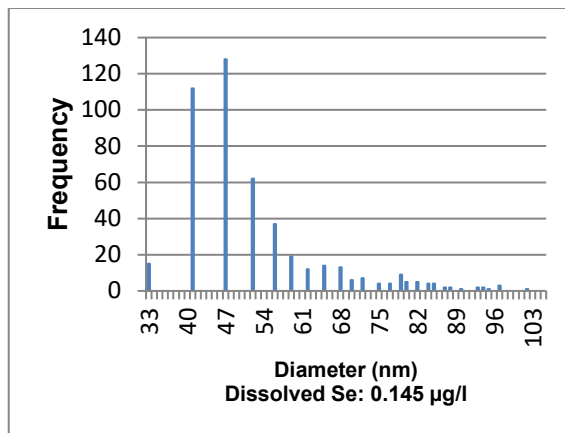


Figure 140: Size histogram of 50 nm SeNP standard (0.02 µg/l), sonicated. Run 3

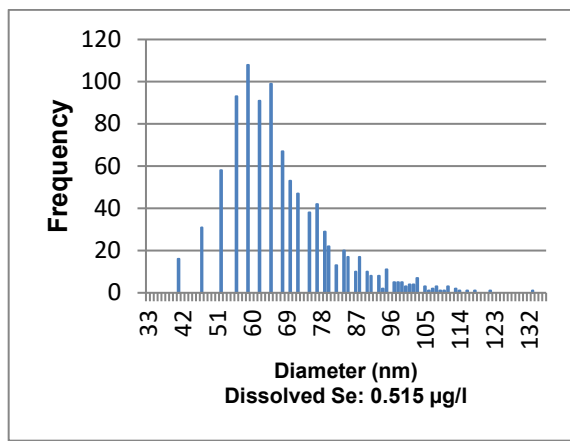


Figure 141: Size histogram of 50 nm SeNP standard (0.08 µg/l), not sonicated. Run 1

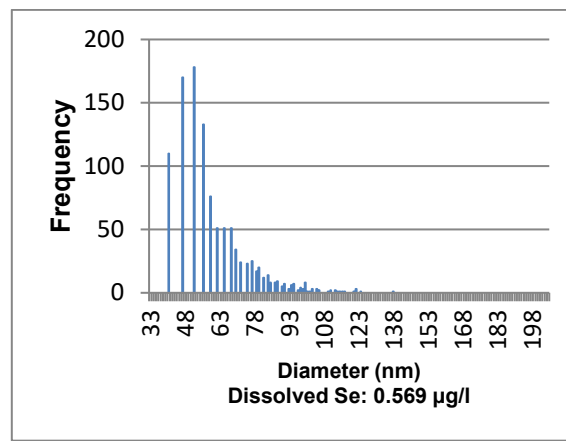


Figure 142: Size histogram of 50 nm SeNP standard (0.08 µg/l), not sonicated. Run 2

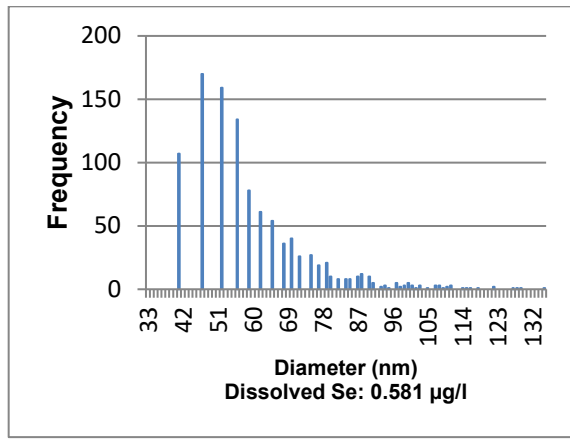


Figure 143: Size histogram of 50 nm SeNP standard (0.08 µg/l), not sonicated. Run 3

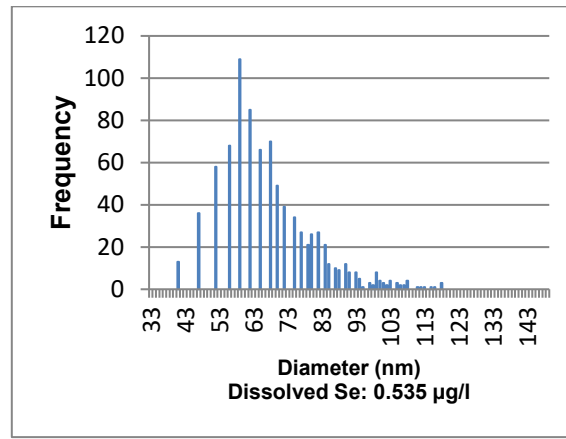


Figure 144: Size histogram of 50 nm SeNP standard (0.08 µg/l), sonicated. Run 1

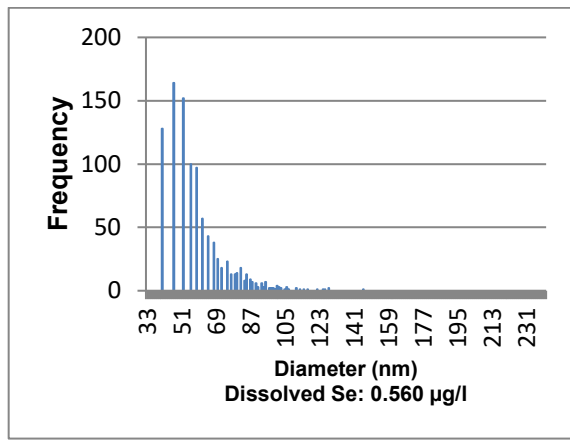


Figure 145: Size histogram of 50 nm SeNP standard (0.08 µg/l), sonicated. Run 2

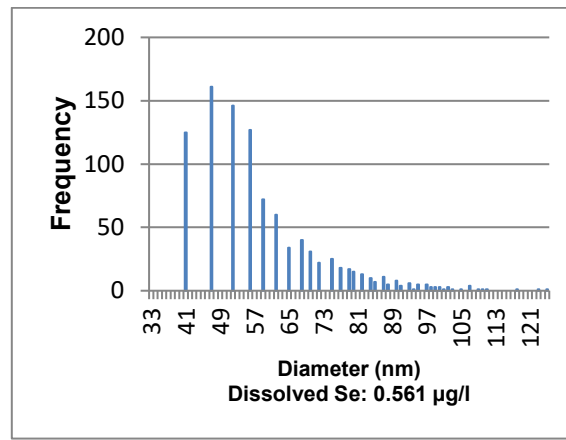


Figure 146: Size histogram of 50 nm SeNP standard (0.08 µg/l), sonicated. Run 3

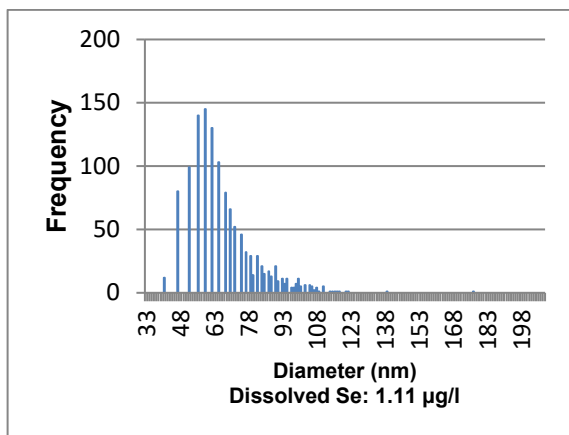


Figure 147: Size histogram of 50 nm SeNP standard (0.2 µg/l), not sonicated. Run 1

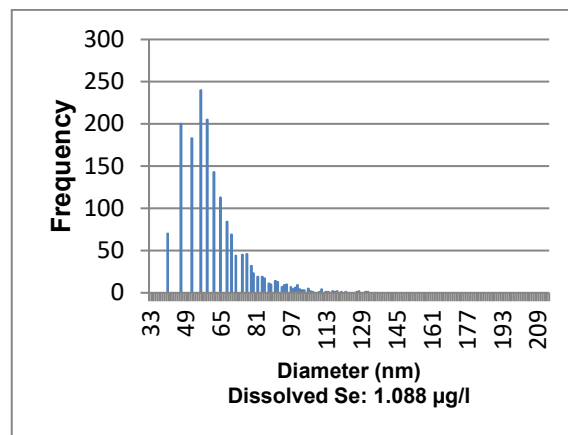


Figure 148: Size histogram of 50 nm SeNP standard (0.2 µg/l), not sonicated. Run 2

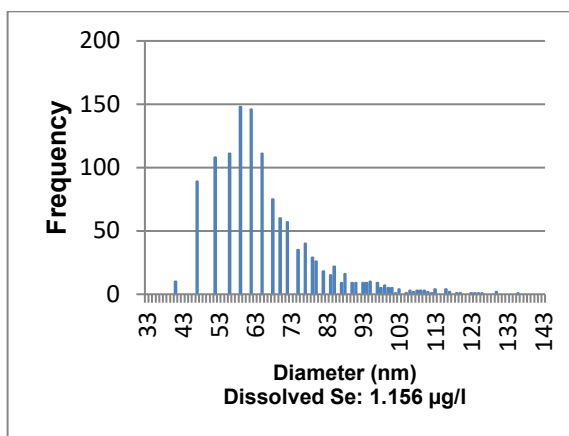


Figure 149: Size histogram of 50 nm SeNP standard (0.2 µg/l), not sonicated. Run 3

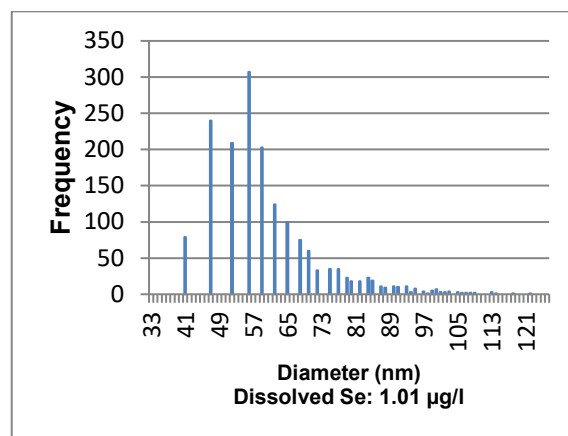


Figure 150: Size histogram of 50 nm SeNP standard (0.2 µg/l), sonicated. Run 1

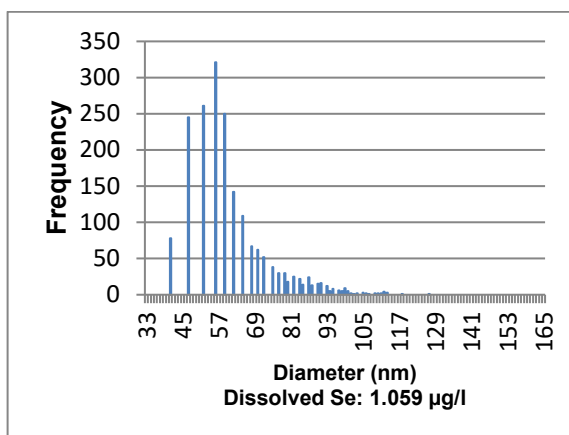


Figure 151: Size histogram of 50 nm SeNP standard (0.2 µg/l), sonicated. Run 2

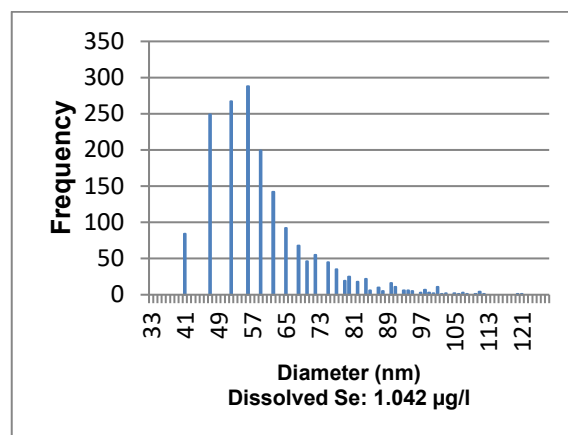


Figure 152: Size histogram of 50 nm SeNP standard (0.2 µg/l), sonicated. Run 3

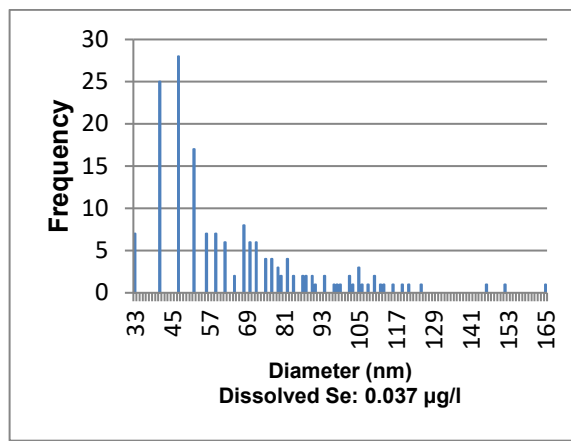


Figure 153: Size histogram of 100 nm SeNP standard (0.02 µg/l), not sonicated. Run 1

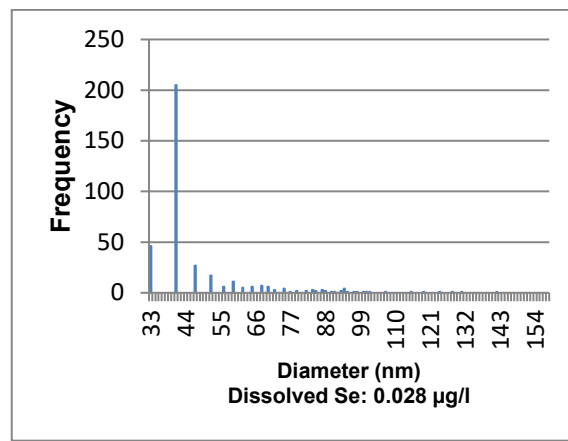


Figure 154: Size histogram of 100 nm SeNP standard (0.02 µg/l), not sonicated. Run 2

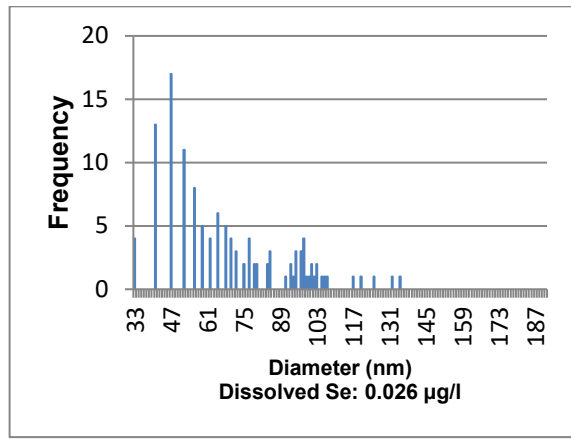


Figure 155: Size histogram of 100 nm SeNP standard (0.02 µg/l), not sonicated. Run 3

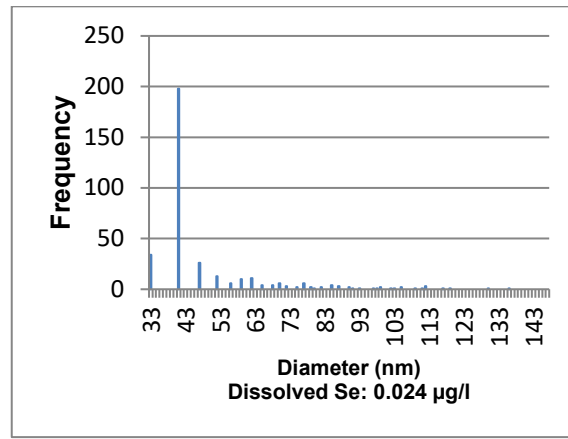


Figure 156: Size histogram of 100 nm SeNP standard (0.02 µg/l), sonicated. Run 1

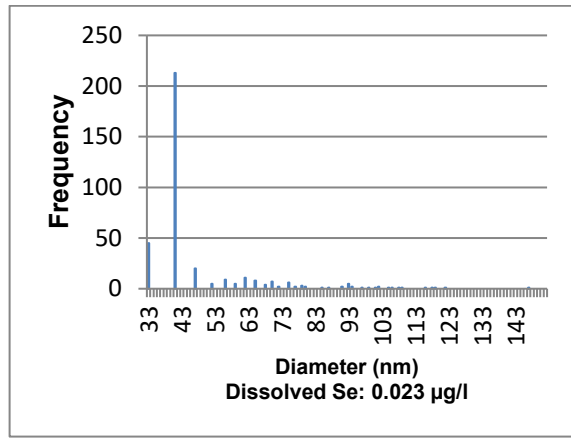


Figure 157: Size histogram of 100 nm SeNP standard (0.02 µg/l), sonicated. Run 2

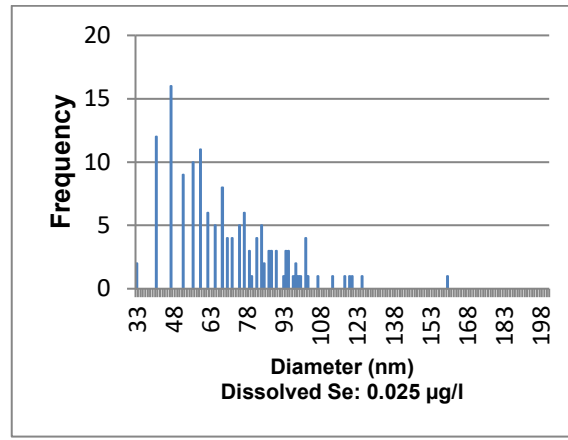


Figure 158: Size histogram of 100 nm SeNP standard (0.02 µg/l), sonicated. Run 3

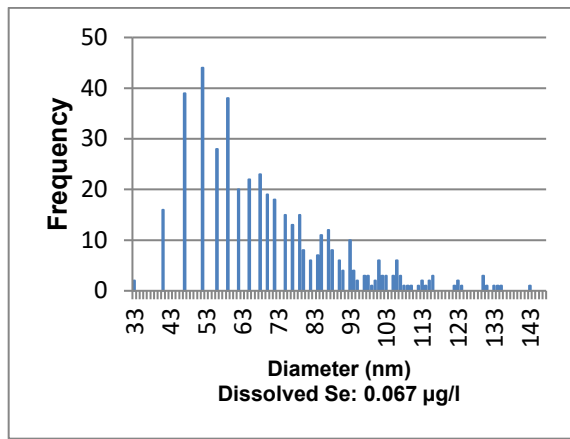


Figure 159: Size histogram of 100 nm SeNP standard (0.067 µg/l), not sonicated. Run 1

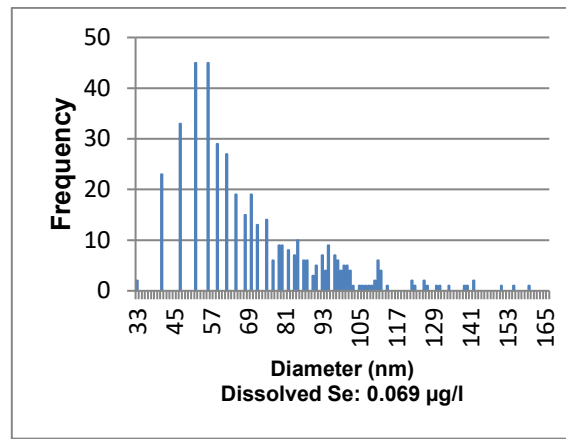


Figure 160: Size histogram of 100 nm SeNP standard (0.069 µg/l), not sonicated. Run 2

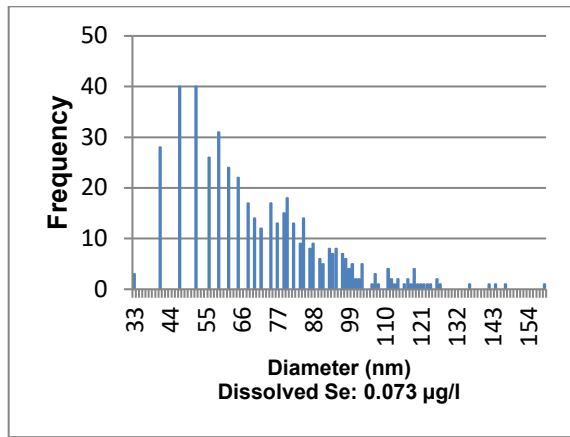


Figure 161: Size histogram of 100 nm SeNP standard (0.073 µg/l), not sonicated. Run 3

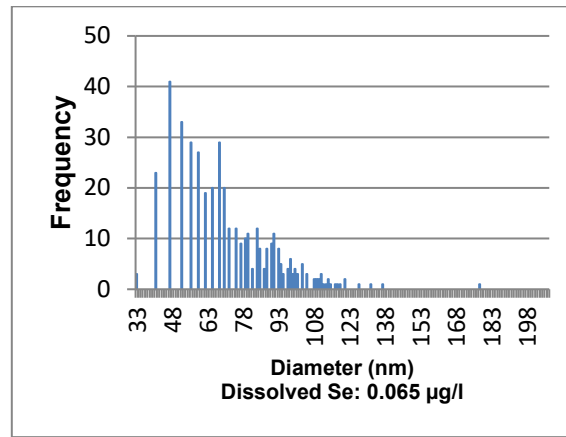


Figure 162: Size histogram of 100 nm SeNP standard (0.065 µg/l), sonicated. Run 1

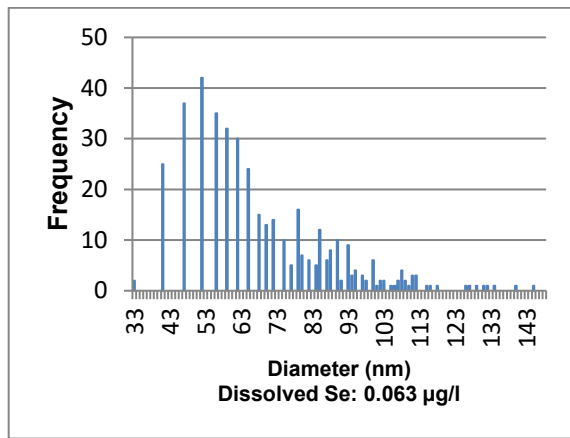


Figure 163: Size histogram of 100 nm SeNP standard (0.063 µg/l), sonicated. Run 2

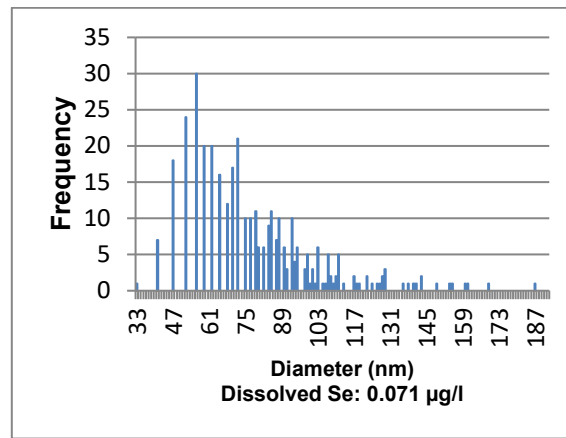


Figure 164: Size histogram of 100 nm SeNP standard (0.071 µg/l), sonicated. Run 3

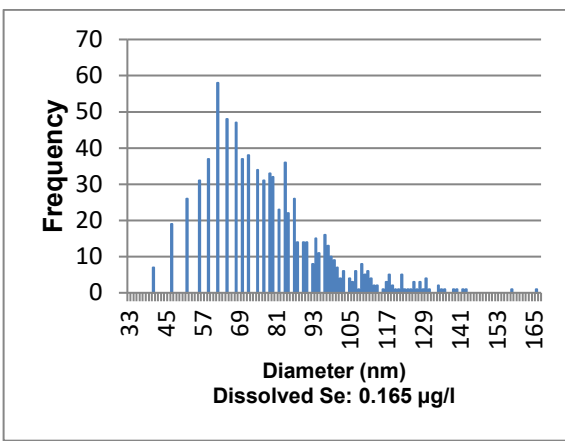


Figure 165: Size histogram of 100 nm SeNP standard (0.2 µg/l), not sonicated. Run 1

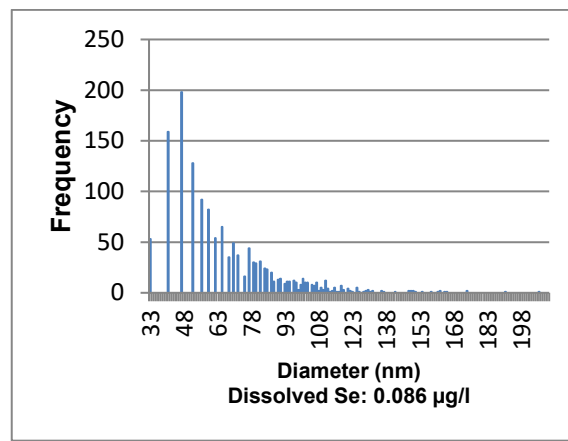


Figure 166: Size histogram of 100 nm SeNP standard (0.2 µg/l), not sonicated. Run 2

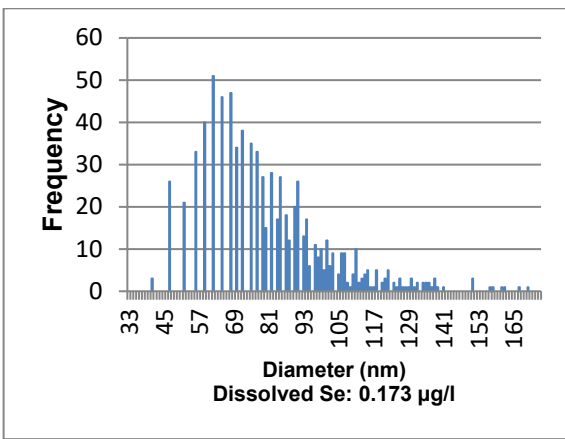


Figure 167: Size histogram of 100 nm SeNP standard (0.2 µg/l), not sonicated. Run 3

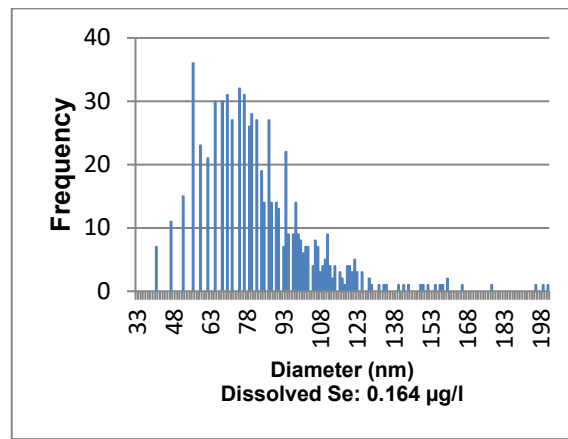


Figure 168: Size histogram of 100 nm SeNP standard (0.2 µg/l), sonicated. Run 1

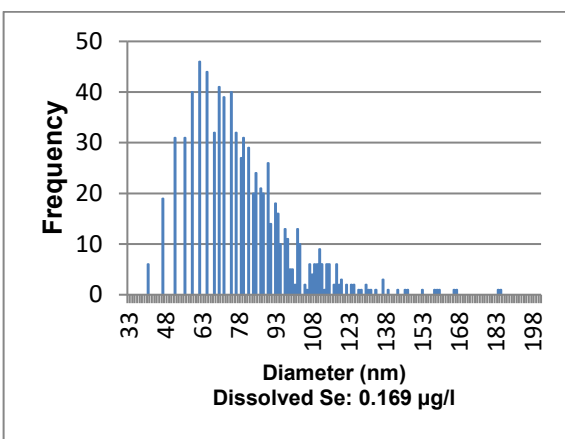


Figure 169: Size histogram of 100 nm SeNP standard (0.2 µg/l), sonicated. Run 2

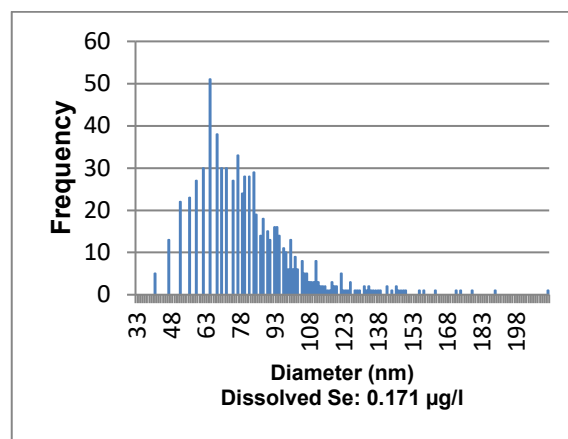


Figure 170: Size histogram of 100 nm SeNP standard (0.2 µg/l), sonicated. Run 3

## Improvement of the daily optimized parameters

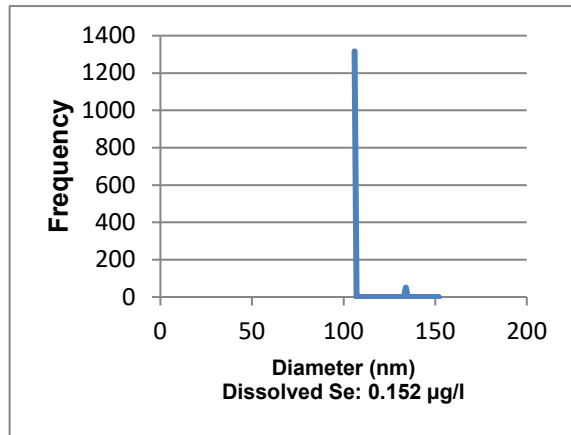


Figure 171: Size histogram of 50 nm SeNP standard (0.02 µg/l) default conditions. Run 1

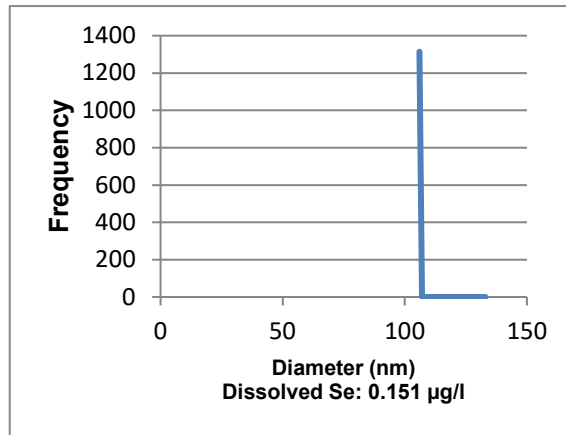


Figure 172: Size histogram of 50 nm SeNP standard (0.02 µg/l) default conditions. Run 2

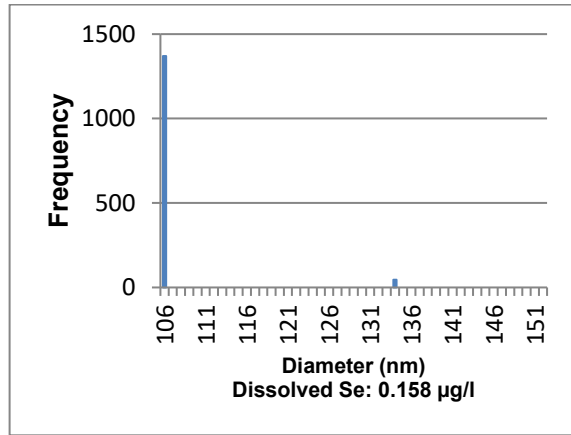


Figure 173: Size histogram of 50 nm SeNP standard (0.02 µg/l) default conditions. Run 3

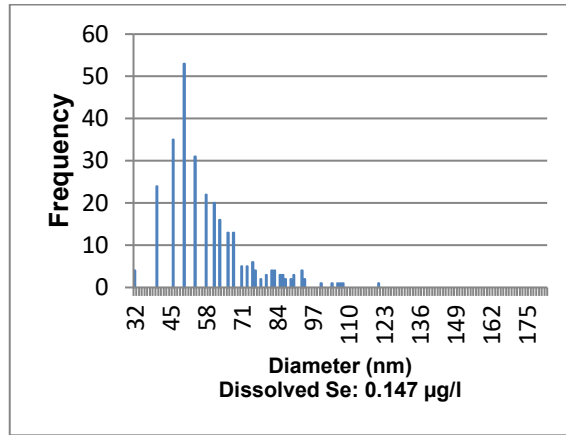


Figure 174: Size histogram of 50 nm SeNP standard (0.02 µg/l) nano conditions. Run 1

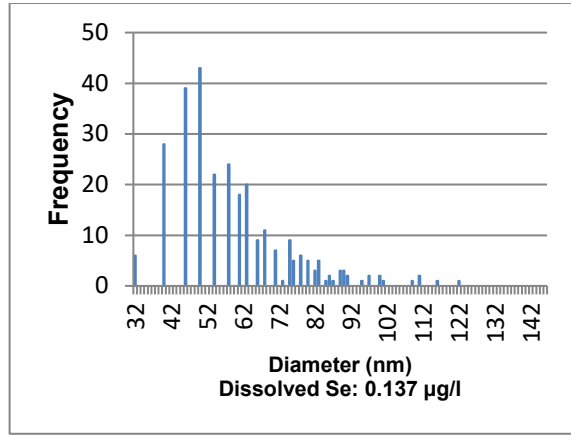


Figure 175: Size histogram of 50 nm SeNP standard (0.02 µg/l) nano conditions. Run 2

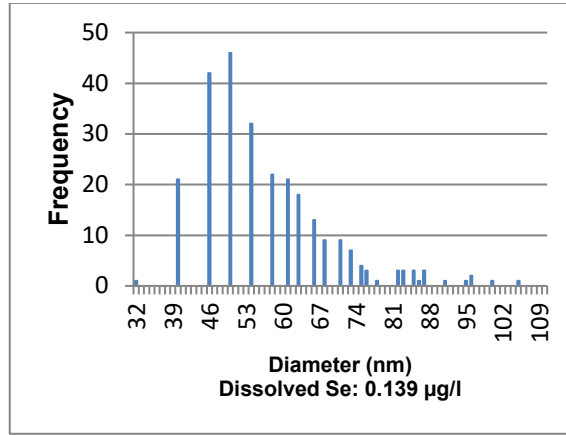


Figure 176: Size histogram of 50 nm SeNP standard (0.02 µg/l) nano conditions. Run 3

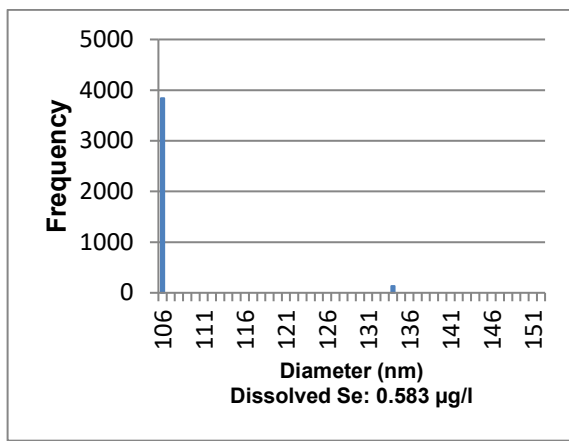


Figure 177: Size histogram of 50 nm SeNP standard (0.08 µg/l) default conditions. Run 1

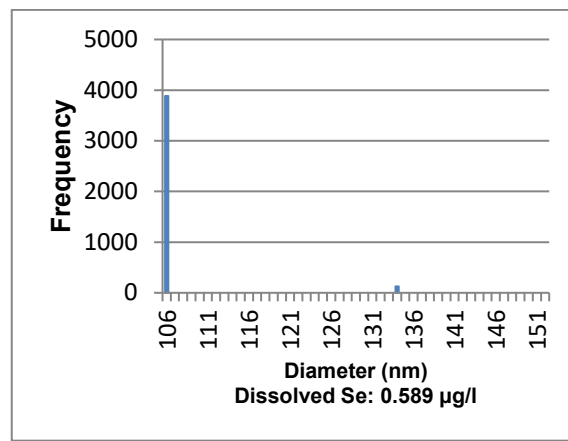


Figure 178: Size histogram of 50 nm SeNP standard (0.08 µg/l) default conditions. Run 2

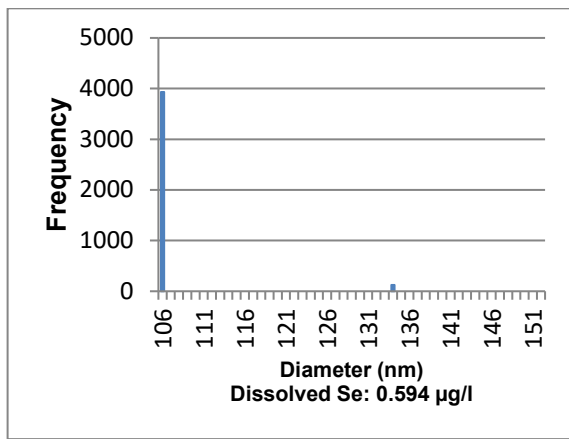


Figure 179: Size histogram of 50 nm SeNP standard (0.08 µg/l) default conditions. Run 3

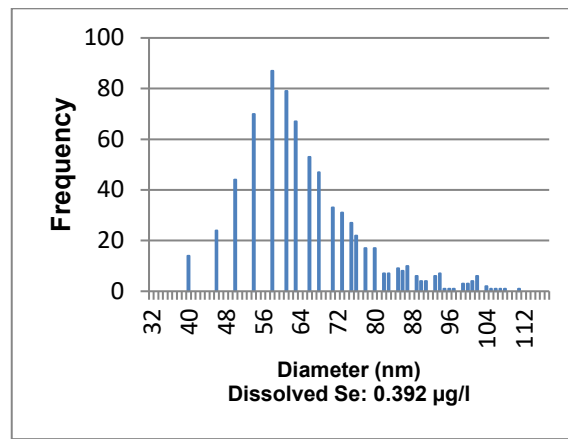


Figure 180: Size histogram of 50 nm SeNP standard (0.08 µg/l) nano conditions. Run 1

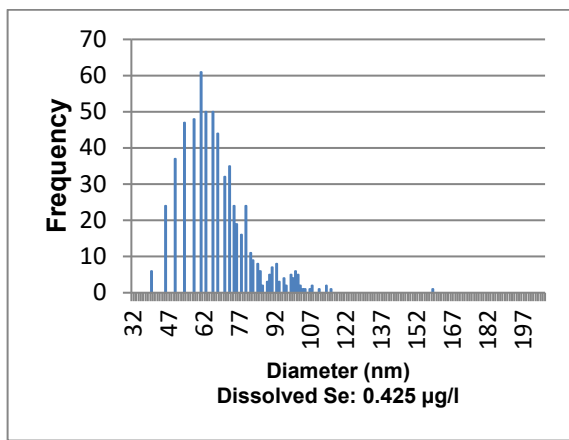


Figure 181: Size histogram of 50 nm SeNP standard (0.08 µg/l) nano conditions. Run 2

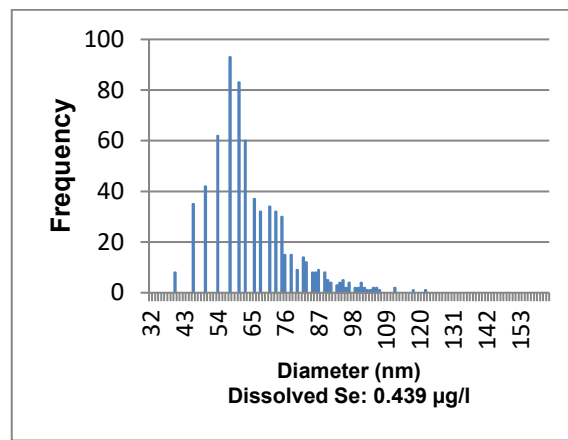


Figure 182: Size histogram of 50 nm SeNP standard (0.08 µg/l) nano conditions. Run 3

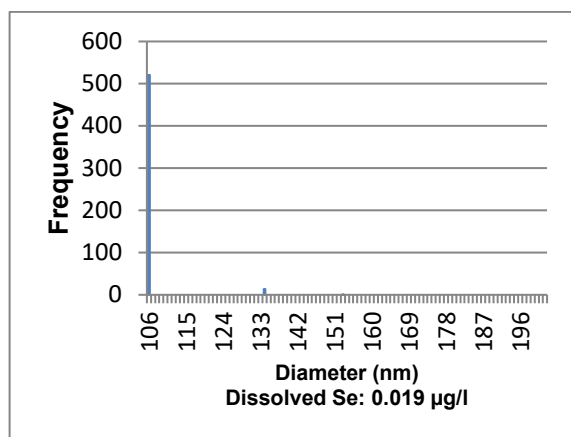


Figure 183: Size histogram of 100 nm SeNP standard (0.02 µg/l) default conditions. Run 1

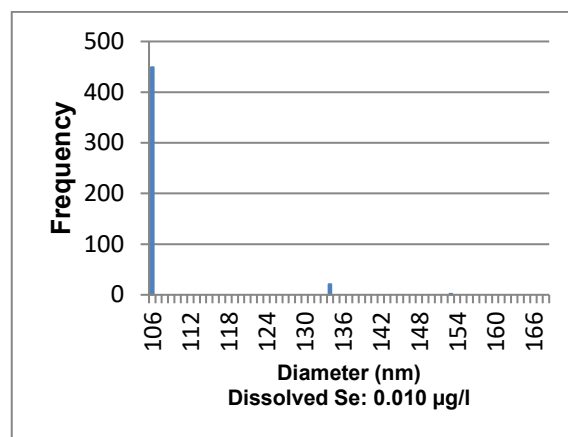


Figure 184: Size histogram of 100 nm SeNP standard (0.02 µg/l) default conditions. Run 2

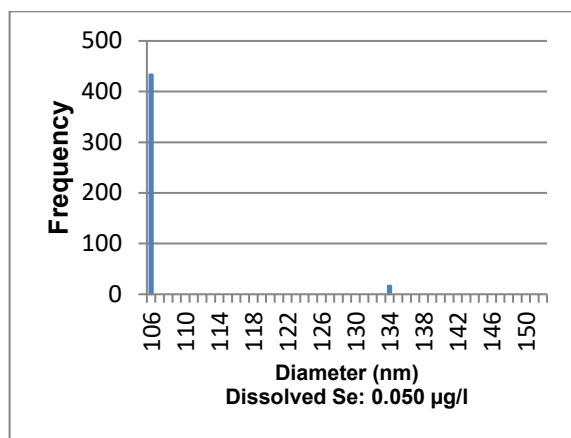


Figure 185: Size histogram of 100 nm SeNP standard (0.02 µg/l) default conditions. Run 3

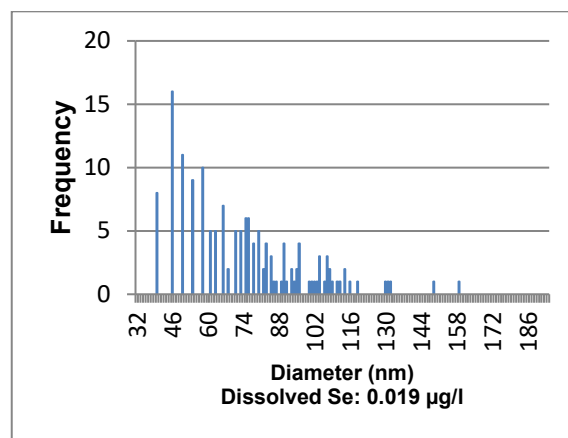


Figure 186: Size histogram of 100 nm SeNP standard (0.02 µg/l) nano conditions. Run 1

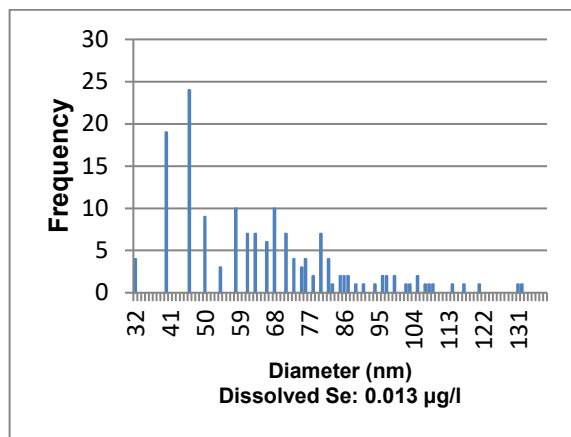


Figure 187: Size histogram of 100 nm SeNP standard (0.02 µg/l) nano conditions. Run 2

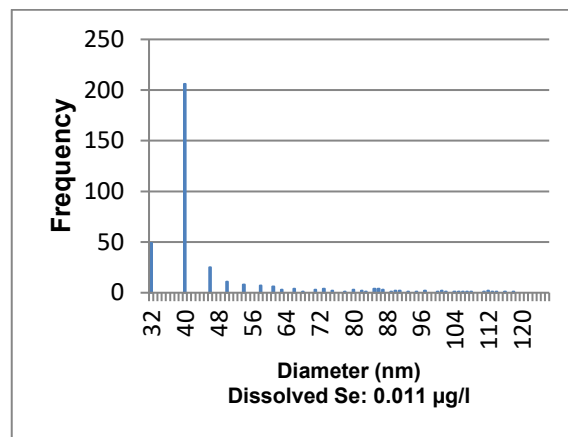


Figure 188: Size histogram of 100 nm SeNP standard (0.02 µg/l) nano conditions. Run 3

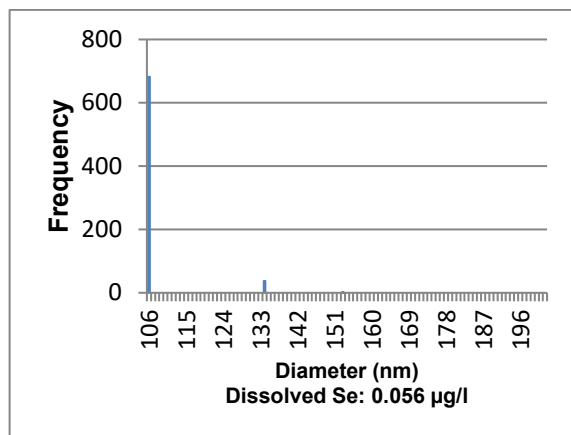


Figure 189: Size histogram of 100 nm SeNP standard (0.08 µg/l) default conditions. Run 1

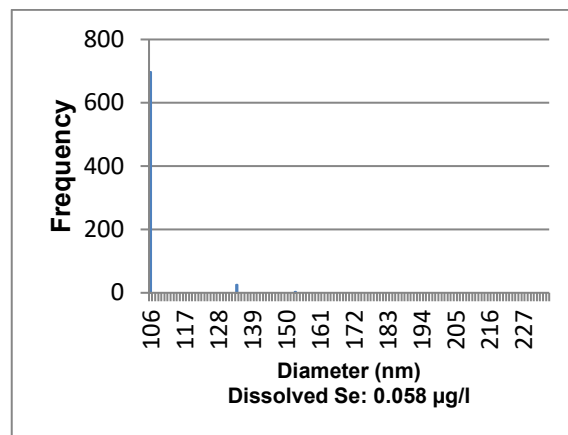


Figure 190: Size histogram of 100 nm SeNP standard (0.08 µg/l) default conditions. Run 2

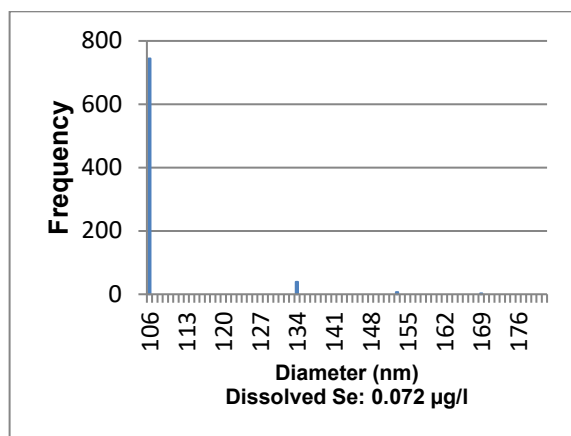


Figure 191: Size histogram of 100 nm SeNP standard (0.08 µg/l) default conditions. Run 3

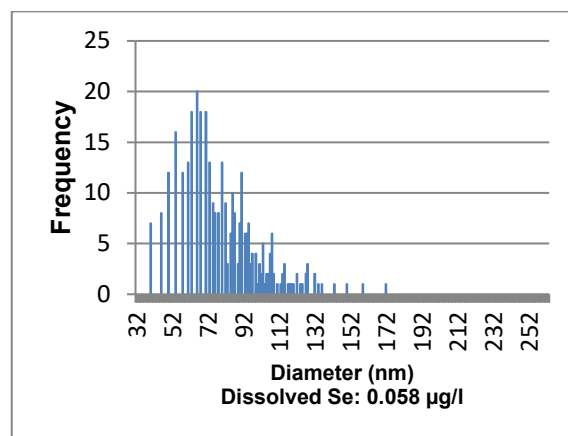


Figure 192: Size histogram of 100 nm SeNP standard (0.08 µg/l) nano conditions. Run 1

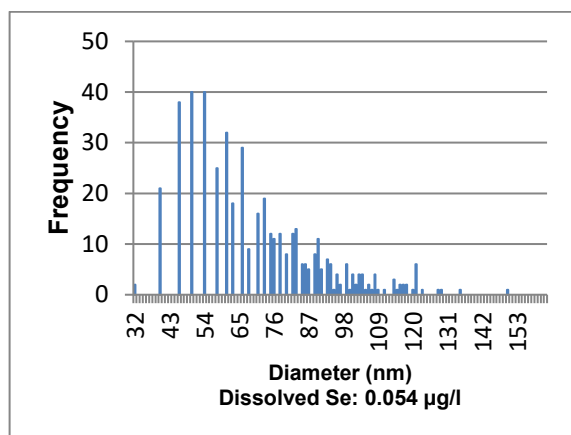


Figure 193: Size histogram of 100 nm SeNP standard (0.08 µg/l) nano conditions. Run 2

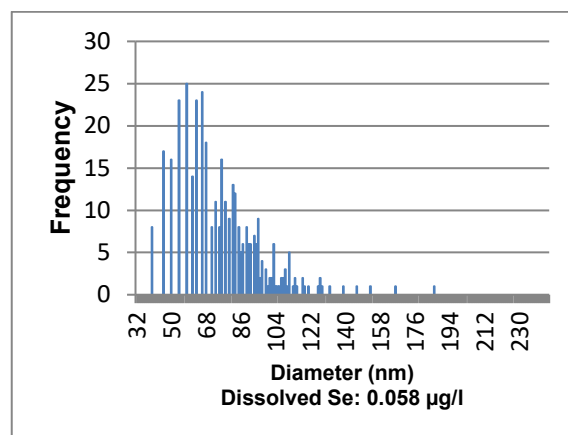


Figure 194: Size histogram of 100 nm SeNP standard (0.08 µg/l) nano conditions. Run 3

## Measuring time optimization

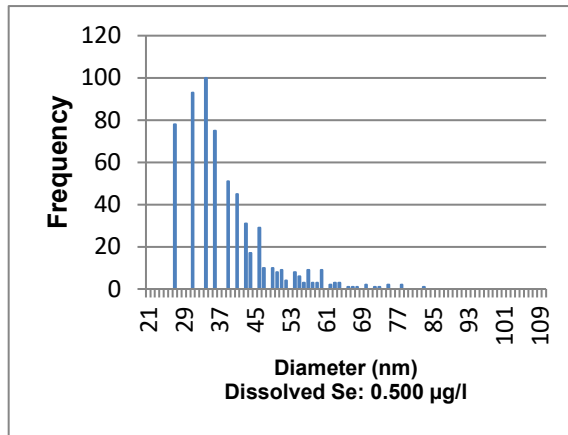


Figure 195: Size histogram of 50 nm SeNP standard (0.1 µg/l)  
30 s Measuring Time. Run 1. Automatic Threshold: 1.09

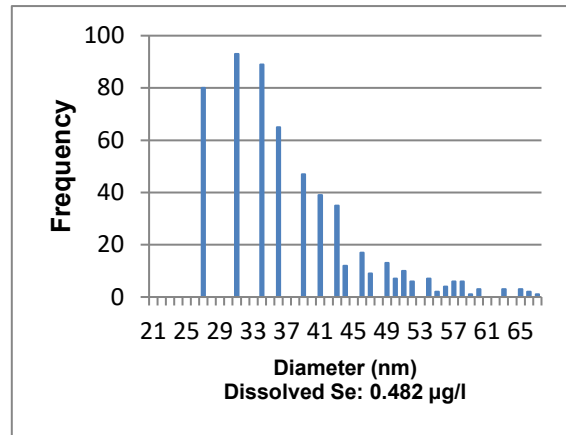


Figure 196: Size histogram of 50 nm SeNP standard (0.1 µg/l)  
30 s Measuring Time. Run 2. Automatic Threshold: 1.07

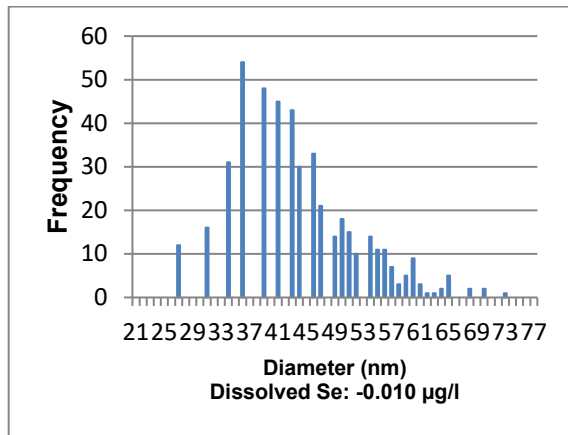


Figure 197: Size histogram of 50 nm SeNP standard (0.1 µg/l)  
30 s Measuring Time. Run 3. Manual Threshold: 1

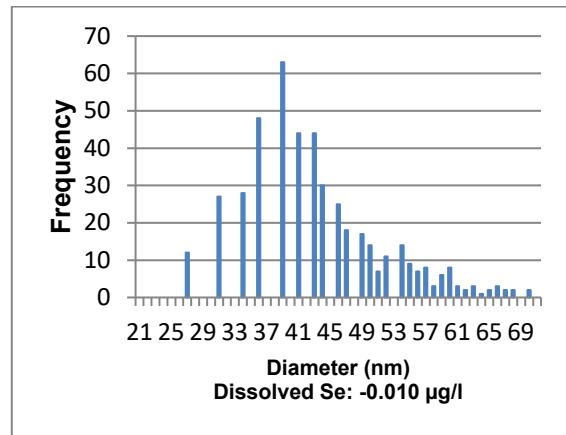


Figure 198: Size histogram of 50 nm SeNP standard (0.1 µg/l)  
30 s Measuring Time. Run 4. Manual Threshold: 1

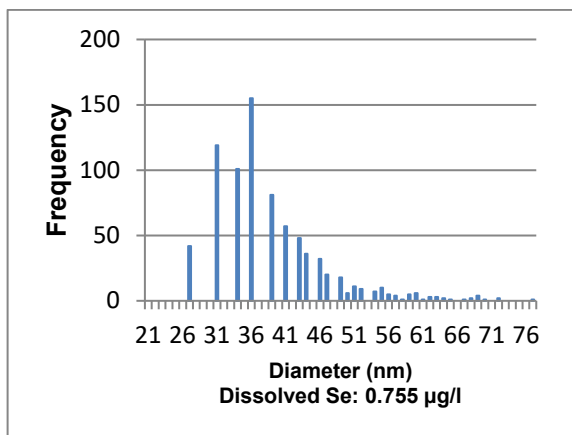


Figure 199: Size histogram of 50 nm SeNP standard (0.2 µg/l)  
30 s Measuring Time. Run 1. Automatic Threshold: 1.33

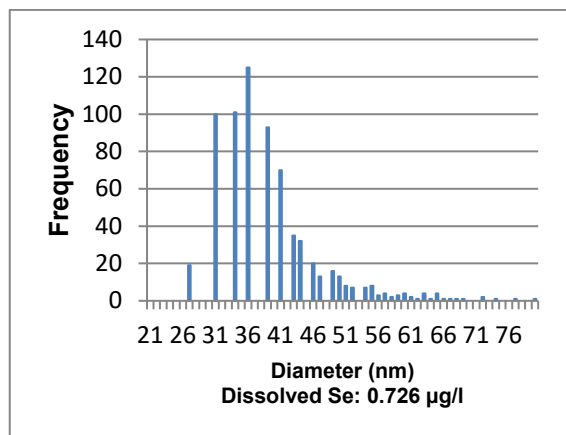


Figure 200: Size histogram of 50 nm SeNP standard (0.2 µg/l)  
30 s Measuring Time. Run 2. Automatic Threshold: 1.30

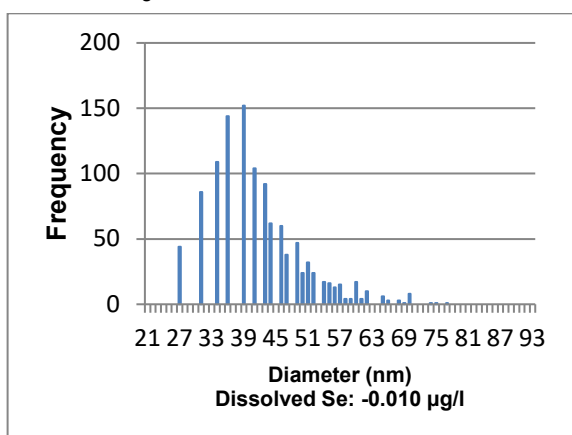


Figure 201: Size histogram of 50 nm SeNP standard (0.2 µg/l)  
30 s Measuring Time. Run 3. Manual Threshold:1

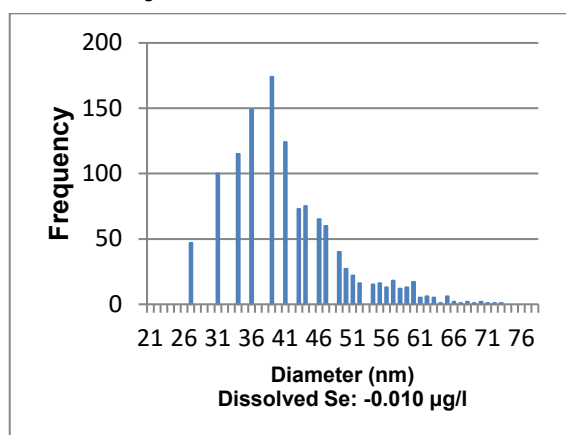


Figure 202: Size histogram of 50 nm SeNP standard (0.2 µg/l)  
30 s Measuring Time. Run 4. Manual Threshold:1

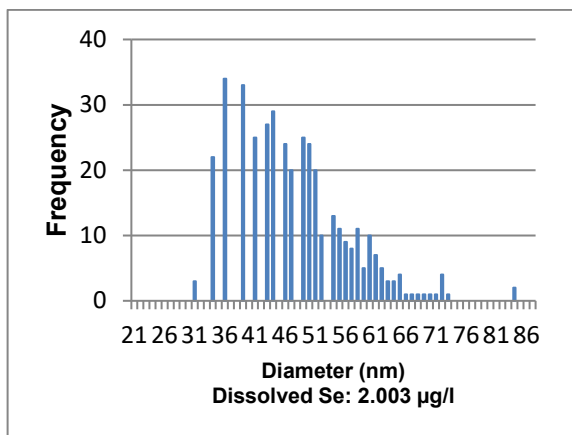


Figure 203: Size histogram of 50 nm SeNP standard (0.5 µg/l)  
30 s Measuring Time. Run 1. Automatic Threshold: 2.41

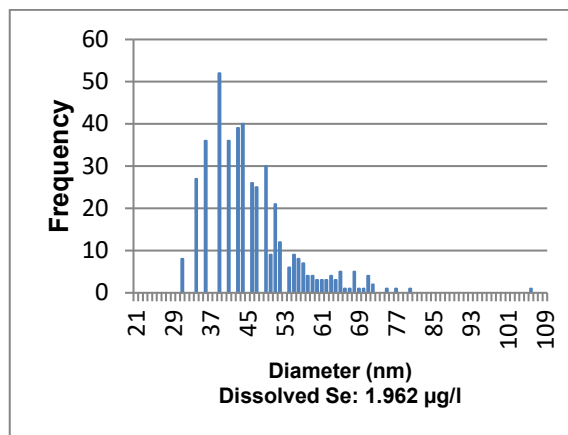


Figure 204: Size histogram of 50 nm SeNP standard (0.5 µg/l)  
30 s Measuring Time. Run 2. Automatic Threshold: 2.38

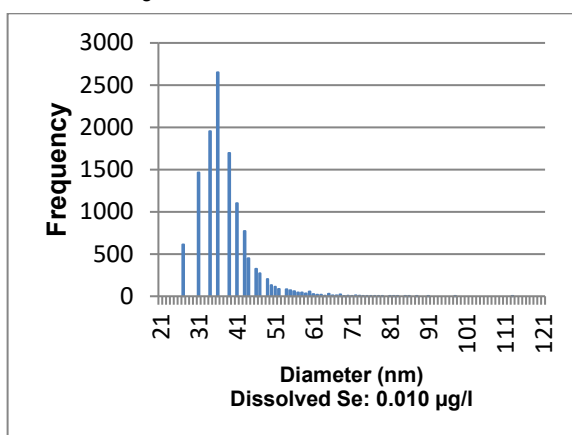


Figure 205: Size histogram of 50 nm SeNP standard (0.5 µg/l)  
30 s Measuring Time. Run 3. Manual Threshold: 1

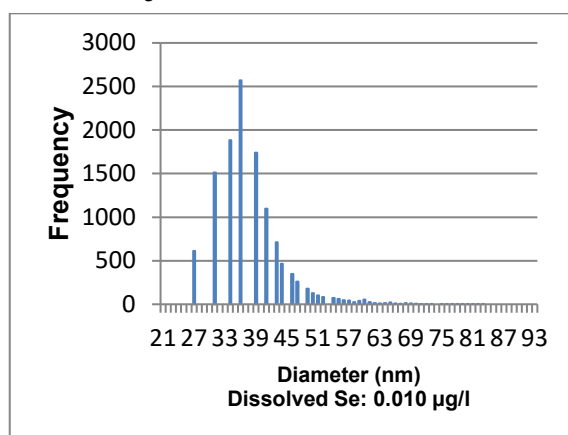


Figure 206: Size histogram of 50 nm SeNP standard (0.5 µg/l)  
30 s Measuring Time. Run 4. Manual Threshold: 1

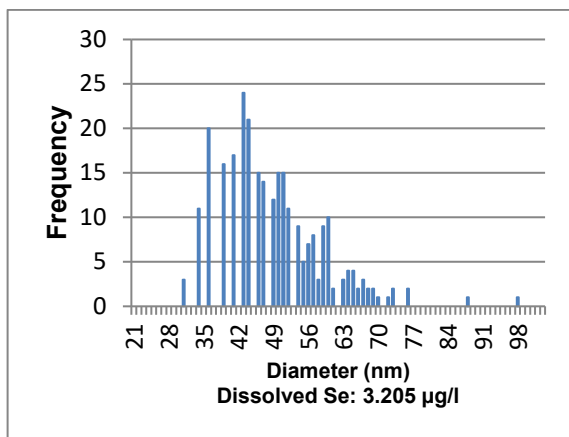


Figure 207: Size histogram of 50 nm SeNP standard (0.8 µg/l)  
30 s Measuring Time. Run 1. Automatic Threshold: 3.29

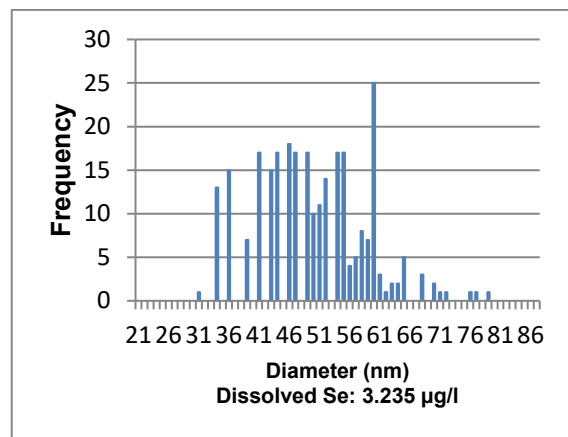


Figure 208: Size histogram of 50 nm SeNP standard (0.8 µg/l)  
30 s Measuring Time. Run 2. Automatic Threshold: 3.20

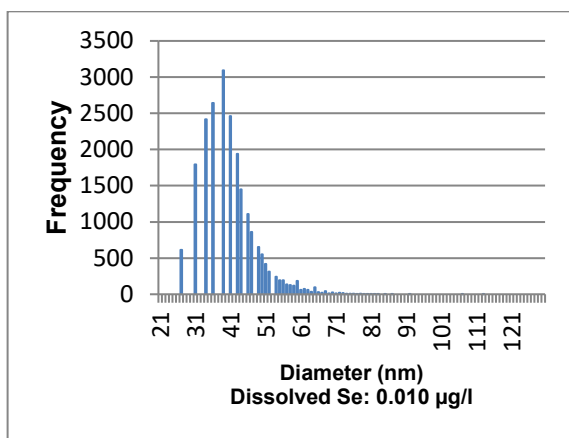


Figure 209: Size histogram of 50 nm SeNP standard (0.8 µg/l)  
30 s Measuring Time. Run 3. Manual Threshold: 1

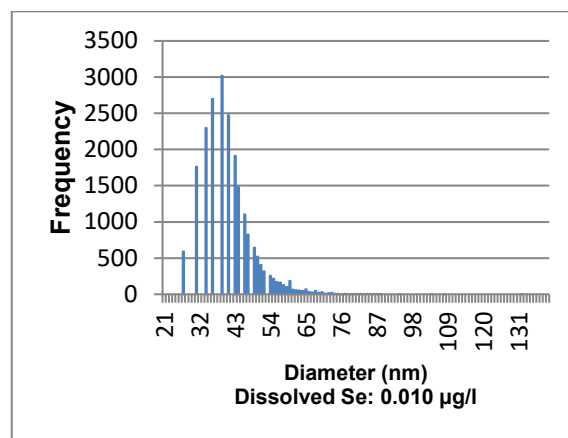


Figure 210: Size histogram of 50 nm SeNP standard (0.8 µg/l)  
30 s Measuring Time. Run 4. Manual Threshold: 1

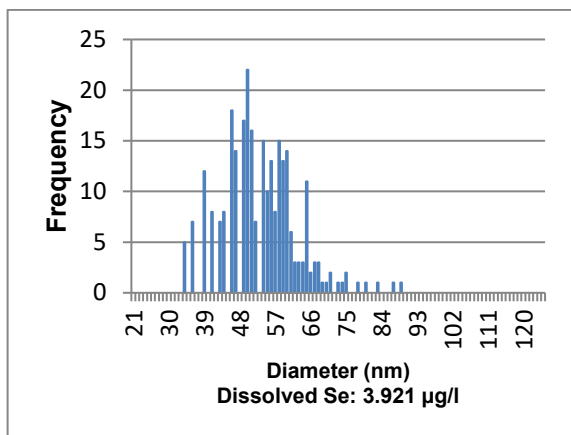


Figure 211: Size histogram of 50 nm SeNP standard (1 µg/l) 30 s Measuring Time. Run 1. Automatic Threshold: 3.65

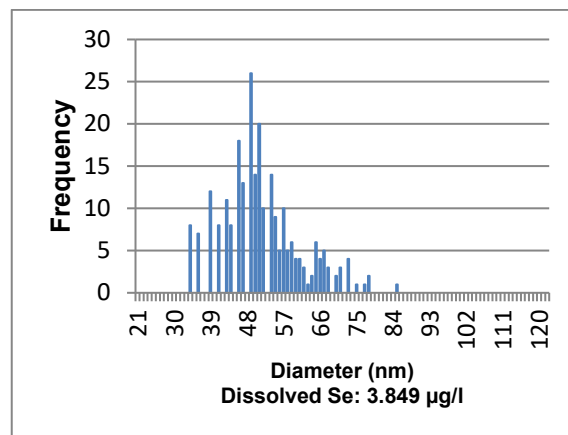


Figure 212 Size histogram of 50 nm SeNP standard (1 µg/l) 30 s Measuring Time. Run 2. Automatic Threshold: 3.61

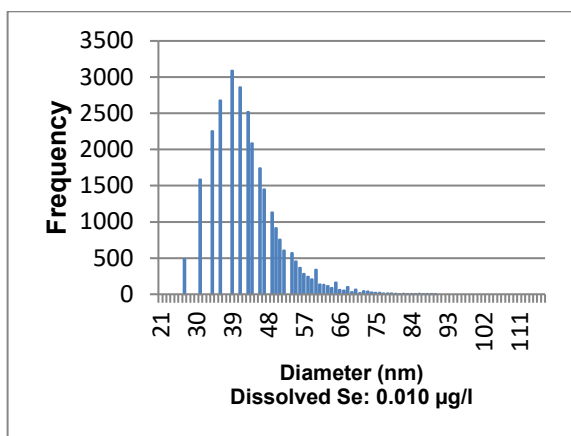


Figure 213 Size histogram of 50 nm SeNP standard (1 µg/l) 30 s Measuring Time. Run 3. Manual Threshold: 1

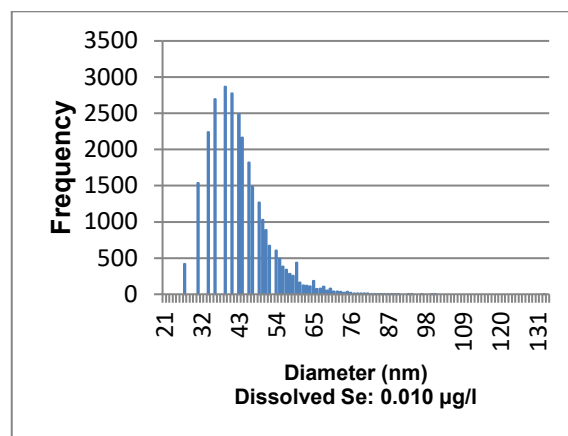


Figure 214 Size histogram of 50 nm SeNP standard (1 µg/l) 30 s Measuring Time. Run 4. Manual Threshold: 1

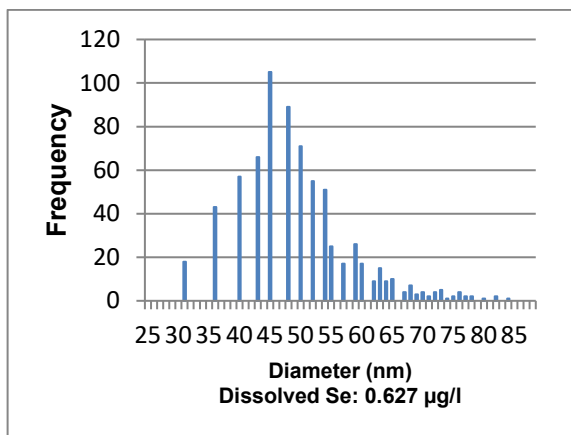


Figure 215: Size histogram of 50 nm SeNP standard (0.1 µg/l)  
60 s Measuring Time. Run 1. Automatic Threshold: 0.95

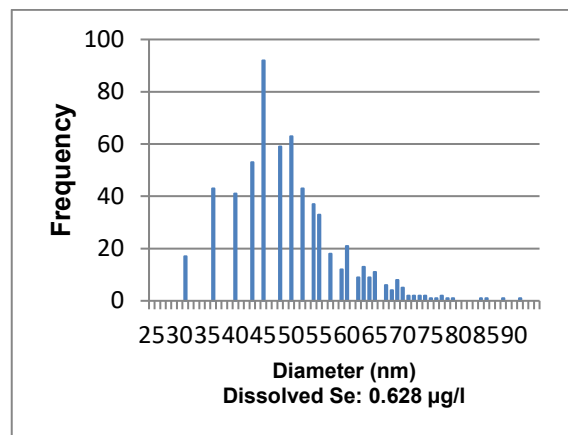


Figure 216: Size histogram of 50 nm SeNP standard (0.1 µg/l)  
60 s Measuring Time. Run 2. Automatic Threshold: 0.95

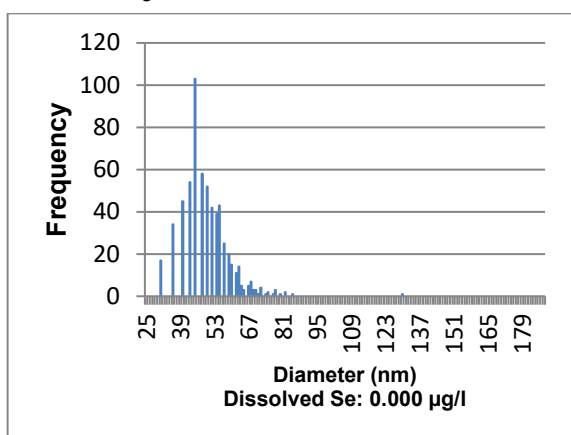


Figure 217: Size histogram of 50 nm SeNP standard (0.1 µg/l)  
60 s Measuring Time. Run 3. Manual Threshold: 1

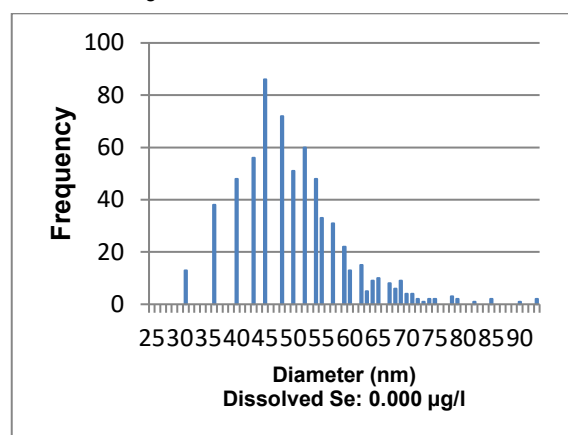


Figure 218: Size histogram of 50 nm SeNP standard (0.1 µg/l)  
60 s Measuring Time. Run 4. Manual Threshold: 1

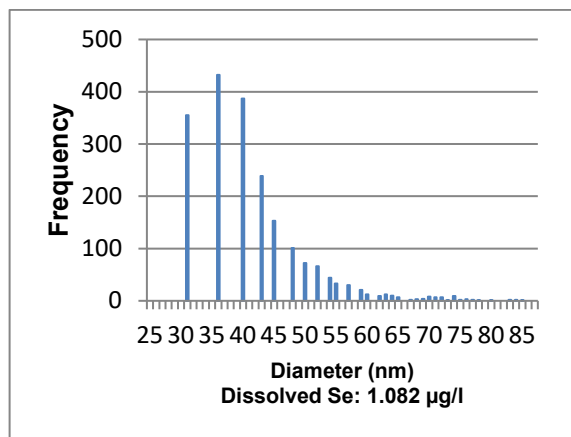


Figure 219: Size histogram of 50 nm SeNP standard (0.2 µg/l)  
60 s Measuring Time. Run 1. Automatic Threshold: 1.25

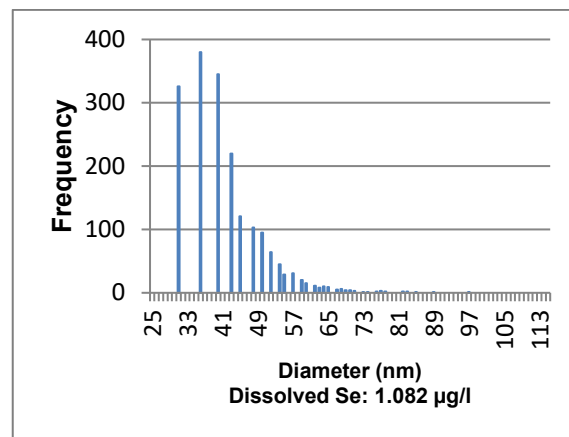


Figure 220: Size histogram of 50 nm SeNP standard (0.2 µg/l)  
60 s Measuring Time. Run 2. Automatic Threshold: 1.25

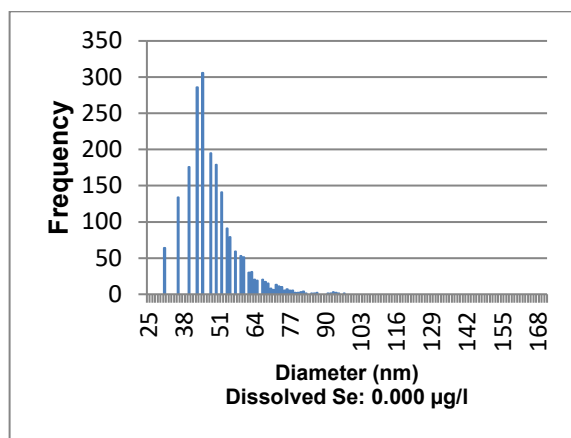


Figure 221: Size histogram of 50 nm SeNP standard (0.2 µg/l)  
60 s Measuring Time. Run 3. Manual Threshold: 1

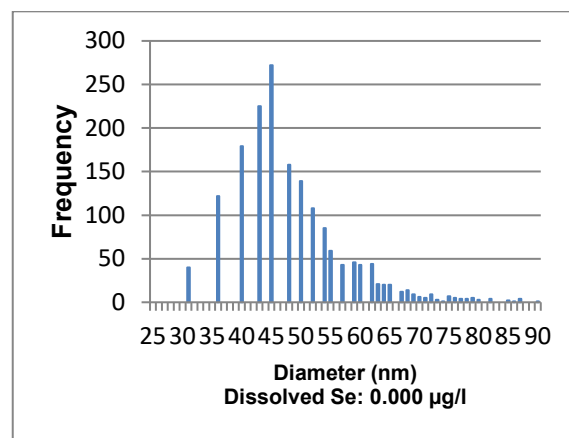


Figure 222: Size histogram of 50 nm SeNP standard (0.2 µg/l)  
60 s Measuring Time. Run 4. Manual Threshold: 1

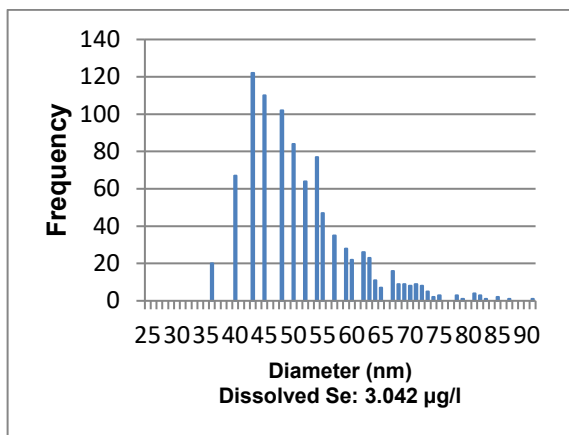


Figure 223: Size histogram of 50 nm SeNP standard (0.5 µg/l)  
60 s Measuring Time. Run 1. Automatic Threshold: 2.33

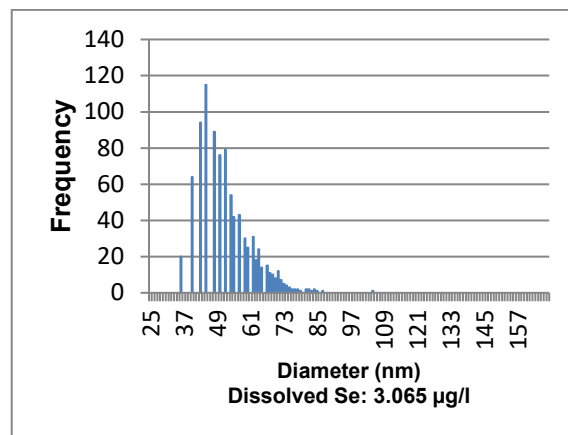


Figure 224: Size histogram of 50 nm SeNP standard (0.5 µg/l)  
60 s Measuring Time. Run 2. Automatic Threshold: 2.34

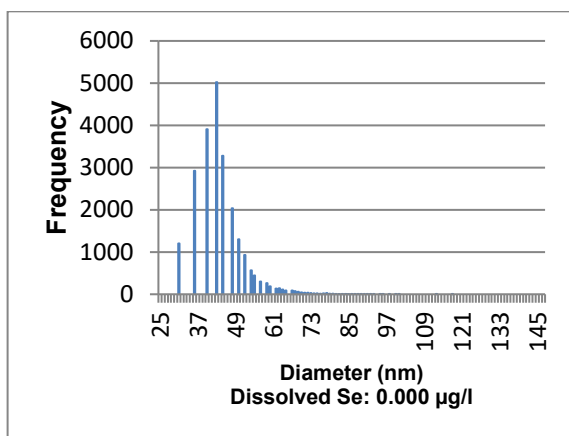


Figure 225: Size histogram of 50 nm SeNP standard (0.5 µg/l)  
60 s Measuring Time. Run 3. Manual Threshold: 1

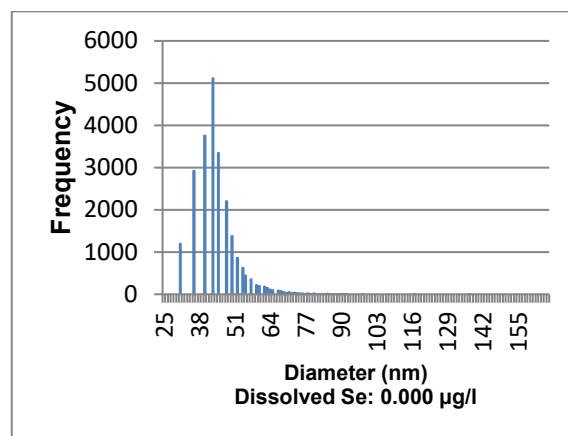


Figure 226: Size histogram of 50 nm SeNP standard (0.5 µg/l)  
60 s Measuring Time. Run 4. Manual Threshold: 1

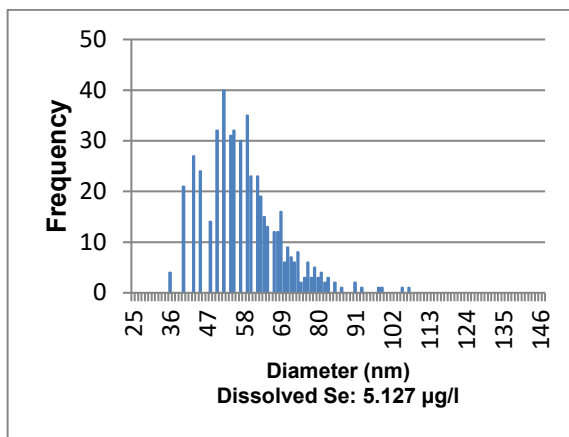


Figure 227: Size histogram of 50 nm SeNP standard (0.8 µg/l)  
60 s Measuring Time. Run 1. Automatic Threshold: 3.27

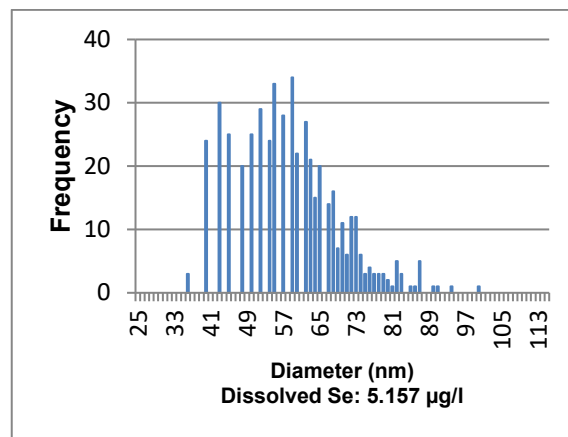


Figure 228: Size histogram of 50 nm SeNP standard (0.8 µg/l)  
60 s Measuring Time. Run 2. Automatic Threshold: 3.28

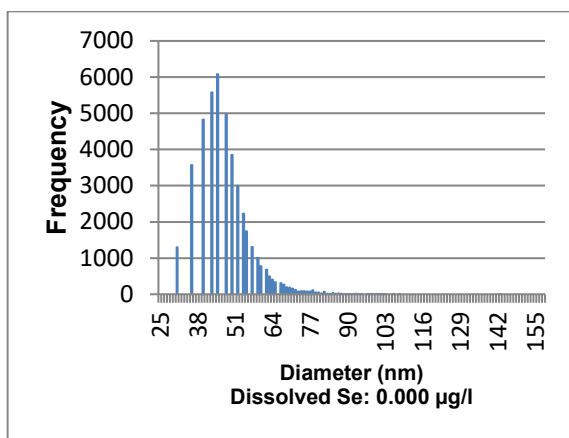


Figure 229: Size histogram of 50 nm SeNP standard (0.8 µg/l)  
60 s Measuring Time. Run 3. Manual Threshold: 1

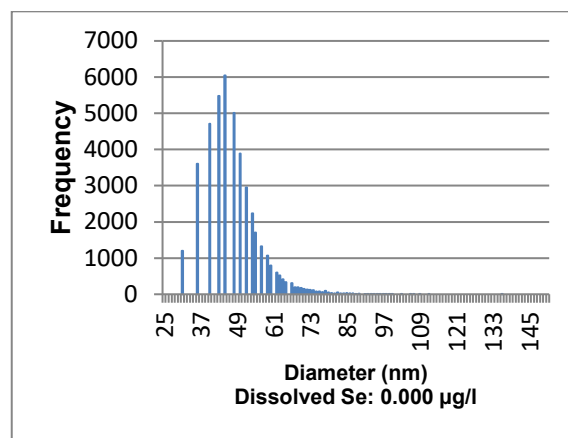


Figure 230: Size histogram of 50 nm SeNP standard (0.8 µg/l)  
60 s Measuring Time. Run 4. Manual Threshold: 1

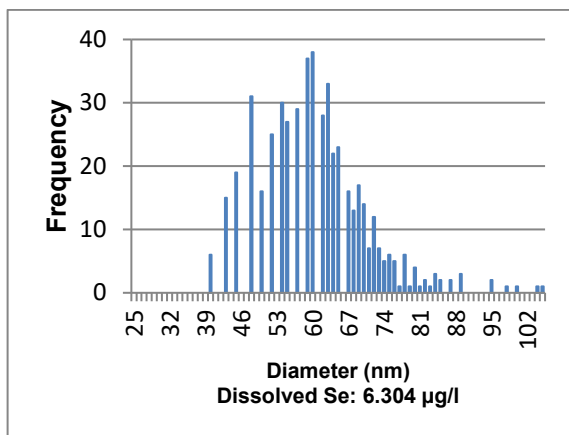


Figure 231: Size histogram of 50 nm SeNP standard (1 µg/l)  
60 s Measuring Time. Run 1. Automatic Threshold: 3.63

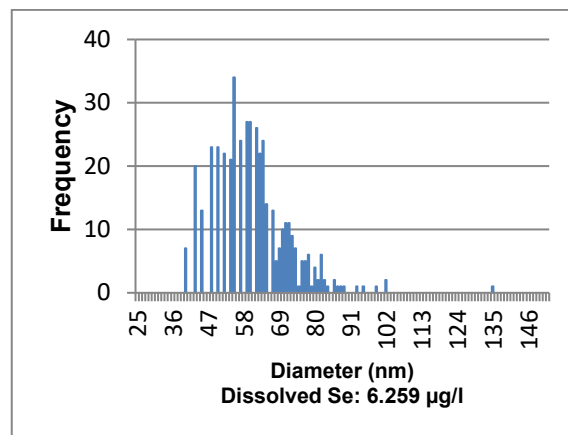


Figure 232: Size histogram of 50 nm SeNP standard (1 µg/l)  
60 s Measuring Time. Run 2. Automatic Threshold: 3.62

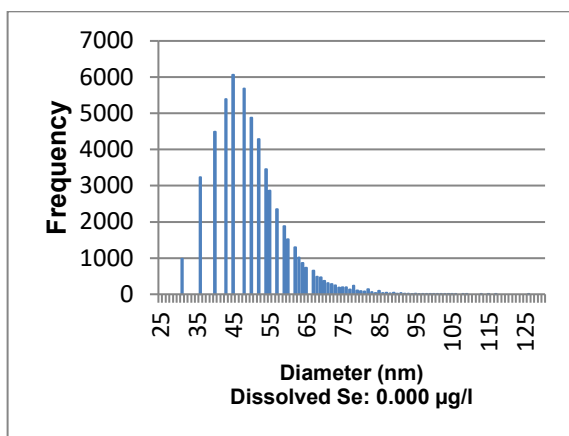


Figure 233: Size histogram of 50 nm SeNP standard (1 µg/l)  
60 s Measuring Time. Run 3. Manual Threshold: 1

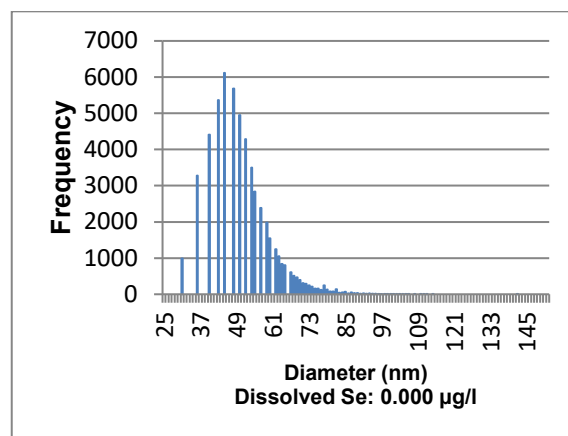


Figure 234: Size histogram of 50 nm SeNP standard (1 µg/l)  
60 s Measuring Time. Run 4. Manual Threshold: 1

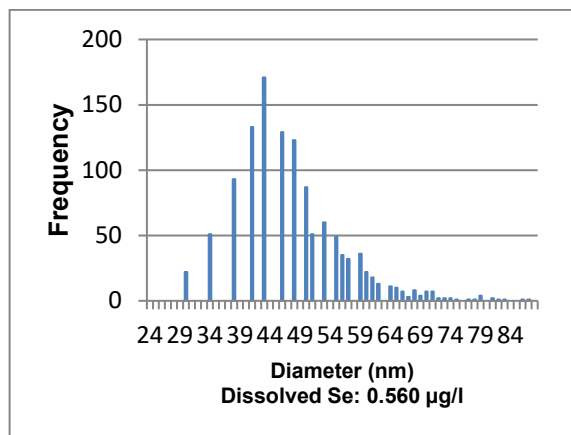


Figure 235: Size histogram of 50 nm SeNP standard (0.1 µg/l)  
120 s Measuring Time. Run 1. Automatic Threshold: 0.96

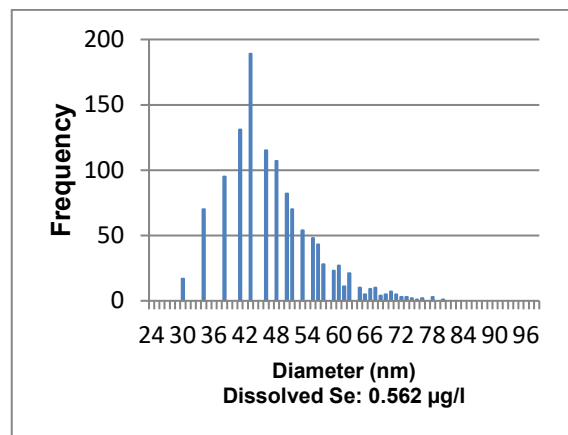


Figure 236: Size histogram of 50 nm SeNP standard (0.1 µg/l)  
120 s Measuring Time. Run 2. Automatic Threshold: 0.96

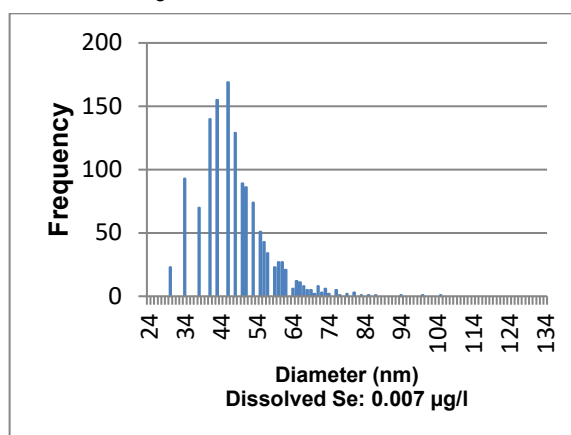


Figure 237: Size histogram of 50 nm SeNP standard (0.1 µg/l)  
120 s Measuring Time. Run 3. Manual Threshold: 1

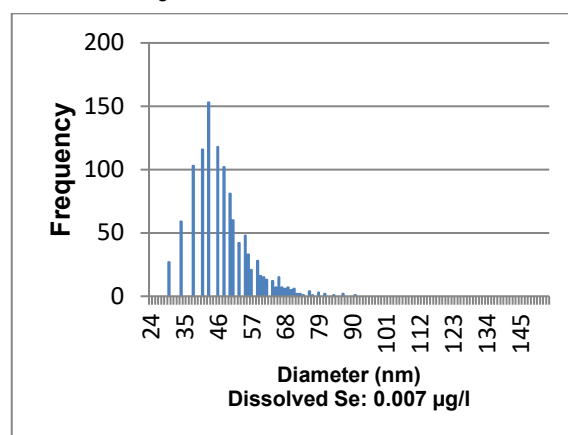


Figure 238: Size histogram of 50 nm SeNP standard (0.1 µg/l)  
120 s Measuring Time. Run 4. Manual Threshold: 1

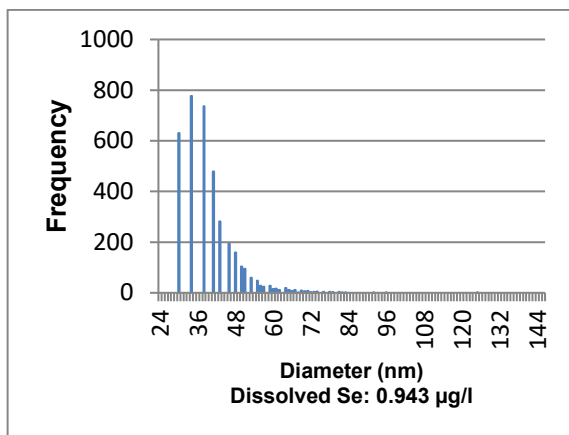


Figure 239: Size histogram of 50 nm SeNP standard (0.2 µg/l)  
120 s Measuring Time. Run 1. Automatic Threshold: 1.24

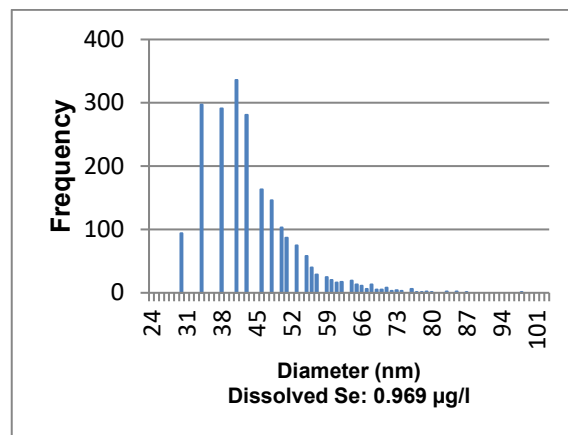


Figure 240: Size histogram of 50 nm SeNP standard (0.2 µg/l)  
120 s Measuring Time. Run 2. Automatic Threshold: 1.26

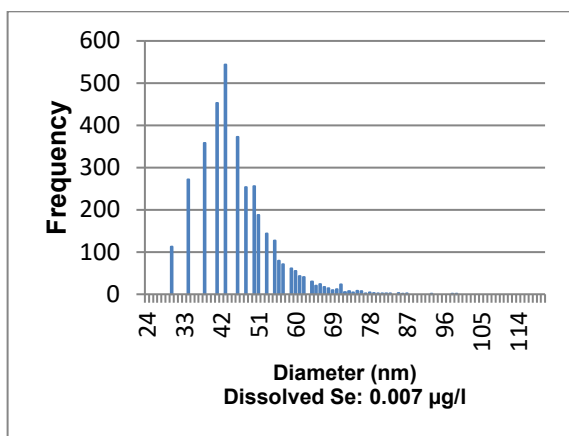


Figure 241: Size histogram of 50 nm SeNP standard (0.2 µg/l)  
120 s Measuring Time. Run 3. Manual Threshold: 1

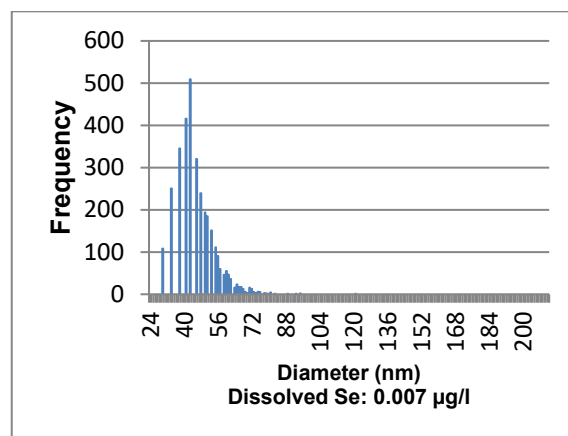


Figure 242: Size histogram of 50 nm SeNP standard (0.2 µg/l)  
120 s Measuring Time. Run 4. Manual Threshold: 1

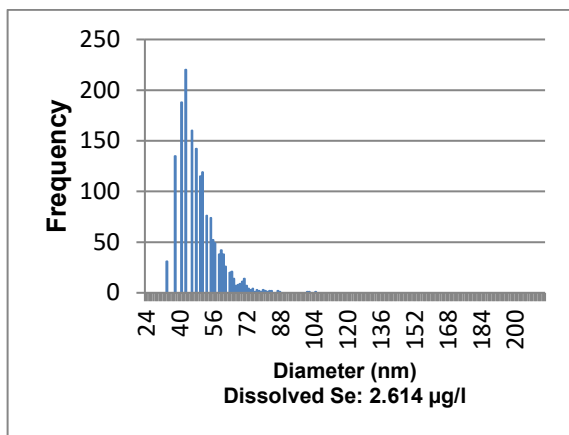


Figure 243: Size histogram of 50 nm SeNP standard (0.5 µg/l)  
120 s Measuring Time. Run 1. Automatic Threshold: 2.31

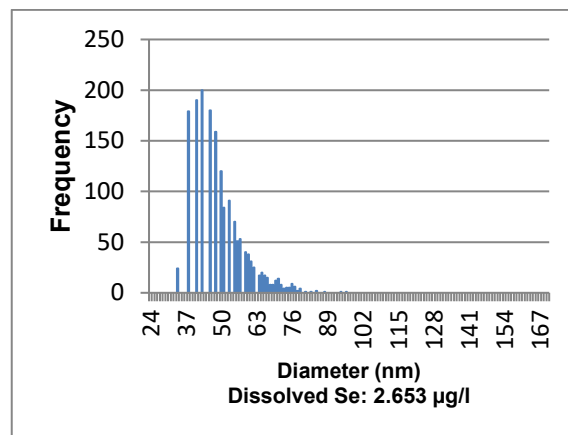


Figure 244: Size histogram of 50 nm SeNP standard (0.5 µg/l)  
120 s Measuring Time. Run 2. Automatic Threshold: 2.33

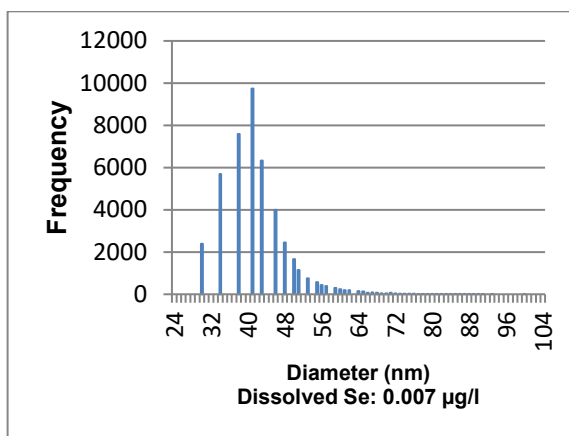


Figure 245: Size histogram of 50 nm SeNP standard (0.5 µg/l)  
120 s Measuring Time. Run 3. Manual Threshold: 1

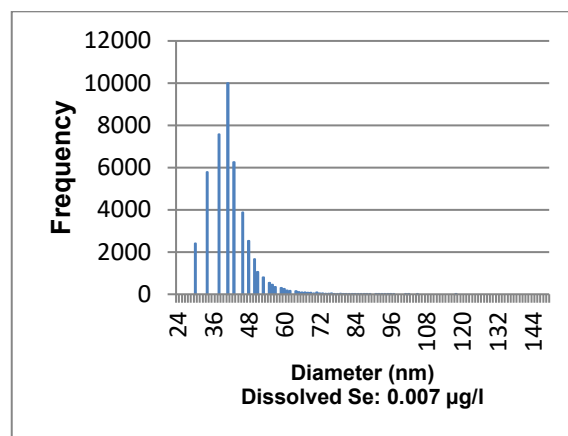


Figure 246: Size histogram of 50 nm SeNP standard (0.5 µg/l)  
120 s Measuring Time. Run 4. Manual Threshold: 1

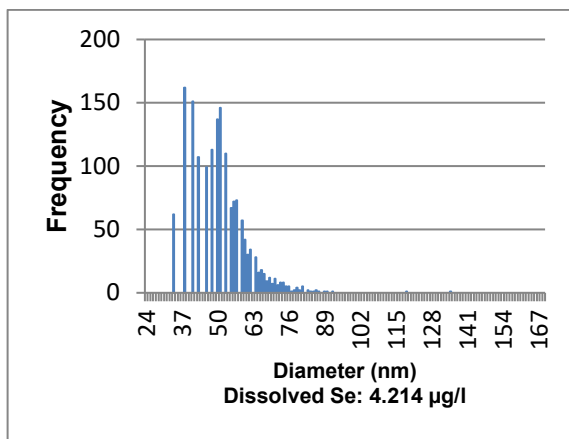


Figure 247: Size histogram of 50 nm SeNP standard (0.8 µg/l)  
120 s Measuring Time. Run 1. Automatic Threshold: 3.20

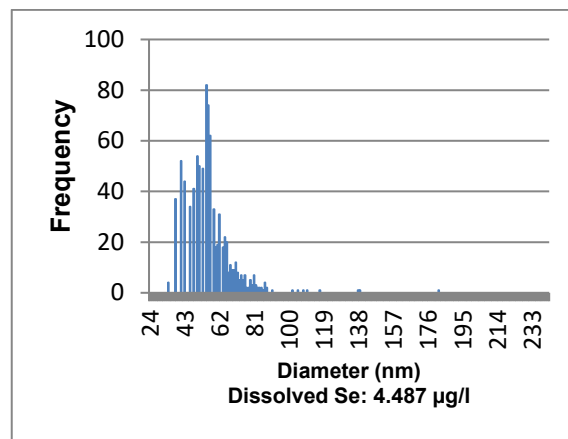


Figure 248: Size histogram of 50 nm SeNP standard (0.8 µg/l)  
120 s Measuring Time. Run 2. Automatic Threshold: 3.27

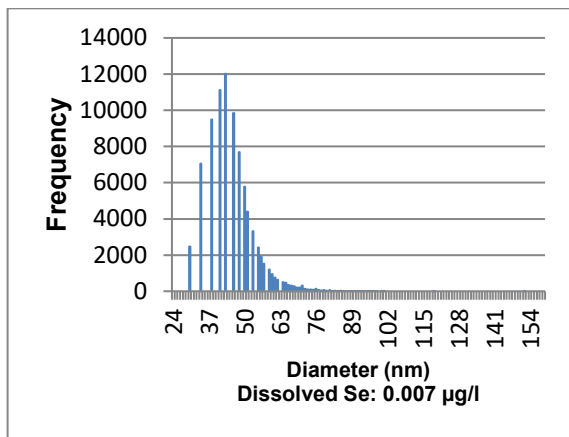


Figure 249: Size histogram of 50 nm SeNP standard (0.8 µg/l)  
120 s Measuring Time. Run 3. Manual Threshold: 1

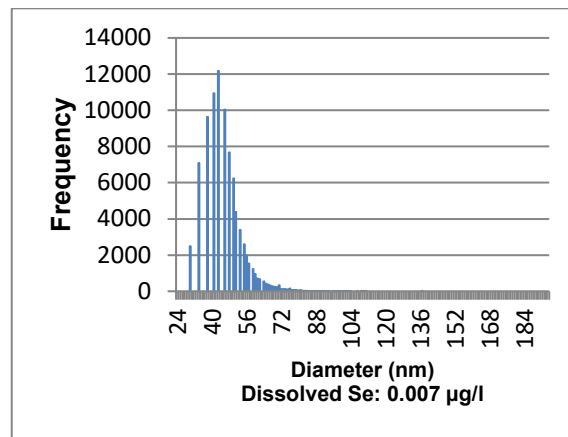


Figure 250: Size histogram of 50 nm SeNP standard (0.8 µg/l)  
120 s Measuring Time. Run 4. Manual Threshold: 1

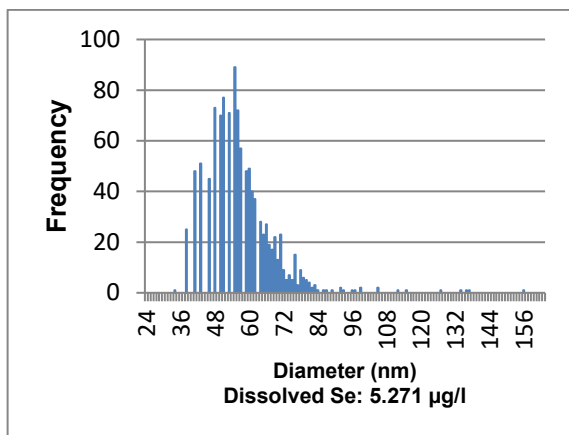


Figure 251: Size histogram of 50 nm SeNP standard (1 µg/l)  
120 s Measuring Time. Run 1. Automatic Threshold: 3.56

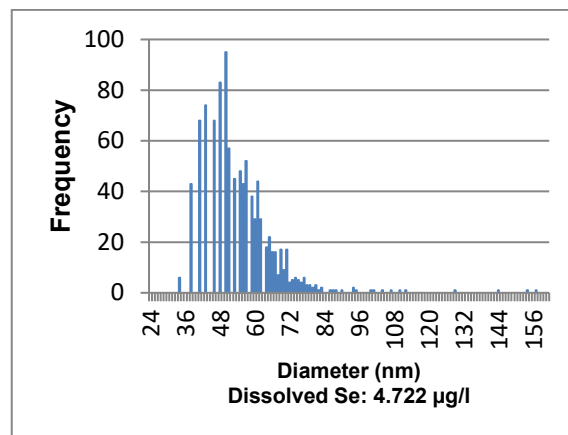


Figure 252: Size histogram of 50 nm SeNP standard (1 µg/l)  
120 s Measuring Time. Run 2. Automatic Threshold: 3.56

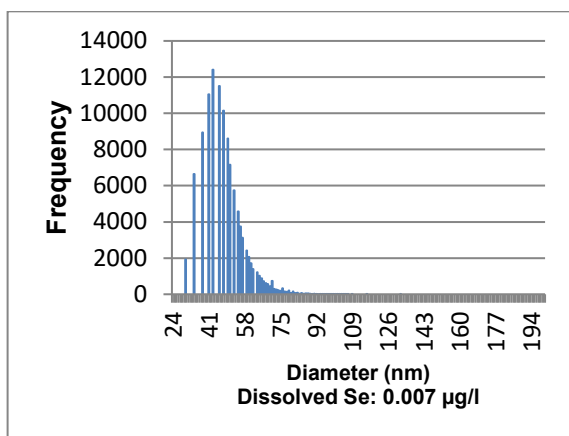


Figure 253: Size histogram of 50 nm SeNP standard (1 µg/l)  
120 s Measuring Time. Run 3. Manual Threshold: 1

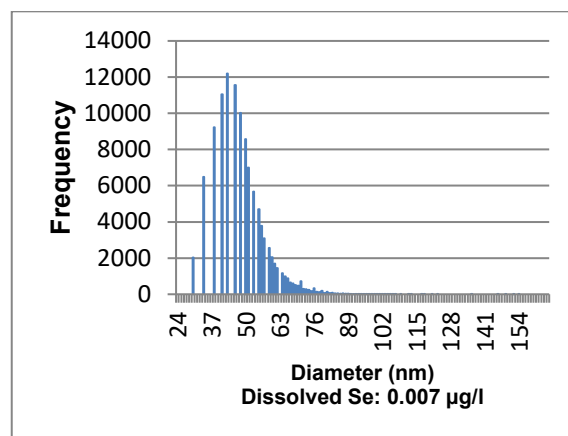


Figure 254: Size histogram of 50 nm SeNP standard (1 µg/l)  
120 s Measuring Time. Run 4. Manual Threshold: 1

## Acknowledgements

Meine Promotionsarbeit durfte ich unter Betreuung von Prof. Dr. Klaus Günther leisten. Für seinen stetigen Ansporn, seine Begeisterung für die Wissenschaft und unser Forschungsprojekt und seine stetige Unterstützung bin ich sehr dankbar. Durch sein mir entgegengebrachtes Vertrauen konnte ich dieses spannende und vielseitige Projekt zu meinem machen.

Dem Fachgebiet Arzneibuch des Bundesinstituts für Arzneimittel und Medizinprodukte möchte ich danken, ganz besonders Dr. Jochen Norwig und Dr. Yvonne Urbach für die freundliche und engagierte Arbeitsatmosphäre und dafür, dass sie es mir möglich gemacht haben, im dortigen Labor meine Untersuchungen durchzuführen.

Ebenfalls herzlich danken möchte ich meinen Kolleg:innen Anette Niederweis, Jana Hinz, Dr. Sarah Leitzen, Eliana Arnold und Dr. Matthias Vogel für den persönlichen und wissenschaftlichen Austausch und dafür, dass sie dazu beigetragen haben, dass ich meine Zeit am BfArM sehr genossen habe.

Sehr dankbar bin ich für meine langjährigen Freunde Max, Daniel, Tobi und Ors und alle, die ihr mir immer zur Seite standet, für all die gute Zeit, die wir zusammen hatten und dafür, dass ihr immer an mich geglaubt habt.

Ganz besonders danke ich auch meiner Familie, Mama, Papa und Oma, Lukas, Leon und Franziska dafür, dass ihr meine Flügel und mein Fangnetz seid, für eure Liebe und Unterstützung und für den Halt und das Verständnis, die ihr mir stets entgegenbringt.